

A COMPARATIVE ANALYSIS OF ELECTRON CORRELATION
IN ATOMIC BE
AND A
MOMENTUM SPACE INVESTIGATION OF LIH

by

Richard John Mobbs

A thesis submitted to the
UNIVERSITY OF LEICESTER
for the degree of
DOCTOR OF PHILOSOPHY
in the Faculty of Science

1985

UMI Number: U353012

All rights reserved

INFORMATION TO ALL USERS

The quality of this reproduction is dependent upon the quality of the copy submitted.

In the unlikely event that the author did not send a complete manuscript and there are missing pages, these will be noted. Also, if material had to be removed, a note will indicate the deletion.



UMI U353012

Published by ProQuest LLC 2015. Copyright in the Dissertation held by the Author.
Microform Edition © ProQuest LLC.

All rights reserved. This work is protected against
unauthorized copying under Title 17, United States Code.



ProQuest LLC
789 East Eisenhower Parkway
P.O. Box 1346
Ann Arbor, MI 48106-1346



To

My Family

Mum & Dad (The Past)

Anne (The Present)

Matthew & Charlotte (The Future)

ACKNOWLEDGEMENTS

I wish to express my thanks to Professors J.L.Beeby and E.A. Davis for the opportunity to work in the Physics Department, University of Leicester.

The receipt of a Science Research Council maintenance grant is gratefully acknowledged.

It is a pleasure to thank all the members, past and present, of the Quantum Molecular Physics Research Group and the staff of the Computer Laboratory, University of Leicester, for their assistance, wittingly or unwittingly, in the preparation of this thesis.

Special thanks must go to Dr. K.E. Banyard for his supervision throughout this research and for many hours of helpful and stimulating discussion on every aspect of this work. His patience, encouragement and advice made this research very enjoyable.

I am especially grateful to my wife, Anne, for her constant support and encouragement throughout this work.

Richard John Mobbs

A COMPARATIVE ANALYSIS OF ELECTRON CORRELATION
IN ATOMIC BE
AND A
MOMENTUM SPACE INVESTIGATION OF LIH

ABSTRACT

In Part I, the electron correlation problem is briefly reviewed and some approaches to its solution are discussed.

In Part II, a partitioning technique used previously to examine correlation trends in individual electronic shells for a series of four-electron ions has been extended and applied to a detailed comparison of four well-correlated wavefunctions for the Be atom. The present analysis of a correlated two-particle density, generalized for any N-electron system, retained all contributions from products of all terms in the wavefunction up to and including the pair-correlation effects. For each correlated description of Be, Coulomb holes and shifts have been evaluated and compared for the K(¹S), L(¹S), KL(¹S) and KL(³S) shells. The inverted nature of the intershell holes, relative to the intrashell effects, has been examined and rationalized in terms of the 2s-2p near-degeneracy which exists in Be. The total Coulomb holes for the two energetically best wavefunctions showed a previously unseen structure which was directly attributable to the intershells. The calculation of partial Coulomb holes and shifts, $\Delta g(r_{12}, r_1)$ vs. r_{12} & $\Delta g(p_{12}, p_1)$ vs. p_{12} , allowed us to examine changes in the components of correlation as the position r_1 or the momentum p_1 of a test electron was varied. Selected one- and two-particle radial and momentum expectation values are also reported along with various radial and angular correlation coefficients.

In Part III the partitioning technique, discussed in Part II, has been applied to a momentum space study of electron correlation in a molecular system. The correlation effects embedded in a CI wavefunction for LiH has been examined in terms of the intra- and intershell Coulomb shifts and several one- and two-particle expectation values.

Finally, in Part IV we present an overview of correlation coefficients as used, quite extensively, in the discussion of electron correlation. We have examined their construction and have reviewed their application towards this subject.

ACKNOWLEDGEMENTS

ABSTRACT

PART I GENERAL INTRODUCTION

1. Introduction	I-1
2. Electron Correlation	I-10
3. Pair Correlation Approximations	I-13
4. Wavefunction Structure	I-23
5. References	I-30

PART II ELECTRON CORRELATION IN ATOMIC BERYLLIUM

1. Introduction	II-1
2. Sinanoglu's MET/Pair function analysis	II-5
3. Partitioning Technique	II-12
4. Wavefunctions	II-22

Position Space

5. Introduction	II-27
6. Results and Calculations	II-30
7. Discussion	II-36

Momentum Space

8. Introduction	II-46
9. Results and Calculations	II-51
10. Discussion	II-56

11. Summary	II-67
12. References	II-70
13. Tables & Figures	II-75

PART III LITHIUM HYDRIDE

1. Introduction	III-1
2. Wavefunction	III-8
3. Results and Calculations	III-11
4. Discussion	III-23
5. References	III-37
6. Tables & Figures	III-40

PART IV CORRELATION COEFFICIENTS

1. Introduction	IV-1
2. Statistical Overview	IV-3
3. An Appraisal of Correlation Coefficients	IV-16
4. An Assessment of the work of King and Rothstein	IV-23
5. Summary	IV-29
6. References	IV-31
7. Figures	IV-33

PART I

GENERAL INTRODUCTION

CHAPTER I.1

INTRODUCTION

The study of the electronic structure of the atom formed an integral part of the development of quantum mechanics at the beginning of this century. Rutherford's (1911) model assumed that all the positive charge of the atom is concentrated in a small region - the nucleus - at the centre of the atom, and that electrons, having negative charge, travel in orbits around this nucleus, rather like planets around the sun. In keeping with Planck's demonstration of the quantization of energy, Bohr (1913) postulated that the possible internal energy values of an atom form a discrete set, and in the case of hydrogen he deduced from this the discrete set of possible values which the radius of the electron's orbit can assume. Experimental evidence for the quantization of the internal energy of atoms was furnished by the Franck-Hertz experiment.

Bohr deduced his discrete set of energies, or energy levels, for the hydrogen atom from the Balmer formula for the wavelength, or the frequency, of a radiated photon. But his semi-classical picture of the atom had a limited success; because of the uncertainty principle, it is not possible to specify completely the orbit of an electron. Indeed, the uncertainty principle required the abandonment of such a deterministic model in favour of a probabilistic

one in which we define a probability per unit volume $|\psi_n|^2$ of finding the electron in a quantum state n . Thus, ψ satisfies the condition given by

$$\int |\psi_n|^2 d\tau = 1. \quad \text{I.1}$$

The equation for the wavefunction $\psi_n(\underline{r}, t)$ was given by Schrödinger⁽¹⁾ (1926):

$$H\psi \equiv (T+V)\psi = ih/2\pi \partial\psi/\partial t \quad \text{I.2}$$

with ψ_n being the appropriate eigenfunction of Equation I.2. The Hamiltonian H is the sum of the quantum-mechanical operators for kinetic (T) and potential (V) energy. The kinetic energy T is obtained from its classical equivalent by the substitution $\underline{p} \rightarrow -ih/2\pi \text{ grad}$, so that for an N -electron atom

$$T = - \{ (h/2\pi)^2 / 2\mu \} \sum_{i=1}^N \nabla_i^2 \quad \text{I.3}$$

where $\mu = m_0 M_A / (m_0 + M_A)$ is the reduced mass of the electron, and M_A is the mass of the nucleus of the atom. The potential energy V used by Schrödinger contains electrostatic interactions which, for an N -electron atom, are

$$V = - Ze^2 \sum_{i=1}^N 1/r_i + e^2 \sum_{i < j}^N 1/|\underline{r}_i - \underline{r}_j| \quad \text{I.4}$$

where \underline{r}_i represents the coordinates of electron i . Mostly we concern ourselves with stationary states of atoms, for which $|\psi(\underline{r}, t)|^2 = |\psi(\underline{r})|^2$, ie independent of time. Writing

$$\Psi(\underline{r}, t) = \Psi(\underline{r}) \exp[-iEt/(h/2\pi)] \quad \text{I.5}$$

then from Equation I.2

$$H\Psi(\underline{r}) = (T+V)\Psi(\underline{r}) = E\Psi(\underline{r}) \quad \text{I.6}$$

which demonstrates the analogy with classical mechanics, but now E is an eigenvalue of the differential operator H .

For hydrogen, only the first part of Equation I.4 arises, and Schrödinger's equation may be solved to give energies satisfying the Balmer formula. But the fine-structure splitting, for example of the $2p^2$ state of hydrogen into two closely spaced levels, is not predicted using this potential. This splitting is correctly given only in a relativistic treatment of atomic structure.

In the quantum theory of the electronic structure of matter, the two-electron systems provide a valuable bridge between the comparatively simple one-electron systems and systems containing many electrons. The structure of an electronic system within a given nuclear framework depends not only on the balance between the kinetic energy of the electrons and their attraction to the nuclei, but also on the mutual electronic repulsion. The last effect causes considerable difficulties in the theory, since it may not be treated within the conventional 'one-electron approximation'. The accurate solution of the many-electron Schrödinger equation therefore demands other methods, and

the results for two-electron systems are then also of guiding importance in treating systems containing many electrons.

In order to understand the present day methods of atomic structure calculations and their motivations, we shall consider the highly accurate calculations that have been performed on the helium isoelectronic sequence. These calculations have used either variational theory or perturbation theory or a combination of the two schemes. We recall that in principle we are seeking the stationary-state solutions of the Schrödinger equation

$$\left[-\frac{1}{2} \sum_{i=1}^N \nabla_i^2 - Z \sum_{i=1}^N \frac{1}{r_i} + \sum_{i < j}^N \frac{1}{r_{ij}} \right] \Psi \equiv H\Psi = E\Psi \quad \text{I.7}$$

which satisfy

$$\langle \Psi | \Psi \rangle \equiv \int \Psi^* \Psi d\tau = 1$$

where N is the number of electrons in the atomic system and $r_{ij} = |\underline{r}_i - \underline{r}_j|$. In writing the electronic Hamiltonian, Equation I.7, we have used atomic units, in which h (Planck's constant) divided by 2π , the electronic charge e , and the electron mass m are all unity. In atomic units, distance is given in bohr radii (bohrs), where 1 bohr is 0.52918×10^{-10} m or 0.52918 Å. The unit of energy is the hartree, equal to 27.21 eV, 627.5 kcal/mole, 2.1948×10^5 cm⁻¹, or 3.1579×10^5 K, depending on one's preference. Equation I.7 can be written in an equivalent variational form by requiring that the functional

$$\langle \Psi | H | \Psi \rangle \equiv \int \Psi^* H \Psi d\tau$$

be stationary with respect to small changes in Ψ which preserve the normalisation condition. If we introduce a Lagrange multiplier E to take into account this normalisation constraint, then the variational equation is

$$\delta \langle \Psi | H - E | \Psi \rangle = \langle \delta \Psi | H - E | \Psi \rangle + \langle \Psi | H - E | \delta \Psi \rangle = 0. \quad \text{I.8}$$

If the energy E and the wavefunction Ψ correspond to the lowest energy of a given symmetry class (eg L,S) then Equation I.8 may be replaced by the minimum principle

$$E \leq E_t = \langle \Psi_t | H | \Psi_t \rangle / \langle \Psi_t | \Psi_t \rangle \quad \text{I.9}$$

where Ψ_t is any function belonging to the same symmetry class as Ψ (see Messiah Ref. 2).

Even for two electron atoms, the eigenfunctions of the Hamiltonian H cannot be found in closed form. It is therefore convenient to form a 'trial' wavefunction Ψ_t which is allowed to depend on a number of variable parameters, for any choice of which Equation I.9 is satisfied. The 'best' choice of these parameters may be considered to be that which makes E_t as low (ie as close to the true energy) as possible. We note that, in practice, this variational method does not provide a pointwise solution of Equation I.7 although, depending on the flexibility of the form of Ψ_t , the resulting wavefunction should be a good representation

of the true wavefunction, at least in those regions of space which are emphasized by the Hamiltonian operator.

Two types of solution of the two-electron Schrödinger equation have been suggested, namely an eigenfunction in the form of a 'superposition of configurations' and a form containing the interelectronic distance as a variable. Both types were first investigated by Hylleraas in his pioneering work on the helium problem⁽³⁻⁵⁾. Hylleraas found that the series of configurations converged rather slowly and that a much quicker convergence could be obtained by introducing r_{12} explicitly in the solution. Wavefunctions containing r_{12} have later been evaluated by James and Coolidge⁽⁶⁾ for the H_2 molecule, by Henrich⁽⁷⁾ for the H^- ion, and for the He series by Eriksson⁽⁸⁾, by Baber and Hasse⁽⁹⁾, and by Chandrasekhar and Herzberg⁽¹⁰⁾. The wavefunctions containing r_{12} have the disadvantage that it seems impossible to give them an interpretation of simple physical visuality, and it is difficult to generalize the approach to many-electron systems⁽¹¹⁾. Nevertheless, the success of the r_{12} method was so large that, for a rather long time, it was almost generally believed in the literature⁽³⁻⁵⁾ that "electronic correlation" could be taken into account only by introducing the inter-electronic distances r_{ij} explicitly into the wavefunction. However, it was already known in the early days of quantum mechanics that the wavefunction for a many-electron system could be expressed as a superposition of configurations built up from one-electron functions, provided that the one-electron set was complete.

The high degree of accuracy achieved for two-electron atoms is not maintained for larger systems. Early variational calculations on the lithium ground state by James and Coolidge⁽¹²⁾ which included interelectronic distances r_{ij} and resulted in an energy value of -7.476au have been extended by Burke⁽¹³⁾ (see also Larson and Burke⁽¹⁴⁾) and more recently by Larson⁽¹⁵⁾ who obtained an energy of -7.478025au with 60 Hylleraas-type basis functions in the wavefunction, although the convergence of this expansion was extremely slow. When relativistic and finite nuclear mass effects are removed from the experimental value, the energy value is estimated to be -7.478069au . Thus even for lithium the accuracy achieved is relatively poor, compared with two-electron systems. One of the difficulties has been the computation of the integrals involving the interelectronic distances r_{12} , r_{23} and r_{13} .

Four-electron systems are the smallest for which the direct use of interelectronic coordinates ceased to be feasible although a limited attempt to include them has been made by Perkins⁽¹⁶⁾. It is natural that the ground state of beryllium should have become the testing ground for many-electron theories, in much the same way as the ground state of helium has been for less elaborate methods. A number of points emerge regarding the correlation energy of beryllium: (1) most of the $2s^2$ correlation arises from the near-degeneracy effect. The two configuration wavefunction used by Watson⁽¹⁷⁾ ($1s^2 2s^2 + 1s^2 2p^2$) contributes most of the outer-shell pair energy as calculated by Hibbert⁽¹⁸⁾ using a large number of configurations. (2) The $1s^2$ correlation energy in

Be is very similar to the correlation energy of the two-electron ion Be^{2+} . (3) The intershell energy is much smaller in magnitude than the intrashell values. This is to be expected since the 1s and 2s orbitals are important in different regions of space and so their motion is already well correlated. We shall return to the pair-energies of Be in a later section.

In order to consider in detail the structure of many-electron atoms, we must seek an alternative approach to the (approximate) solution of Schrödinger's equation. The approximations introduced above are essentially mathematical, arising from the representation of the wavefunction in terms of a finite basis set. Probably the most widely used alternative to this scheme is based on a proposal by Hartree^(19,20). In his method, Hartree approximated the physics of the problem, and thereby was able to set up a mathematical model which was tractable even for large atoms. The scheme allowed each electron to move independently of the others. Hence the probability density function $\Psi^*\Psi$ should be a product of the probability density functions of the individual electrons. This requires each electron to be described by a function of its own coordinates: $\phi_k(k)$. The N-electron wavefunction Ψ becomes

$$\Psi = \phi_1(1)\phi_2(2)\dots\phi_N(N) \quad . \quad \text{I.10}$$

Each orbital function $\phi_k(k)$, $k=1,2,\dots,N$, may be determined by setting up a Schrödinger-type equation for each electron:

$$[-1/2 \nabla^2 - z/r + V_k(\underline{r})]\phi_k = \epsilon_k \phi_k \quad \text{I.11}$$

where $V_k(\underline{r})$ is the electrostatic potential experienced by the k th electron:

$$V_k(\underline{r}) = \sum_{i \neq k} \int |\phi_i(\underline{s})|^2 / |\underline{r}-\underline{s}| \, d\underline{s} \quad \text{I.12}$$

A simplification may be made by taking a spherical average of $V_k(\underline{r})$ to produce a purely radial potential:

$$V_k(r) = 1/4\pi \int V_k(\underline{r}) \, d\underline{r} \quad \text{I.13}$$

If this radial potential is used instead of $V_k(\underline{r})$ in Equation I.13, the entire potential term is purely radial, and we have a central-field model.

No mention has been made of electron spin. Indeed Equation I.10 fails to satisfy Pauli's exclusion principle. To overcome this difficulty, Fock^(21,22) expressed the wavefunction in the form of a determinant:

$$\Psi = 1/\sqrt{N!} \det |\phi_1(1)\phi_2(2)\dots\phi_N(N)| \quad \text{I.14}$$

The exclusion principle is now satisfied, for elementary properties of determinants show that $\Psi=0$ if $\phi_i=\phi_j$, while the wavefunction is antisymmetric with respect to interchange of pairs of coordinate rows without changing the 'value' of the determinant, it is possible to choose the ϕ_i 's to form an orthonormal set. The factor $1/\sqrt{N!}$ ensures that Ψ is also normalised for an orthonormal basis set.

CHAPTER I.2
ELECTRON CORRELATION

The correlation problem is still a field of active research and many methods of analysing and studying correlation have been proposed. The work of Nesbet⁽²³⁾, Brueckner^(24, 25, 36), Goldstone⁽²⁶⁾ and Sinanoglu⁽²⁷⁻³⁶⁾ has been particularly noteworthy. Much of the early work on the problem was due to Hylleraas⁽³⁻⁵⁾ who proposed three methods of constructing a correlated wavefunction, all of which are still in use today.

In the Hartree-Fock approximation, the motion of each electron is solved in the presence of the average potential created by the remaining (N-1) electrons. As such, the HF approximation neglects the instantaneous (rather than the averaged) repulsions between pairs of electrons. The contribution to the total energy due to instantaneous repulsions is called the correlation energy⁽³⁷⁾, since the motion of the electrons is correlated in that two electrons are unlikely to get very close to each other, given Coulomb's law. To be more specific the correlation energy E_c is usually accepted⁽³⁸⁾ to be the difference between the restricted Hartree-Fock energy and the exact non-relativistic energy of a particular system.

The correlation energy is usually a relatively small percentage of the total energy of an atom or molecule. For example, for the neon atom the correlation energy, 0.38 hartrees, is only 0.3% of the total energy -129.06 hartrees⁽³⁹⁾. This small percentage might lead an unsuspecting observer to conclude that the RHF approximation, which neglects electron correlation, is adequate. For many purposes the RHF approximation is an excellent one; for example, molecular geometries, some one-electron properties, and ionization potentials predicted from RHF wavefunctions are frequently in good agreement with experiment. However, though 0.3% is a small percentage, the actual value of the correlation energy of neon is more than 10 eV, which is larger than the amount of energy required to break most chemical bonds.

Since energy differences are of primary importance to chemists, one might hope the correlation energy to be constant as a function of molecular geometry. Were this the case, accurate dissociation energies and potential energy surfaces could be obtained from Hartree-Fock wavefunctions. For chemical reactions involving only closed-shell species, Snyder and Basch⁽⁴⁰⁾ have in fact found SCF calculations to give fair agreement with experiment for heats of reaction. However, for most diatomic molecules the molecular RHF wavefunctions do not dissociate to RHF wavefunctions describing the correct states of the separated atoms⁽⁴¹⁾. The F_2 molecule is predicted to have a negative dissociation energy in the restricted Hartree-Fock approximation⁽⁴²⁾ and the RHF dissociation energy for O_2 is slightly more than one-fourth

of the experimental value⁽⁴³⁾. The barrier height or activation energy for the simple chemical reaction $\text{Cl} + \text{H}_2 \rightarrow \text{HCl} + \text{H}$ is predicted from accurate SCF calculations⁽⁴⁴⁾ to be three or more times greater than experiment. In general, perhaps the most serious drawback of the Hartree-Fock approximation is its inability to describe molecular formation and dissociation.

The most frequently used method for approaching the electron correlation problem is configuration-interaction⁽³⁻⁵⁾, abbreviated CI. For any atom or molecule, there are an infinite number of orbitals in addition to the occupied Hartree-Fock orbitals. These higher orbitals can of course be used to construct other (after the RHF) configurations. A CI wavefunction is just a linear combination of such configurations with coefficients variationally determined. The CI method is in principle exact because, as the basis set of one-electron functions (orbitals) approaches completeness and we include in our wavefunction all configurations which can be constructed from these orbitals, we approach the exact solution to the Schrödinger equation. Although in practice it is never possible to use a complete set of orbitals, the CI method is a very reasonable procedure for going beyond Hartree-Fock. The CI approach will be discussed in greater detail later.

CHAPTER I.3

PAIR CORRELATION APPROXIMATIONS

It is convenient and physically meaningful to separate the problem of the wavefunction and energy of an atom with N electrons into two parts: (1) the self-consistent field (SCF) orbitals of the Hartree-Fock method, and (2) the remaining correlation part. This of course is not the only way to separate the problem into parts, nor is it even clear at the outset that the problem should be divided at all. Various more "classical" approaches have looked at the N -electron problem without such a division. Hylleraas in 1929 dealt with Helium directly in terms of a power series in r_1 , r_2 and r_{12} not in two distinct and explicit stages. The Bacher-Goudsmit method⁽⁴⁵⁾ relates energies to one another.

Should it be indeed convenient to have the two-stage problem, why take the HF SCF orbitals as the start, other than that they are readily available for many atoms. In other many-body problems the same type of HF orbitals often are not convenient. In the uniform electron gas the HF orbitals are the trivial solution for translational invariance, ie plane waves.

In the simplest possible description of an N -electron system, one one-electron function (spin-orbital) is

associated with each electron and the N-electron wavefunction is a Slater determinant built up of from these spin-orbitals. The one-to-one correspondence between electrons and spin-orbitals gives an acceptable first-order description only for closed-shell and certain open-shell states. A one-electron theory that is applicable in general to open-shell states as well is characterized by assigning sets of electrons of degenerate spin-orbitals, where the number of electrons within one set can be equal to or smaller than the dimension of the irreducible representation spanned by the degenerate set of spin-orbitals. An example is the characterization of an atomic state by its configuration⁽⁴⁶⁾, eg for the carbon ground state $1s^2 2s^2 2p^2$, without specifying the m_s and m_l values.

An electron-pair theory for a closed-shell state is characterized by as many two-electron functions as there are electron pairs, ie $N(N-1)/2$ for an N-electron system, and possibly in addition by N one-electron functions. Some of the two-electron functions can be built from just two one-electron functions. If this holds for all two-electron functions, we have a one-electron theory.

The very general definition of electron-pair theories includes theories based on the two-particle density matrices, as well as those originating from cluster expansion of the wavefunction. Second-order perturbation theory of electron correlation automatically leads to a pair theory. There are many more pair theories compatible with the above definition but we shall concentrate on pair-

cluster expansions of the wavefunction.

There are essentially two reasons why one can expect that electron-pair theories to furnish a good approximation for N-electron systems: (1) The Hamiltonian contains only one- and two-particle operators; (2) the Pauli principle prevents three electrons from occupying the same region of space.

If the Hamiltonian contained just one-electron operators, ie had the form

$$H(1,2,\dots,N) = \sum_{i=1}^N h(i)$$

a one-electron theory would be exact, namely the N-electron wavefunction Ψ would be a Slater determinant built up from the eigenfunctions of h.

Unfortunately it is not true that for the Hamiltonian

$$H(1,2,\dots,N) = \sum_i^N h(i) + \sum_{i < j}^N g(i,j) = H(1) + H(2)$$

an electron-pair theory is exact. The situation is not so bad, however, since the average electron interaction can readily be taken into account by a one-electron theory (Hartree-Fock approximation) so that the pair functions have only to take care of that part of the electron interaction which is beyond the average interaction (sometimes referred to as "instantaneous interaction" or "fluctuations")^(30,31,33,36).

Since two of three electrons must have the same spin, and since two electrons with the same spin cannot occupy the same point of space⁽⁴⁷⁾ (Fermi hole), only two electrons can come close to each other. Therefore, three-particle contributions to the correlation energy (the difference between Hartree-Fock and exact nonrelativistic energy), which are already small because they occur only indirectly (in higher order of perturbation theory), do not contain short-range contributions and are therefore likely to be negligible in many cases⁽⁴⁸⁾.

If it were not necessary to calculate all of the correlation energy at once, the problem would be much simpler. The essential motivation behind the idea of pair correlations is the goal of dividing the correlation energy into many small pieces, each of which may be computed separately. Ever since the 1916 manifesto of G.N. Lewis, chemists have found it useful to think of electronic structure in terms of electron pairs, imagined to be localized in space, separable, and transferable in many cases from molecule to molecule. One of the earliest version of an electron-pair theory is the "separated-pair" approximation introduced by Hurley et al⁽⁴⁹⁾.

One of the two related methods is usually employed in the theoretical evaluation of pair correlations. The first method is the many body perturbation theory (MBPT) of Brueckner^(50,51) and Goldstone⁽⁵²⁾, extended to atomic systems by Kelly⁽⁵³⁾. Kelly⁽⁵⁴⁻⁵⁶⁾ and Das and co-

workers⁽⁵⁷⁾ have shown MBPT to be a very powerful method for the treatment of a variety of problems involving electron correlation. However, MBPT makes extensive use of Feynman Diagrams, which most scientists are not familiar with, and for this reason we will not discuss MBPT here. The second method, usually called pair correlation theory and associated with the names Sinanoglu⁽⁵⁸⁾ and Nesbet⁽⁵⁹⁾ fits in nicely with our development of configuration interaction. The rather complicated and intensely debated relationship between MBPT and pair correlation theory has been discussed in detail by Freed^(60,61).

The Hartree-Fock approximation leaves out the instantaneous repulsion between pairs of electrons. Therefore it is reasonable to assume that most of the correlation energy can be accounted for by consideration of a set of functions describing in more detail the interaction between each pair of electrons. A particularly happy situation would arise if the pair correlation functions describing the different pairs of electrons were independent and their contributions to the correlation energy were additive.

In pair correlation approximations for closed shell systems one assumes that the energy E_c is given by⁽³⁰⁾

$$E_c = \sum_{ij} e(i,j) \quad \text{I.15}$$

In its usual form the pair correlation approximation summation in Equation I.15 goes over all the occupied spin-

orbitals ϕ_i in the RHF wavefunction. Each pair correlation energy, $e(i,j)$ is calculated independently. It is possible to make formal arguments as to why Equation I.15 should be approximately correct⁽³³⁾. Nonetheless, the pair correlation approximation is essentially intuitive, arising from our confidence in the orbital theory of electronic structure. As to its merits as a quantitative theory, these can only be determined by detailed calculations which make comparisons with accurate variational calculations and with experiment.

As a concrete example, consider the $1s$ ground state of the beryllium atom. The RHF wavefunction is of the form

$$\Psi_{\text{RHF}} = 1s\alpha 1s\beta 2s\alpha 2s\beta$$

For Be there are six pair correlation energies of the usual kind: $e(1s\alpha, 1s\beta)$, $e(1s\alpha, 2s\alpha)$, $e(1s\alpha, 2s\beta)$, $e(1s\beta, 2s\alpha)$, $e(1s\beta, 2s\beta)$ and $e(2s\alpha, 2s\beta)$. These pair correlation energies have been accurately evaluated by Nesbet⁽⁶²⁾ and his results are seen in Table I.1. It may be noted, as one might expect, that $e(1s\alpha, 2s\alpha) = e(1s\beta, 2s\beta)$ and $e(1s\alpha, 2s\beta) = e(1s\beta, 2s\alpha)$. The results of Table I.1 show many features in common with Bunge's⁽⁶³⁾ Be calculation. In particular, the $1s^2$ and $2s^2$ pair correlation are large and the contributions to the $1s2s$ correlations are small. Table I.1 also upholds a cherished belief among theoretical scientists that "electrons with the same spin (function) avoid each other". The pair correlation energy due to a $1s$ and a $2s$ orbital with α spin is 2.5 times less than that obtained when one of

the electrons being correlated is $1s\alpha$ and the other is $2s\beta$.

<u>Pair Correlation</u>	<u>Energy</u>
$e(1s\alpha, 1s\beta)$	0.04183
$e(1s\alpha, 2s\alpha)$	0.00081
$e(1s\alpha, 2s\beta)$	0.00212
$e(1s\beta, 2s\alpha)$	0.00212
$e(1s\beta, 2s\beta)$	0.00081
$e(2s\alpha, 2s\beta)$	0.04535

Table I.1 Spin-orbital pair correlation energies of Nesbet for the ground state of Be.

We have not yet mentioned how the spin-orbital pair correlation energies were obtained. It turns out that Nesbet calculated the $e(i,j)$'s using a CI approach in terms of Slater determinants⁽⁶²⁾. First a large set of s, p, d and f orbitals is chosen and an SCF calculation is carried out. Then to calculate, for example, $e(1s\alpha, 1s\beta)$, a CI is carried out including the SCF determinant plus all determinants of the type $2s\alpha 2s\beta xy$, where x and y are all the spin-orbitals besides $1s$ and $2s$ in the basis set. $e(1s\alpha, 1s\beta)$ is then just the difference between the energy of the above CI and the SCF energy. Put in another way, the $1s^2$ pair correlation energy $e(1s\alpha, 1s\beta)$ is just the energy lowering (below the SCF) due to Slater determinants which may be designed $1s\alpha 1s\beta \rightarrow xy$. Similarly $e(1s\alpha, 2s\alpha)$ is obtained by performing a CI including the SCF determinant plus all determinants $1s\beta 2s\beta xy$ which result from the replacement of the $1s\alpha$ and $2s\beta$ spin-orbitals from the SCF determinant. $e(1s\alpha, 2s\alpha)$ is just the difference between the above CI energy and the SCF energy.

The usefulness of the pair correlation idea depends on how well the approximation relation given by Equation I.15 holds. The sum of the six spin-orbital pair correlation energies in Table I.1 is 0.09304 hartrees. For comparison the "experimental" correlation energy of Be is 0.094 hartrees⁽³⁹⁾. The sum of the pairs is therefore 99% of the true correlation energy. Thus it appears that for beryllium the spin-orbital pair correlation approximation is in an excellent approximation. It should be pointed out that Nesbet's basis set is unavoidably less than complete, and a comparable calculation using a complete set of functions might yield 101% or 102% of the true correlation energy. In a variational calculation, of course, we can never obtain more than 100% of the correlation energy, since the calculated energy is a rigorous upper bound to the exact nonrelativistic energy.

There is at least one theoretical objection to the idea of spin-orbital pair correlations, in addition to the fact that the sum of the pairs is not an upper bound to the true correlation energy. This objection is that in many of the spin-orbital pair correlation CI calculations discussed above, the wavefunction obtained is not an exact eigenfunction of the symmetry operators L^2 and S^2 . For example, in the $(1s\alpha, 2s\beta)$ Be calculation, the determinants $1s\beta \ 2s\alpha \ 3s\alpha \ 4s\beta$ and $1s\beta \ 2s\alpha \ 3s\beta \ 4s\alpha$ would be included, corresponding to the excitation $1s\alpha \ 2s\beta \rightarrow 3s\alpha \ 4s\beta$ and $1s\alpha \ 2s\beta \rightarrow 3s\beta \ 4s\alpha$. In the $(1s\beta, 2s\alpha)$ beryllium calculation would be included the two determinants $1s\alpha 2s\beta 3s\alpha 4s\beta$ and $1s\alpha 2s\beta 3s\beta 4s\alpha$. Unfortunately, the simplest 1S configuration

which can be constructed from the orbital occupancy $1s2s3s4s$ includes all four of the above Slater determinants. Since the $(1s\alpha, 2s\beta)$ and $(1s\beta, 2s\alpha)$ calculations are completely independent, neither of the two wavefunctions will be 1S L-S eigenfunction.

The most general way of guaranteeing that each pair correlation wavefunction will be an exact eigenfunction of all the symmetry operators of the point group is to include in the same calculation all configurations arising from each particular orbital occupancy. For the Be atom, the $e(1s\alpha, 2s\alpha)$, $e(1s\alpha, 2s\beta)$, $e(1s\beta, 2s\alpha)$, $e(1s\beta, 2s\beta)$ calculation will no longer be independent but incorporated into a single pair correlation, the $(1s, 2s)$ symmetry-adapted pair correlation^(64, 65). Although there are four times as many Slater determinants in the symmetry-adapted $(1s, 2s)$ calculation, the size of the eigenvalue problem will not be four times as large as that required to evaluate $e(1s\alpha, 2s\alpha)$. This is because the symmetry-adapted pair calculations are carried out in terms of configurations, which are symmetrized linear combinations of determinants. For the $1s2s3s4s$ problem, only two linearly independent 1S eigenfunctions may be constructed from the six acceptable Slater determinants.

It is of course possible that the question of symmetry-adapted versus spin-orbital pairs is not of practical importance. For Be, the summation of the spin-orbital pair correlation energies was in close agreement with experimental correlation energy. To test the difference

between the two pair correlation schemes, a direct comparison, using the same basis set and the same Slater determinants, is needed. Such a comparative study has been made of Ne by Viers, et al⁽⁶⁵⁾.

CHAPTER 1.4

WAVEFUNCTION STRUCTURE

The Hartree-Fock (HF) formalism yields approximate solutions of the many-electron Hamiltonian. These solutions are in considerable error if we use them to predict many physically observable quantities. The two standard methods for improving on the HF wavefunction are (1) the Hylleraas⁽³⁻⁵⁾ approach where the interelectronic coordinates (r_{ij}) are explicitly included in the wavefunction and (2) that of configuration-interaction where the variational principle is applied to a trial wavefunction which is a linear combination of Slater determinants. (Hylleraas outlined a more approximate method for handling electron correlation effects within He. This involved the concept of singly-occupied "inner" and "outer" shells. Consequently, the independent-particle representation $(1s)^2$ becomes $(1s', 1s'')$, where $1s'$ and $1s''$ are different singly-occupied space orbitals associated with different spins. The splitting of the $(1s)^2$ configuration by using different orbitals for different spins naturally introduces some correlation effects into the total wavefunction and so lowers the energy of the system). Both methods increase in difficulty with increasing number of particles. This increase is most serious for the Hylleraas approach since the number of interelectronic coordinates increases quadratically with the number of particles while the number of independent one-

electron coordinates increases only linearly. When going from the HF wavefunction to more exact functions for systems of four or more electrons there often is a problem of orbital degeneracy along with that of the correlation problem. As we shall see the orbital degeneracy problem is important for the ground state of Be which in the case involves the near degeneracy of the Be 2s and 2p one-electron functions or orbitals. The method of configuration-interaction is the more appropriate way of handling the orbital degeneracy problem.

The Method of Configuration-Interaction

The configuration-interaction (CI) method is a straightforward application of the Ritz⁽⁶⁶⁾ method of linear variations to the calculation of electronic wavefunctions. It has been used for both atoms⁽³⁻⁵⁾ and molecules (either in terms of atomic orbitals⁽⁶⁷⁾, the valence bond method, or in terms of molecular orbitals⁽⁶⁸⁾ since the early days of quantum mechanics, but until electronic computers became available its application was mostly limited to very small systems or to semiempirical treatments. Some of the more ambitious precomputer CI calculations were carried out on the π -electron system of benzene (with some serious approximations) by Parr et al⁽⁶⁹⁾, on some atomic systems by Bernal and Boys⁽⁷⁰⁾ and by Boys^(71,72) and on the HF molecule by Kastler⁽⁷³⁾. The earliest CI calculation which employed an electronic computer were probably those of Meckler⁽⁷⁴⁾ on O₂ (using the computer only for the solution of the matrix eigenvalue problem), of Boys and Price⁽⁷⁵⁾ on

Cl, Cl⁻, S and S⁻ and of Boys et al⁽⁷⁶⁾ on BH, H₂O and H₃.

Two characteristics of the CI method make it particularly attractive and important. First, unlike methods which rely on more restricted forms of trial wavefunctions (such as self-consistent field, separated pairs etc), it is capable in principle of providing accurate solutions of the nonrelativistic, clamped nuclei Schrödinger equation. Second, it is a general method, applicable in principle to any stationary state of an atomic or molecular system. While the qualification "in principle" in the above statements is significant because of the slow convergence of the CI expansion and of difficulties in dealing with highly excited states, it should be seen in the context of the very rapid improvement in our capabilities for such calculations over the last two decades. Even if it is overoptimistic to expect the same rate of improvement in computer design, computational procedures and theoretical methods in the near future, it is safe to assume that over the long run the configuration-interaction method, or one of its variations, will become a standard practical tool for obtaining highly accurate answers to questions involving the electronic structure of small- and medium-size systems.

While the computational difficulties of the CI method are formidable, its conceptual simplicity and generality are very appealing. It results from the application of the variation principle to a trial function which is written as a linear combination of many predetermined terms, each of which is expressed in terms of products of one-electron

orbitals. These expansion terms are usually made to satisfy some or all of the boundary and symmetry conditions which apply to the desired final wavefunction. This can be done for open-shell states almost as easily as for closed-shell systems, for excited states almost as easily as for ground states, and far from equilibrium as easily as near the equilibrium geometry of the system. The very generality of the method can, however, be a disadvantage in some cases, particularly those involving highly excited states. Thus, for example, the restricted form of the SCF wavefunction makes it possible to use that method to obtain an approximate solution for a core-vacancy state, while it would be very difficult (or even impossible) to prevent a CI wavefunction for a stationary state embedded in a continuum from acquiring the character of lower states.

The self-consistent field (SCF) method has by now become fairly standardized, at least for closed-shell systems, and several "black box" programs are now available even for the casual user who does not want to learn much about the theory or its implementation. The situation is still far from realization for CI calculations. While very much has been learned in recent years about optimum procedures for various stages of the calculation, the size and complexity of the programs are considerable and many choices and decisions have to be made by the user.

Before proceeding a few words on the name of the method are in order. The term "configuration-interaction" dates from the early days of quantum mechanics, and was taken to

imply the cooperative effect of several electronics configurations of a system in stabilizing it, relative to the energy of a single configuration⁽⁷⁷⁾. As recently pointed out by Mulliken⁽⁷⁸⁾, it has often been argued that this name is not appropriate for the CI method as commonly practiced, and alternative terms, such as "superposition of configurations" (SOS) and "configuration mixing" (CM), have been proposed and used by various authors. The terms configuration-interaction, and particularly the abbreviation CI, are well entrenched, however, and will be used throughout this thesis.

The basic assumption is the existence of an expansion theorem

$$\psi(\underline{x}) = \sum_K c_K \phi_K(\underline{x}) \quad \text{I.16}$$

for every normalised function $\psi(\underline{x})$ of the space-spin coordinate $\underline{x} = (r, \sigma)$ of a single electron in terms of an orthogonal complete and discrete set $\{\phi_K(\underline{x})\}$ of one electron functions, or spin-orbitals. For a many electron Ψ , Löwdin applies the same theorem, one coordinate at a time⁽⁷⁹⁾. After introducing the antisymmetrizer (since electrons are fermions) he obtains:

$$\Psi(\underline{x}_1, \underline{x}_2, \dots, \underline{x}_N) = \sum_K c_K \Psi_K(\underline{x}_1, \underline{x}_2, \dots, \underline{x}_N) \quad \text{I.17}$$

where

$$\Psi_K(\underline{x}_1, \underline{x}_2, \dots, \underline{x}_N) = 1/\sqrt{N!} \det\{\psi_k, \psi_1, \psi_m, \dots\}$$

is a normalised Slater determinant K corresponding to an ordered configuration defined by the set $k < l < m \dots$

The expansion, given by Equation I.16, without any other symmetry restrictions other than to be antisymmetric with respect to exchange of any two space-spin coordinates, allowed Löwdin to treat the convergence problem from a most general point of view⁽⁷⁹⁻⁸¹⁾. He considered the first order density matrix $\Gamma(x'_1|x_1)$ given by

$$\begin{aligned} \Gamma(x'_1|x_1) &= N \int \psi^*(x'_1, x_2, \dots, x_N) \psi(x_1, x_2, \dots, x_N) dx_2 \dots dx_N \\ &= \sum_{kl} \psi_K^*(x'_1) \psi_l(x_1) g_{kl} \end{aligned}$$

and observed that the diagonal elements g_{kk} were given by

$$g_{kk} = \sum_K^{(k)} |c_K|^2$$

where K runs over all configurations containing the specific index k . Then, a new basis $\{X_k(x)\}$ was introduced so that the $\Gamma(x'_1|x_1)$ became diagonal. The X_k 's associated with the exact wavefunction were called natural spin-orbitals (NSO's). The most important configuration in a CI wavefunction based on natural orbitals is called the first natural configuration and is frequently very similar to the SCF wavefunction.

This result may appear to be of little value, since in

order to determine the NSO's it is necessary to calculate the density, which in turn requires a knowledge of the exact wavefunction. However, a number of workers have made use of this result by firstly performing an approximate CI calculation, determining approximate natural orbitals and then repeating the procedure but now using those NSO's of highest occupation number and augmenting the basis set with a number of new functions (the occupation number provides a useful index of the importance of each orbital). In particular, the noteworthy calculation of Bender and Davidson⁽⁸⁴⁾ on the LiH molecule, and the work of Watson⁽⁸²⁾, Bunge⁽⁶³⁾ and Olympia & Smith⁽⁸³⁾ whose work on atomic Be is the subject of the next part of this thesis.

CHAPTER I.5

REFERENCES

1. E. Schrodinger, *Ann. der Physik* 79, 361 (1926).
2. A. Messiah, *Quantum Mechanics* Vol 2 (Amsterdam, 1962).
3. E.A. Hylleraas, *Z. Physik* 48, 469 (1928).
4. E.A. Hylleraas, *Z. Physik* 45, 347 (1929).
5. E.A. Hylleraas, *Z. Physik* 65, 209 (1930).
6. H.M. James and A.S. Coolidge, *J. Chem. Phys.* 1, 825 (1933).
7. L.R. Henrich, *Astrophys. J.* 99, 59 (1944).
8. H.A.S. Eriksson, *Z. Physik* 109, 762 (1938).
9. T.D.H. Baber and H.R. Hasse, *Proc. Cambridge Phil. Soc.* 33, 253 (1937).
10. S. Chandrasekhar and G. Herzberg, *Phys. Rev.* 98, 1050 (1955).
11. E. Wigner, *Phys. Rev.* 46, 1002 (1934).
12. H.M James and A.S. Coolidge, *Phys. Rev.* 49, 688 (1936).
13. E.A. Burke, *Phys. Rev.* 130, 1871 (1963).
14. S. Larsson and E.A. Burke, *Phys. Rev.* 184, 248 (1969).
15. S. Larsson, *Phys. Rev.* 169, 49 (1968).
16. J.F. Perkins, *Phys. Rev.* A8, 700 (1973).
17. R.E. Watson, *Ann. Phys. NY* 13, 250 (1961).
18. A. Hibbert, *J. Phys. B: Atom. Molec. Phys.* 7, 1417 (1974).
19. D.R. Hartree, *Proc. Camb. Phil. Soc.* 24, 89 (1928).
20. D.R. Hartree, *Proc. Camb. Phil. Soc.* 24, 111 (1928).
21. V. Fock, *Z. Physik* 61, 126 (1930).
22. V. Fock, *Z. Physik* 62, 795 (1930).

23. R.K. Nesbet, Adv. Chem. Phys. 9, 321 (1965).
24. K.A. Brueckner, Phys. Rev. 97, 1353 (1955).
25. K.A. Brueckner, Phys. Rev. 100, 36 (1955).
26. J. Goldstone, Proc. R. Soc. A239, 267 (1957).
27. O. Sinanoglu, J. Chem. Phys. 33, 1212 (1960).
28. O. Sinanoglu, Phys. Rev. 122, 493 (1961).
29. O. Sinanoglu, Proc. Roy. Soc. A260, 379 (1961).
30. O. Sinanoglu, J. Chem. Phys. 36, 706 (1962).
31. O. Sinanoglu, J. Chem. Phys. 36, 3198 (1962).
32. O. Sinanoglu, Rev. Mod. Phys. 35, 517 (1963).
33. O. Sinanoglu, Advan. Chem. Phys. 6, 315 (1964).
34. O. Sinanoglu, Nucl. Instrum. Meth. 110, 193 (1970).
35. O. Sinanoglu and D.F. Tuan., J. Chem. Phys. 38, 1740 (1963).
36. O. Sinanoglu and K.A. Brueckner, Three Approaches to Electron Correlation in Atoms, (Yale University Press, 1970).
37. P.O. Lowdin, Advan. Chem. Phys. 2, 207 (1959).
38. E. Clementi, J. Chem. Phys. 38, 2248 (1963).
39. A. Veillard & E. Clementi, J. Chem. Phys. 49, 2415 (1968).
40. L.C. Snyder & H. Basch, J. Am. Chem. Soc. 91, 2189 (1969).
41. J.C. Slater, Quantum Theory of Molecules and Solids, Vol I and II (McGraw-Hill, New York, 1963).
42. A.C. Wahl, J. Chem. Phys. 41, 2600 (1964).
43. H.F. Schaefer, J. Chem. Phys. 41, 2207 (1971).
44. S. Rothenberg & H.F. Schaefer, Chem. Phys. Letters 10, 565 (1971).
45. R.F. Bacher & S. Goudsmit, Atomic Energy States (McGraw-Hill, 1932).
46. E.U. Condon and G.H. Shortley, The Theory of Atomic Spectra (Cambridge University Press, New York, 1951).
47. E.P. Wigner & F. Seitz, Phys. Rev. 46, 509 (1934).
48. N.R. Kestner & O. Sinanoglu, J. Chem. Phys. 45, 194

(1966).

49. A.C. Hurley, J.E. Lennard-Jones & J.A. Pople, Proc. Roy. Soc (London) A220, 446 (1953).
50. K.A. Brueckner, Phys. Rev. 97, 1353 (1955).
51. K.A. Brueckner, Phys. Rev. 100, 36 (1955).
52. J. Goldstone, Proc. R. Soc. A239, 267 (1957).
53. H.P. Kelly, Advan. Chem. Phys. 14, 129 (1969).
54. H.P. Kelly, Phys. Rev. 144, 39 (1966).
55. H.P. Kelly, Phys. Rev. 173, 142 (1968).
56. H.P. Kelly, Phys. Rev. 180, 55 (1969).
57. N.C. Dutta, C. Matsubara, R.T. Pu & T.P. Das, Phys. Rev. 177, 33 (1969).
58. O. Sinanoglu, Advan. Chem. Phys. 14, 237 (1969).
59. R.K. Nesbet, Advan. Chem. Phys. 14, 1 (1969).
60. K.F. Freed, Phys. Rev. 173, 1 (1968).
61. K.F. Freed, Ann. Rev. Phys. Chem. 21, 313 (1971).
62. R.K. Nesbet, Phys. Rev. 155, 51, 56 (1967).
63. C.F. Bunge, Phys. Rev. 168, 92 (1968).
64. H.F. Schaefer & F.E. Harris, Phys. Rev. 167, 67 (1968).
65. J.W. Viers, F.E. Harris & H.F. Schaefer, Phys. Rev. A1, 24 (1970).
66. W. Ritz, J. Reine Angew. Math. 135, 1 (1909).
67. S. Weinbaum, J. Chem. Phys. 1, 593 (1933).
68. H.M. James & A.S. Coolidge, J. Chem. Phys. 1, 825 (1933).
69. R.G. Parr, D.P. Craig & I.G. Ross, J. Chem. Phys. 18, 1561 (1950).
70. M.J.M. Bernal & S.F. Boys, Philos. Trans. R. Soc. London, Ser. A 245, 139 (1952).
71. S.F. Boys, Proc. R. Soc. London, Ser. A 217, 136 (1953).
72. S.F. Boys, Proc. R. Soc. London, Ser. A 217, 235 (1953).
73. D. Kastler, J. Chem. Phys. 50, 556 (1953).
74. A. Meckler, J. Chem. Phys. 21, 1750 (1953).

- 75 S.F. Boys & V.E. Price, Philos. Trans. R. Soc. London, Ser. A 246, 451 (1954).
- 76 S.F. Boys, G.B. Cook, C.M. Reeves & I. Shavitt, Nature 178, 1207 (1956).
- 77 E.U. Condon & G.H. Shortley, The Theory of Atomic Spectra, (Cambridge U.P., London, 1935).
- 78 R.S. Mulliken, Chem. Phys. Lett. 25, 305 (1974).
- 79 P.O. Löwdin, Phys. Rev. 97, 1474 (1955).
- 80 P.O. Löwdin, J. Phys. Chem. 61, 55 (1957).
- 81 P.O. Löwdin, Adv. Chem. Phys. 32, 328 (1960).
- 82 R.E. Watson, Phys. Rev. 119, 170 (1960).
- 83 P.L. Olympia & D.W. Smith, J. Chem. Phys. 52, 67 (1970).
- 84 C.F. Bender & E.R. Davidson, J. Phys. Chem. 70, 2675 (1966).

PART II

ELECTRON CORRELATION IN ATOMIC BERYLLIUM

CHAPTER II.1

INTRODUCTION

In a well-known review, McWeeny⁽¹⁾ wrote that 'one of the outstanding problems of quantum mechanics is the precise determination of the form of the correlation holes when strong interactions are admitted'. Since then, much has been done to elucidate the consequences of electron correlation in atoms and molecules examined in terms of the Coulomb hole $\Delta f(r_{12})$ ⁽²⁻¹³⁾. This quantity, defined by Coulson and Neilson⁽²⁾, is the difference between the correlated and the Hartree-Fock (HF) distribution functions for the interparticle separation r_{12} for electrons 1 and 2. However, such an analysis has generally been confined to two-electron systems⁽²⁻¹³⁾. In an endeavour to gain insight into correlation effects for specific electronic shells, within an N-electron system, Banyard and Mashat⁽¹⁴⁾ used the many-electron theory (MET), proposed by Sinanoglu⁽¹⁵⁻²⁴⁾, to partition the correlated two-particle density which, along with the partitioned form of the HF density, enable $\Delta f(r_{12})$ to be determined for each shell. In this way, Coulomb holes were evaluated for the intra- and inter-electronic shells within a series of Be-like ions, using the correlated wave-functions of Weiss⁽²⁵⁾ and the HF functions of Clementi⁽²⁶⁾.

The K-shell "holes" for the Be-like ions were found to be very similar to those obtained for the two-electron

series whereas, by comparison, the influence of correlation on the L-shells was quite striking. Of especial interest were the characteristics of the Coulomb holes for the $K\alpha_L\alpha$ - and $K\alpha_L\beta$ -shells. In particular, it was observed that the $K\alpha_L\alpha$ curves were inverted by comparison with the "holes" obtained by Boyd and Katriel⁽¹⁰⁾ for the 2^3S state of the He-like ions. Clearly, such findings could be dependent on the restrictions imposed by Weiss⁽²⁵⁾ when constructing his wavefunctions and, as a consequence, this observation stimulated the present analysis.

Thus, for the ground state of Be, an examination has been carried out into the inter- and intrashell correlation effects embodied in four configuration-interaction (CI) wavefunctions reported by Watson⁽²⁷⁾, Bunge⁽²⁸⁾, and Olympia and Smith⁽²⁹⁾. Two functions were taken from the work of Olympia and Smith. All four correlated functions possess the restricted HF wavefunction of Watson⁽²⁷⁾ as the leading configuration. The correlation effect is achieved by using an orthonormal basis set to form additional configurations involving various excitations from this HF reference state.

During recent years there has been an increasing interest in the study of the effects of electron correlation in momentum space⁽³⁰⁻⁵⁰⁾. R.J. Weiss⁽⁵¹⁾ was probably the first to enquire into the possible effects of correlation on momentum distributions by suggesting that they could account for the enhanced high momentum tail observed in the experimental Compton profiles. Such a conclusion could not be supported by the subsequent work of Benesch, Smith and

Brown⁽³⁰⁻³⁴⁾ but was substantiated by the recent work of Banyard and Moore⁽³⁹⁾. The work of Ahlberg and Lindner⁽³⁸⁾ analysed Fermi correlation, by calculating so-called correlation quotients, in the Be, Ne, Ar and Zn atoms; they concluded that the same rules govern Fermi correlation between electrons whether described in position space or in momentum space. The Coulomb correlation work of Banyard and Moore⁽³⁹⁾, on the iso-electronic series H^- , He and Li^+ , has subsequently been extended by Banyard and Reed⁽⁴⁰⁾ who have represented the Coulomb hole in momentum space for the same series. Following such analysis, we have presented, for the Be atom, a comparative study of electron correlation in momentum space invoking the properties of the momentum space equivalent of the Coulomb hole.

When forming the Coulomb hole in position space, the effects of radial and angular correlation are known to work in unison whereas, by contrast, in momentum space, these components yield characteristics which are in opposition^(39,40). Consequently, momentum space is a particularly useful, and sensitive, medium for highlighting the differences between the radial and angular components of correlation for both atoms and molecules. From the study of two-electron systems, it has been found that, by comparison with position space, such differences give rise to a relatively complicated structure for the Coulomb hole; thus, for momentum space, it is preferable to use the term 'shift' rather than 'hole' ⁽⁴⁰⁾.

Since position and momentum co-ordinates are conjugate quantities, our subsequent findings for Be in both position and momentum space should provide an overall view of correlation within the individual intra- and inter-electronic shells for this example of a many-electron atom.

CHAPTER II.2

SINANOGLU'S MANY ELECTRON THEORY

Though Coulomb repulsions are of long range and would be expected to add to the complications introduced by the finiteness of an N-body system, a number of theoretical developments have indicated that correlations in atoms and molecules may have simplifying features. A crucial question in these developments is how the complicated behaviour of N electrons all coupled together may be simplified into that of a few sub-problems⁽⁵²⁾. One such approach is that of Sinanoglu, whose method is outlined in this section.

The exact wavefunction of an N-electron closed shell or single determinantal state may be written as

$$\Psi(\underline{x}_1, \underline{x}_2, \dots, \underline{x}_N) = \phi_0 + X \quad \text{II.1}$$

such that

$$\langle \phi_0 | X \rangle = 0$$

and

$$\langle \phi_0 | \phi_0 \rangle = 1$$

and hence $\langle \phi_0 | \Psi \rangle = 1$. Where X represents the correlation relative to the N-electron orbital theory wavefunction ϕ_0 .

given by

$$\phi_0 = A(1,2,3,\dots,i,\dots,N) \quad \text{II.2}$$

with $i = i(\underline{x}_i)$ representing the i th spin-orbital and $\underline{x}_i = (\underline{r}_i, \sigma_i)$ are space and spin coordinates, A is the N particle antisymmetrizer.

The correlation part of the wavefunction, X , may be analysed into 1,2,3,..., etc up to N -electron effects⁽⁵²⁾. One then obtains

$$\begin{aligned} X = & \sum_{i=1}^N \{f_i\} + \sum_{i<j}^N \{U_{ij}\} + \sum_{i<j<k}^N \{U_{ijk}\} + \dots \\ & + \sum_{i<j<\dots<n} \{U_{ij\dots n}\} + \dots + \{U_{123\dots N}\} \end{aligned} \quad \text{II.3}$$

where $\{\}$ indicates antisymmetrization with the product of the remaining $(N - n)$ spin-orbitals. For example:

$$\{U_{ijk}\} = 1/3! A_N(1,2,3\dots N/ijk U_{ijk}) \quad \text{II.4}$$

The U 's are closed form "cluster" functions⁽²¹⁾ with the properties

$$U_{ij}(\underline{x}_i, \underline{x}_j) = - U_{ij}(\underline{x}_j, \underline{x}_i) \quad \text{II.5}$$

and strong orbital orthogonality,

$$\begin{aligned}
\langle f_i | \phi_k \rangle &= 0 \\
\langle U_{ij} | \phi_k \rangle &= 0 \\
\langle U_{ijk\dots N} | \phi_k \rangle &= 0
\end{aligned}
\tag{II.6}$$

for $k = 1, 2, 3, \dots, N$. In Equation II.6 it is an $(N - 1)$ electron function that is rigorously zero, ie,

$$\langle U_{ij\dots n} | \phi_k \rangle = \int_0^\infty U_{ij\dots n}^*(\underline{x}_1, \underline{x}_2, \dots, \underline{x}_n) \phi_k(\underline{x}_i) d\underline{x}_i = 0 \tag{II.7}$$

The form of Equations II.1 - II.6 is general for any $\phi_0 = A(1, 2, \dots, N)$ in Equation II.2 so long as these N spin-orbitals form an orthonormal set. A convenient and quite standard choice, however, is the Hartree-Fock (HF) ϕ_0 whereupon one has correlation in the traditional sense⁽⁵³⁾.

In Sinanoglu's Many Electron Theory (MET) (12, 13 & 32) the wavefunction is written, without approximation, in the following form:

$$\begin{aligned}
\Psi(\underline{x}_1, \underline{x}_2, \dots, \underline{x}_N) &= A\{(\phi_1(\underline{x}_1), \phi_2(\underline{x}_2), \dots, \phi_N(\underline{x}_N)) [1 + \\
&\sum_i^N f_i(\underline{x}_i) / \phi_i(\underline{x}_i) + 1/\sqrt{2}! \sum_{i < j}^N U_{ij}(\underline{x}_i, \underline{x}_j) / \phi_i(\underline{x}_i) \phi_j(\underline{x}_j) + \dots + \\
&1/\sqrt{N}! U_{12\dots N}(\underline{x}_1, \underline{x}_2, \dots, \underline{x}_N) / \phi_1(\underline{x}_1) \phi_2(\underline{x}_2) \dots \phi_N(\underline{x}_N)] \} \tag{II.8}
\end{aligned}$$

The $\phi_i(\underline{x}_i)$ are HF orbitals, so that the first term in this expansion corresponds to the HF approximation, the $f_i(\underline{x}_i)$ are known as orbital correction functions, the $U_{ij}(\underline{x}_i, \underline{x}_j)$ functions account for correlations between two electrons,

the $U_{ijk}(\underline{x}_i, \underline{x}_j, \underline{x}_k)$ functions account for correlation between three electrons, and so on for the higher terms.

Sinanoglu decomposed these various functions into a cluster expansion thus:

$$\begin{aligned}
 U_{ij} &= A_2(f_i f_j) + U'_{ij} \\
 U_{ijk} &= A_3(f_i f_j f_k + 1/2 f_i U'_{jk} + \dots) + U'_{ijk} \quad \text{II.9}
 \end{aligned}$$

where A_m is the usual m electron normalised antisymmetriser. The terms in brackets are referred to as unlinked clusters while the U_{ij} , U_{ijk} etc functions are referred to as linked clusters. Various considerations suggest that the linked clusters of three or more electrons may be ignored and that, from an energy viewpoint, the f functions are expected to be small. A good approximation to Equation II.1 is thus assumed to be the following 'unlinked-cluster' expansion:

$$\begin{aligned}
 \Psi(\underline{x}_1, \underline{x}_2, \dots, \underline{x}_N) &= A\{(\phi_1(\underline{x}_1), \phi_2(\underline{x}_2), \dots, \phi_N(\underline{x}_N)) [1 + \\
 &1/\sqrt{2}! \sum_{i < j}^N U_{ij}(\underline{x}_i, \underline{x}_j) / \phi_i(\underline{x}_i) \phi_j(\underline{x}_j) + \\
 &1/2 \sum_{\substack{i < j, k < l \\ i, j \neq k, l}}^N U_{ij} U_{kl} / \phi_i(\underline{x}_i) \phi_j(\underline{x}_j) \phi_k(\underline{x}_k) \phi_l(\underline{x}_l)] \} \quad \text{II.10}
 \end{aligned}$$

where the explicit functional dependence on electron coordinates has been omitted. This form so far appears satisfactory for the correlation energy of single determinantal states, the ground states of $1s^2 2s^n 2p^m$

atoms^(54,55), benzene⁽⁵⁶⁾, and possibly also the second-row atoms⁽⁵⁷⁾, and some diatomic and larger molecules⁽⁵⁸⁾.

The problem reduces to finding the orbital correction functions and the pair correlation functions which satisfy the orthogonality condition of Equation II.6.

The exact wavefunction, Equation II.8, for an N-electron atomic or molecular system may be rewritten in the following abbreviated form:

$$\Psi = A\{(\phi_1 \dots \phi_N) [1 + \sum_{i=1}^N f_i / \phi_i + 1/2! \sum_{i < j}^N U_{ij} / \phi_i \phi_j + \dots + U_{12\dots N} / \phi_1 \dots \phi_N]\} \quad \text{II.11}$$

where, with no loss of generality, all the cluster functions are assumed to satisfy the strong orthogonality requirement of Equation II.6. It is assumed in Equation II.11 that, before the antisymmetriser acts, the functions f_i and HF orbitals ϕ_i are functions of space-spin coordinates of electron i and a similar dependence on electron coordinates is implied for the cluster functions. Multiplication of Equation II.11 by the orbital product:

$$\prod_i (\underline{x}_1, \dots, \underline{x}_{i-1}, \underline{x}_{i+1}, \dots, \underline{x}_N) = \phi_1(\underline{x}_1) \dots \phi_{i-1}(\underline{x}_{i-1}) \phi_{i+1}(\underline{x}_{i+1}) \dots \phi_N(\underline{x}_N) \quad \text{II.12}$$

together with integration over the space-spin variables

$\underline{x}_1 \dots \underline{x}_{i-1} \underline{x}_{i+1} \dots \underline{x}_N$ results in the following expression:

$$\begin{aligned} & \langle \Psi(\underline{x}_1, \dots, \underline{x}_N) | \phi_1(\underline{x}_1) \dots \phi_{i-1}(\underline{x}_{i-1}) \phi_{i+1}(\underline{x}_{i+1}) \dots \phi_N(\underline{x}_N) \rangle \\ & = N [\phi_i(\underline{x}_i) + f_i(\underline{x}_i)] \end{aligned} \quad \text{II.13}$$

The constant, N , in Equation II.13 arises from the normalisation constant implicit in the antisymmetriser operator A . From Equation II.13 we obtain:

$$N = \langle \Psi(\underline{x}_1, \dots, \underline{x}_N) | \phi_1(\underline{x}_1) \dots \phi_N(\underline{x}_N) \rangle \quad \text{II.14}$$

hence

$$f_i(\underline{x}_i) = \langle \Psi | \Pi_i \rangle / \langle \Psi | \Pi \rangle - \phi_i(\underline{x}_i) \quad \text{II.15}$$

By means of a similar process, which Sinanoglu has called the method of successive partial orthogonalisations⁽²⁴⁾ (MSPO), we may obtain explicit formulae for the pair functions. Thus, multiplication of Equation II.11 by the orbital product $(\underline{x}_1, \dots, \underline{x}_{i-1}, \underline{x}_{i+1}, \dots, \underline{x}_{j-1}, \underline{x}_{j+1}, \dots, \underline{x}_N)$, which is equivalent to Π_i though with the omission of the orbital $\phi_j(\underline{x}_j)$, yields, after integration over the space-spin coordinates $\underline{x}_1 \dots \underline{x}_{i-1} \underline{x}_{i+1} \dots \underline{x}_{j-1} \underline{x}_{j+1} \dots \underline{x}_N$:

$$\begin{aligned} \langle \Psi | \Pi_{ij} \rangle = N [& \phi_i(\underline{x}_i) \phi_j(\underline{x}_j) - \phi_i(\underline{x}_j) \phi_j(\underline{x}_i) \\ & + \phi_i(\underline{x}_i) f_j(\underline{x}_j) - \phi_i(\underline{x}_j) f_j(\underline{x}_i) \\ & + f_i(\underline{x}_i) \phi_j(\underline{x}_j) - f_i(\underline{x}_j) \phi_j(\underline{x}_i) \\ & + 2U_{ij}(\underline{x}_i, \underline{x}_j)] \end{aligned} \quad \text{II.16}$$

Substitution of N from Equation II.14 gives the following relationship for the pair function $U_{ij}(\underline{x}_i, \underline{x}_j)$:

$$U_{ij}(\underline{x}_i, \underline{x}_j) = 1/\sqrt{2} [\langle \Psi | \Pi_{ij} \rangle / \langle \Psi | \Pi \rangle - \phi_i \phi_j + \phi_j \phi_i - f_i \phi_j + \phi_j f_i - \phi_i f_j + f_j \phi_i] \quad \text{II.17}$$

If required, an expression for the linked cluster pair U'_{ij} may be obtained from the cluster expansion given in Equation II.9. In Equation II.17 the complete orbital product $\phi_1 \dots \phi_N$ has been represented by the function Π and explicit dependence on electron coordinates is indicated by the ordering of the product functions, thus:

$$\phi_i \phi_j - \phi_j \phi_i = \phi_i(\underline{x}_i) \phi_j(\underline{x}_j) - \phi_i(\underline{x}_j) \phi_j(\underline{x}_i) \quad \text{II.18}$$

It is clear that this procedure may be extended to obtain explicit expressions for any of the cluster functions $U_{ij\dots k}$, or with the aid of Equation II.9 for any linked cluster $U'_{ij\dots k}$. Although the analysis given here has been for the exact wavefunction, it is obvious that with a knowledge of the Hartree-Fock orbitals $\phi_i(\underline{x}_i)$ we may apply this procedure to any approximate wavefunction and thereby analyse the various correlation effects which are implicitly contained in that wavefunction. By this procedure, we may separate correlation effects due to purely intrashell or intershell interactions, or we may, for example, extract such correlation functions as might reasonably be expected to remain constant, for use in semiempirical type calculations on related atoms or molecules.

CHAPTER II.3

THE PARTITIONING TECHNIQUE

Wavefunctions for atoms and molecules involve the coordinates and spins of all the electrons, and usually consist of large numbers of determinants constructed from orbitals which may in turn be linear combinations of basis functions containing various numerical parameters; they have also become more and more elaborate as computational facilities have improved. Consequently, the wavefunction itself gives us no clear and simple picture of the electron distribution and how it determines physical and chemical properties. If wavefunctions are to give any understanding of electronic structure, and any general means of relating different properties and comparing the merits of one description with those of another, we must try to extract in some way information about the physically essential features of the electron distribution. Since common atomic and molecular properties are expectation values of one- and two-particle operators, this information is in fact contained in a small number of density functions which are comparatively easy to visualize; of particular interest are the one- and two-particle densities. The one-particle density, for example, depends on the coordinates of a simple point in space, whereas the wavefunction itself depends on N sets of coordinates and spins in a multi-dimensional configuration space. The two-particle density, as defined

by McWeeny and Sutcliffe⁽⁵⁹⁾, may be written as:

$$\Gamma_2(\underline{x}_1, \underline{x}_2) = N(N-1) \int \Psi(\underline{x}_1, \underline{x}_2, \dots, \underline{x}_N) \Psi^*(\underline{x}_1, \underline{x}_2, \dots, \underline{x}_N) d\underline{x}_3 \dots d\underline{x}_N. \quad \text{II.19}$$

The two-particle density, and along with the one-particle counterpart, contains all the information required to formulate many of the properties of an N-electron system.

Investigations into electron correlation have extensively used both the one- and two-particle densities for the evaluation of expectation values and other functions depending upon two particle interactions. These studies have mainly concentrated on the two-electron systems of H^- , He and particular two-electron ions⁽⁶⁻¹⁰⁾. However, once we leave the simpler problem of two electron wavefunctions the two-particle density contains terms which are associated with intra- and intershell electron correlation effects. It need not be clear in many wavefunctions which effect is which; for instance, if the wavefunction is constructed from a set of non-orthogonal functions all terms of the wavefunction contribute, to a greater or lesser extent, to the various intra- and intershell correlation effects. Banyard and Mashat⁽¹⁴⁾ proposed that the two-particle density may be partitioned into pairwise components yielding the intra- and intershell effects of interest, thus:

$$\Gamma_2(\underline{x}_1, \underline{x}_2) \approx \sum_{i < j}^N \Gamma_{ij}(\underline{x}_1, \underline{x}_2) \quad \text{II.20}$$

The (i,j) labels refer to the occupied normalized spin-orbitals ϕ in the restricted HF description. The (i,j) pairs (1,2) and (3,4), for example, reference, respectively, the K-shell and L-shell intrashell contributions to the total two-particle density. Other combinations of (i,j) will reference the various intershell effects, for example, the pairing (1,3) references the KL intershell effect of (3S) symmetry for any 'atomic' two-particle density. The total number of combinations will, of course, depend on the the value of N. For N=3 there are only 3 combinations of (i,j) pairings, that is, (1,2), (1,3) and (2,3). For N=4 there are 6 unique pairings; N=5 there are 10 and so on for higher N values. The total number of pairings for any N is given the expression $N!/(2(N-2)!)$.

Given a complex wavefunction for any system, the influence of electron correlation on the charge distribution can be assessed in terms of the changes which occur in the distribution function $f(r_{12})$, for the inter-electronic separation r_{12} , when compared with the corresponding HF distribution. Such a distribution has been defined by Coulson and Neilson⁽²⁾, and its representation associated with the spin-orbital pair (i,j) is given by:

$$f_{ij}(r_{12}) = \int \Gamma_{ij}(\underline{x}_1, \underline{x}_2) d\underline{x}_1 d\underline{x}_2 / dr_{12} \quad \text{II.21}$$

The integrations for electrons 1 and 2 are performed over spin and all space coordinates except r_{12} .

For the Hartree-Fock two-particle density, the partitioning into pairwise components (i,j) is both exact and straightforward, yielding:

$$\Gamma_{\text{HF}}(\underline{x}_1, \underline{x}_2) = \frac{1}{2} \sum_{i < j}^N \{ [\phi_i(\underline{x}_1)\phi_j(\underline{x}_2) - \phi_j(\underline{x}_1)\phi_i(\underline{x}_2)]^* [\phi_i(\underline{x}_1)\phi_j(\underline{x}_2) - \phi_j(\underline{x}_1)\phi_i(\underline{x}_2)] \} \quad \text{II.22}$$

where, for example, ϕ_i is the *i*th occupied normalised HF spinorbital. The partitioning of $\Gamma_{\text{corr}}(\underline{x}_1, \underline{x}_2)$, the two-particle density associated with any correlated wavefunction, however, is approximate and the method used for the partitioning will now be outlined.

For a closed-shell system we may write the correlated wavefunction as:

$$\Psi(\underline{x}_1, \underline{x}_2, \dots, \underline{x}_N) = A\{(\phi_1(\underline{x}_1), \phi_2(\underline{x}_2), \dots, \phi_N(\underline{x}_N)) [1 + \sum_i^N f_i(\underline{x}_i)/\phi_i(\underline{x}_i) + 1/\sqrt{2}! \sum_{i < j}^N U_{ij}(\underline{x}_i, \underline{x}_j)/\phi_i(\underline{x}_i)\phi_j(\underline{x}_j) + \dots + 1/\sqrt{N}! U_{12\dots N}(\underline{x}_1, \underline{x}_2, \dots, \underline{x}_N)/\phi_1(\underline{x}_1)\phi_2(\underline{x}_2)\dots\phi_N(\underline{x}_N)] \}. \quad \text{II.23}$$

The Hartree-Fock approximation leaves out the instantaneous repulsion between pairs of electrons. Therefore it is reasonable to assume that most of the correlation energy can be accounted for by considering functions that describe in more detail the interactions between each pair of electrons. Thus Equation II.23 may be rewritten in an approximate form to include terms upto and including the pair function U_{ij} as:

$$\Psi \approx A\pi \left[1 + \sum_i^N f_i(\underline{x}_i)/\phi_i(\underline{x}_i) + 1/\sqrt{2}! \sum_{i < j}^N U_{ij}(\underline{x}_i, \underline{x}_j)/\phi_i(\underline{x}_i)\phi_j(\underline{x}_j) \right] \quad \text{II.24}$$

where π is the product of all occupied HF spin-orbitals. A is an N -particle antisymmetrizer such that $A\pi$ represents the normalized N -particle HF wavefunction, the properties of the f_i and U_{ij} functions have been discussed earlier. Equation II.24 may be factorised yielding

$$\begin{aligned} \Psi = & \sum_{i < j}^N \{ (\phi_i(\underline{x}_1)\phi_j(\underline{x}_2) - \phi_j(\underline{x}_1)\phi_i(\underline{x}_2))(-1)^P A' \pi_{ij} \\ & + [(f_i(\underline{x}_1)\phi_j(\underline{x}_2) - \phi_j(\underline{x}_1)f_i(\underline{x}_2)) \\ & + (\phi_i(\underline{x}_1)f_j(\underline{x}_2) - f_j(\underline{x}_1)\phi_i(\underline{x}_2))](-1)^P A' \pi_{ij} \\ & + 2/\sqrt{2}! U_{ij}(\underline{x}_1, \underline{x}_2)(-1)^P A' \pi_{ij} \\ & + (\phi_i(\underline{x}_1)\phi_j(\underline{x}_2) - \phi_j(\underline{x}_1)\phi_i(\underline{x}_2)) (-1)^P A' f_k \pi_{ijk} \\ & + 1/\sqrt{2} (\phi_i(\underline{x}_1)\phi_j(\underline{x}_2) - \phi_j(\underline{x}_1)\phi_i(\underline{x}_2))(-1)^P A' U_{kl} \pi_{ijkl} \\ & + 1/\sqrt{2} (-1)^P \bar{A} U_{ij} \pi_{ij} \} . \quad \text{II.25} \end{aligned}$$

A' is an $(N-2)$ -particle antisymmetrizer and permutes the electron coordinate combination $(\underline{x}_3, \underline{x}_4, \dots, \underline{x}_N)$ with the associated $(N-2)$ spin-functions. \bar{A} is an N -particle antisymmetrizer with the exclusion of the combination $(\underline{x}_1, \underline{x}_2, \underline{x}_3, \dots, \underline{x}_N)$ and $(\underline{x}_2, \underline{x}_1, \underline{x}_3, \dots, \underline{x}_N)$. These combinations are represented by the term $2/\sqrt{2} U_{ij}(\underline{x}_1, \underline{x}_2)(-1)^P A' \pi_{ij}$ of Equation II.25. In this analysis, π_{ij} represents the

product of all occupied HF spin orbitals except $\phi_i(\underline{x}_1)$ and $\phi_j(\underline{x}_2)$ and, owing to the antisymmetrizer A in Equation II.23, the remaining (N-2) electron coordinates can be arranged arbitrarily among the available (N-2) spin-orbitals.

Upon expansion of the pair function $U_{ij}(\underline{x}_1, \underline{x}_2)$ in Equation II.25 we obtain

$$\begin{aligned} \Psi = & \sum_{i < j}^N \langle \Psi | \Pi_{ij} \rangle / \langle \Psi | \Pi \rangle (-1)^P A' \Pi_{ij} \\ & + (\phi_i \phi_j - \phi_j \phi_i) (-1)^P A' (f_k \Pi_{ijk} + 1/\sqrt{2} U_{kl} \Pi_{ijkl}) \\ & + 1/\sqrt{2} (-1)^P \bar{A} U_{ij} \Pi_{ij} \end{aligned} \quad \text{II.26}$$

The integrations in $\langle \Psi | \Pi_{ij} \rangle$ are over all the coordinates occurring in Π_{ij} and thus we obtain a function of \underline{x}_1 and \underline{x}_2 only. The dependence on electron coordinates is to be taken as

$$\phi_i \phi_j - \phi_j \phi_i = \phi_i(\underline{x}_1) \phi_j(\underline{x}_2) - \phi_j(\underline{x}_1) \phi_i(\underline{x}_2)$$

For simplicity we introduce the following short hand notation

$$\begin{aligned} \text{term 1} & = \langle \Psi | \Pi_{ij} \rangle / \langle \Psi | \Pi \rangle (-1)^P A' \Pi_{ij} , \\ \text{term 2} & = (\phi_i \phi_j - \phi_j \phi_i) (-1)^P A' (f_k \Pi_{ijk}) , \\ \text{term 3} & = (\phi_i \phi_j - \phi_j \phi_i) (-1)^P 1/\sqrt{2} A' (U_{kl} \Pi_{ijkl}) , \\ \text{and term 4} & = 1/\sqrt{2} (-1)^P \bar{A} U_{ij} \Pi_{ij} . \end{aligned}$$

Thus, the evaluation of the two-particle density, which may be written in a partitionable form, reduces to the following integral:

$$\langle \text{term 1} + \dots + \text{term 4} | \text{term 1} + \dots + \text{term 4} \rangle_{3,4,\dots,N} \quad \text{II.27}$$

where the integral $\langle \dots | \dots \rangle_{3,4,\dots,N}$ is to be interpreted as

$$\langle \dots | \dots \rangle_{3,4,\dots,N} = \int \dots dx_3 dx_4 \dots dx_N .$$

The resulting overlaps may be summarised in the following table.

	term 1	term 2	term 3	term 4
term 1	R1	Ø	Ø	Ø
term 2	Ø	R2	Ø	R3
term 3	Ø	Ø	R4	Ø
term 4	Ø	R3	Ø	R5

The non-zero results R1, R2, R3 and R4 are given by:

$$R1 = \langle \Psi | \Pi_{ij} \rangle^* \cdot \langle \Psi | \Pi_{ij} \rangle / \langle \Psi | \Pi \rangle^2 ,$$

$$R2 = 2(\phi_i \phi_j - \phi_j \phi_i)^2 \langle f_k | f_k \rangle - 4(\phi_i \phi_k - \phi_k \phi_i)(\phi_j \phi_k - \phi_k \phi_j) \langle f_i | f_j \rangle ,$$

$$R3 = 8/\sqrt{2} (\phi_i \phi_j - \phi_j \phi_i) A_{12} (-f_k^{ij} \phi_k + f_k^{ik} \phi_j + f_k^{kj} \phi_i) ,$$

$$R4 = 2A' (\langle U_{ij} | U_{ij} \rangle_{s k k} \phi_i \phi_j + 4 \langle U_{ik} | U_{kj} \rangle_{s i j} \phi_i \phi_j) ,$$

$$\text{and } R5 = 2(\phi_i \phi_j - \phi_j \phi_i) \left\{ \sum_{s < t}^N (\phi_s \phi_t - \phi_t \phi_s) \sum_{(g < h)}^N \sum_{(p < q)}^N \langle U_{gh} | U_{pq} \rangle \right\} .$$

≠ i, j ≠ s, t

Overlaps of zero value will occur in the above table as a consequence of the orthogonality conditions presented in Equation II.6. Thus, combining the non-zero results we obtain the partitioned form of a general two-particle density for the correlated description of the N-electron closed shell system.

$$\begin{aligned}
 \Gamma_{\text{corr}}(\underline{x}_1, \underline{x}_2) &= \sum_{i < j}^N \sum_{k=i, j}^N C'_{ij} [\langle \Psi | \Pi_{ij} \rangle^* \cdot \langle \Psi | \Pi_{ij} \rangle / \langle \Psi | \Pi \rangle^2 \\
 &+ 8/\sqrt{2} (\phi_i \phi_j - \phi_j \phi_i) A_{12} (- f_k^{ij} \phi_k + f_k^{ik} \phi_j + f_k^{kj} \phi_i) \\
 &+ 2 A'_{12} (\langle U_{ij} | U_{ij} \rangle \phi_s \phi_k + 4 \langle U_{ik} | U_{kj} \rangle \phi_s \phi_i) \\
 &+ 2 (\phi_i \phi_j - \phi_j \phi_i) \{ \sum_{s < t}^N (\phi_s \phi_t - \phi_t \phi_s) \sum_{\substack{g < h \\ \neq i, j}}^N \sum_{\substack{p < q \\ \neq s, t}}^N \langle U_{gh} | U_{pq} \rangle \} \\
 &+ 2 (\phi_i \phi_j - \phi_j \phi_i)^2 \langle f_k | f_k \rangle \\
 &- 4 (\phi_i \phi_k - \phi_k \phi_i) (\phi_j \phi_k - \phi_k \phi_j) \langle f_i | f_j \rangle
 \end{aligned} \tag{II.28}$$

The constant C'_{ij} has been introduced to ensure, as in Equation II.22, that the individual densities for each pair (i,j) are normalised to unity. The summations over g and h each span all the spin-orbital labels except i and j, with the restriction that $g < h$; corresponding restrictions hold for the ranges of p and q. For compactness, we have introduced the following antisymmetrizers for the electronic coordinates

$$A_{12} \equiv \underline{x}_1 \underline{x}_2 - \underline{x}_2 \underline{x}_1 \tag{II.29}$$

and

$$A'_{12} = \underline{x}_1 \underline{x}_2 \underline{x}_2 \underline{x}_1 - \underline{x}_2 \underline{x}_2 \underline{x}_1 \underline{x}_1 - \underline{x}_1 \underline{x}_1 \underline{x}_2 \underline{x}_2 + \underline{x}_2 \underline{x}_1 \underline{x}_2 \underline{x}_1. \quad \text{II.30}$$

In addition, the abbreviated notation for terms like $f_{k\phi_k}^{ij}$ and the single integration $\langle U_{ij} | U_{ij} \rangle_s$, for example, are to be interpreted as

$$f_{k\phi_k}^{ij} = \left(\int U_{ij}(\underline{x}_a, \underline{x}_r) f_k(\underline{x}_r) d\underline{x}_r \right) \phi_k(\underline{x}_b) \quad \text{II.31}$$

and

$$\langle U_{ij} | U_{ij} \rangle_s = \int U_{ij}^*(\underline{x}_a, \underline{x}_r) U_{ij}(\underline{x}_b, \underline{x}_r) d\underline{x}_r, \quad \text{II.32}$$

where a and b are chosen according to the prescription given by A_{12} and A'_{12} , respectively. Finally, the dependence on electron coordinates for the remaining terms in Equation I.28 is to be taken as

$$U_{ij} = U_{ij}(\underline{x}_1, \underline{x}_2) \quad \text{II.33}$$

and

$$\phi_i \phi_j - \phi_j \phi_i = \phi_i(\underline{x}_1) \phi_j(\underline{x}_2) - \phi_j(\underline{x}_1) \phi_i(\underline{x}_2). \quad \text{II.34}$$

In passing, we note that if we multiply Equation II.25 by the HF product $A\Pi$ and integrate over the electron coordinates, as prescribed by Equation II.19, we obtain

$$\langle \Psi | A\Pi \rangle = \langle \text{term 1} + \dots + \text{term 4} | A\Pi \rangle_{3,4,\dots,N}, \quad \text{II.35}$$

where the notation used in Equation II.35 has been defined earlier. Equation II.35 is an approximate two-particle density, Γ'_{corr} , which may be partitioned into the various intra- and intershell effects. Evaluating the integral in Equation II.35 we obtain

$$\Gamma'_{\text{corr}}(\underline{x}_1, \underline{x}_2) = \sum_{i < j}^N [\langle \Psi | \Pi_{ij} \rangle^* / \langle \Psi | \Pi \rangle (\phi_i \phi_j - \phi_j \phi_i) + (\phi_i \phi_j - \phi_j \phi_i)^* (\phi_i \phi_j - \phi_j \phi_i)] \quad \text{II.36}$$

which is the original approach of Banyard and Mashat⁽¹⁴⁾.

CHAPTER II.4

WAVEFUNCTIONS

For the ground state of Be we have taken, as the correlated description, the wavefunctions of Bunge⁽²⁸⁾, Watson⁽²⁷⁾ and Olympia and Smith⁽²⁹⁾. The function of Bunge consisted of 180 orthogonal configuration constructed from a set of 7s, 7p and 4d basis functions. Olympia and Smith extended the work of Bunge in their density matrix study of atomic ground states. They produced three wavefunctions and the two functions with the best energy have been included in this investigation. In particular, their 85 configuration-wavefunction represents an almost full CI expansion over a limited basis set of 4s, 2p and 1d. To qualify the term 'almost' these authors omitted the unimportant d^4 configuration. The work of Bunge⁽²⁸⁾ was based on the earlier work of Watson⁽²⁷⁾ whose wavefunction is considered here for completeness. Watson's CI calculation involved 37 selected configurations and included the HF function. Approximately ninety percent of the correlation energy was incorporated into the final wavefunction using an extensive basis set consisting of 6s, 5p, 4d, 3f and 3g functions. A summary of the construction of all wavefunctions investigated may be found in Tables II.3 and II.4.

The most sophisticated and rapidly convergent configuration-interaction wavefunctions reported in the

literature for first-row atoms are those obtained by Bunge and coworkers^(28,60-62). These calculations introduce a number of new theoretical ideas and shed considerable light on the nature of electron correlation in many-electron systems. The Bunge calculations make use of natural orbital concepts, but in a somewhat different manner than either pseudonatural orbitals (PSNO) or iterative natural orbitals⁽⁶³⁾ methods. The calculation on the ground state of beryllium illustrates the approach taken⁽²⁸⁾. The first step is a self-consistent-field calculation, carried out using a large basis set of Slater functions. Then a calculation is carried out including the RHF configuration $1s\alpha 1s\beta 2s\alpha 2s\beta$ plus all configurations whose orbital occupancies may be specified $x_i x_j (2s)^2$ and $(1s)^2 x_i x_j$ where x_i and x_j are all orbitals in the basis set except the SCF orbitals $1s$ and $2s$. After the expansion coefficients are obtained for this CI wavefunction, the density matrix is set up and diagonalized, yielding a set of natural orbitals.

The above procedure corresponds to obtaining a set of orbitals to describe both the $(1s)^2$ and $(2s)^2$ correlation. Bunge in fact finds that the natural orbitals with the highest occupation number are quite similar to either the $(1s)^2$ or $(2s)^2$ PSNO's. The advantage in finding these natural orbitals from a single calculation is that the optimum orbitals for correlating $(1s)^2$ and $(2s)^2$ are determined in the presence of each other.

Using the natural orbitals thus obtained, Bunge proceeds to carry out a CI calculation designed to account for as

much of the correlation energy as possible. An exhaustive search is carried out, using perturbation theory as well as numerous trial variational calculations, to determine which configurations should be included in the final wavefunction. Eventually a 180 configuration wavefunction, constructed from 1492 Slater determinants, was decided upon⁽²⁸⁾. The variational energy of this wavefunction is -14.6642 hartrees, which may be compared to the estimated RHF energy -14.5730 and the estimated nonrelativistic exact energy -14.6664 hartrees. It may be seen that 98% of the correlation energy of Be has been obtained⁽²⁸⁾.

All singly-excited configurations have zero H matrix elements with the SCF configuration for the closed shell $1s^2$ ground state of beryllium. Therefore these configurations can only contribute to the final wavefunction by way of interaction with doubly- and triply-excited configurations. Bunge finds for Be that single excitations lower the energy by only -0.00058 hartrees, or 0.6% of the calculated correlation energy. Triple excitations are found to lower the energy by 0.00025 hartrees and quadruple excitations by 0.00352 hartrees. The latter two numbers correspond to 0.3% and 3.8% of the calculated correlation energy. Perhaps the most important aspect of the Bunge calculation is the unequivocal demonstration of the relative unimportance (4.1% of the correlation energy) of configurations differing by more than two orbitals from the SCF wavefunction, a fact supporting the negligible three particle, and four particle etc., interactions and hence a justification for truncating Equation II.23 after the pair function term U_{ij} .

If triple and quadruple excitations had turned out to be important, the quantitative calculation of the correlation energy would be extremely difficult. This is because of the very large number of triple- and quadruple-excited configurations.

The double excitations for $1s$ Be are of three types: (a) the two $1s$ SCF orbitals are replaced, (b) the two $2s$ SCF orbitals are replaced, and (c) one of the $1s$ and one of the $2s$ orbitals are replaced. Double excitations of type (c) are the most difficult to deal with since an orbital occupancy of the type $1s2s x_i x_j$ will give rise to two linearly independent $1s$ configurations. Table II.1 shows the most important configurations of each type in the Be wavefunction of Bunge⁽²⁸⁾.

After the SCF the most important configuration is the $(1s)^2(2p)^2$ or $(2s)^2 \rightarrow (2p)^2$ in the excitation notation. The importance of this configuration is well known and it has been called the degeneracy effect⁽²⁷⁾ since the $2s$ and $2p$ orbitals are degenerate in the hydrogenic approximation. The $1s2s$ expansion converges the slowest since the natural orbitals were determined for the $(1s)^2$ and $(2s)^2$ pairs. Were it possible to rigorously divide the correlation energy into contributions from the $(1s)^2$, $(2s)^2$ and $1s2s$ pairs, Bunge estimates that these contributions would be 0.0426, 0.0455 and 0.0053 hartrees.

The exact restricted Hartree-Fock wavefunction for Be may be obtained using a basis set consisting only of s orbitals. However, Table II.1 shows clearly that p and d orbitals must be included to obtain a significant fraction of the correlation energy. Bunge has also estimated the effect of f and g orbitals on the correlation energy of Be and these estimates are seen in Table II.2. As one goes across the first row of the periodic table to larger atoms it has been shown by a variety of calculations^(60-62,64-66) that the effects of higher spherical harmonics become more important. On the basis of accurate calculations, such as that discussed above, Bunge and coworkers have estimated the effects of g,h,i,... for the ground states of carbon and neon to be 3% and 8% of the correlation energy. Since it is very difficult to include even g orbitals in atomic calculations Bunge's estimates show clearly that the quantitative calculation of correlation energies for atoms larger than neon may be nearly intractable within an orbital framework.

CHAPTER II.5

INTRODUCTION TO POSITION SPACE

Electron correlation can be examined in terms of the Coulomb hole $\Delta f(r_{12})^{(2)}$, however, such an analysis has generally been confined to two-electron systems⁽²⁻¹⁰⁾. Banyard and Mashat⁽¹⁴⁾ used the many-electron theory (MET) of Sinanoglu⁽¹⁵⁻²⁴⁾ to partition the two-particle density, required for the evaluation of $\Delta f(r_{12})$, calculated from a four-electron wave function. Their partitioning technique was carried out to within certain approximations to include terms up to and including the pair-correlation functions, as shown by Equation II.36. They performed a comparative analysis of a series of Be-like ions using the wavefunctions of Weiss⁽²⁵⁾ and the HF functions of Clementi⁽²⁶⁾.

The partitioning of the two-particle densities for the four electron ions gave K-shell characteristics which were close to those obtained for the He-like series when described by either explicitly correlated (EC) or configuration-interaction (CI) wavefunctions^(6,7). For the L-shells, Banyard and Mashat found Coulomb holes of similar shape to the K-shell curves but they were greatly enhanced in magnitude. The inverted nature of the Coulomb holes calculated for the intershell distribution $K\alpha L\alpha$ were in direct conflict with those evaluated by Boyd and Katriel⁽¹⁰⁾ for the 2^3S state of the He-like ions. It has been

suggested⁽⁶⁷⁾ that the Weiss wavefunctions for the Be-like series may possess K-shell descriptions which are somewhat less reliable than those used for the He-like ions. Consequently, the work contained in this part of this thesis has been to compare their observations for Be with the results of a corresponding analysis of other highly correlated wavefunctions and, in the process, one could then establish whether the intershell behavior was acceptable or not. An examination has been performed into the inter- and intrashell correlation effects embodied in four configuration-interaction (CI) wavefunctions reported by Watson⁽²⁷⁾, Bunge⁽²⁸⁾, and two functions of Olympia and Smith⁽²⁹⁾. In addition to calculating the Coulomb holes $\Delta f(r_{12})$, also determined were the partial 'holes' $\Delta g(r_{12}, r_1)$, as defined by Boyd and Coulson⁽⁸⁾.

Due to the relative sophistication of the wavefunctions studied it was thought advisable to use the complete partitioning technique for the two-particle correlated density as described by Equation II.28; which has been evaluated to include all cross-product terms up to and including the pair-correlation terms U_{ij} . A limited comparison has been made between these results and those obtained for the Bunge⁽²⁸⁾ wavefunction when partitioned according to the original, and more limited, approach used by Banyard and Mashat.

The four CI wavefunctions analyzed here each possess the restricted HF wavefunction of Watson⁽²⁷⁾ as the leading configuration. The correlation effect is achieved by using

an orthonormal basis set to form additional configurations involving various excitations from this HF reference state. Thus, to assist the discussion, Tables I.3 and I.4 not only include the total energies E but also quoted, for each shell, are the number of single- and double-excitation terms used in the construction of the wavefunction and, in addition, we also present a summary of their composition.

The complexity represented by the partitioned two-particle density was eased by defining the present Coulomb and partial Coulomb holes for Be with respect to the HF wavefunction of Watson. Pilot calculations indicate that differences due to changing from the Clementi⁽²⁶⁾ to the Watson⁽²⁷⁾ HF function were negligible. Ideally, it would have been desirable to include in our analysis of Be the 650-term CI wavefunction of Bunge⁽⁶⁸⁾ but the added labour and the required computer time proved to be prohibitive.

CHAPTER II.6

RESULTS AND CALCULATIONS FOR POSITION SPACE

The $f(r_{12})$ and $g(r_{12}, r_1)$ distributions

Correlation effects obviously have their most marked influence on two-electron properties. One may define a function $f_{ij}(r_{12})$ ^(2,69) giving the normalised distribution for the interelectronic distance r_{12} , associated with the spin-orbital pair (i,j) , according to the definition

$$f_{ij}(r_{12}) = \int \Gamma_{ij}(\underline{r}_1, \underline{r}_2) d\underline{r}_1 \cdot d\underline{r}_2 / dr_{12} \quad \text{II.37}$$

where r_{12} is the difference $|\underline{r}_1 - \underline{r}_2|$. $\Gamma_{ij}(\underline{r}_1, \underline{r}_2)$ is evaluated from $\Gamma_{ij}(\underline{x}_1, \underline{x}_2)$ by integrating over the spin coordinates. The details concerning the evaluation of $f(r_{12})$ is discussed in Ref. 70 Appendix A.2. Following the definition of Coulson and Neilson⁽²⁾, the Coulomb hole is evaluated from the expression

$$\Delta f(r_{12}) = f_{\text{corr}}(r_{12}) - f_{\text{HF}}(r_{12}) \quad \text{II.38}$$

where $f(r_{12})$ is derived, respectively, at correlated and HF level.

The intra- and intershell Coulomb holes are shown in Figures II.1, II.2 and II.3. The sum total of these holes,

for each correlated description, is given in Figure II.4 and the total Coulomb hole is compared with its individual components for the Bunge wavefunction only in Figure II.5.

In addition to calculating the Coulomb holes we have obtained insight into the shape of the $f(r_{12})$ curves by evaluating the expectation values

$$\langle r_{12}^n \rangle = \int f(r_{12}) r_{12}^n dr_{12} \quad \text{II.39}$$

for $n = -1, 1$ and 2 . Clearly, different regions of the $f(r_{12})$ curve will be emphasised by the function r_{12}^n for each value of n .

Since the $\Delta f(r_{12})$ curves are obtained from averaged distributions it is of interest to investigate the shape of the Coulomb hole when electron 1, say, has a specific position. Thus, following the procedure of Boyd and Coulson⁽⁸⁾ we have evaluated partial Coulomb holes $\Delta g(r_{12}, r_1)$ such that:

$$\begin{aligned} \int \Delta g(r_{12}, r_1) dr_1 &= \int [g_{\text{corr}}(r_{12}, r_1) - g_{\text{HF}}(r_{12}, r_1)] dr_1 \\ &= \Delta f(r_{12}) \end{aligned} \quad \text{II.40}$$

Again, details of the evaluation of the $g(r_{12}, r_1)$ function are presented in Ref. 70 Appendix A.2.

For the Bunge wavefunction only, the partial Coulomb holes $\Delta g(r_{12}, r_1)$ have been evaluate for each shell and the

results are displayed in Figure II.6.

Two-particle expectation values

An assessment of the effects of electron correlation on the partitioned two-particle density can be further assisted by calculating the expectation values:

$$\langle \underline{r}_1 \cdot \underline{r}_2 / r_1^n r_2^n \rangle = \int (\underline{r}_1 \cdot \underline{r}_2 / r_1^n r_2^n) \Gamma_{ij}(\underline{r}_1, \underline{r}_2) d\underline{r}_1 d\underline{r}_2 \quad \text{II.41}$$

for $n = 0, 1$ and 2 . Each of these expectation values involve the angle γ_{12} between the position vectors \underline{r}_1 and \underline{r}_2 of electrons 1 and 2, and is therefore particularly sensitive to angular correlation. The expectation value corresponding to $n=1$ is $\langle \cos \gamma_{12} \rangle$ which is the average of the cosine of the angle between \underline{r}_1 and \underline{r}_2 and, therefore, reflects only the influence of angular correlation.

The radial density, $D(r_1, r_2)$, defined by

$$D(r_1, r_2) = \int \Gamma_{ij}(\underline{r}_1, \underline{r}_2) r_1^2 r_2^2 \sin \theta_1 \sin \theta_2 d\theta_1 d\theta_2 d\phi_1 d\phi_2 \quad \text{II.42}$$

and normalised such that

$$\int D(r_1, r_2) dr_1 dr_2 = 1$$

is particularly sensitive to radial correlation thus to aid the discussion we have evaluated the radial expectation values

$$\langle r_1^n r_2^n \rangle = \iint r_1^n r_2^n D(r_1, r_2) dr_1 dr_2 \quad \text{II.43}$$

for $n = -1$ and 1 .

One-particle expectation values

We can study the effects of correlation in different regions of the one-particle distribution by calculating the expectation values defined by

$$\langle r_1^n \rangle = \int r_1^n d(r_1) r_1^2 dr_1 \quad \text{II.44}$$

where $d(r_1)$ represents the one-particle distribution function defined by

$$d(r_1) = \int D(r_1, r_2) r_2^2 dr_2$$

The expectation values have been evaluated for $n = -2, -1, 1$ and 2 .

Standard Deviation

A useful concept in assessing the spread of the various distribution functions about their means is the standard deviation defined by

$$\Delta(z) = \sqrt{[\langle z^2 \rangle - \langle z \rangle^2]} \quad \text{II.45}$$

Where z is a general coordinate. We have calculated this quantity for the $f(r_{12})$ and $d(r_1)$ distributions.

Selected one- and two-particle expectation values and standard deviations are given in Tables II.5 to II.9. γ_r presented in Table II.9 is the percentage of each $f_{HF}(r_{12})$ density which has been redistributed due to correlation. For reference, all tables include the expectation values derived from the Watson HF function.

Correlation Coefficients

Statistical correlation coefficients were first applied to the analysis of electron correlation by Kutzelnigg, Del Re and Berthier⁽⁷¹⁾ who suggested that they may be used in assessing the global effects of electron correlation in atoms and molecules. These coefficients are based on the concepts of probability theory and mathematical statistics and have already been introduced in the present context by Banyard and Moore⁽³⁹⁾. For our two-electron shells we evaluated the radial coefficients

$$\tau_{\text{radial}} = [\langle r_1^n r_2^n \rangle - \langle r_1^n \rangle^2] / [\langle r_1^2 \rangle - \langle r_1 \rangle^2] \quad \text{II.46}$$

n taking the values of +1 and -1 and the angular coefficients

$$\tau_{\text{angular}} = \langle \underline{r}_1 / r_1^n \cdot \underline{r}_2 / r_2^n \rangle / \langle r_1^{2(1-n)} \rangle \quad \text{II.47}$$

n having the allowed value of 0, 1, and 2. The special case when $n = 0$ for the angular coefficients yields $\tau_{\gamma} = \langle \cos \gamma_{12} \rangle$ where γ_{12} is the angle between the electronic vectors \underline{r}_1 and

τ_2 . This selection of τ enables us to emphasize different regions of the two-particle density when assessing either radial or angular effects. We also note that each τ is bounded between +1 and -1. For consistency, we follow the definition of the Coulomb hole and formed $\Delta\tau = \tau_{\text{corr}} - \tau_{\text{HF}}$. The results are presented in Tables II.10 and II.11 for all four CI wavefunctions.

CHAPTER II.7

DISCUSSION: POSITION SPACE

From Table II.3 and II.4 it is seen that the wavefunction due to Bunge is not only the best energetically but, not surprisingly, it is also the most complex in its description of each shell. The E values in Table II.3 also indicate that the correlated wavefunctions fall into two groups: the Bunge⁽²⁸⁾ (B) and 95-term Olympia and Smith⁽²⁹⁾ (OS95) functions followed by the Watson⁽²⁷⁾ (W) and 85-term Olympia and Smith⁽²⁹⁾ (OS85) descriptions. The Weiss⁽²⁵⁾ wavefunction for Be, analysed by Banyard and Mashat⁽¹⁴⁾, has an energy of -14.66090au and therefore lies between these two groups. However, since the Weiss configurations were constructed from a non-orthogonal basis set, his 55-term wavefunction does not lend itself to a summary in the form of Table II.4; nevertheless, the truncated natural expansion of the Weiss wavefunction presented by Barnett, Linderberg and Shull⁽⁶⁷⁾ should provide a useful comparison in this context. As a preliminary to our main discussion, we note that the HF expectation values in Tables II.5, II.6, II.7 and II.8 are in excellent accord with those derived previously from the HF wavefunction of Clementi.

Figure II.1 reveals a high degree of correspondence between the K-shell Coulomb holes derived from the B and OS95 functions. By comparison, the Watson curve is seen to

be slightly too compact and the OS85 function yields a K-shell hole which is too diffuse. The cross-over points for the B and OS95 functions are almost coincident with the value obtained from the earlier analysis and, like the Weiss result, both curves show a strong similarity with the Coulomb hole for $\text{Be}^{++(6)}$. In Figure II.2 the L-shell holes for the B and OS95 wavefunctions are coincident and, along with the Watson curve, their cross-over points are comparable with that of the Weiss curve. Relative to the Bunge curve, the Watson L-shell hole is somewhat too shallow whereas the OS85 function produces a hole which is not only too deep but is, once again, too diffuse. A comparison between the L-shell effect and that for the K-shell can be obtained in terms of the percentage of each $f_{\text{HF}}(r_{12})$ -density which has been redistributed due to correlation: these results - labelled γ_r - are given in Table II.9. For the four wavefunctions analysed here, the L-shell percentages are about 6.5 times those for the K-shell, an exception is the L-shell for the OS85 function. Note also the comparison of these γ_r -values with those derived from the previous $\Delta f(r_{12})$ -curves obtained from the first-order partitioning of the Weiss wavefunction.

For the W wavefunction, Barnett, Linderberg and Shull⁽⁶⁷⁾ suggested that a deficiency appeared to exist in the description of the outer-shell p-character, thus influencing angular correlation. However, inspection of Table II.4 indicates that, for the L-shell of Watson, a greater inadequacy may exist when describing radial correlation: this is confirmed by the correlation

coefficients in Tables II.10 and II.11 where the consequences are seen to be quite marked for $\Delta\tau_r$ and $\Delta\tau_{1/r}$. The OS85 wavefunction is, with the exclusion of the configuration d^4 , a complete CI expansion over a small basis set. Therefore, the over diffuseness in both shells must be associated with an imbalance between the radial and angular components of correlation due to the restricted number of basis orbitals.

For the L-shell, correlation causes a significant contraction in the one- and two-particle radial density distributions. This is illustrated in Tables II.5, II.6, and II.7 for all wavefunctions by the changes in $\langle r^n \rangle$, $\langle r_1^{-1} r_2^{-1} \rangle$ and $\langle r_1 r_2 \rangle$. Such radial contractions are only compatible with the sizeable increase in the inter-particle separation, see Table II.8, because of the 2s - 2p near-degeneracy in the Be which produces a large angular correlation effect. The magnitude of the angular separation for each shell can be judged by inspection of $\Delta\tau_\gamma$, $\Delta\tau_\gamma$, and $\Delta\tau_\gamma$ in Table II.11 and, as seen, the L-shell coefficients are by far the largest.

The intershell Coulomb holes shown in Figure II.3 for the B and OS95 wavefunctions and the similarity between these curves is quite impressive. The intershell curves for the two remaining CI wavefunctions were, by comparison, small (less than 8% of the Bunge values) and are contracted towards the origin. A measure of each $\Delta f(r_{12})$ is provided by the values of Y_r in Table II.9. In passing we note that, for the B and OS95 wavefunctions, the Y_r values for the

intershells are comparable with those for the K-shell. Figure II.3 reveals that the $3s$ curves are of the same shape as the $K\alpha$ hole derived previously from the Weiss function. Although the maxima and minima of the $3s$ curves are about 14% larger than those of the Weiss curve, the cross-over values of $r_{12} = 2.91$ and 2.95 are only slightly smaller than the $K\alpha$ result of 3.08 . Like the Weiss result, these $3s$ intershell curves are inverted by comparison with the 2^3s holes obtained by Boyd and Katriel⁽¹⁰⁾ for the He-like ions. Nevertheless, at small r_{12} , each Be curve follows the He-like trend by being vanishingly small, a feature which arises from the influence of Fermi correlation on $f_{\text{corr}}(r_{12})$ and $f_{\text{HF}}(r_{12})$. By contrast, we note that the $1s$ curves in Figure II.3 possess a structure very similar to that reported by Boyd and Coulson⁽⁸⁾ for the 2^1s hole in He. Although not strictly comparable, the $1s$ curves are also seen to be of the same shape as the $K\alpha$ Weiss curve and their final cross-over point at $r_{12} = 3.00$ is remarkably close to the Weiss result of 3.13 . Therefore, it would appear that the intershell characteristics contained in the Weiss Be-like wavefunctions are indeed quite reliable.

To rationalise the shape of the intershell curves we recall that, for Be, the pair-correlation energies for the K- and L-shells are about seven times larger than those for the intershells^(72,73), thus illustrating the dominance of intrashell correlation. In addition, it is noted from Table II.6 that, for the K-shell, correlation produces only a marginal expansion of the radial density whereas, for the L-shell, a significant contraction occurs as discussed

above. That correlation has brought the K- and L-shells closer together implies that, at large r_{12} , the interparticle distribution function $f(r_{12})$ for each intershell should decrease relative to the HF values. At small r_{12} , the interpenetration of the the L-shell into the K-shell region will provide the major contribution to the evaluation of $f(r_{12})$. Thus, for the $1s$ intershell, we would expect that $\Delta f(r_{12})$ may be of conventional Coulomb hole shape when $r_{12} < 1$ say, this r_{12} value being comparable with the extent of $\Delta f(r_{12})$ for the K-shell. By contrast, as already mentioned, the Fermi effect is operative at small r_{12} for the $3s$ case and, consequently, this will obviate the need for Coulomb correlation. For both intershells, the effect at large r_{12} should be greater than at small r_{12} since a large interparticle separation can, of course, span the distance between the K- and L-shell regions of maximum density. Finally, the requirement that each $\Delta f(r_{12})$ curve should integrate to zero implies the existence of a maximum at intermediate r_{12} for both $1s$ and $3s$. The magnitude and extent of the characteristics outlined above are clearly dependent on the quality of the intershell pair descriptions contained in the correlated wavefunction. Consequently, only the B and OS95 wavefunctions produce $\Delta f(r_{12})$ curves with such features. That the $3s$ intershell curves for the Be-like ions should be different from the 2^3s Coulomb holes for the two-electron systems is now clear since the correlation effect within the excited state of a He-like ion is not constrained by the presence of any intrashell effects.

The total holes in Figure II.4 fall into two quite different pairs with the similarity between the B and OS95 wavefunctions being very good. In marked contrast with the previous Coulomb holes for $\text{Be}^{(14,74)}$, these two functions produce some well-defined structure which is directly attributable to the improved description of the two intershells. This is substantiated by a comparison with the component curves in Figure II.5 for the Bunge wavefunction. The $1s$ and $3s$ contributions also cause a significant reduction in the size of the L-shell maximum. The W and OS85 functions yield total holes which appear reasonable within the K-shell region but elsewhere Figure II.4 shows that these curves are too exaggerated and, as expected, they possess no intershell features. A relative measure of the four total holes is provided by the corresponding Y_r -values in Table II.9. That the major differences between the two sets of Coulomb holes in Figure I.4 are due to the inadequate descriptions of the intershell correlation effects in the W and OS85 functions can be illustrated as follows. If, when forming total holes for the W and OS85 functions, one replaced their $1s$ and $3s$ contributions by those derived from either the B or OS95 functions (see Figure II.3), then the resulting curves would be found to be comparable in shape and magnitude with the total holes shown in Figure II.4 for the B and OS95 functions. We note that the $\text{KL}(3s)$ contribution has to be multiplied by 3 when evaluating the total Coulomb hole.

Having discussed the changes in the distribution functions for the interparticle separation, let us now make

a brief comment about the individual $f(r_{12})$ -distributions. The spread or diffuseness of $f(r_{12})$ about the mean value $\langle r_{12} \rangle$ is measured by the magnitude of Δr_{12} . Table II.8 shows that, for each shell, the correlated value of Δr_{12} derived from either the B or OS95 wavefunction is less than the corresponding HF result. This indicates that the introduction of electron correlation has caused each $f(r_{12})$ -distribution to sharpen-up around its $\langle r_{12} \rangle$ value. However, when comparing the Δr_{12} values for the whole atom (determined from the total $f(r_{12})$ -distributions) we observe that the correlated results are now larger than the HF value. This contrast between the behaviour of the total distributions and that for their component parts arises from the varying effect of correlation of $\langle r_{12} \rangle$ for the individual electronic shells. Because correlation produces a large increase in $\langle r_{12} \rangle$ for the L-shell but causes a small decrease in $\langle r_{12} \rangle$ for both intershells, for example, it immediately suggests that the correlated description of the total $f(r_{12})$ -distribution will be more diffuse about the mean than its HF counterpart. This behaviour of the $f(r_{12})$ -distributions, illustrated by the results in Table II.8, also occurs for the Be-like ions⁽¹⁴⁾ when described by the correlated wavefunctions of Weiss⁽²⁵⁾.

The partial Coulomb holes $\Delta g(r_{12}, r_1)$ are shown in Figure II.6 evaluated for the Bunge wavefunction. For the K- and L-shells they are of conventional 'Coulomb hole' shape for all locations r_1 of the test electron. The K-shell diagram shows that the largest hole occurs when $r_1 \approx 0.5 \langle r_1 \rangle_K$ whereas, for the L-shell, the surface is not only

more extensive but the greatest effect, which is considerably larger than that for the K-shell, occurs at $r_1 \approx \langle r_1 \rangle_L$. The structure of each intershell surface is comparatively complicated, although the inverted nature of the 'holes' is immediately apparent in both cases. The $1s$ surface, presented in Figure II.6(C), shows structure at small r_1 and r_{12} which is directly attributable to the penetration of the L-shell electron into the K-shell region. The integrated effect is clearly shown in Figure II.3 as a small Coulomb hole effect at small r_{12} . The Fermi effect forbids such a penetration hence this effect is absent on the intershell $3s$ surface shown in Figure II.6(D) and the integrated effect shown in Figure II.3. Both intershell surfaces show two distinct features one which is located parallel to the r_{12} axis and the other arranged about the $r_1 = r_{12}$ diagonal. Each structure can be attributed to locating the test electron either in the K-shell or the L-shell, indeed, the maximum effects are located at either $r_1 \approx \langle r_1 \rangle_K$ or $r_1 \approx \langle r_1 \rangle_L$. The diagonal structure is associated with the test electron being located in the L-shell; the other electron having a higher probability of being located in the K-shell gives an r_{12} value of approximately equal to the test electron distance of r_1 . As r_1 changes so does r_{12} , this type of correlation is statistically referred to as 'harmony-correlation'. For the parallel structure the reverse is true; the test electron is now located in the very tightly bound K-shell, the other electron has now a higher probability of being located in the L-shell and any variation in r_1 will have little effect on the inter-particle separation r_{12} . In this particular

case the variables r_1 and r_{12} are, statistically, referred to as being 'uncorrelated'. Further discussion concerning the definition and interpretation of these statistical correlation terms will be reserved until Part IV of this thesis.

To examine the sensitivity of our $\Delta f(r_{12})$ -curves with respect to the partitioning technique, we calculated the Coulomb holes for the Bunge wavefunction using the first order analysis of Banyard and Mashat⁽¹⁴⁾. The K-shell curve was essentially unchanged to within graphical accuracy and, as indicated by the crosses in Figure II.3, the changes for the intershells are not large. The greatest effect occurred for the L-shell. The crosses in Figure II.2 show that retaining only first-order terms in the correlated density gives rise to $\Delta f(r_{12})$ -values which are too large when compared with the previous Bunge curve. Extending the partitioning of $\Gamma_{\text{corr}}(\underline{x}_1, \underline{x}_2)$ to the present level of analysis but adding only those contributions involving the $(s_1^2 p_1^2)$ -configuration reduced the magnitude of the L-shell hole and made it virtually coincident with the solid curve. Graphical coincidence was also achieved for the intershell curves. This not only re-emphasizes the importance of the 2s-2p near degeneracy effect but also suggests that part of the difference between the Bunge and Weiss L-shell curves will, in this instance, be due to the level of partitioning for $\Gamma_{\text{corr}}(\underline{x}_1, \underline{x}_2)$.

The changes in τ provide a global measure of electron correlation since each coefficient involves expectation

values based on both the one- and two-particle densities. A common scale for each τ allows inter-comparisons to be made. Tables II.10 and II.11 shows that an overall similarity exists between the $\Delta\tau$ for the B and OS95 wavefunctions. For the K-shells, we observe that $\Delta\tau_r$ and $\Delta\tau_\gamma$ are of roughly comparable magnitude but, for the L-shells, the angular effect is seen to be at least three times larger than $\Delta\tau_r$. We note that the Watson L-shell values for $\Delta\tau_{1/r}$ and $\Delta\tau_r$ are exceedingly small thus indicating a lack of radial correlation; by contrast, the angular coefficients are of a more reasonable magnitude. This is understandable by inspection of Table II.4 where it is seen that the correlation configurations listed for the L-shell of Watson are of angular form. For the intershells, the $\Delta\tau$ values are found to be more varied; in particular, we observe that for the B and OS95 functions $\Delta\tau_{1/r}$ and $\Delta\tau_r$ are now of opposite sign. The positive value of $\Delta\tau_{1/r}$ arise from an increase in $\langle r_1^{-1} r_2^{-1} \rangle$, thus indicating that correlation causes a contraction in the inner regions of the intershell two-particle radial density. However, from an angular viewpoint, the signs of $\Delta\tau_\gamma$, $\Delta\tau_\gamma$, and $\Delta\tau_\gamma$ imply an increase in interparticle separation; an exception is the W-function this being due to an inadequacy in the number of correlation configurations. The net effect of correlation on $\langle r_{12} \rangle$ for the intershells in the wavefunctions can be seen from Table II.8.

CHAPTER II.8

INTRODUCTION TO MOMENTUM SPACE

During the last decade the study of electron momentum distributions in atoms and molecules has received renewed attention. Knowledge and analysis of these distributions should give information about electron-nuclear and electron-electron interactions. It is these interactions in particular which dictate the chemical and physical properties of the species and the study of electron momentum distributions should be a useful technique by which we may investigate the nature of, for example, the chemical bond. Although the momentum distribution of an electronic system can be measured in a variety of ways, the first employed the inelastic photon-electron interaction or, as it is more commonly known, the Compton effect. It has been recent experimental developments in this technique⁽⁷⁵⁻⁷⁷⁾ that have stimulated a renewed interest in the theoretical determination of momentum distributions and, as a consequence, molecular physicists and theoretical chemists are beginning to recognise the importance of such calculations in describing electronic systems. In particular, the influence of electron correlation on the Compton profile and on the associated one-particle momentum distribution⁽³⁹⁾.

Earlier⁽⁷⁸⁾ we examined and compared the intra- and intershell correlation effects in position space for the ground state of Be when described by several configuration-interaction (CI) wavefunctions⁽²⁷⁻²⁹⁾. The analysis was performed by determining Coulomb holes⁽²⁾ and various expectation values for each electronic shell. The expectation values were used to calculate several statistical correlation coefficients τ , which were of special interest when assessing the angular and radial components of electron correlation in the intrashells. The description of an individual shell, at both a correlated and Hartree-Fock (HF) level, was obtained by partitioning the second-order density for the total system into its pairwise components. To achieve such partitioning we neglected the three- and four-particle correlation terms in the many-body representation⁽⁵²⁾ of the correlated wavefunction. Variations in the importance of correlation throughout different regions of position space were studied by means of partial holes. We now present a parallel investigation for Be carried out in momentum space.

When forming the Coulomb hole in position space, the effects of radial and angular correlation are known to work in unison whereas, by contrast, in momentum space, these components yield characteristics which are in opposition⁽³⁹⁾. Consequently, momentum space is a particularly useful and sensitive medium for highlighting the differences between the radial and angular components of correlation for both atoms and molecules. In a study of some two-electron systems⁽⁴⁰⁾, it has been found that, by

comparison with position space, such differences give rise to a relatively complicated structure for the Coulomb hole; thus, for momentum space, it is preferable to use the term 'shift' rather than 'hole'⁽⁴⁰⁾. At small momenta, the behaviour of a partial Coulomb shift allows us to examine the influence of correlation on the motion of the valence electrons. This will be especially relevant in consideration of molecular formation.

For Be(¹s), the Coulomb shift and the changes in τ in momentum space reported here are derived from the CI wavefunctions reported earlier⁽²⁷⁻²⁹⁾. In each instance, the HF reference state for Be is taken, as before, from the work of Watson⁽²⁷⁾. The partitioned two-particle densities in momentum space for the K(¹s), L(¹s), KL(¹s) and KL(³s) shells were obtained by applying the Dirac transformation procedure⁽⁷⁹⁾ to the primitive spin-orbitals in position space used to represent each Be wavefunction. The definition of the Coulomb shift is completely analogous to that discussed by Coulson and Neilson in position space. The Coulomb shift $\Delta f(p_{12})$ is the change, due to correlation, in the distribution function $f(p_{12})$ for a given magnitude of the momentum difference $p_{12} = |p_1 - p_2|$ between electrons 1 and 2. Since position and momentum co-ordinates are conjugate quantities, the present results, taken together with our earlier findings, will provide an overall view of correlation within the individual intra- and inter-electronic shells for this example of a many-electron atom.

Let us now examine in more detail the theoretical determination of momentum distributions and also the limitations of any theoretical model. Bearing in mind that the momentum density is simply the modulus of the momentum-space wavefunction squared, one may formally consider the problem as one of evaluating the electronic wavefunction, not in the usual position space representation, but in the momentum-space representation. There are two fundamentally different approaches to this calculation; one is to formulate the Schrödinger equation directly in terms of the electronic momenta:

$$\frac{p^2}{2m} \chi(p) + [V(p) - E]\chi(p) = 0 \quad \text{II.48}$$

Here $\chi(p)$ is the wavefunction in the momentum representation and $V(p)$ is the Fourier transform of the potential energy $V(r)$. Thus, the Schrödinger equation is transformed from a differential equation in position space to an integral equation in momentum space and, for this reason, evaluation of the momentum-space wavefunction by this method has received very little attention. In fact, the most successful workers to use this procedure are McWeeny and Coulson^(80,81) who manage to solve the equation iteratively and obtained approximate wavefunctions for the helium atom and the hydrogen molecule. However, the computational difficulties that arise rendered their approach impracticable for larger systems.

Fortunately, there is an alternative approach by which a wavefunction in momentum representation may be obtained.

The position space wavefunction may be converted into momentum representation via a simple transformation which is associated with the name Dirac⁽⁷⁹⁾. Because of the abundance of position-space wavefunctions already available, this approach has enjoyed considerably more success than the direct approach. Podolsky and Pauling⁽⁸²⁾ were among the first to use this procedure by calculating the momentum functions from hydrogenic orbitals. The attractive feature of the Dirac transform is that it is isomorphic, that is, it preserves the original wavefunction. Overlap and other integrals are also preserved by the transformation.

Dirac has shown that the Fourier transform

$$\chi(\underline{P}, \sigma) = \int e^{-i\underline{P} \cdot \underline{R}} \psi(\underline{R}, \underline{\sigma}) d\underline{R} \quad \text{II.49}$$

is the bridge between the position- and momentum-space representation of the N-electron wavefunction. Here \underline{P} , \underline{R} and $\underline{\sigma}$ stand for the the collection of momentum coordinates (p_1, p_2, \dots, p_N) , position coordinates (r_1, r_2, \dots, r_N) and spin coordinates $(\sigma_1, \sigma_2, \dots, \sigma_N)$ respectively. The element of volume $d\underline{R}$ is $(dr_1, dr_2, \dots, dr_N)$. In the case of a wavefunction $\psi(\underline{R}, \underline{\sigma})$ which is expanded in terms of Slater determinants⁽⁸³⁾ over a set of position-space spin-orbitals, the transformation of each individual orbital leads to $\chi(\underline{P}, \underline{\sigma})$ expressed as the same expansion of Slater determinants but over the transformed set of spin-orbitals.

CHAPTER II.9

RESULTS AND CALCULATIONS FOR MOMENTUM SPACE

Using the notation of Bunge⁽²⁸⁾, the Be wavefunctions are formed from primitive spin-orbitals in position space of the type

$$N_{jl} r^{(nj+1)} e^{-Zjlr} Y_{l,m}(\theta_r, \varphi_r) \epsilon_{ms}(\sigma_s) \quad \text{II.50}$$

Combining II.49 and II.50 we obtain

$$\chi(p) = \int N_{jl} r^{(nj+1)} e^{-Zjlr} e^{-i\mathbf{p}\cdot\mathbf{r}} Y_{l,m}(\theta_r, \varphi_r) d\mathbf{r} \quad \text{II.51}$$

where spin has been omitted for convenience. Using the expansion of a plane wave in terms of spherical harmonics and Bessel functions⁽⁸⁴⁾:

$$e^{-i\mathbf{p}\cdot\mathbf{r}} = \sqrt{(2\pi/pr)} \sum_{l=0}^{\infty} (2l+1)/2 i^{-l} J_{l+1/2}(pr) P_l(\cos\theta_{pr}) \quad \text{II.52}$$

where

$$P_l(\cos\theta_{pr}) = 4\pi/(2l+1) \sum_{m=-l}^l Y_{lm}^*(\theta_r, \varphi_r) Y_{lm}(\theta_p, \varphi_p) \quad \text{II.53}$$

and integrating over all angles we obtain

$$\chi(p) = N_{j1} (p)^{-1/2} Y_{lm}(\theta_p, \phi_p) i^l \int_0^\infty r^{n_j+1+3/2} e^{-Z_{j1}r} J_{l+1/2}(pr) dr \quad \text{II.54}$$

The solution of Equation II.54 is evaluated by repeated differentiation of the appropriate integration formula for Hankel transforms given in Ref. 85 where by we then obtain

$$\chi(p) = N_{j1} \frac{(-1)^{n+1}}{\sqrt{\pi}} \frac{(2p)^{l+1/2}}{\sqrt{p}} i^{-l} l! \frac{\partial^{n+1}}{\partial z_{j1}^{n+1}} \left[\frac{1}{[z_{j1}^2 + p^2]^{l+1}} \right] \quad \text{II.55}$$

as the momentum-space representation of the Be orbitals.

Coulomb Shifts and Partial Coulomb Shifts

The Coulomb shift associated with the HF spin-orbital pair (i,j) is given by

$$\Delta f_{ij}(p_{12}) = \int \Delta \Gamma_{ij}(p_1, p_2) dp_1 dp_2 / dp_{12} \quad \text{II.56}$$

where the limits of integration are analogous to those discussed by Coulson and Neilson⁽²⁾ in position space; spin has been integrated out of Equation II.56. $\Delta f_{ij}(p_{12})$ is the change, due to correlation, in the distribution function $f_{ij}(p_{12})$ for a given magnitude of the momentum difference $p_{12} = |p_1 - p_2|$ between electrons 1 and 2 and $\Delta \Gamma_{ij}(p_1, p_2)$ is the change in the partitioned two-particle density after transformation into momentum space. Each $f_{ij}(p_{12})$ is

normalized to unity. The Coulomb shifts $\Delta f(p_{12})$ vs p_{12} for the intra- and intershells of Be are shown in Figures II.7 to II.10. The sum total shifts for the various correlated wavefunctions are presented in Figure II.11 and, following the position space investigation, Figure II.12 shows the individual curves for each shell compared with the total shift for the Bunge wavefunction, only.

The partial Coulomb shift $\Delta g_{ij}(p_{12}, p_1)$ measures the influence of correlation when a test electron, say electron 1, has a momentum of a given magnitude p_1 . These shifts are defined such that

$$\int \Delta g_{ij}(p_{12}, p_1) dp_1 = \Delta f_{ij}(p_{12}) \quad \text{II.57}$$

and, for the energetically best wavefunction⁽²⁸⁾, the Δg results for each of the electronic shells are displayed in Figure II.13.

Expectation values

The global effects of correlation may be investigated via expectation values. Equations II.41 to II.45 discussed in connection with our position space investigation have the following representation in momentum space.

The two-particle expectation values

$$\langle p_1 \cdot p_2 / p_1^n p_2^n \rangle = \int (p_1 \cdot p_2 / p_1^n p_2^n) \Gamma_{ij}(p_1, p_2) dp_1 dp_2 \quad \text{II.58}$$

and

$$\langle p_1^n p_2^n \rangle = \int p_1^n p_2^n D(p_1, p_2) dp_1 dp_2 \quad \text{II.59}$$

have been evaluated for $n = 0, 1$ and 2 and $n = -1$ and 1 respectively. Equation II.58 involves the angle γ_{12} between the momentum vectors p_1 and p_2 and is therefore sensitive to angular correlation whilst Equation II.59 is particularly sensitive to radial correlation. The radial density $D(p_1, p_2)$ is given by

$$D(p_1, p_2) = \int r_{ij}(p_1, p_2) p_1^2 p_2^2 \sin\theta_1 \sin\theta_2 d\theta_1 d\theta_2 d\phi_1 d\phi_2 \quad \text{II.60}$$

and is normalised such that

$$\int D(p_1, p_2) dp_1 dp_2 = 1$$

The one-particle expectation values defined by

$$\langle p_1^n \rangle = \int p_1^n d(p_1) dp_1 \quad \text{II.61}$$

assesses correlation in different regions of the one-particle distribution $d(p_1)$ given by

$$d(p_1) = \int D(p_1, p_2) p_2^2 dp_2 \quad \text{II.62}$$

Equation II.61 has been evaluated for $n = -2, -1, 1$ and 2 . The one- and two-particle expectation values discussed here are presented in Tables II.12 to II.16. $\Delta(z)$, shown in Tables II.13 and II.15, is the standard deviation of the

function z as is defined by Equation II.45.

Correlation Coefficients

The radial and angular components of electron correlation can be assessed in a global manner by evaluating various correlation coefficients⁽⁷¹⁾. The radial coefficient take the form

$$\tau_{\text{radial}} = [\langle p_1^n p_2^n \rangle - \langle p_1^n \rangle^2] / [\langle p_1^{2n} \rangle - \langle p_1^n \rangle^2] \quad \text{II.63}$$

where $n = 1$ and -1 corresponds to τ_p and $\tau_{1/p}$ respectively. These quantities give emphasis, in turn, to large and small values of the magnitude of p . The angular coefficients are given by

$$\tau_{\text{angular}} = \langle p_1/p_1^n \cdot p_2/p_2^n \rangle / \langle p_1^{2(1-n)} \rangle \quad \text{II.63}$$

where, to conform with our previous notation⁽⁷⁸⁾, $n = 0, 1$ and 2 yields τ_γ , $\tau_{\gamma''}$ and $\tau_{\gamma'}$, respectively. The angle between the electronic momentum vectors p_1 and p_2 is denoted by γ . The results for $\Delta\tau = \tau_{\text{corr}} - \tau_{\text{HF}}$ for each shell are given in Tables II.17 and II.18. Finally, Table II.16 also contains the value of γ_p - the percentage of each $f_{\text{HF}}(p_{12})$ probability density which has been redistributed due to correlation.

CHAPTER II.10

DISCUSSION: MOMENTUM SPACE

In Figures II.7 we note that the K-shell curves derived from the B and OS95 wavefunctions are graphically indistinguishable. By comparison, it is seen that the OS85 function gives a Coulomb shift which is not only of greater magnitude at its peak but is also somewhat more diffuse. The Watson wavefunction produces a curve which crosses the axis at a point coincident with the B and OS95 curves but differs from them slightly in magnitude. Included in Figure II.7 is the Coulomb shift for Be^{++} since a comparison between it and the K-shell of Be is of obvious interest; the ionic curve was obtained by Reed⁽⁸⁶⁾ using the CI wavefunction of Weiss⁽²⁵⁾ and the HF function of Clementi⁽²⁶⁾. We observe that although the B and OS95 functions give results which are very similar to the Be^{++} curve when $p_{12} > 6$, significant differences exist for $0 < p_{12} < 6$. For two-electron systems it has been established⁽³⁹⁾ that, at small p_{12} the radial component of electron correlation gives rise to negative values for $\Delta f(p_{12})$ whereas, by contrast, angular correlation produces a curve which is initially positive. Thus, when p_{12} is small, Figure II.7 shows that, like the other two-electron ions, the overall effect in Be^{++} is one of radial correlation. However, for the K-shell in Be, it appears that the occupation of the L-shell causes an initial cancellation between the angular and radial components.

These differences between Be^{++} and Be at small p_{12} are in general accord with a comparison between the corresponding $\Delta\tau$ values. Although the K-shell angular correlation coefficients for Be were found to be only marginally larger than those for Be^{++} , it was noted that the $\Delta\tau_{1/p}$ value of -0.0058 for the K-shell was considerably smaller than the ionic result of -0.0197. Thus, by comparison with Be^{++} , radial correlation at small momenta in the Be K-shell is inhibited by the presence of the L-shell electrons. In the light of the momentum analysis by Banyard and Reed⁽⁴⁰⁾, the overall behaviour of the curves in Figure II.7 suggests that angular correlation has, on balance, the major influence in the K-shell of Be.

The L-shell Coulomb shifts in Figure II.8 indicate that the B and OS95 wavefunctions yield results which are graphically coincident, as was found in position space. However, unlike position space, these $\Delta f(p_{12})$ values are noticeably different from the results derived from both the W and OS85 functions. All four curves reveal the dominance of angular correlation at small p_{12} , the effect being greatest for the energetically poorer W and OS85 functions. The magnitude of the L-shell Coulomb shift is considerably greater than that for the K-shell although, as would be expected, it is much less extensive in its p_{12} -range. The relative size of the various K- and L-shell curves can be gauged from the γ values given in Table II.16. As in position space, the L-shell effect is about 6.5 times larger than that for the K-shell.

In position space, correlation caused a significant contraction of the L-shell distribution in Be. This is reflected here as an expansion in the one- and two-particle radial densities, as indicated by the changes in $\langle p_1^n \rangle$ and $\langle p_1^n p_2^n \rangle$ in Tables II.12, II.13 and II.14. For the angular-related properties in Table II.16 and II.18, we see that each intrashell value possesses a positive sign. Thus, correlation has enhanced the alignment of the two momentum vectors, a result which is in keeping with the ground-state studies of the He-like ions^(39,40). The change in the angular correlation coefficients suggests that this effect has greatest absolute magnitude in the L-shell at intermediate p ; see $\Delta\tau_{\gamma}$. However, inspection of Table II.16 also indicates that the ratio of the L- to K-shell angular effects is largest for $\Delta\tau_{\gamma}$, thus showing that the relative change in the angular effects is greatest at small p ; see Equation II.63 when $n = 2$. The large amount of angular correlation in the L-shell in both momentum and position space is due, of course, to the high degree of near 2s-2p degeneracy in Be and, as such, is a non-dynamical effect⁽⁵⁵⁾.

The intershell Coulomb shift shown in Figures II.9 and I.10 are derived from the B and OS95 wavefunctions. The remaining CI functions produced intershell curves which were, by comparison, both small and contracted towards the origin. This is not surprising in view of the limited number of correlating configurations used to describe the intershells, see Table II.4. Therefore, the $\Delta f(p_{12})$ curves for the W and OS85 functions are omitted from Figures II.9

and II.10. However, a measure of their respective sizes is provided by a comparison of the γ - values in Table II.16.

In position space⁽⁷⁸⁾, the $KL(1S)$ and $KL(3S)$ intershell Coulomb holes were found to be of similar shape and magnitude except in the region of small r_{12} . However, in momentum space, the opposing effects of angular and radial correlation produce intershell shifts which are quite distinct in character and range. Figure II.9 suggests that angular correlation is dominant for $p_{12} < 1.5$ whereas, from the $3S$ curves in Figure II.10, it appears that radial correlation is paramount and remains so over a somewhat larger p_{12} -region. That the influence of correlation is generally more extensive in p_{12} -space for $1S$ than $3S$ is, no doubt, related to the presence of the Fermi effect in the $3S$ case. When $p_{12} = |p_1 - p_2|$ is close to zero, Fermi correlation causes $f_{\text{corr}}(p_{12})$ and $f_{\text{HF}}(p_{12})$ to be vanishingly small, thus accounting for the graphically negligible values of $\Delta f(p_{12})$ in Figure II.10 when $p_{12} < 0.25$. Inspection of Tables II.12, II.13 and II.14 shows that, for the inter-shells, electron correlation has produced an expansion in the one- and two-particle radial momentum densities. As for the K- and L-shells, Table II.16 and II.18 reveal a reduction in the average angle between the momentum vectors in each intershell when the B and OS95 results are compared with the HF values.

The rationalisation of the shape of these Coulomb shifts requires, of necessity, some general comments about the HF model. Since each shell within the HF reference state for

Be uses basis orbitals with zero angular momentum, the momentum vector \underline{p} for an electron will be parallel to its position vector \underline{r} . In addition, the HF description indicates that the average angle between the electronic vectors is 90° in each space. If, for a given shell in position space for Be, the two electrons can be thought of as oscillating about the nucleus along mutually perpendicular axes then, to minimize the electron-electron repulsion energy, it is reasonable to assume a phase difference between their motions of $\pi/2$. As the initial example, let us now comment on the expected behaviour of $\Delta f(p_{12})$ for the L-shell. The introduction of correlation was found^(14,87) to cause a relatively large increase in the average angle between the position vectors r_1 and r_2 . In the context of the HF model discussed above, this implies that correlation produces a corresponding decrease in the average angle between p_1 and p_2 , as observed. Such a change in angle predicts an increase in $f(p_{12})$ for small p_{12} . Correlation also produced a contraction of the L-shell in position space which, as seen from Tables II.12 and II.13, means a move towards higher momentum values. Consequently, the Coulomb shifts should also be positive at large p_{12} . Because each $f(p_{12})$ -distribution is normalised, a compensating decrease in probability is to be expected at intermediate p_{12} . These correlation characteristics are indeed seen in Figure II.8.

For the K-shell of Be in position space, we found that the radial and angular correlation coefficients were not only of the same sign but, in contrast with the L-shell,

they were also of roughly similar magnitude when applied to a common region of space. This similarity of magnitude also occurs in momentum space but, as Tables II.17 and II.18 shows, the K-shell radial and angular coefficients are now of opposite sign. Thus, as seen in Figure II.7, the almost equal and opposing effects of radial and angular correlation in the K-shell produces maximum values for $\Delta f(p_{12})$ which are very small by comparison with the L-shell. In passing, we recall that, in position space, the extremum values of $\Delta f(p_{12})$ for the K-shell were comparable with those for the L-shell. The approximate balance between the correlation components in momentum space for the K-shell makes it difficult to predict a shape for the Coulomb shift. Figure II.7 indicates that the K-shell curves are, in fact, characterized by angular correlation effect.

The pair correlation energies for Be^(72,73) suggest that the behaviour of the $1s$ and $3s$ intershell Coulomb shifts may be largely dictated by the intrashell correlation effects. For the $1s$ intershell, the interpenetration of the K- and L-shell orbitals will give rise to overlap regions where the occupying electron pair will experience K($1s$)- or L($1s$)-type correlation. At small p_{12} it is reasonable to suggest that the main contribution to $f(p_{12})$ should arise from this double-occupancy effect within the individual intrashell regions. Therefore, one expects that $\Delta f(p_{12})$ for KL($1s$) will follow the common feature of the K($1s$)- and L($1s$)-curves by being positive at small p_{12} . A large p_{12} value implies that the intershell electrons will be physically separated by being located essentially in their

respective shells. The correlation effect ought now to be dominated by the significant shift of the L-shell electron towards a region of higher momentum; the change in the K-shell momentum due to correlation is comparatively small. Since the average angle between p_1 and p_2 for the $KL(1s)$ is barely decreased by correlation from its HF value of 90° (see $\Delta\tau_{\gamma} \equiv \langle \cos\gamma_{12} \rangle$ in Table II.18), the increase in L-shell momentum will produce a transfer in p_{12} -probability towards larger p_{12} values. Thus, $\Delta f(p_{12})$ should be positive at large p_{12} and negative at intermediate p_{12} , as seen in Figure II.9. The behaviour of the $3s$ Coulomb shift at large p_{12} may be rationalized in the same way. However, since the $\langle p_1^n p_2^n \rangle$ values in Table II.14 indicate that the $KL(3s)$ two-particle radial momentum density is less extensive than that for $KL(1s)$, it is not surprising that the $3s$ curve has the smaller p_{12} -range. When p_{12} is small, the $3s$ and $1s$ curves in Figure II.10 are seen to be quite different in shape. The presence of the Fermi effect in the $3s$ intershell stops the Coulomb shifts from possessing any $K(1s)$ or $L(1s)$ characteristics at small p_{12} . Consequently, the structure of the $KL(3s)$ curve will be governed mainly by the increase in the L-shell momentum vector which, as seen from Table II.18, retains an average orientation of almost 90° with respect to the marginally increased K-shell vector. Thus, after the initial flat part of the curve, due to the near-zero values of $f_{\text{corr}}(p_{12})$ and $f_{\text{HF}}(p_{12})$, correlation will reduce $f(p_{12})$ and increase it at the larger p_{12} values, as mentioned above.

Examination of the intra- and intershell Coulomb shifts presented in Figure II.12 for the B wavefunction highlights the different characteristics of the four curves. The most noticeable feature is the massive influence of the $L(1s)$ curve which, in Be, almost completely masks any variation in the other curves when forming the sum total Coulomb shift. This is in marked contrast with position space where intershell effects were discernable in the total $\Delta f(r_{12})$ curve. The change in behaviour on transforming to momentum space arises because, as noted earlier, angular and radial correlation effects are now in opposition. An approximate balance between these correlation components in the $K(1s)$, $KL(1s)$ and $KL(3s)$ shells produce small $\Delta f(p_{12})$ - values whereas, in the $L(1s)$ -shell, the large non-dynamical angular component clearly over-rides the radial effect. Figure II.11 shows that the sum total Coulomb shifts derived from the four CI wavefunctions fall into two pairs. We note that, except at small p_{12} , the distinction between the pairs is, however, by no means as great as that found in position space. A comparison with Figure II.8 shows that the difference at small p_{12} in Figure II.11 arises from variations in the correlated description of the L-shell electrons, whereas at large p_{12} , the total shifts will essentially reflect K-shell characteristics. Figure II.11 also shows that the B and OS95 wavefunctions produce results which are in good agreement over the whole p_{12} -range. An overall assessment of the four sum total curves and their components is provided by the Y_p values in Table II.16. The W and OS85 wavefunctions appear to be poor, relatively

speaking, not only in their intershell descriptions but also in their L-shells. The over-large L-shell effects are due to an exaggerated imbalance between angular and radial correlation, the latter component being too small in the W and OS85 functions.

The $\Delta(p_{12})$ results in Table II.15 measure the diffuseness or spread of an individual $f(p_{12})$ distribution about its mean value $\langle p_{12} \rangle$. Correlation has caused each shell, except L, to sharpen-up about $\langle p_{12} \rangle$; the L-shell has expanded. The net effect for the atom is that correlation produces a slight sharpening-up of $f(p_{12})$ about a marginally reduced $\langle p_{12} \rangle$ value.

Variations in correlation characteristics with increasing momentum are revealed by the partial Coulomb shifts in Figure II.13. For the L-shell, the initial decrease in Δg vs. p_{12} at small p_1 indicates a radial effect. However, when the test electron has a momentum $p_1 > 0.35$, the sharp increase in Δg vs. p_{12} denotes the existence of angular correlation. The angular effect is seen to extend over a large p_1 -range and is observed to be a maximum when $p_1 \approx \langle p_1 \rangle_L$. For the K-shell, the $\Delta g(p_{12}, p_1)$ surface appears to have three distinct but unequal regions. At very small p_1 there is some evidence of a small angular effect. However, when $0.6 < p_1 < 2.0$, the sizeable negative region in the surface clearly indicates the dominance of radial correlation. For $p_1 > 2.0$, angular correlation is now uppermost. Radial and angular correlation are seen to have their maximum effects when the test electron has momentum

values of about 1.4 and 3.4, respectively.

Figure II.9 and II.10 reveal that the intershells possess an overall similarity in their $\Delta g(p_{12}, p_1)$ -surfaces. However, variations do exist. For 3S , the principal maximum and minimum are of slightly smaller magnitude than those for 1S and, in addition, they are located at larger p_{12} -values. Such differences are reasonable in view of the Fermi effect mentioned earlier. The almost zero Δg -values at small p_{12} which occur in Figure II.13(D) for all p_1 are also a consequence of Fermi correlation. Both intershell surfaces possess a major positive region located roughly at $p_1 = \langle p_1 \rangle_L$. This implies that the test electron is in the L-shell and, in view of the spread of the p_{12} -values about each peak, the principal maxima could involve some K-shell effects. Conversely, when p_1 is large, the test electron is in the K-shell and therefore the diagonal structure, common to both intershell surfaces, refers to the L-shell electron. Correlation increases the L-shell momenta which means, in the latter instance, that p_2 becomes larger. Therefore, for a fixed large p_1 value, the magnitude of $p_{12} = |p_1 - p_2|$ will be decreased or increased depending on the orientation of the vectors. The intershell surfaces show this behaviour as a decrease in Δg along the diagonal axis and an increase in probability when p_{12} is either greater or smaller than the chosen large p_1 value. Comparing these surfaces with those for the intrashell, it is seen from the ordinates that the Δg -range for each intershell is bigger than that for the K-shell but is significantly smaller than the L-shell variation. Figure II.13 indicates that, of the four

surfaces, the Δg -values for the L-shell are largest by, at least, a factor of 30. This emphasizes, once again, the enormous importance of the L-shell contribution to the correlation effect in momentum space for Be.

An overall assessment of angular and radial correlation components in different regions of momentum space is provided by the change in the correlation coefficients listed in Tables II.17 and II.18. As seen, these results support our findings not only for the K- and L-shells but also for the total atom. The B and OS95 wavefunctions produce $\Delta\tau$ values which are remarkably similar and, as expected, they differ appreciably from the W and OS85 results. In passing, we note that when the average $\gamma_{12} = \text{arc cos} \{ \Delta\tau_{\gamma} \equiv \langle \cos \gamma_{12} \rangle_{\text{corr}} \}$ in momentum space is added to the corresponding interparticle angle in position space, the total is $180^\circ (\pm 0.3^\circ)$ for each shell, except L, within each correlated wavefunction. The L-shell values are always somewhat in excess of 180° may be a consequence of the large non-dynamical angular correlation effect which occurs in this shell. Generally, however, the sum of the two angles is in keeping with our HF and correlated models discussed above.

CHAPTER II.11

SUMMARY

The first-order partitioning technique used by Banyard and Mashat for studying Coulomb holes for electronic shells in Be-like ions has been extended and applied to a comparison of different wavefunctions for Be. When partitioning the second order correlated density, the present inclusion of all products of terms up to and including the pair-correlation functions U_{ij} produced greatest change, relative to the earlier work, in the Coulomb hole for the L-shell. This was related to the 2s-2p near-degeneracy effect which exists in Be. For systems in which such effects do not occur it is felt that first-order partitioning may prove adequate.

The total energies, E , of the four CI wavefunctions examined here group into two pairs and this was clearly reflected in the behaviour of the Coulomb holes for each shell. The effect was particularly noticeable for the intershells, where the $\Delta f(r_{12})$ curves for the 1S and 3S intershell states were inverted by comparison with the intrashell holes, thus substantiating the characteristics observed earlier when analysing the Weiss wavefunctions for the Be-like ions. The shape of such curves was rationalised in terms of the significant contraction of the L-shell towards the nucleus which, in turn, arises primarily from a

large non-dynamical angular correlation effect.

The total Coulomb holes for the energetically best descriptions of Be revealed that, even when combined with the K- and L-shell holes, the intershell effects were of significant magnitude to produce clearly identifiable characteristics not seen in earlier work.

Because angular and radial correlation produces opposing effects in momentum space, the structure of the Coulomb shift $\Delta f(p_{12})$ vs. p_{12} reflects the nature of the dominant correlation component for a given electronic shell. The Coulomb shift for the Be K-shell indicates that, overall, the angular component is slightly in excess of the radial effect. A partial Coulomb shift $\Delta g(p_{12}, p_1)$ highlights the changes in relative importance of the components as the momentum of a test electron, say p_1 , is increased. For the K-shell, it was found that radial correlation is the more influential constituent at small to intermediate p_1 whereas, at large p_1 , angular correlation is dominant. Compared with the K-shell, the correlation effects in momentum space for the L-shell are massive. A large effect exists for all momenta except at quite small values, when the radial constituent is prevalent. The disparity between the K- and L-shell Coulomb shifts in Be is so great that, irrespective of the contributions from the intershells, the $\Delta f(p_{12})$ -curve for the atom as a whole is almost completely dominated by the L-shell component. This is in contrast with position space where not only did the K- and L-shells possess comparable extremum values for $\Delta f(r_{12})$ but, more

interestingly, the total Coulomb hole for Be exhibited distinct intershell features. With these points in mind, it would be intriguing to examine a system like Ne, with a completed L-shell, in both position and momentum space.

Finally, for the ground state of a many-electron system, we have established in toto that the Coulomb holes and Coulomb shifts display characteristics which arise, respectively, from the sum and difference of the radial and angular correlation effects. This, along with the partitioning technique, enables us to assess and compare these correlation components for different correlated descriptions of a given electronic shell.

CHAPTER II.12
REFERENCES

- 1 R. McWeeny, Rev. Mod. Phys. 32, 335 (1960).
- 2 C.A. Coulson and A.H. Neilson, Proc. Phys. Soc. London 78, 831 (1961).
- 3 W.A. Lester, Jr., and M. Krauss, J. Chem. Phys. 41, 1407 (1964).
- 4 R.F. Curl and C.A. Coulson, Proc. Phys. Soc. London 85, 647 (1965).
- 5 W.A. Lester, Jr. and M. Krauss, J. Chem. Phys. 44, 207 (1966).
- 6 K.E. Banyard and G.J. Seddon, J. Chem. Phys. 58, 1132 (1973).
- 7 G.J. Seddon and K.E. Banyard, J. Chem. Phys. 59, 1065 (1973).
- 8 R.J. Boyd and C.A. Coulson, J. Phys. B: Atom. Molec. Phys. 6, 782 (1973).
- 9 R.J. Boyd, Theoret. Chim. Acta (Berl) 33, 79 (1974).
- 10 R.J. Boyd and J. Katriel, Int. J. Quantum Chem. 8, 255 (1974).
- 11 R. Benesch and V.H. Smith, Jr., Chem. Phys. Lett. 5, 601 (1970).
- 12 N. Moiseyev, J. Katriel and R.J. Boyd, Theor. Chim. Acta 45, 61 (1977).
- 13 K.E. Banyard and P.K. Youngman, J. Phys. B 15, 853 (1982).
- 14 K.E. Banyard and M.M. Mashat, J. Chem. Phys. 67, 1405 (1976).
- 15 O. Sinanoglu, J. Chem. Phys. 33, 1212 (1960).
- 16 O. Sinanoglu, Phys. Rev. 132, 493 (1961).
- 17 O. Sinanoglu, Proc. Roy. Soc. A260, 379 (1961).
- 18 O. Sinanoglu, J. Chem. Phys. 36, 706 (1962).
- 19 O. Sinanoglu, J. Chem. Phys. 36, 3198 (1962).
- 20 O. Sinanoglu, Rev. Mod. Phys. 35, 517 (1963).
- 21 O. Sinanoglu, Advan. Chem. Phys. 6, 315 (1964)

- 22 O. Sinanoglu, Nucl. Instrum. Meth. 110, 193 (1970).
- 23 O. Sinanoglu and D.F. Tuan., J. Chem. Phys. 38, 1740 (1963)
- 24 O. Sinanoglu and K.A. Brueckner, Three Approaches to Electron Correlation in Atoms, (Yale University Press, New Haven, 1970)
- 25 A.W. Weiss, Phys. Rev. 122, 1826 (1961).
- 26 E. Clementi, 'Tables of Atomic Functions', a supplement to IBM J. Res. Dev. 9, 2 (1965).
- 27 R.E. Watson, Phys. Rev. 119, 170 (1960).
- 28 C.F. Bunge, Phys. Rev. 168, 92 (1968).
- 29 P.L. Olympia Jr. and D.W. Smith, J. Chem. Phys. 52, 67 (1970).
- 30 R. Benesch and V.H. Smith, Jr., Chem. Phys. Lett. 5, 601 (1970).
- 31 R. Benesch and V.H. Smith, Jr., Int. J. Quant. Chem. 4S, 131 (1971).
- 32 R. Benesch and V.H. Smith, Jr., Phys. Rev. 5A, 114 (1972).
- 33 R.E. Brown and V.H. Smith, Jr., Phys. Rev. 5A, 140 (1972).
- 34 R. Benesch, Phys. Rev. 6A, 573 (1972).
- 35 V.H. Smith, Jr., and R.E. Brown, Chem. Phys. Lett. 20, 424 (1973).
- 36 M. Naon and M. Cornille, J. Phys. B: Atom. Molec. Phys. 6, 954 (1973).
- 37 R. Benesch, J. Phys. B: Atom. Molec. Phys. 9, 2587 (1976).
- 38 R. Ahlberg and P. Lindner, J. Phys. B: Atom. Molec. Phys. 9, 2963 (1976).
- 39 K.E. Banyard and J.C. Moore, J. Phys. B: Atom. Molec. Phys. 10, 2781 (1977).
- 40 K.E. Banyard and C.E. Reed, J. Phys. B: Atom. Molec. Phys. 10, 2781 (1978).
- 41 S.R. Gadre, J. Chem. Phys. 71, 1510 (1979).
- 42 J.R. Lombardi, Phys. Rev. A 22, 797 (1980).
- 43 S.R. Gadre and R.L. Matcha, J. Chem. Phys. 74, 589 (1981).

- 44 R.K. Pathak and S.R. Gadre, J. Chem. Phys. 74, 5925 (1981).
- 45 J. Navaza and G. Tsoucaris, Phys. Rev. A 24, 683 (1981).
- 46 S.R. Gadre, S.P. Gejji and N. Venkatalaxmi, Phys. Rev A 26, 1768 (1982).
- 47 A.J. Thakkar, J. Chem. Phys. 76, 747 (1982).
- 48 M.S. Alfredo, A.J. Thakkar and V.H. Smith, Int. J. Quan. Chem. 21, 419 (1982).
- 49 S.R. Gadre, S. Chakravorty and R.K. Pathak, J. Chem. Phys. 78, 4581 (1983).
- 50 S.R. Gadre and S.P. Gejji, J. Chem. Phys. 80, 1175 (1984).
- 51 R.J. Weiss, Acta. Cryst. 25A, 248 (1969).
- 52 O. Sinanoglu, Proc. Natl. Acad Sci. USA, 47, 1217 (1961)
- 53 P.O. Lowdin, Advances in Chemical Physics, Vol. 2. Interscience Publishers, New York, (1964) p. 207
- 54 D.F. Tuan and O. Sinanoglu, J. Chem. Phys., 41, 2677 (1964)
- 55 V. McKoy and O. Sinanoglu, J. Chem Phys. 41, 2689 (1964)
- 56 J. Koutecky, J. Cizek, J. Dubsy and K. Hlavaty, Theoret. Chim. Acta, 2, 462 (1964)
- 57 V. McKoy and O. Sinanoglu, in Modern Quantum Chemistry, Istanbul Lectures, Ed. O. Sinanoglu, Vol II, Academic Press, New York, 1965, p. 23
- 58 C. Hollister and O. Sinanoglu, J. Am. Chem. Soc. 88, 13 (1966).
- 59 R. McWeeny and B.T. Sutcliffe, 'Methods of Molecular Quantum Mechanics' (Academic, New York 1969).
- 60 A. Bunge and C.F. Bunge, Phys. Rev. A1, 1599 (1970).
- 61 A. Bunge, J. Chem. Phys. 53, 20 (1970).
- 62 C.F. Bunge and E.M.A. Peixoto, Phys. Rev. 168, 92 (1970).
- 63 C.F. Bender and E.R. Davidson, J. Phys. Chem. 70, 2675 (1966).
- 64 H.P. Kelly, Phys. Rev. 131, 690 (1963).
- 65 R.K. Nesbet, T.L. Barr and E.R. Davidson, Chem. Phys. Lett. 4, 203 (1969).

- 66 J.W. Viers, F.E. Harris and H.F. Schaefer, Phys. Rev. A1, 24 (1970).
- 67 G.P. Barnett, J. Linderberg and H. Shull, J. Chem. Phys. 43, 580 (1965).
- 68 C.F. Bunge, Phys. Rev. A 14, 1965 (1976).
- 69 J.L. Calais and P.O. Lowdin, J. Mol. Spect. 8, 203 (1962).
- 70 K.H. Al-Bayati, Ph.D. Thesis, Electron Correlation in the $(1s^2 2s)^2 S$ & $(1s^2 2p)^2 P$ states of the Lithium Isoelectronic Sequence in Position & Momentum Space, University of Leicester, (1984).
- 71 W. Kutzelnigg, G Del Re and G. Berthier, Phys. Rev. 172, 49 (1968).
- 72 F.W. Pyron and C.J. Joachain, Phys. Rev. 157, 7 (1967).
- 73 K.E. Banyard and G.K. Taylor, Phys. Rev. A 10, 1972 (1974).
- 74 R. Benesch and V.H. Smith Jr. J. Chem. Phys. 55, 482 (1971).
- 75 W.A. Reed, Acta. Cryst. 32A, 676 (1976).
- 76 B.G. Williams, Physica Scripta, 15, 92 (1977).
- 77 M.J. Cooper, Contemp. Phys. 18, 489 (1977).
- 78 K.E. Banyard and R.J. Mobbs, J. Chem. Phys. 75, 3433 (1981).
- 79 P.A.M. Dirac Quantum Mechanics (Oxford University Press, Oxford, 1935), P.103.
- 80 R. McWeeny and C.A. Coulson, Proc. Phys. Soc. (London) 62A, 509 (1949).
- 81 R. McWeeny, Proc. Phys. Soc. (London) 62A, 519 (1949).
- 82 B. Podolsky and L. Pauling, Phys. Rev. 34, 109 (1929).
- 83 J.C. Slater, Phys. Rev. 34, 1293 (1929).
- 84 H. Margenau and G.M. Murphy, The Mathematics of Physics and Chemistry (Van Nostrand, Princeton, 1956).
- 85 G.N. Watson, A Treatise on the Theory of Bessel Functions, Cambridge University Press, 2nd. Edition (1966) p286.
- 86 C.E. Reed, Ph.D. Thesis, Properties of Electron Momentum Distributions: A Study of Correlation Effects in some Two-Electron Systems & An Examination of Directional Compton Profiles for the Lithium Halides, University of Leicester (1980).

87 K.E. Banyard and D.J. Ellis, Mol. Phys. 24, 1291 (1972).

Excitation	Coefficient	Energy Criterion
$(1s)^2(2s)^2$	0.9531	--
$(1s)^2 - (3p)^2$	0.0285	0.0203
$(1s)^2 - (4s)^2$	0.0168	0.0079
$(1s)^2 - 3s4s$	0.0139	0.0039
$(1s)^2 - 2p3p$	0.0085	0.0011
$(1s)^2 - (3s)^2$	0.0065	0.0006
$(1s)^2 - (4d)^2$	0.0064	0.0026
$(1s)^2 - (5p)^2$	0.0051	0.0019
$(2s)^2 - (2p)^2$	0.2933	0.0409
$(2s)^2 - (3s)^2$	0.0396	0.0023
$(2s)^2 - (3d)^2$	0.0166	0.0014
$1s2s - 2p3p$	0.0093	0.0009
	0.0058	0.0004
$1s2s - 3p4p$	0.0077	0.0007
$1s2s - (2p)^2$	0.0057	0.0002
$1s2s - (4s)^2$	0.0055	0.0007

Table II.1 Important configurations in the 180 configuration wavefunction of Bunge⁽²⁸⁾ for the ground state of Be. The energy criterion is defined by Bunge and gives an idea of the contributions of each configuration to the correlation energy.

E (s limit)	-14.5920
% Correaltion Energy	20.3
E (sp limit)	-14.6608
% Correaltion Energy	94.0
E (spd limit)	-14.66453
% Correaltion Energy	98.0
E (spdf limit)	-14.66570
% Correaltion Energy	99.3
E (spdfg limit)	-14.66598
% Correaltion Energy	99.6
Exact	-14.66639

Table II.2 Estimated contributions of orbitals with different l values to the correlation energy in Be.

Wavefunction ψ^a	TOTAL energy E(a.u.)	% Correlation energy ^b	Description of the total ψ^c
BUNGE (B) ^d	-14.66419	96.55%	180 configurations 7s, 7p and 4d Orthonormal basis set
OLYMPIA & SMITH (OS95) ^e	-14.66355	95.87%	95 configurations 7s, 7p and 4d Orthonormal basis set
WATSON (W) ^f	-14.65740	89.36%	37 configurations 6s, 5p, 4d, 2f and 2g Orthonormal basis set
OLYMPIA & SMITH (OS85) ^e	-14.65534	87.18%	85 configurations 4s, 2p and 1d Orthonormal basis set
HARTREE-FOCK ^f (HF)	-14.57299	0.0%	...

Table II.3 The Be ground-state wavefunctions: their total energies E , in atomic units, and their composition. The reference Hartree-Fock (HF) wavefunction is that determined by Watson.

^a For comparison, the 55-term CI wavefunction of Weiss (Ref. 25) for Be used a nonorthogonal basis set and yielded $E = -14.66090$ au, giving 93.06% of the correlation energy.

^b The exact nonrelativistic energy for Be is -14.66745 (quoted from Ref 29)

^c The leading configuration is the RHF wavefunction of Watson (Ref. 27)

^d Reference 28

^e Reference 29

^f Reference 27

Wavefunction	Number of correlation configurations considered			
	K(¹ s)	L(¹ s)	KL(¹ s)	KL(³ s)
BUNGE (B)	39	22	46	34
	14[s] 19[p] 6[d]	14[s] 7[p] 1[d]	15[s] 22[p] 9[d]	13[s] 16[p] 5[d]
OLYMPIA & SMITH (OS95)	26	15	28	21
	11[s] 12[p] 3[d]	10[s] 4[p] 1[d]	8[s] 16[p] 4[d]	6[s] 13[p] 2[d]
WATSON (W)	22	6	4	1
	6[s] 8[p] 4[d] 2[f] 2[g]	5[p] 1[d]	1[s] 3[p]	1[p]
OLYMPIA & SMITH (OS85)	9	9	11	6
	5[s] 3[p] 1[d]	5[s] 3[p] 1[d]	7[s] 3[p] 1[d]	5[s] 1[p]

Table II.4 The Be ground-state correlated wavefunctions: a summary of the correlation configurations considered for each shell. For a given shell, N[l] indicates that N correlation configurations were formed by either a single- or double-excitation from that shell into a basis orbital of l-type symmetry, the remaining electrons retaining their Hartree-Fock description.

Wavefunction	Shell	$\langle r_1^{-2} \rangle$	$\langle r_1^{-1} \rangle$
BUNGE (B)	K(¹ S)	27.7368	3.6803
	L(¹ S)	1.1048	0.5331
	KL(¹ S)	14.4254	2.1084
	KL(³ S)	14.4314	2.1088
	TOTAL	14.4269	2.1080
OLYMPIA & SMITH (OS95)	K(¹ S)	27.7412	3.6799
	L(¹ S)	1.0709	0.5325
	KL(¹ S)	14.4557	2.1092
	KL(³ S)	14.4576	2.1095
	TOTAL	14.4401	2.1083
WATSON (W)	K(¹ S)	27.7938	3.6824
	L(¹ S)	1.0017	0.5236
	KL(¹ S)	14.4084	2.1022
	KL(³ S)	14.4074	2.1021
	TOTAL	14.4043	2.1024
OLYMPIA & SMITH (OS85)	K(¹ S)	27.8203	3.6868
	L(¹ S)	0.9579	0.5227
	KL(¹ S)	14.4249	2.1071
	KL(³ S)	14.4237	2.1070
	TOTAL	14.4124	2.1063
HARTREE-FOCK (HF)	K(¹ S)	27.7599	3.6819
	L(¹ S)	1.0560	0.5225
	KL(¹ S)	14.4080	2.1022
	KL(³ S)	14.4080	2.1022
	TOTAL	14.4080	2.1022

Table II.5 Some one-particle expectation properties for the intra- and intershells of Be. The sum total listed for each expectation value is given by $1/6 [K(^1S) + L(^1S) + KL(^1S) + 3KL(^3S)]$.

Wavefunction	Shell	$\langle r_1 \rangle$	$\langle r_1^2 \rangle$	Δr_1
BUNGE (B)	K(¹ S)	0.4152	0.2334	0.2470
	L(¹ S)	2.5794	7.9423	1.1357
	KL(¹ S)	1.4969	4.0954	1.3618
	KL(³ S)	1.4970	4.0959	1.3619
	TOTAL	1.4971	4.0931	1.3608
OLYMPIA & SMITH (OS95)	K(¹ S)	0.4149	0.2328	0.2464
	L(¹ S)	2.5798	7.9632	1.1435
	KL(¹ S)	1.4992	4.1151	1.3666
	KL(³ S)	1.4995	4.1154	1.3663
	TOTAL	1.4987	4.1095	1.3651
WATSON (W)	K(¹ S)	0.4153	0.2348	0.2495
	L(¹ S)	2.6250	8.2804	1.1788
	KL(¹ S)	1.5325	4.3327	1.4086
	KL(³ S)	1.5323	4.3322	1.4086
	TOTAL	1.5283	4.3074	1.4042
OLYMPIA & SMITH (OS85)	K(¹ S)	0.4136	0.2314	0.2457
	L(¹ S)	2.5956	8.0763	1.1571
	KL(¹ S)	1.5088	4.1855	1.3816
	KL(³ S)	1.5089	4.1856	1.3816
	TOTAL	1.5074	4.1750	1.3794
HARTREE-FOCK (HF)	K(¹ S)	0.4150	0.2330	0.2465
	L(¹ S)	2.6498	8.4318	1.1875
	KL(¹ S)	1.5324	4.3323	1.4086
	KL(³ S)	1.5324	4.3323	1.4086
	TOTAL	1.5324	4.3323	1.4086

Table II.6 Some one-particle expectation properties for the intra- and intershells of Be. The sum total listed for each expectation value is given by $1/6 [K(^1S) + L(^1S) + KL(^1S) + 3KL(^3S)]$.

Wavefunction	Shell	$\langle r_1^{-1} r_2^{-1} \rangle$	$\langle r_1 r_2 \rangle$
BUNGE (B)	K(¹ S)	13.2886	0.1702
	L(¹ S)	0.2788	6.5462
	KL(¹ S)	2.1425	1.0781
	KL(³ S)	1.7802	1.0603
	TOTAL	3.5084	1.8291
OLYMPIA & SMITH (OS95)	K(¹ S)	13.1860	0.1702
	L(¹ S)	0.2791	6.5547
	KL(¹ S)	2.1666	1.0825
	KL(³ S)	1.7803	1.0623
	TOTAL	3.4954	1.8324
WATSON (W)	K(¹ S)	13.1917	0.1702
	L(¹ S)	0.2742	6.8980
	KL(¹ S)	2.0859	1.1089
	KL(³ S)	1.7398	1.0897
	TOTAL	3.4619	1.9077
OLYMPIA & SMITH (OS85)	K(¹ S)	13.3517	0.1687
	L(¹ S)	0.2662	6.6297
	KL(¹ S)	2.0826	1.0805
	KL(³ S)	1.7712	1.0805
	TOTAL	3.5023	1.8534
HARTREE -FOCK (HF)	K(¹ S)	13.5565	0.1722
	L(¹ S)	0.2730	7.0215
	KL(¹ S)	2.1077	1.1096
	KL(³ S)	1.7399	1.0897
	TOTAL	3.5261	1.9287

Table II.7 Some two-particle expectation properties for the intra- and intershells of Be. The sum total listed for each expectation value is given by $1/6 [K(^1S) + L(^1S) + KL(^1S) + 3KL(^3S)]$.

Wave-function	Shell	$\langle r_{12}^{-1} \rangle$	$\langle r_{12} \rangle$	$\langle r_{12}^2 \rangle$	Δr_{12}
BUNGE	K(¹ S)	2.1925	0.6194	0.4798	0.3100
	L(¹ S)	0.2789	4.1966	19.8952	1.5111
	KL(¹ S)	0.5119	2.6490	8.4253	1.1866
	KL(³ S)	0.4600	2.6586	8.4308	1.1675
	TOTAL	0.7272	2.5734	9.0154	1.5469
OLYMPIA & SMITH (OS95)	K(¹ S)	2.1946	0.6194	0.4799	0.3102
	L(¹ S)	0.2789	4.2028	19.9555	1.5137
	KL(¹ S)	0.5125	2.6519	8.4433	1.1877
	KL(³ S)	0.4594	2.6601	8.4478	1.1711
	TOTAL	0.7274	2.5757	9.0370	1.5500
WATSON (W)	K(¹ S)	2.1899	0.6187	0.4781	0.3087
	L(¹ S)	0.2793	4.2178	20.2455	1.5671
	KL(¹ S)	0.5080	2.6817	8.6545	1.2095
	KL(³ S)	0.4557	2.6915	8.6608	1.1902
	TOTAL	0.7240	2.5988	9.2267	1.5726
OLYMPIA & SMITH (OS85)	K(¹ S)	2.2038	0.6195	0.4804	0.3108
	L(¹ S)	0.2700	4.2976	20.8087	1.5295
	KL(¹ S)	0.5058	2.6833	8.6622	1.2092
	KL(³ S)	0.4549	2.6922	8.6666	1.1911
	TOTAL	0.7240	2.6128	9.3252	1.5806
HARTREE -FOCK (HF)	K(¹ S)	2.2732	0.6071	0.3119	0.3119
	L(¹ S)	0.3432	3.7559	1.6602	1.6602
	KL(¹ S)	0.5063	2.6819	1.2099	1.2099
	KL(³ S)	0.4555	2.6921	1.1902	1.1902
	TOTAL	0.7482	2.5202	1.5204	1.5204

Table II.8 Some two-particle expectation properties for the intra- and intershells of Be. The sum total listed for each expectation value is given by $1/6 [K(^1S) + L(^1S) + KL(^1S) + 3KL(^3S)]$.

Wavefunction	Shell	$\langle \frac{r_1}{r_1^2} \cdot \frac{r_2}{r_2^2} \rangle$	$\langle r_1 \cdot r_2 \rangle$	Charge Shifted $\gamma_r \%$
BUNGE (B)	K(¹ S)	-0.3132	-0.0070	2.130
	L(¹ S)	-0.0608	-2.0008	13.919
	KL(¹ S)	-0.0247	-0.0044	2.350
	KL(³ S)	-0.0071	-0.0065	2.266
	TOTAL	-0.0700	-0.3386	0.999
OLYMPIA & SMITH (OS95)	K(¹ S)	-0.3076	-0.0071	2.181
	L(¹ S)	-0.0599	-1.9957	13.975
	KL(¹ S)	-0.0194	-0.0042	2.158
	KL(³ S)	-0.0059	-0.0059	2.122
	TOTAL	-0.0674	-0.3374	1.323
WATSON (W)	K(¹ S)	-0.3058	-0.0056	2.141
	L(¹ S)	-0.0576	-1.8287	13.437
	KL(¹ S)	0.0097	0.0020	0.124
	KL(³ S)	0.0063	0.0020	0.036
	TOTAL	-0.0653	-0.3070	2.252
OLYMPIA & SMITH (OS85)	K(¹ S)	-0.2801	-0.0069	2.157
	L(¹ S)	-0.0608	-2.0284	15.889
	KL(¹ S)	-0.0047	-0.0021	0.085
	KL(³ S)	-0.0049	-0.0042	0.063
	TOTAL	-0.0600	-0.3417	2.728
HARTREE-FOCK (HF)	K(¹ S)	0.0	0.0	.
	L(¹ S)	0.0	0.0	.
	KL(¹ S)	0.0	0.0	.
	KL(³ S)	0.0	0.0	.
	TOTAL	0.0	0.0	.

Table II.9 Some two-particle expectation properties for the intra- and intershells of Be. The sum total listed for each expectation value is given by $1/6 [K(^1S) + L(^1S) + KL(^1S) + 3KL(^3S)]$. Also included is γ_r , the percentage of the interparticle distribution function $f_{HF}(r_{12})$ which has been redistributed due to correlation.

Wavefunction	Shell	$\Delta\tau_r$	$\Delta\tau_{1/r}$
BUNGE (B)	K(¹ S)	-0.0358	-0.0180
	L(¹ S)	-0.0832	-0.0066
	KL(¹ S)	-0.0026	+0.0007
	KL(³ S)	-0.0024	+0.0011
	TOTAL	-0.0111	-0.0043
OLYMPIA & SMITH (OS95)	K(¹ S)	-0.0316	-0.0250
	L(¹ S)	-0.0773	-0.0056
	KL(¹ S)	-0.0004	+0.0034
	KL(³ S)	-0.0013	+0.0015
	TOTAL	-0.0106	-0.0056
WATSON (W)	K(¹ S)	-0.0367	-0.0259
	L(¹ S)	+0.0053	-0.0001
	KL(¹ S)	-0.0005	-0.0021
	KL(³ S)	+0.0005	+0.0000
	TOTAL	-0.0057	-0.0066
OLYMPIA & SMITH (OS85)	K(¹ S)	-0.0389	-0.0169
	L(¹ S)	-0.0804	-0.0102
	KL(¹ S)	-0.0022	-0.0046
	KL(³ S)	+0.0027	+0.0010
	TOTAL	-0.0114	-0.0042

Table II.10 The change in radial correlation coefficient τ .

Wavefunction	Shell	$\Delta\tau_{\gamma}$	$\Delta\tau_{\gamma'}$	$\Delta\tau_{\gamma''}$
BUNGE (B)	K(¹ S)	-0.0301	-0.0113	-0.0331
	L(¹ S)	-0.2519	-0.0550	-0.3035
	KL(¹ S)	-0.0010	-0.0017	-0.0060
	KL(³ S)	-0.0015	-0.0005	-0.0048
	TOTAL	-0.0827	-0.0053	-0.0595
OLYMPIA & SMITH (OS95)	K(¹ S)	-0.0306	-0.0111	-0.0333
	L(¹ S)	-0.2506	-0.0559	-0.3021
	KL(¹ S)	-0.0010	-0.0013	-0.0053
	KL(³ S)	-0.0014	-0.0004	-0.0048
	TOTAL	-0.0816	-0.0053	-0.0592
WATSON (W)	K(¹ S)	-0.0239	-0.0110	-0.0306
	L(¹ S)	-0.2208	-0.0575	-0.2819
	KL(¹ S)	+0.0046	+0.0006	+0.0059
	KL(³ S)	+0.0046	+0.0004	+0.0040
	TOTAL	-0.0707	-0.0039	-0.0491
OLYMPIA & SMITH (OS85)	K(¹ S)	-0.0299	-0.0100	-0.0337
	L(¹ S)	-0.2511	-0.0634	-0.3064
	KL(¹ S)	-0.0010	-0.0003	-0.0017
	KL(³ S)	+0.0049	-0.0003	-0.0036
	TOTAL	-0.0818	-0.0042	-0.0588

Table II.11 The change $\Delta\tau$ in angular correlation coefficient τ .

Wavefunction	Shell	$\langle p_1^{-2} \rangle$	$\langle p_1^{-1} \rangle$
BUNGE (B)	K(¹ S)	0.3930	0.4736
	L(¹ S)	10.7772	2.4979
	KL(¹ S)	5.9709	1.5380
	KL(³ S)	5.9725	1.5384
	TOTAL	5.8431	1.5208
OLYMPIA & SMITH (OS95)	K(¹ S)	0.3932	0.4737
	L(¹ S)	10.7502	2.4963
	KL(¹ S)	6.0130	1.5424
	KL(³ S)	6.0136	1.5426
	TOTAL	5.8862	1.5233
WATSON (W)	K(¹ S)	0.3943	0.4736
	L(¹ S)	11.4436	2.5715
	KL(¹ S)	6.3363	1.5805
	KL(³ S)	6.3367	1.5806
	TOTAL	6.1974	1.5612
OLYMPIA & SMITH (OS85)	K(¹ S)	0.3682	0.4673
	L(¹ S)	11.0499	2.5280
	KL(¹ S)	6.1379	1.5563
	KL(³ S)	6.1382	1.5563
	TOTAL	5.9951	1.5368
HARTREE-FOCK (HF)	K(¹ S)	0.3934	0.4739
	L(¹ S)	12.2805	2.6874
	KL(¹ S)	6.3370	1.5806
	KL(³ S)	6.3370	1.5806
	TOTAL	6.3370	1.5806

Table II.12 Some one-particle expectation properties for the intra- and intershells of Be. The sum total listed for each expectation value is given by $1/6 [K(^1S) + L(^1S) + KL(^1S) + 3KL(^3S)]$.

Wavefunction	Shell	$\langle p_1 \rangle$	$\langle p_1^2 \rangle$	Δp_1
BUNGE (B)	K(¹ S)	3.0947	13.5927	2.0038
	L(¹ S)	0.6712	1.0574	0.7791
	KL(¹ S)	1.8692	7.3118	1.9539
	KL(³ S)	1.8696	7.3103	1.9531
	TOTAL	1.8740	7.3154	1.9502
OLYMPIA & SMITH (OS95)	K(¹ S)	3.0950	13.5970	2.0044
	L(¹ S)	0.6690	1.0559	0.7800
	KL(¹ S)	1.8695	7.3197	1.9557
	KL(³ S)	1.8692	7.3189	1.9557
	TOTAL	1.8735	7.3216	1.9523
WATSON (W)	K(¹ S)	3.0934	13.6036	2.0086
	L(¹ S)	0.6531	1.0144	0.7667
	KL(¹ S)	1.8587	7.2861	1.9573
	KL(³ S)	1.8584	7.2834	1.9569
	TOTAL	1.8634	7.2924	1.9545
OLYMPIA & SMITH (OS85)	K(¹ S)	3.1045	13.6406	2.0007
	L(¹ S)	0.6550	0.9947	0.7521
	KL(¹ S)	1.8661	7.3051	1.9552
	KL(³ S)	1.8659	7.3034	1.9550
	TOTAL	1.8705	7.3084	1.9518
HARTREE-FOCK (HF)	K(¹ S)	3.0919	13.5681	2.0020
	L(¹ S)	0.6251	1.0021	0.7819
	KL(¹ S)	1.8585	7.2851	1.9573
	KL(³ S)	1.8585	7.2851	1.9573
	TOTAL	1.8585	7.2851	1.9573

Table II.13 Some one-particle expectation properties for the intra- and intershells of Be. The sum total listed for each expectation value is given by $1/6 [K(^1S) + L(^1S) + KL(^1S) + 3KL(^3S)]$.

Wavefunction	Shell	$\langle p_1^{-1} p_2^{-1} \rangle$	$\langle p_1 p_2 \rangle$
BUNGE (B)	K($1s$)	0.2233	9.4361
	L($1s$)	6.2530	0.4422
	KL($1s$)	1.3580	2.3542
	KL($3s$)	1.1079	1.6327
	TOTAL	1.8597	2.8551
OLYMPIA & SMITH (OS95)	K($1s$)	0.2234	9.4369
	L($1s$)	6.2454	0.4394
	KL($1s$)	1.3641	2.3670
	KL($3s$)	1.1116	1.6294
	TOTAL	1.8613	2.8552
WATSON (W)	K($1s$)	0.2236	9.4062
	L($1s$)	6.7641	0.4355
	KL($1s$)	1.3990	2.2760
	KL($3s$)	1.1480	1.5809
	TOTAL	1.9718	2.8101
OLYMPIA & SMITH (OS85)	K($1s$)	0.2173	9.4915
	L($1s$)	6.4129	0.4217
	KL($1s$)	1.3471	2.2951
	KL($3s$)	1.1255	1.6160
	TOTAL	1.8923	2.8427
HARTREE -FOCK (HF)	K($1s$)	0.2246	9.5598
	L($1s$)	7.2219	0.3908
	KL($1s$)	1.3994	2.2846
	KL($3s$)	1.1480	1.5810
	TOTAL	2.0483	2.8297

Table II.14 Some two-particle expectation properties for the intra- and intershells of Be. The sum total listed for each expectation value is given by $1/6 [K(1s) + L(1s) + KL(1s) + 3KL(3s)]$.

Wave-function	Shell	$\langle p_{12}^{-1} \rangle$	$\langle p_{12} \rangle$	$\langle p_{12}^2 \rangle$	Δp_{12}
BUNGE (B)	K(1S)	0.3102	4.4735	26.3423	2.5160
	L(1S)	1.8073	0.9638	2.0525	1.0600
	KL(1S)	0.5003	3.1678	14.5947	2.1354
	KL(3S)	0.4070	3.2727	14.4514	1.9341
	TOTAL	0.6398	3.0705	14.3906	2.2276
OLYMPIA & SMITH (OS95)	K(1S)	0.3102	4.4718	26.3076	2.5120
	L(1S)	1.8098	0.9621	2.0463	1.0586
	KL(1S)	0.5007	3.1672	14.5961	2.1366
	KL(3S)	0.4072	3.2720	14.4497	1.9348
	TOTAL	0.6404	3.0695	14.3832	2.2274
WATSON (W)	K(1S)	0.3103	4.4852	26.5044	2.5273
	L(1S)	1.8545	0.9493	2.0272	1.0611
	KL(1S)	0.5023	3.1575	14.5147	2.1318
	KL(3S)	0.4089	3.2664	14.4192	1.9365
	TOTAL	0.6490	3.0652	14.3840	2.2335
OLYMPIA & SMITH (OS85)	K(1S)	0.3100	4.4848	26.3986	2.5070
	L(1S)	1.8622	0.9385	1.9923	1.0542
	KL(1S)	0.5022	3.1590	14.5602	2.1403
	KL(3S)	0.4093	3.2656	14.4002	1.9328
	TOTAL	0.6504	3.0631	14.3586	2.2307
HARTREE -FOCK (HF)	K(1S)	0.3082	4.5248	27.0648	2.5673
	L(1S)	1.7747	0.9591	1.9926	1.0357
	KL(1S)	0.4999	3.1589	14.5098	2.1286
	KL(3S)	0.4090	3.2652	14.4112	1.9365
	TOTAL	0.6350	3.0731	14.4668	2.2412

Table II.15 Some two-particle expectation properties for the intra- and intershells of Be. The sum total listed for each expectation value is given by $1/6 [K(^1S) + L(^1S) + KL(^1S) + 3KL(^3S)]$.

Wavefunction	Shell	$\langle \left(\frac{p_1}{2}\right) \cdot \left(\frac{p_2}{2}\right) \rangle$	$\langle p_1 \cdot p_2 \rangle$	Charge Shifted $\gamma_p \%$
BUNGE (B)	K(¹ S)	0.0033	0.4287	0.781
	L(¹ S)	0.5898	0.0298	4.967
	KL(¹ S)	0.0019	0.0101	0.486
	KL(³ S)	0.0025	0.0075	0.286
	TOTAL	0.1004	0.0818	0.942
OLYMPIA & SMITH (OS95)	K(¹ S)	0.0032	0.4282	0.786
	L(¹ S)	0.5887	0.0302	4.959
	KL(¹ S)	0.0017	0.0134	0.405
	KL(³ S)	0.0019	0.0079	0.265
	TOTAL	0.0999	0.0826	0.935
WATSON (W)	K(¹ S)	0.0014	0.3514	0.736
	L(¹ S)	0.5027	0.0196	6.187
	KL(¹ S)	-0.0077	-0.0243	0.165
	KL(³ S)	-0.0006	-0.0036	0.020
	TOTAL	0.0824	0.0559	1.079
OLYMPIA & SMITH (OS85)	K(¹ S)	0.0029	0.4413	0.868
	L(¹ S)	0.5893	0.0316	6.607
	KL(¹ S)	0.0022	0.0250	0.024
	KL(³ S)	0.0015	0.0070	0.053
	TOTAL	0.0998	0.0865	1.112
HARTREE-FOCK (HF)	K(¹ S)	0.0	0.0	...
	L(¹ S)	0.0	0.0	...
	KL(¹ S)	0.0	0.0	...
	KL(³ S)	0.0	0.0	...
	TOTAL	0.0	0.0	...

Table II.16 Some two-particle expectation properties for the intra- and intershells of Be. The sum total listed for each expectation value is given by $1/6 [K(^1S) + L(^1S) + KL(^1S) + 3KL(^3S)]$. Also included is γ , the percentage of the interparticle distribution function $f_{HF}(r_{12})$ which has been redistributed due to correlation.

Wavefunction	Shell	$\Delta\tau_p$	$\Delta\tau_{1/p}$
BUNGE (B)	K(¹ S)	-0.0352	-0.0058
	L(¹ S)	-0.0136	+0.0029
	KL(¹ S)	+0.0067	+0.0069
	KL(³ S)	+0.0006	+0.0027
	TOTAL	-0.0097	-0.0111
OLYMPIA & SMITH (OS95)	K(¹ S)	-0.0354	-0.0058
	L(¹ S)	-0.0134	+0.0031
	KL(¹ S)	+0.0104	+0.0070
	KL(³ S)	+0.0014	+0.0029
	TOTAL	-0.0088	-0.0115
WATSON (W)	K(¹ S)	-0.0404	-0.0042
	L(¹ S)	+0.0152	+0.0314
	KL(¹ S)	-0.0025	+0.0000
	KL(³ S)	-0.0001	+0.0000
	TOTAL	-0.0104	-0.0066
OLYMPIA & SMITH (OS85)	K(¹ S)	-0.0366	-0.0068
	L(¹ S)	-0.0131	+0.0047
	KL(¹ S)	-0.0053	-0.0029
	KL(³ S)	+0.0008	+0.0029
	TOTAL	-0.0093	-0.0119

Table II.17 The change $\Delta\tau$ in radial correlation coefficient τ .

Wavefunction	Shell	$\Delta\tau_{\gamma}$	$\Delta\tau_{\gamma'}$	$\Delta\tau_{\gamma''}$
BUNGE (B)	K(¹ S)	+0.0315	+0.0083	+0.0284
	L(¹ S)	+0.0282	+0.0547	+0.1404
	KL(¹ S)	+0.0014	+0.0003	+0.0007
	KL(³ S)	+0.0010	+0.0004	+0.0038
	TOTAL	+0.0112	+0.0172	+0.0302
OLYMPIA & SMITH (OS95)	K(¹ S)	+0.0315	+0.0082	+0.0283
	L(¹ S)	+0.0300	+0.0549	+0.1397
	KL(¹ S)	+0.0018	+0.0003	+0.0013
	KL(³ S)	+0.0011	+0.0003	+0.0034
	TOTAL	+0.0113	+0.0170	+0.0299
WATSON (W)	K(¹ S)	+0.0258	+0.0035	+0.0176
	L(¹ S)	+0.0193	+0.0439	+0.1151
	KL(¹ S)	-0.0033	-0.0012	-0.0038
	KL(³ S)	-0.0005	-0.0001	-0.0012
	TOTAL	+0.0077	+0.0133	+0.0209
OLYMPIA & SMITH (OS85)	K(¹ S)	+0.0323	+0.0078	+0.0280
	L(¹ S)	+0.0318	+0.0533	+0.1410
	KL(¹ S)	+0.0034	+0.0004	+0.0032
	KL(³ S)	+0.0010	+0.0002	+0.0027
	TOTAL	+0.0118	+0.0167	+0.0300

Table II.18 The change $\Delta\tau$ in angular correlation coefficient τ .

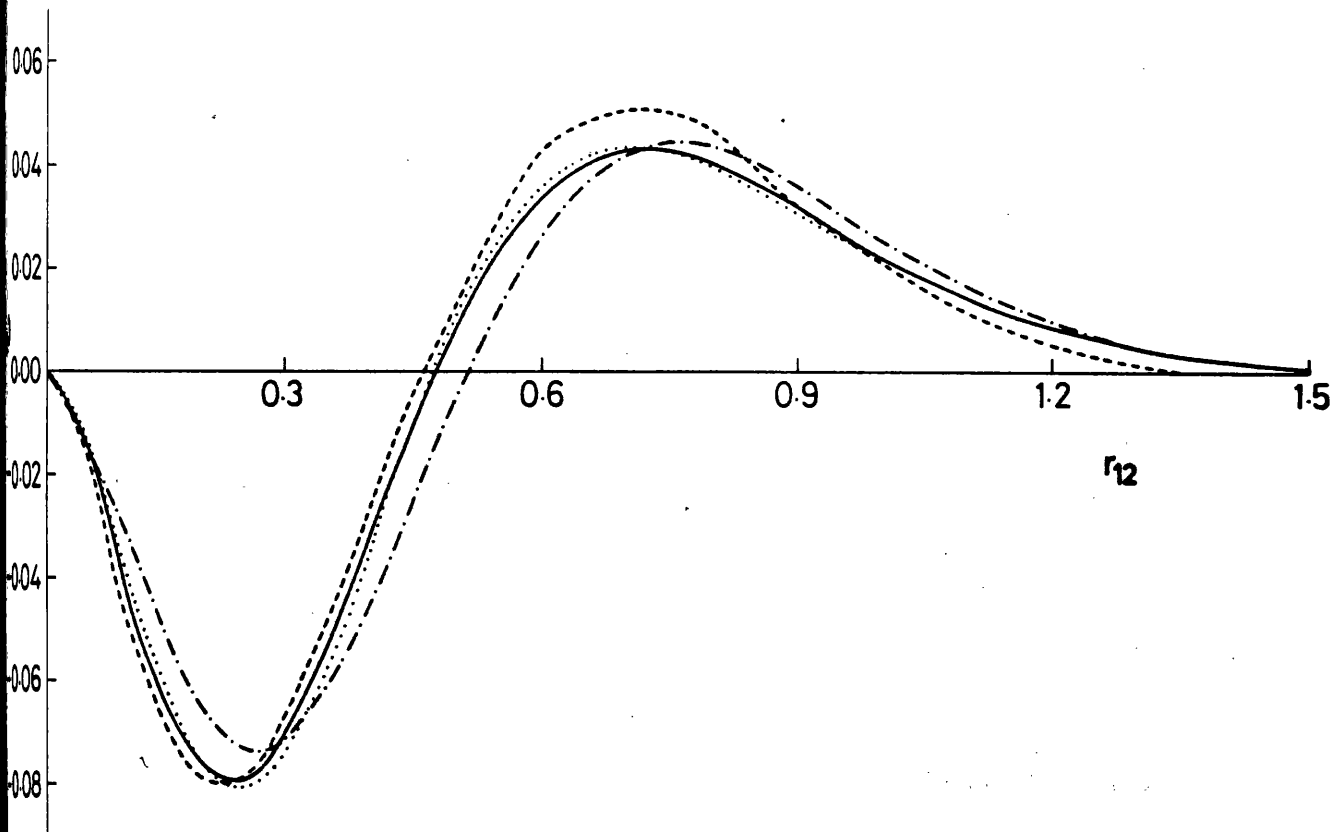


Figure II.1 The Be K-shell Coulomb holes.

Bunge wavefunction (B) (solid curve)

Olympia & Smith 95 term wavefunction (OS95) (dotted curve)

Watson wavefunction (W) (dashed curve)

Olympia & Smith 85 term wavefunction (OS85) (dot-dashed curve)

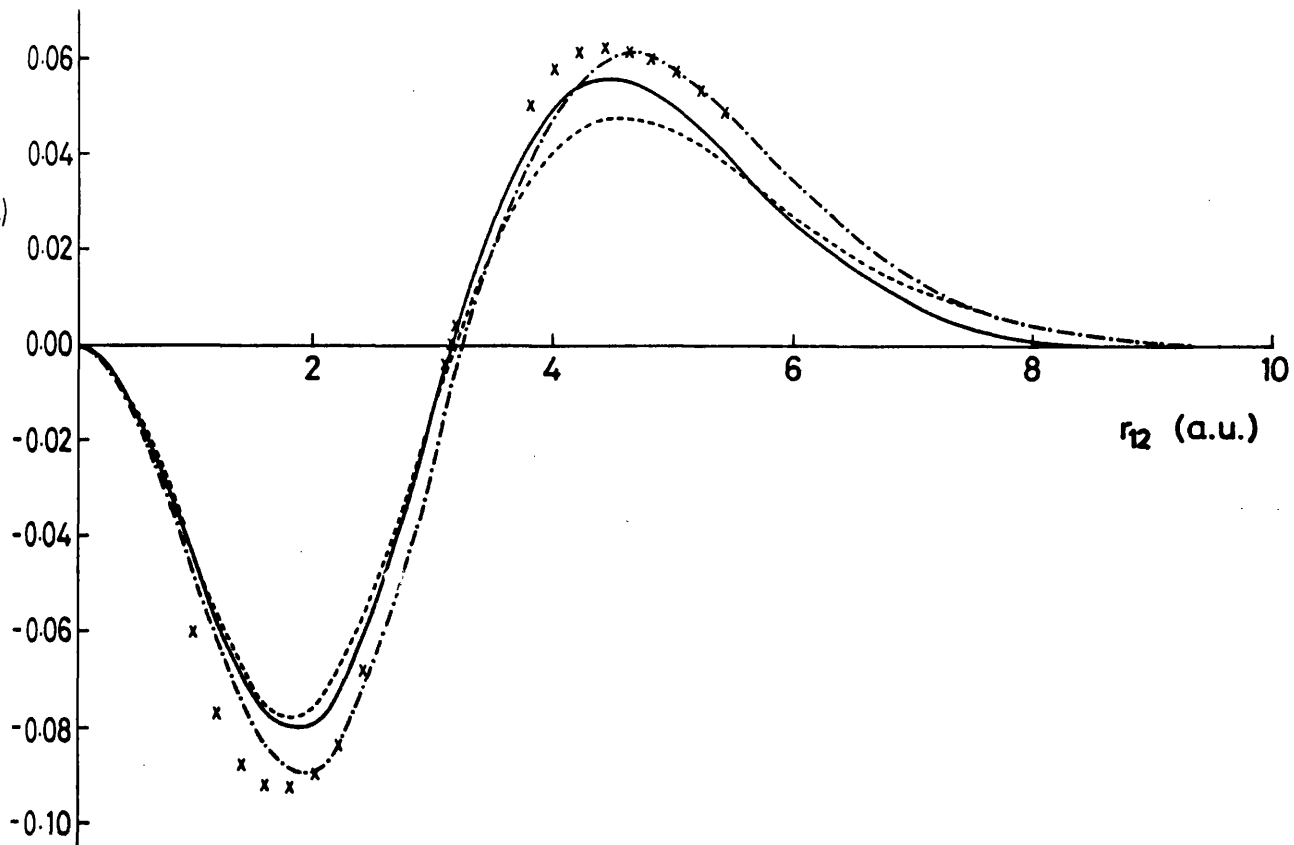


Figure II.2 The Be L-shell Coulomb holes.

Bunge wavefunction (B) (solid curve)

Olympia & Smith 95 term wavefunction (OS95) (dotted curve)

Watson wavefunction (W) (dashed curve)

Olympia & Smith 85 term wavefunction (OS85) (dot-dashed curve)

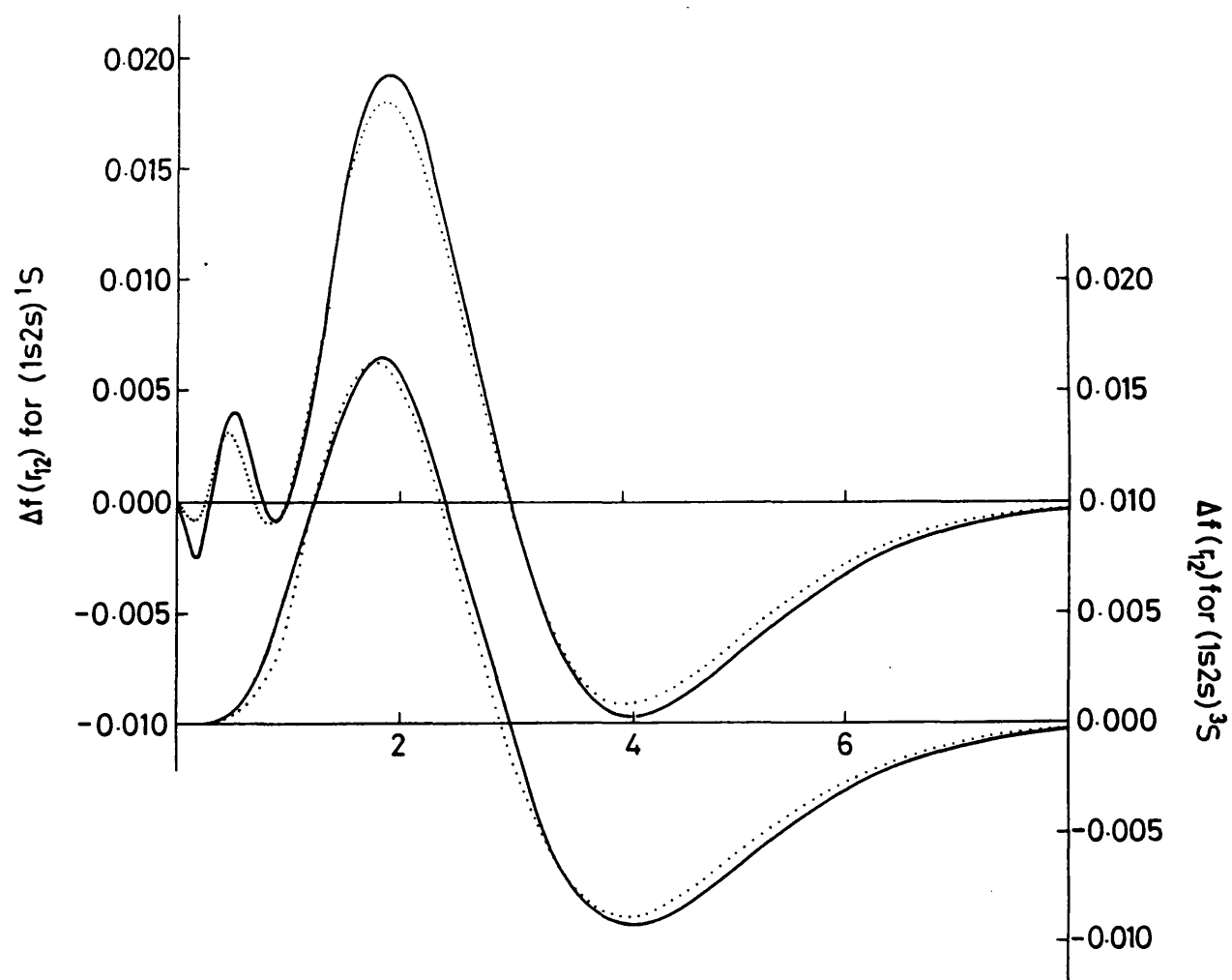


Figure II.3 The Be intershell Coulomb holes.

Bunge wavefunction (B) (solid curve)

Olympia & Smith 95 term wavefunction (OS95) (dotted curve)

Watson wavefunction (W) (dashed curve)

Olympia & Smith 85 term wavefunction (OS85) (dot-dashed curve)

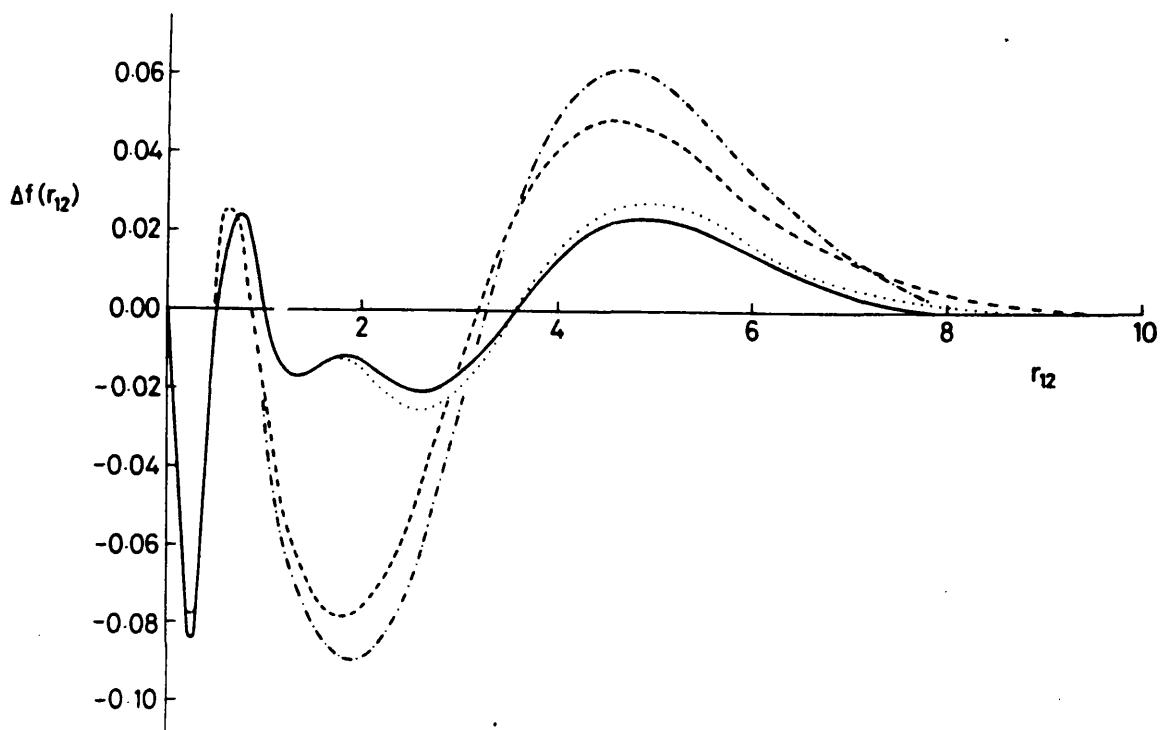


Figure II.4 Total Coulomb holes for the Be atom.

Bunge wavefunction (B) (solid curve)

Olympia & Smith 95 term wavefunction (OS95) (dotted curve)

Watson wavefunction (W) (dashed curve)

Olympia & Smith 85 term wavefunction (OS85) (dot-dashed curve)

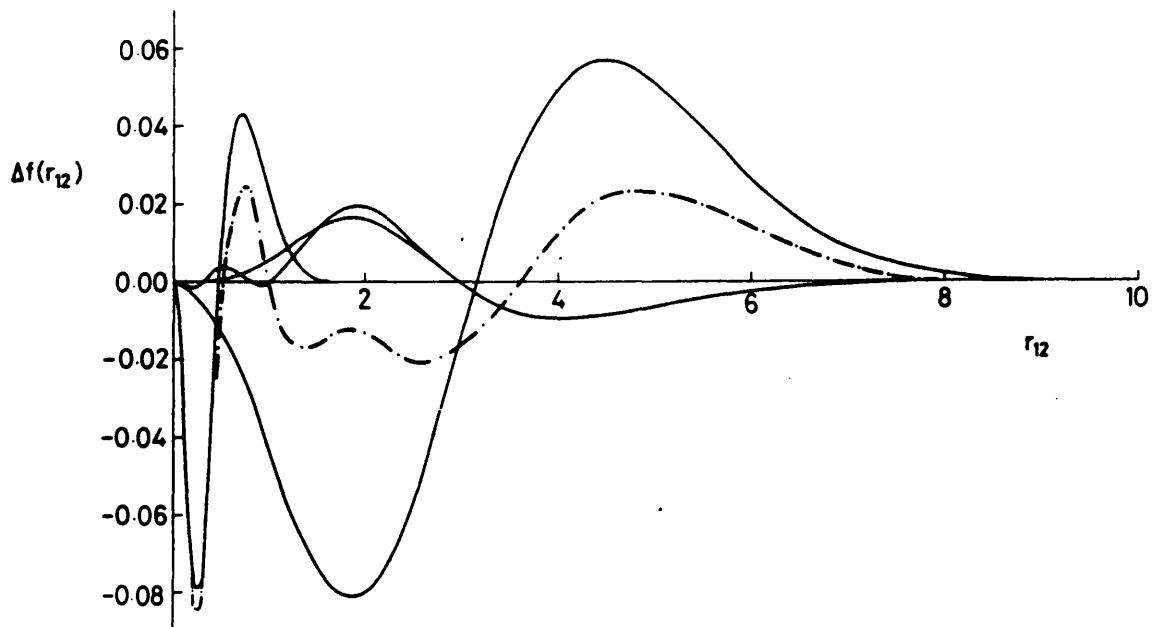
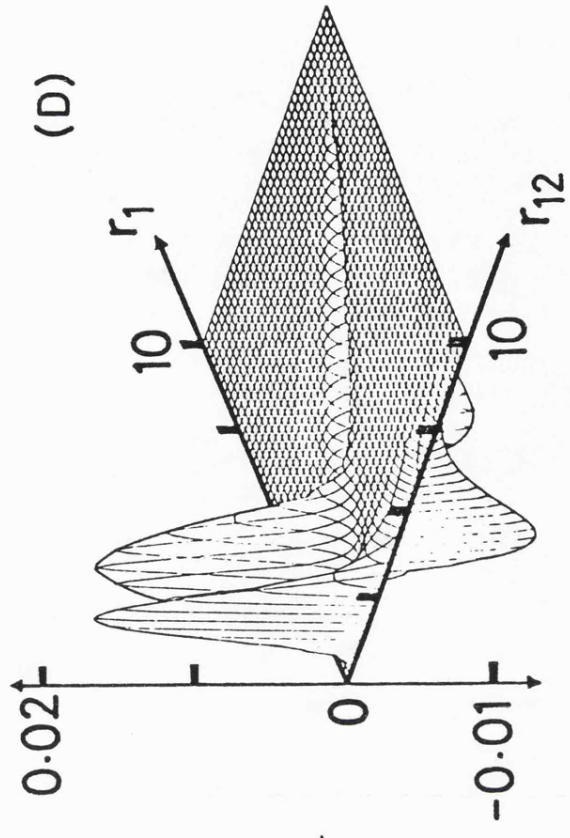
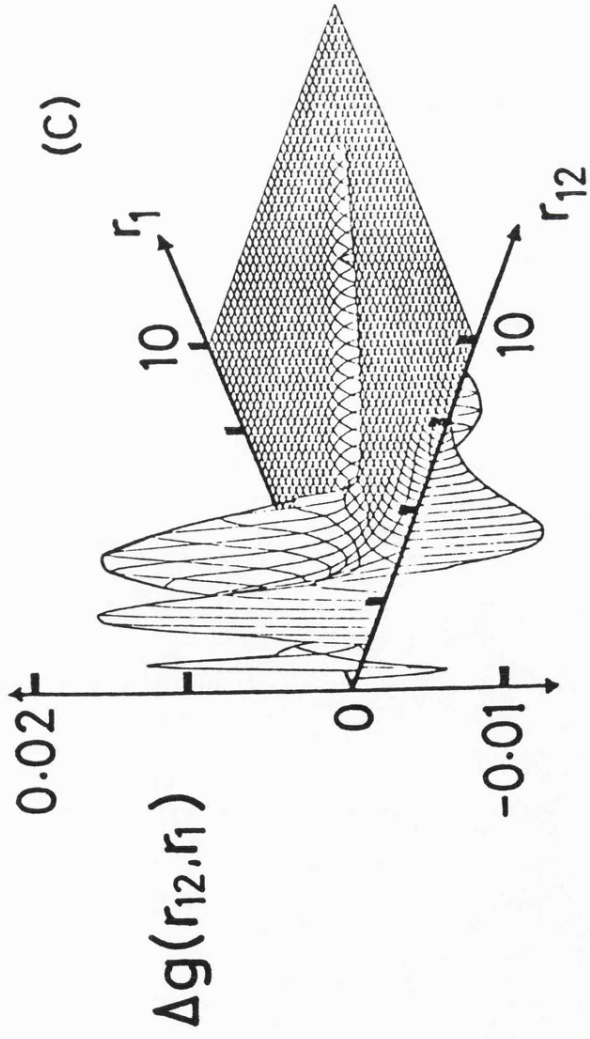
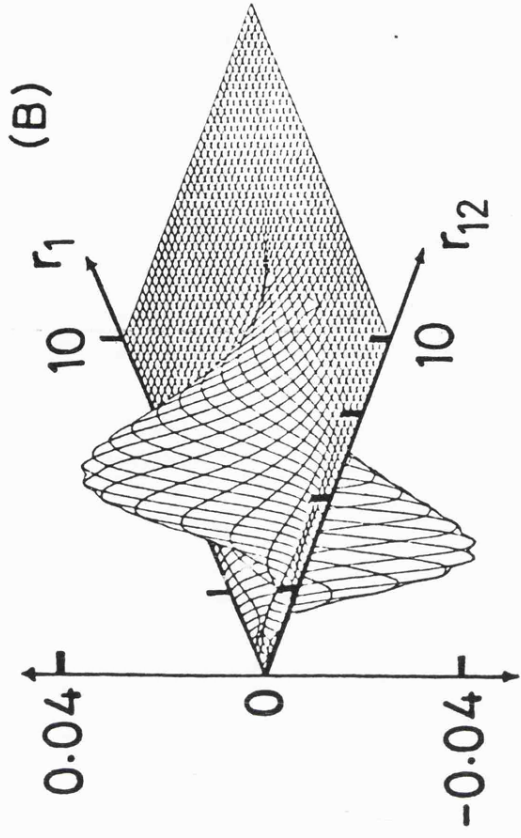
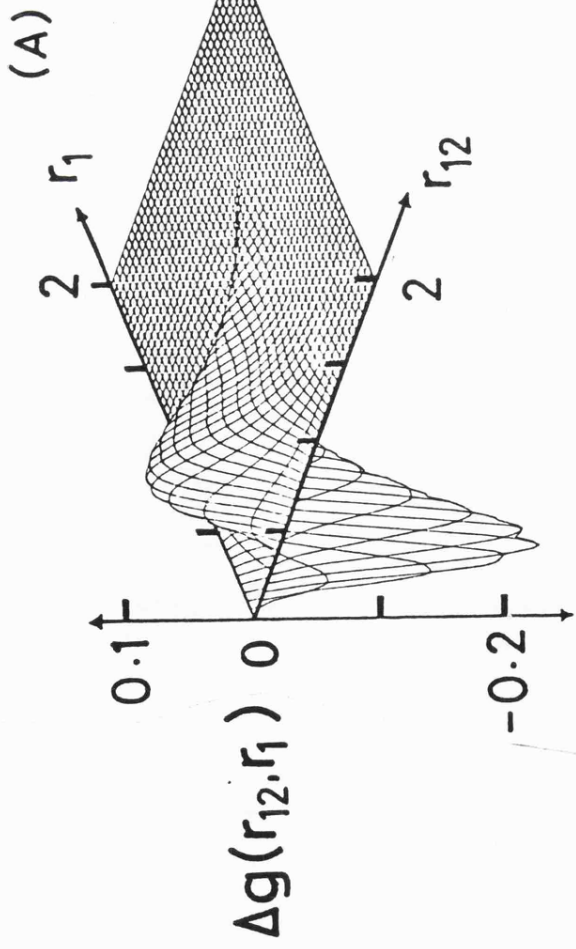


Figure II.5 Total and component Coulomb holes for the Bunge wavefunction.

Figure II.6

(see over)

Figure II.6 The partial Coulomb hole surfaces, $\Delta g(r_{12}, r_1)$, for the intra- and intershells of Be evaluated for the Bunge wavefunction.



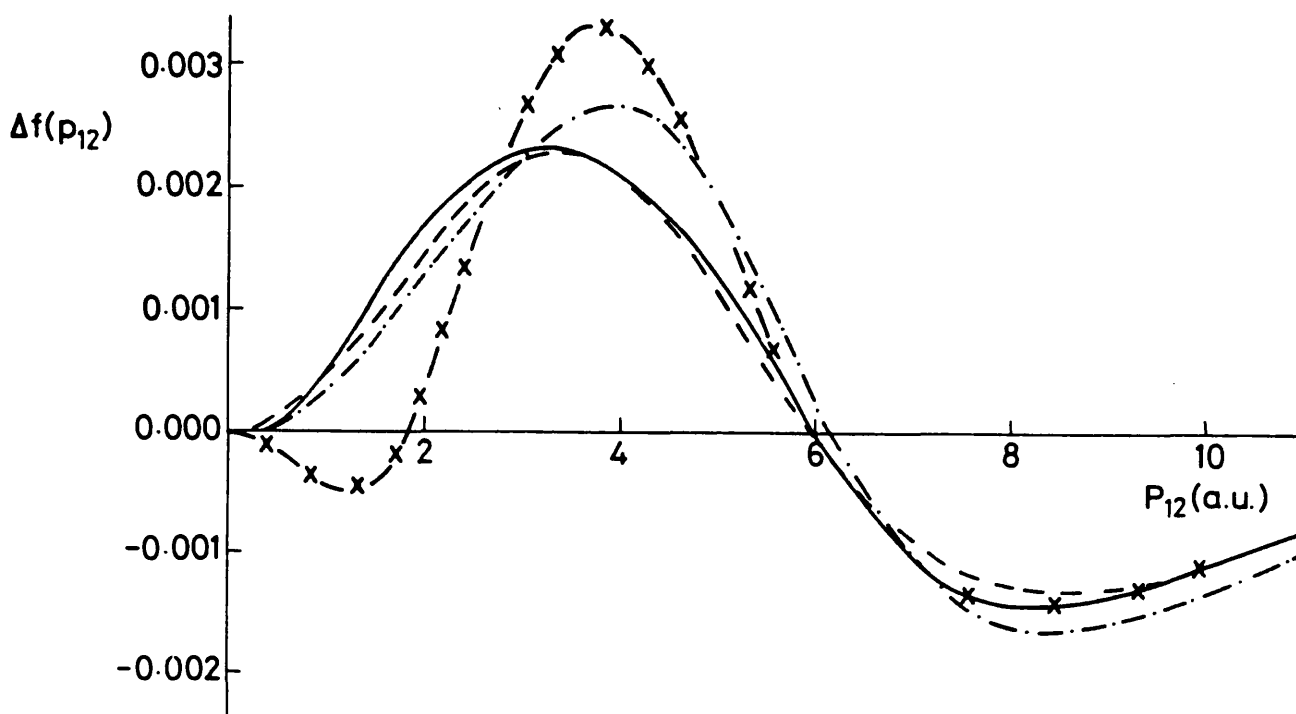


Figure II.7 - The Be atom K-shell Coulomb shifts.

Bunge wavefunction (B) (solid curve)

Olympia & Smith 95 term wavefunction (OS95) (dotted curve)

Watson wavefunction (W) (dashed curve)

Olympia & Smith 85 term wavefunction (OS85) (dot-dashed curve)

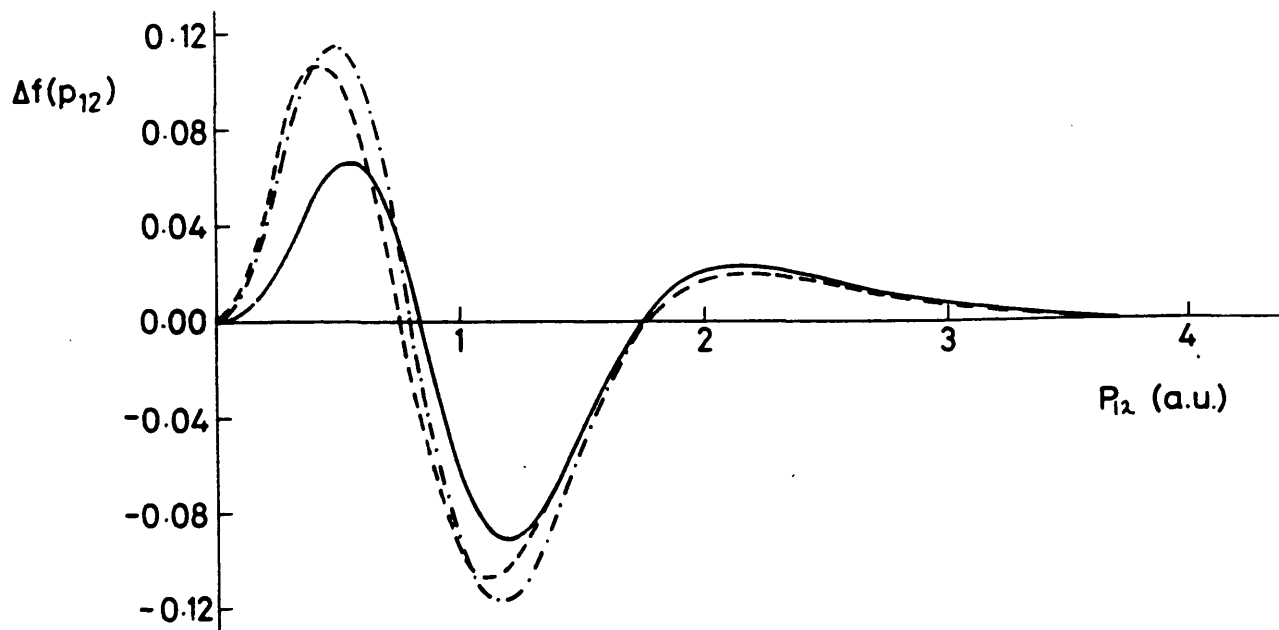


Figure II.8 The Be atom L-shell Coulomb shifts.

Bunge wavefunction (B) (solid curve)

Olympia & Smith 95 term wavefunction (OS95) (dotted curve)

Watson wavefunction (W) (dashed curve)

Olympia & Smith 85 term wavefunction (OS85) (dot-dashed curve)

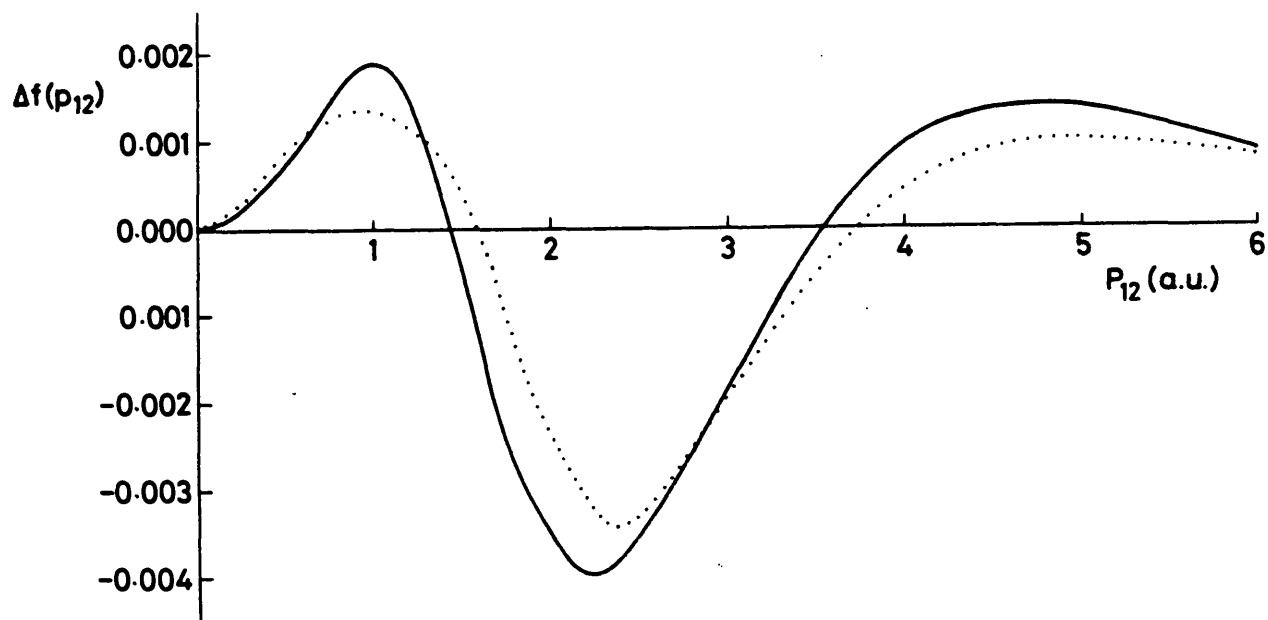


Figure II.9 The Be atom intershell ($1s$) Coulomb shifts.

Bunge wavefunction (B) (solid curve)

Olympia & Smith 95 term wavefunction (OS95) (dotted curve)

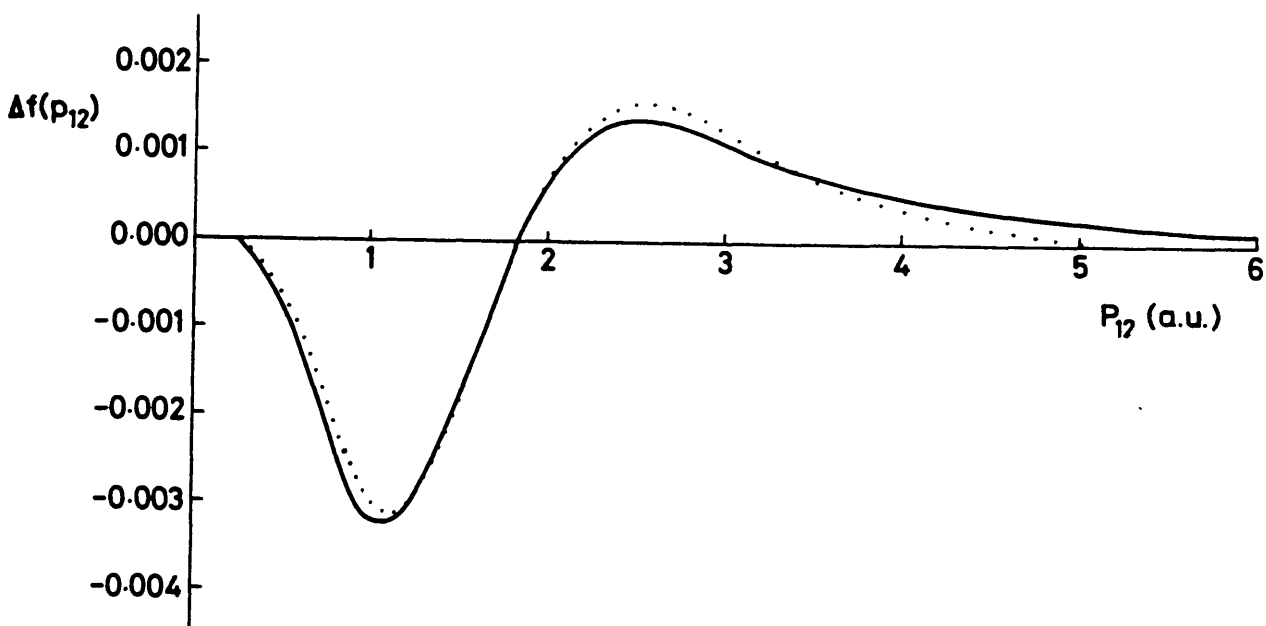


Figure II.10 The Be atom intershell (3S) Coulomb shifts.
 Bunge wavefunction (B) (solid curve)
 Olympia & Smith 95 term wavefunction (OS95) (dotted curve)

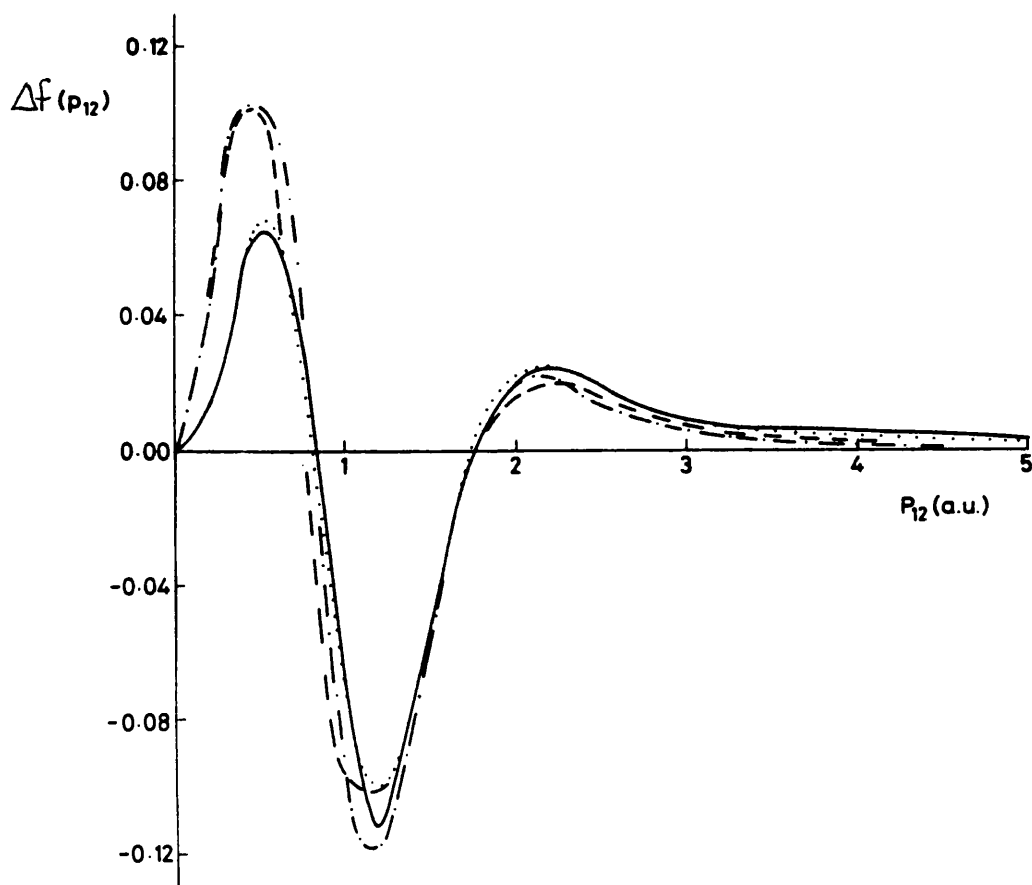


Figure II.11 Total Coulomb shifts for the Be atom.

Bunge wavefunction (B) (solid curve)

Olympia & Smith 95 term wavefunction (OS95) (dotted curve)

Watson wavefunction (W) (dashed curve)

Olympia & Smith 85 term wavefunction (OS85) (dot-dashed curve)

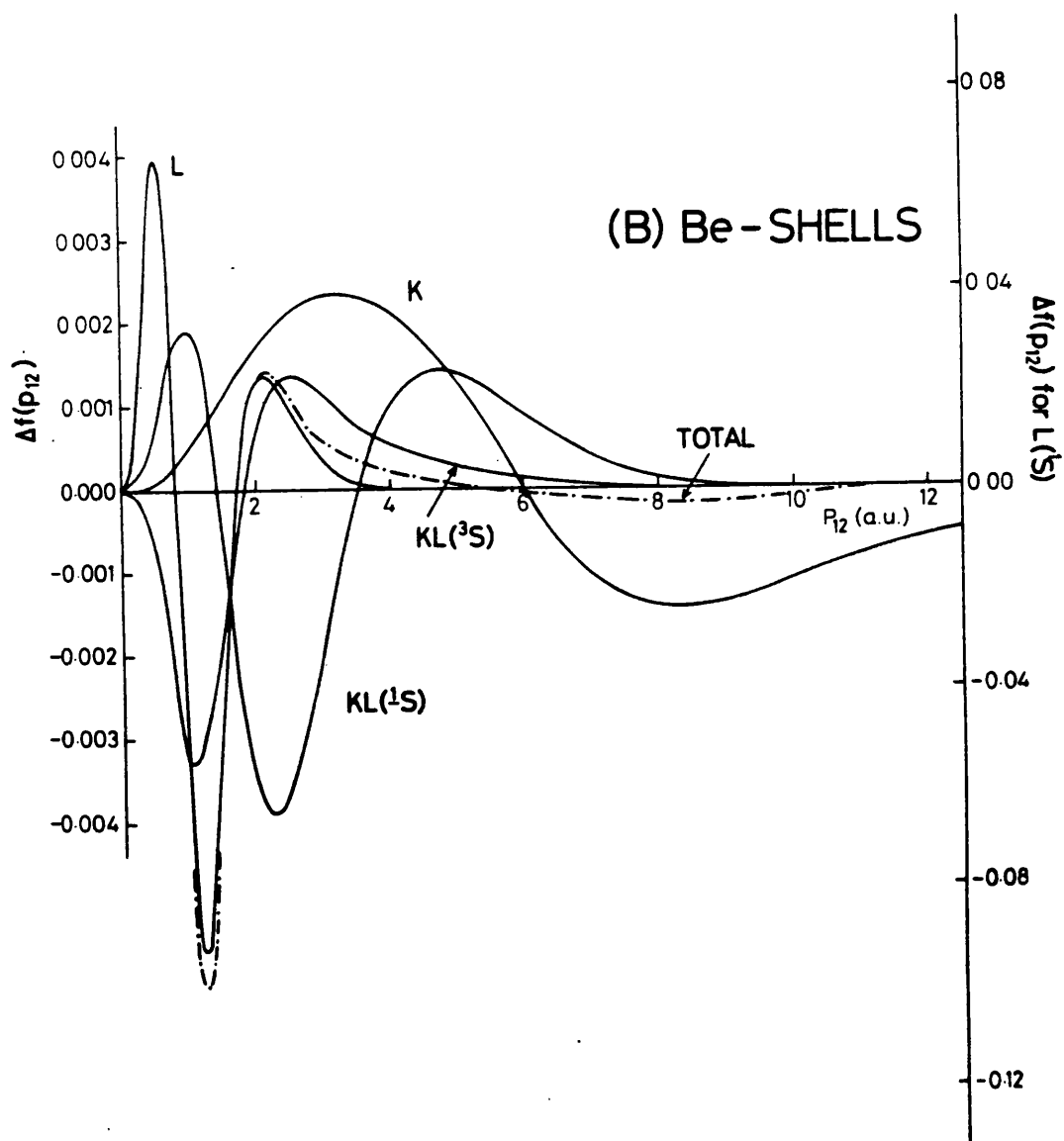
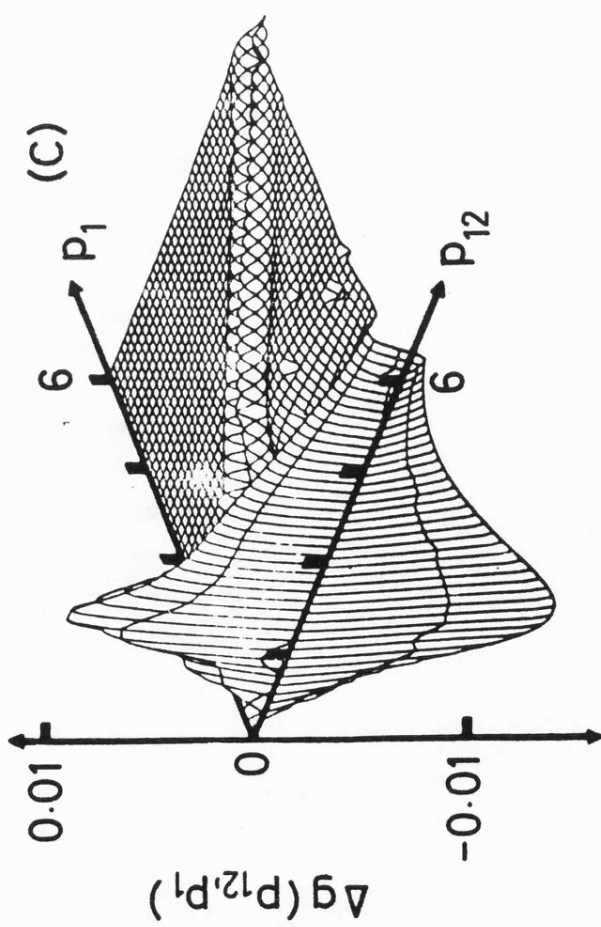
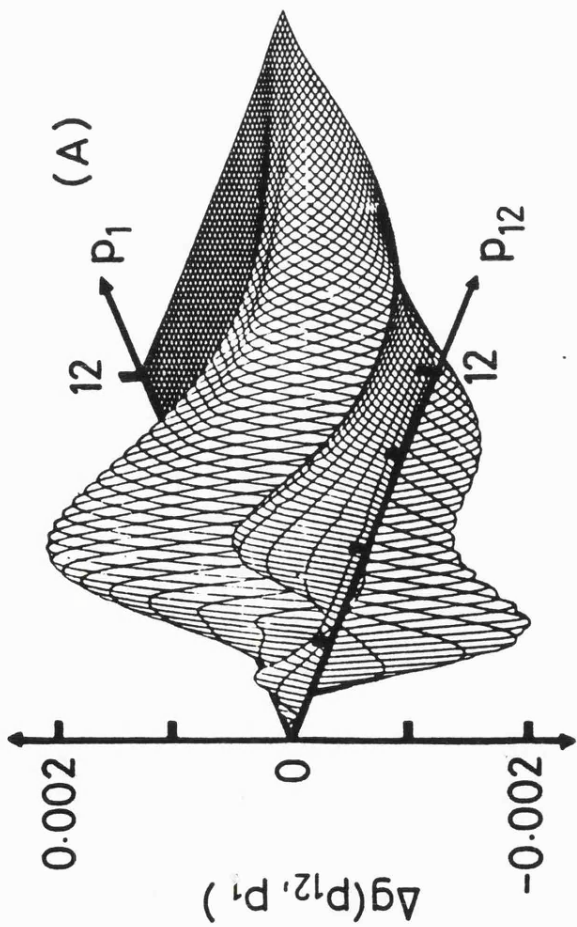
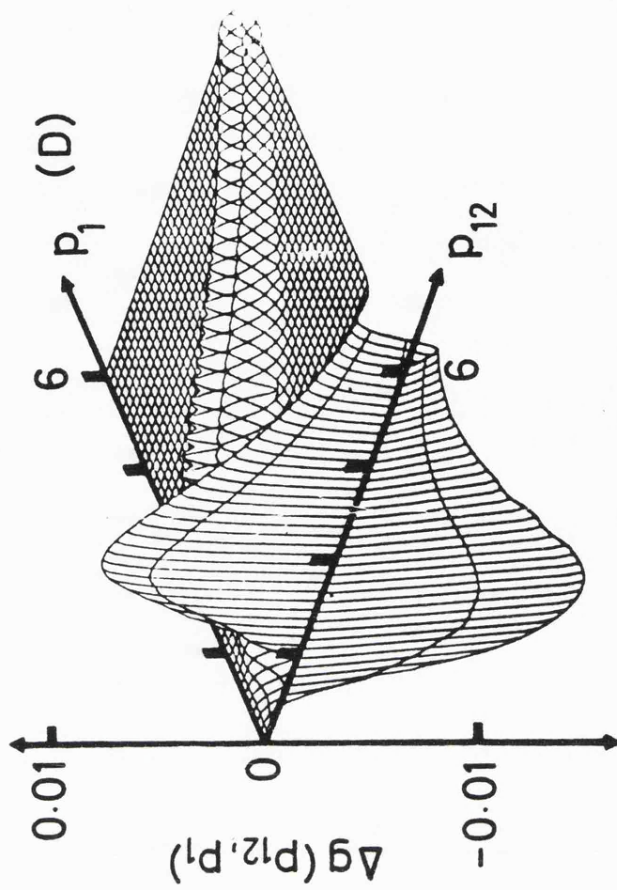
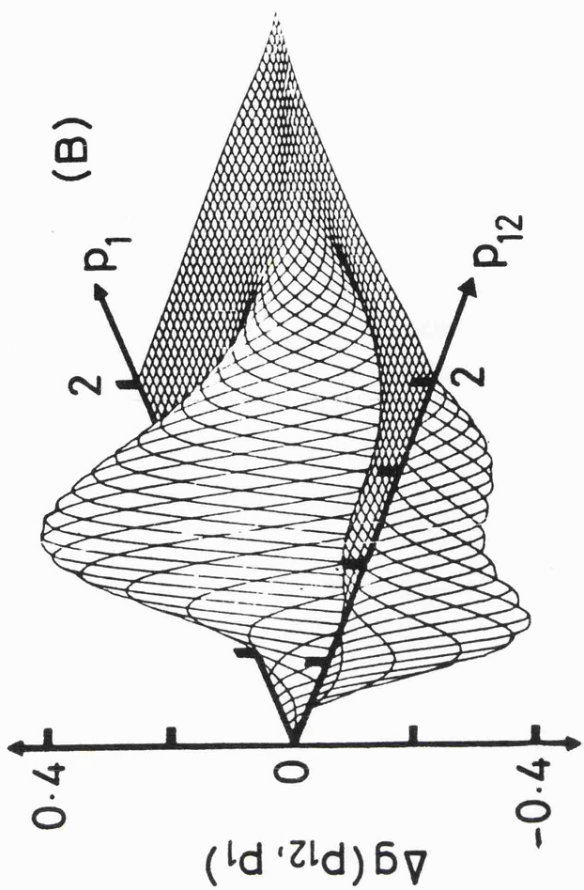


Figure II.12 Total and component Coulomb shifts for the Bunge wavefunction.

Figure II.13
(see over)

Figure II.13 The partial Coulomb shift surfaces $\Delta g(p_{12}, p_1)$, for the intra- and intershells of Be evaluated for the Bunge wavefunction.



PART III
LITHIUM HYDRIDE

CHAPTER III.1

INTRODUCTION

The problem of electron correlation is central to our understanding of the detailed electronic structure of atomic and molecular systems⁽¹⁾. The correlated behaviour of electronic motions in two-electron atoms and ions has been the focus of much attention, both for electrons of like-⁽²⁻⁵⁾ and unlike-⁽⁶⁻⁹⁾ spin components (Fermi and Coulomb effects respectively). Much less work has been carried out on molecules, although Fermi correlation holes have been examined in H_2 and H_6 ⁽¹⁰⁾, and LiH and Li_2 ⁽¹¹⁾. The most comprehensive treatment of 'correlation holes' in diatomic molecules to date has been presented by Doggett^(12,13), who has analyzed the average longitudinal and transverse hole functions in H_2 , BH and LiH. Great attention has been devoted to the LiH molecule by theorists, the main reason being that it provides the simplest closed-shell system of immediate interest after the hydrogen molecule.

For a two-electron system, Coulson and Neilson⁽⁶⁾ examined the influence of electron correlation in position space by means of the Coulomb hole. Subsequently, the concept of the Coulomb hole has been used to study correlation effects in many electron atoms; see, for example, the work on Be by Benesch and Smith⁽¹⁴⁾ and Banyard

and Mobbs⁽¹⁵⁾. However, its application to molecular systems has been very limited due to the multi-centre nature of the wavefunctions. The recent example of the HeH^+ molecular ion in position space⁽¹⁷⁾ was tractable largely because of the availability of an energetically acceptable one-centre correlated wavefunction. Besides analysing ground state correlation effects in terms of the $\Delta f(r_{12})$ vs. r_{12} curves, it has also been demonstrated that a complementary investigation in momentum space can be equally informative. This arises because the radial and angular components of electron correlation produce differing characteristics in the analogous $\Delta f(p_{12})$ vs. p_{12} curves. Such curves, known as Coulomb shifts, have provided insight into the variation of the relative importance of radial and angular correlation effects throughout a series of He-like ions^(18,19) and as a function of R for HeH^+ ⁽¹⁶⁾, where R is the internuclear separation. For molecules, momentum space has the computational advantage of making the problem effectively single-centred.

The study of momentum distributions within molecules should provide a fresh perspective from which to view the mechanisms governing the formulation of the chemical bond and the influence of electron correlation on the charge density. Coulson and Duncanson⁽²⁰⁻²⁷⁾ pioneered the calculation of electron momentum distributions for molecules forty years ago. In the first of a series of papers Coulson⁽²²⁾ considered the single bond with especial reference to the systems H_2^+ and H_2 . He showed that, with respect to non-interacting atoms, the formation of a bond

decreases the mean component of the momentum in the direction of the bond, increases the mean component perpendicular to the bond and increases the mean momentum average over all directions. The innovative studies of Coulson and Duncanson were, however, severely handicapped by lack of good atomic and molecular wavefunctions. Henneker and Cade⁽²⁸⁾ have since used wavefunctions of Hartree-Fock (HF) quality to give a more qualitative explanation of the above observations by considering the diatomic molecules LiF and N_2 . Nowadays, correlated wavefunctions of quality beyond that of the HF are readily available and enquiries have been made into electron correlation effects on the calculated momentum distribution in molecules^(12,13). Brown and Smith⁽²⁹⁾ have analysed the consequences of correlation on the electronic momentum distribution in the simplest two-electron molecule, H_2 .

It is over fifty years since Heitler and London⁽³⁰⁾ published their classic paper on the quantum theory of the chemical bond in the simplest of all molecules, H_2 . In the same year Burrau⁽³¹⁾ calculated with astonishing accuracy, by direct numerical solution of the Schrödinger equation, the bond length and dissociation energy of the hydrogen molecule ion H_2^+ . These papers marked not only the beginning of quantum chemistry but also the beginning of two rival theories: the valence bond (VB) theory which emphasises the role of electron pairs, the the molecular orbital (MO) theory which emphasises the quasi-independence of electrons by assigning each to its own 'orbital'. These two approaches were to dominate the subject for many years

to come.

An atom is a special case of a molecule, in which there are N electrons but only one nucleus, and it is not surprising that many techniques used in atomic structure calculations (see a review by Hibbert⁽³²⁾) are also employed in molecular theory. Many of the aims will also be similar. Besides calculating the ground-state electronic structure (the wavefunction and electron density) we ought to be able to deal with excited states and to calculate spectroscopic terms values, oscillator strengths for transitions, the fine and hyperfine structure of the energy levels resulting from relativistic corrections to the Hamiltonian, and so on. In short, we should be able to calculate not only structure but properties. In the case of a molecule, however, the challenge is even more overwhelming, for in addition to the physical properties we should also be able to calculate the chemical properties. A molecule has a geometry which we indicate by drawing straight lines to connect pairs of 'bonded' atoms, and we ought to be able to calculate bond lengths, bond angles, force constants for stretching and bending, the energy needed to break a specific bond, dissociating the molecule into two fragments; the interactions between molecules and the chemical reactions which may occur when they come into close proximity, and all the properties revealed by modern spectroscopic methods including electron spin resonance (ESR), nuclear magnetic resonance (NMR), nuclear quadrupole resonance (NQR), photoelectron spectroscopy (PES) and many more.

The demands on the theory itself are no less severe. The energy required to break a bond is typically of the order of 5eV, but the total electronic energy (given by the solution of the Schrödinger equation) may be thousands of times larger; to estimate a dissociation energy as a difference of two such large quantities is clearly a hazardous exercise. Nor are there, in general, any elegant methods of reducing the complexity of the problem, for polyatomic molecules usually lack symmetry and powerful methods of angular momentum theory, used to such good effect in atomic calculations, are no longer applicable.

SCF calculations of increasing degrees of complexity have led to results for the energy which have reached the HF limit⁽³³⁾; at the same time, more sophisticated techniques have enabled a large portion of the correlation energy to be taken into account⁽³⁴⁻⁴⁰⁾. The LCAO-MO-SCF procedure developed by Roothaan⁽⁴¹⁾ has been applied to a great many molecules and wavefunctions produced by this method are a good zeroth-order approximation to the true wavefunction. Attempts to improve this approximation by adding correlating terms, via configuration-interaction methods, initially did not share the success produced in atomic systems. Ebbing⁽³⁴⁾, for instance, carried out a calculation on LiH using 53 configurations and obtained only 65% of the correlation energy. This lack of success led to a resurgence of interest in the nonorthogonal or valence bond formalism. Harris and Taylor⁽³⁵⁾ published a four configuration wavefunction which nearly matched that of Ebbing, and Browne and Matsen⁽³⁶⁾ published a 28

configuration function which gave 85% of the correlation energy. In a landmark paper, Löwdin⁽⁴²⁾ introduced the concept of natural spin orbitals and the equations for computing them. These orbitals form an orthonormal set and an orbitals occupation number gives a direct measure of its importance in the wavefunction. The natural orbital expansion for two-electron systems has been much studied⁽⁴³⁻⁴⁵⁾ and it is now clear, from the work of Davidson and Jones⁽⁴³⁾, that only four configurations built from natural orbitals are required to obtain 90% of the correlation energy of H_2 . Bender and Davidson⁽⁴⁶⁾ outlined a new procedure for calculating natural orbitals without actually solving the integrodifferential equations. Their procedure consisted simply of the following steps: a) make an initial guess to the natural orbitals in terms of some basis set; b) construct an approximate wavefunction from a reasonable number of configurations formed from these orbitals; c) compute the natural orbitals for this wavefunction; and d) using these orbitals as a guess, repeat steps b and c until the wavefunction and orbitals converge. Bender and Davidson's work on LiH produced an energy of -8.0604 which remains the best available variational approximation to the LiH ground state energy. Their basis set consisted of 12σ , 6π and 5δ functions expanded on elliptic orbitals. Bender and Davidson in their subsequent work on the first row diatomic hydrides⁽⁴⁷⁾ pointed out the limitations of elliptic type orbitals when applied to systems with more than one electronic shell.

In this initial study of a two-centre wavefunction, we restrict ourselves to R (the bond length) = 3.015au and, because of the essential convenience of its structure and its STO basis set, we use the 262 term configuration-interaction (CI) wavefunction of Arrighini, Tomasi and Guidotti⁽⁴⁸⁾. The leading term in their ground state wavefunction for LiH is, by design, a good approximation to the restricted near HF description. The correlation terms are formed from 17 virtual orthonormal basis orbitals by considering all possible single and double excitations from the HF reference state; triple and quadruple excitations were not included. As in Part I of this thesis for Be, the partitioning of the correlated two-particle density into its pairwise components was eased considerably by the orthogonality of the basis set and by the fact that we could use the leading configuration as the uncorrelated (\sim HF) description of LiH. With respect to their SCF-reference state, the 262-term function of Arrighini et al accounted for 82.1% of the correlation energy.

CHAPTER III.2
THE WAVEFUNCTION

As discussed in Part II of this thesis the difficulty in the partitioning of an N-electron two-particle density into its pairwise components can be eased considerably if the wavefunction is constructed from an orthonormal basis set and includes the HF term as the leading configuration. The wavefunction of Arrighini et al, published in 1970, fulfills these requirements. Although not the best, energy wise, wavefunction available in the literature, for LiH, the structure of its basis set and the construction of the wavefunction itself made it a favourable function to initiate investigative studies of electron correlation in a simple molecular system. In addition, an overriding factor in selecting this particular function was the availability of all of the expansion data; a factor so often overlooked in the publication of modern wavefunctions.

Arrighini et al expanded the unknown HF MO's ϕ_i in terms of a finite basis set of STO's $\{\varphi\}$ centered at both nuclei, ie.,

$$\phi_i = \sum_k c_k \{\varphi\} \quad \text{III.1}$$

The basis set consisted of 11 STO's, 1s 1s' 2s 2s' 2s" 2p & 2p' centred on the Li atom and 1s 1s' 2p & 2p' centred on

the H atom. Their associated orbital exponents were carefully selected by preliminary investigations on the Li^+ ion and hydrogen atom. The resulting HF wavefunction, which was normalised to unity, gave an HF energy value $E = -7.98624\text{au}$ and should be compared to the calculation of Cade and Huo⁽³³⁾ who obtained, what is regarded as a true HF limit, a value of -7.98731au .

The CI wavefunction can be considered as being constructed from an innershell, outershell and an intershell component, denoted by $\text{CI}[\text{rs}, 2\sigma^2]$, $\text{CI}[1\sigma^2, \text{tv}]$ and $\text{CI}[1\sigma 2\sigma, \text{rt}]$ respectively. The wavefunction $\text{CI}[\text{rs}, 2\sigma^2]$ includes the configurations arising from promotions of the molecular innershell electrons into orbitals r & s: all possible configurations were considered, 9 of single substitution (SS) type and 65 double substitution (DS) type. The resulting energy improvement, -0.035876au could be interpreted as the correlation energy of the LiH innershell. An analogous remark can be made for the wavefunction $\text{CI}[1\sigma^2, \text{tv}]$ where the two 2σ electrons have been promoted into orbitals t & v. This includes the configurations arising from excitations of the outershell electrons, 9 SS type and 65 DS type. Finally, the wavefunction $\text{CI}[1\sigma 2\sigma, \text{rt}]$ contains all configurations resulting from simultaneous excitations of the electrons from the 1σ and 2σ orbitals, one from each of them. In this case only DS configurations result (113 in number).

In order to make possible a CI procedure involving π orbitals, the basis set was enlarged to include, for any $2p_z$

function already present in the basis set, a pair ($2p_x, 2p_y$) with the same orbital exponent. The basis set so enlarged leads to 17 virtual orbitals (8 of π -type), in terms of which the configurations are to be built up. Taking into account only singly and doubly excited configurations, the total number of these which interact with the HF ground state ($^1\Sigma$) is 261, 18 of which are single substituted; the remaining 243 are double substituted configurations. Table III.2 shows the distribution of these configurations in contributing to the various intra and intershell correlation effects. 148 configurations are used to represent the intrashell correlation effects (74 in each of the outer- and innershells) whilst the remaining 195 configurations contribute to the intershell correlation effects. The final energy for the 262-term CI wavefunction (normalised to unity) for LiH gave a total energy of -8.05545au representing, as mentioned previously, 82.1% of the correlation energy.

CHAPTER III.3

RESULTS AND CALCULATIONS

Electron correlation within a wavefunction may be investigated by examining the differences between the correlated two-particle density and the corresponding HF density. The definition of Γ , the two-particle density, in terms of an N-particle wavefunction has been described in Part II of this thesis and is normalized to equal the number of independent electron pairs within the system. The two-particle density for the individual electronic shells is obtained by partitioning Γ into its pairwise components Γ_{ij} ; where the (i,j) label the occupied normalized spin-orbitals in the restricted HF description of our system. As discussed earlier, for Γ_{HF} the partitioning is both straight forward and exact but, the resolution of Γ_{corr} , the correlated two-particle density, into its intra and inter-shell components can only be carried out approximately; see, once again, Part II of this thesis.

Following our earlier work on Be, it is clear that the original approach of Banyard and Mashat⁽⁴⁹⁾, whose evaluation of the partitioning technique has been outlined in Equations II.35 and II.36, can be considered to be an excellent 'first order' approximation when used to partition Γ_{corr} and that the full partitioning technique given by Equation II.28 need only be applied to wavefunctions that

exhibit, in the case of an orthonormal basis set, configurations with large coefficients as a result of degenerate orbitals. In the case of Be the large coefficient for the $1s^2 2p^2$ configuration came from the degeneracy which exists between the '2s' and '2p' orbitals in Be. In Table III.1 we present a comparable table to Table II.1 showing the leading configurations of the Arrighini et al wavefunction. As can be seen from this table no degenerate orbitals exist for LiH; the second largest coefficient is for the $1s^2 6\sigma^2$ configuration having a value of -0.06987 (the largest coefficient is of course for the leading HF term, with a value of 0.98537). Thus the CI function of Arrighini et al⁽⁴⁸⁾ was restricted in terms of the many body expansion proposed by Sinanoglu⁽⁵⁰⁾ and Γ_{corr} was then formed by retaining only 'first order' terms as far as, and including, the pair correlation functions U_{ij} ; integrations were carried out over all electron coordinates except those associated with electrons 1 and 2. The resulting expressions for Γ_{HF} and Γ_{ij} in terms of Ψ_{corr} , the Arrighini correlated wavefunction for LiH, and ϕ , the HF spin orbitals are:

$$\Gamma_{\text{HF}}(\underline{z}_1, \underline{z}_2) = 1/2 \sum_{i < j}^{N=4} \{ \phi_i(\underline{z}_1) \phi_j(\underline{z}_2) - \phi_j(\underline{z}_1) \phi_i(\underline{z}_2)^* \\ \phi_i(\underline{z}_1) \phi_j(\underline{z}_2) - \phi_j(\underline{z}_1) \phi_i(\underline{z}_2) \}, \text{ III.2}$$

$$\Gamma_{\text{corr}}(\underline{z}_1, \underline{z}_2) = \sum_{i < j}^{N=4} \{ \phi_i(\underline{z}_1) \phi_j(\underline{z}_2) - \phi_j(\underline{z}_1) \phi_i(\underline{z}_2) \} [$$

$$\langle \Psi_{\text{corr}} | \Pi_{ij} \rangle / \langle \Psi_{\text{corr}} | \Pi \rangle - 1/2 \{ \phi_i(\underline{z}_1) \phi_j(\underline{z}_2) \\ - \phi_j(\underline{z}_1) \phi_i(\underline{z}_2) \}] \quad \text{III.3}$$

where z has been used to represent a general coordinate denoting either position or momentum space. The integrations in $\langle \Psi_{\text{corr}} | \Pi_{ij} \rangle$ are over all the coordinates occurring in Π_{ij} and thus we obtain a function of z_1 and z_2 only.

Conversion of position MO to momentum space MO

A general coordinate, z , has been used in Equations III.2 and III.3 to emphasize that the partitioning technique can be accomplished in either position or momentum space. Having partitioned the two-particle density into its pairwise components in position space, say, the various orbitals are then converted to momentum space coordinates or, of course, we can convert the original wavefunction, Ψ_{corr} , and then partition the resulting momentum two-particle density. Either way a basis set function, in this particular instance a Slater type orbital (STO), has to be converted from position to momentum space coordinates.

Momentum space electronic wavefunctions can be obtained through the Fourier transformation⁽⁵¹⁾ of ordinary position-space wavefunctions. Thus, we may write, using the notation of Equation III.1

$$X(p) = h^{-3/2} \int \phi_i(\underline{r}') e^{-ip \cdot \underline{r}} d\underline{r} \quad \text{III.4}$$

where $\phi_i(\underline{r}')$ is a position space molecular orbital and $X(p)$ is its momentum space counterpart. From Equation III.1 it

can be seen that ϕ_i is constructed from primitive basis functions centred on both nuclei, thus Equation III.4 may be written as follows:

$$\chi(\underline{p}) = h^{-3/2} \int [\{\varphi\}_{Li}(\underline{r}_A) + \{\varphi\}_H(\underline{r}_B)] e^{-i\underline{p} \cdot \underline{r}} d\underline{r} \quad \text{III.5}$$

where $\{\varphi\}_{Li}(\underline{r}_A)$ and $\{\varphi\}_H(\underline{r}_B)$ are the sets of primitive STO functions centred on the Li and H nuclei, respectively. The vectors \underline{r}_A , \underline{r}_B and \underline{r} are the position vector of the electron from, respectively, the Li nucleus, the H nucleus and an arbitrary origin. Taking site A, the Li nucleus, as the origin these vectors take more simpler form thus:

$$\underline{r} = \underline{r}_A = \underline{R} + \underline{r}_B$$

where \underline{R} is the bond length. With this substitution for \underline{r} Equation III.5 may be written as

$$\begin{aligned} \chi(\underline{p}) &= \int \{\varphi\}_{Li}(\underline{r}_A) e^{-i\underline{p} \cdot \underline{r}_A} d\underline{r}_A \\ &\quad + \int \{\varphi\}_H(\underline{r}_B) e^{-i\underline{p} \cdot (\underline{R} + \underline{r}_B)} d\underline{r}_B \\ &= \chi_A(\underline{p}) + e^{-i\underline{p} \cdot \underline{R}} \chi_B(\underline{p}) \end{aligned} \quad \text{III.6}$$

where $\chi_A(\underline{p})$ and $\chi_B(\underline{p})$ are the momentum space representation of orbitals on centres A and B. In order to transform $\{\varphi\}_{Li}(\underline{r}_A)$, or $\{\varphi\}_H(\underline{r}_B)$, we use Bauer's⁽⁵²⁾ expansion of $e^{-i\underline{p} \cdot \underline{r}_A}$, or $e^{-i\underline{p} \cdot (\underline{r}_B)}$, given by the following expression:

$$e^{-i\underline{p} \cdot \underline{r}} = 4\pi \sum_{l=0}^{\infty} (-i)^l j_l(pr) \sum_{m=-l}^l Y_{lm}^*(\omega_r) Y_{lm}(\omega_p), \quad \text{III.7}$$

where \underline{r} has been used to represent either \underline{r}_A or \underline{r}_B , ω_r and ω_p represents the combined angular variables in position and momentum space, and $j_l(pr)$ is a spherical Bessel function⁽⁵³⁾.

The functions $\{\varphi\}_{Li}(\underline{r}_A)$ and $\{\varphi\}_{H}(\underline{r}_B)$ are constructed from Slater-type orbitals (STOs) given by

$$\varphi(\underline{r}) = N R(r) Y_{l, m'}(\omega_r) \quad \text{III.8}$$

In Equation III.8, $R(r)$ is the radial part of the function defined as

$$R(r) = e^{-\xi r} r^{n-1},$$

where r is measured from the appropriate atomic centre; N is the normalization factor expressed as

$$N = [2\xi]^{n+1/2} / \sqrt{[(2n)!]}$$

and $Y_{l, m'}(\omega_r)$ is a normalized spherical harmonic.

The primitive STO functions contained within $\{\varphi\}_{Li}(\underline{r}_A)$, or $\{\varphi\}_{H}(\underline{r}_B)$, are converted, individually, to momentum space coordinates in the following way

$$\chi(\underline{p}) = h^{-3/2} \int \varphi(\underline{r}) e^{-i\underline{p} \cdot \underline{r}} d\underline{r} \quad \text{III.9}$$

where $\chi(\underline{p})$ is the momentum space representation of a

particular φ function. Combining Equations III.8 and III.9, and expressing $e^{-i\mathbf{p}\cdot\mathbf{r}}$ in terms of spherical harmonics, as shown by Equation III.7, we obtain the following expression for $\chi(\mathbf{p})$

$$\chi(\mathbf{p}) = N \sqrt{2/\pi} \sum_{l'=0}^{\infty} \sum_{m'=-l'}^{l'} (-i)^{l'} Y_{l'm'}(\omega_{\mathbf{p}}) \int_0^{\infty} j_{l'}(pr) R(r) r^2 dr \int_0^{2\pi} \int_0^{\pi} Y_{l'm'}^*(\omega_r) Y_{lm}(\omega) \delta\omega. \quad \text{III.10}$$

The angular integrations are carried out over all values of the solid angle ω , resulting in the two delta functions $\delta_{ll'} \delta_{mm'}$ which cancel all terms in the summation except when $l = l'$ and $m = m'$. Thus, we obtain

$$\chi(\mathbf{p}) = N R(p) Y_{lm}(\omega_{\mathbf{p}}), \quad \text{III.11}$$

where

$$R(p) = \sqrt{2/\pi} (-i)^l \int_0^{\infty} j_l(pr) R(r) r^2 dr. \quad \text{III.12}$$

Equation III.12 can be written as

$$R(p) = (-i)^l \int_0^{\infty} 1/\sqrt{pr} J_{l+1/2}(pr) R(r) r^2 dr, \quad \text{III.13}$$

where $J_{l+1/2}(pr)$ is an ordinary Bessel function of order $(l + 1/2)$ and can be written in terms of a spherical Bessel function through the relationship

$$J_{l+1/2}(pr) = \sqrt{2pr/\pi} j_l(pr). \quad \text{III.14}$$

Substituting Equation III.13 into III.11 and including the expression for $R(r)$ yields

$$\chi(\underline{p}) = N(-1)^l / \sqrt{(p)} Y_{lm}(\omega_p) \int_0^{\infty} J_{l+1/2}(pr) e^{-\xi r} r^{n+1/2} dr \quad \text{III.15}$$

The radial integral is evaluated by making use of the definite integral⁽⁵³⁾

$$\int_0^{\infty} e^{-at} J_{\nu}(bt) t^{\nu} dt = (2b)^{\nu} \Gamma(\nu+1/2) / [\sqrt{\pi}(A)^{\nu+1/2}] , \quad \text{III.16}$$

$$\text{where } A = a^2 + b^2 .$$

Differentiating this function q times with respect to the quantity a we obtain

$$\begin{aligned} & \int_0^{\infty} e^{-at} J_{\nu}(bt) t^{\nu+q} dt \\ &= (-1)^{-q} (2b)^{\nu} / \sqrt{\pi} \Gamma(\nu+1/2) \frac{\partial^q}{\partial \xi^q} (1/A^{\nu+1/2}) . \end{aligned} \quad \text{III.17}$$

Comparing Equations III.17 and III.15 if we let $\nu = (l+1/2)$, $\nu+q = n + 1/2$ (ie., $q = n-l$), $t=r$ and $b=p$, the integral in Equation III.15 becomes equal to the integral expression of Equation III.17. Thus in atomic units,

$$\begin{aligned} \chi(\underline{p}) &= N (-1)^{n-l} (2p)^{l+1/2} l! i^{-l} 1/\sqrt{(p\pi)} \\ & \frac{\partial^{n-l}}{\partial \xi^{n-l}} (\xi^2 + p^2)^{-(l+1)} Y_{lm}(\theta_p, \phi_p) . \end{aligned} \quad \text{III.18}$$

With this knowledge of the individual $\chi(\underline{p})$'s the complex function $X(\underline{p})$ may then be produced. Examples of the functional form of the momentum-space STOs used in this work may be found in Ref. 54, Appendix A.1.

Expectation values

As discussed in Part II of this thesis, we can define a two-particle radial density $D(p_1, p_2)$ given by

$$D(p_1, p_2) = \int r_{ij}(p_1, p_2) p_1^2 p_2^2 d\omega_1 d\omega_2, \quad \text{III.19}$$

where the integrations in Equation III.19 are taken over all values of the solid angles ω_1 and ω_2 . Associated with $D(p_1, p_2)$ is the mean radial distribution function, $I(p_1)$, defined for molecular systems by Duncanson and Coulson⁽²⁷⁾ such that $I(p_1)dp_1$ is the probability that the electron has a momentum between p_1 and p_1+dp_1 . Such a definition is completely analogous to the atomic momentum one-particle distribution function $d(p_1)$ discussed in Part II and is given by Equation II.62. Thus $I(p_1)$ may be evaluated by integration of Equation III.19 as follows:

$$I(p_1) = \int D(p_1, p_2) p_2^2 dp_2. \quad \text{III.20}$$

Both distributions represented by Equation III.19 and III.20 are normalised such that

$$\int D(p_1, p_2) dp_1 dp_2 = 1$$

and

$$\int I(p_1) dp_1 dp_2 = 1 .$$

The effects of correlation may be investigated via pictorial representation of the $I(p_1)$ function at both the HF and correlated levels, as discussed by Duncanson and Coulson⁽²⁷⁾. In Figures III.1 and III.2 we present the innershell and outershell $I_{HF}(p_1)$ and the associated functions $\Delta I(p_1)$ expressed as the difference between the two $I(p_1)$ distributions calculated using the correlated wavefunction and the HF wavefunction, thus

$$\Delta I(p_1) = I_{\text{corr}}(p_1) - I_{\text{HF}}(p_1) . \quad \text{III.21}$$

In Figure III.3 we present the $I(p_1)$, and $\Delta I(p_1)$, calculated for the whole atom.

The effect that electron correlation has on this one-particle function can also be investigated, more traditionally, with the aid of expectation values. In Table III.4 we present the one-particle expectation values defined by

$$\langle p_1^n \rangle = \int p_1^n I(p_1) dp_1 \quad \text{III.22}$$

evaluated for $n = -2, -1, 1$ and 2 and, as such, are used to assess the effects of electron correlation in different regions of the $I(p_1)$ distribution.

Electron correlation has a more influential effect upon the two-electron properties. Thus, to assist the discussion the two-particle expectation values

$$\langle p_1 \cdot p_2 / p_1^n p_2^n \rangle = \int (p_1 \cdot p_2 / p_1^n p_2^n) r_{ij}(p_1, p_2) dp_1 dp_2, \quad \text{III.23}$$

and

$$\langle p_1^n p_2^n \rangle = \int p_1^n p_2^n D(p_1, p_2) dp_1 dp_2, \quad \text{III.24}$$

have been evaluated for various values of n . Equation III.23, which involves the angle γ_{12} between the momentum vectors p_1 and p_2 and is therefore sensitive to angular correlation, has been evaluated for n values of 0, 1 and 2, whilst Equation III.24, which is particularly sensitive to radial correlation, has associated n values of -1 and 1. These results can be found in Tables III.6 and III.10.

The angular integrations of Equation III.23 are solved by expanding $\cos \gamma_{12}$ in terms of spherical harmonics by using the Addition theorem given by:

$$P_l(\cos \theta) = 4\pi / (2l+1) \sum_{m=-l}^l Y_{lm}^*(\theta_1, \varphi_1) Y_{lm}(\theta_2, \varphi_2) \quad \text{III.25}$$

evaluated for $l=0$. Then the angular integrations of Equation III.23 may be carried out by repeatedly using the coupling rule for spherical harmonics which permits an easy evaluation of the product of three spherical harmonics thus:

$$\int Y_{l_3 m_3}^* Y_{l_2 m_2} Y_{l_1 m_1} d\Omega = \int \sqrt{[(2l_1+1)(2l_2+1)/(4\pi(2l+1))]} d\Omega$$

$$C(l_1 l_2 l; m_1 m_2 m) C(l_1 l_2 l; 000) \int Y_{l_3 m_3}^* Y_{l_1 m_1 + m_2} d\Omega \quad \text{III.26}$$

The elements of the transformation in Equation III.26 are called Clebsch-Gordan (or Wigner) coefficients and are defined by Rose⁽⁵⁵⁾. These coefficients are also referred to as vector-addition coefficients, since we add l_1 to l_2 to get l and m_1 to m_2 to get m .

The $\Delta(z)$ values, shown in Tables III.4 and III.5, are the standard deviations of the functions associated with z . The standard deviation, defined by Equation II.45, measures the spread, or dispersion, of a particular distribution about its mean value and, as such, gives as a single index a measure of the effect that correlation has had on that distribution.

Coulomb Shifts and Partial Coulomb Shifts

As discussed in Part II, for a given $p_{12} = |p_1 - p_2|$ the Coulomb shift corresponding to the HF spin orbital pair (i, j) is given by

$$\Delta f_{ij}(p_{12}) = \int \Delta \Gamma_{ij}(p_1, p_2) dp_1 dp_2 / dp_{12} \quad \text{III.27}$$

where $\Delta \Gamma_{ij}(p_1, p_2)$ is the change, due to correlation, in the partitioned two-particle density after transformation into momentum space. Spin has been intergrated out of Equation III.27 and the limits of integration have been discussed

earlier. The Coulomb shifts for the individual intra and intershells in LiH are shown in Figures III.4 to III.7. It is to be noted that the (i,j) pairs (1,4) and (2,3) have once again been combined and rewritten to yield pure spin states $^1\Gamma$ and $^3\Gamma$ for the intershells. In Figure III.8, we compare the sum total Coulomb shift for LiH with its individual components. The γ_p -values in Table III.10 represent the percentage of each $f_{HF}(p_{12})$ probability density which has been redistributed due to correlation.

It was shown earlier, see Part II, that the effects of electron correlation may be discussed and visualised in terms of the partial Coulomb shift, $\Delta g_{ij}(r_{12}, p_1)$, which measures the influence of correlation when a test electron, say electron 1, has a momentum of a given magnitude p_1 . These shifts are defined such that

$$\int \Delta g_{ij}(p_{12}, p_1) dp_1 = \Delta f_{ij}(p_{12}) \quad \text{III.28}$$

and the Δg results for each of the electronic shells are displayed in Figure III.9.

CHAPTER III.4

DISCUSSION

As shown in Part II of this thesis, and in the earlier work of Banyard and Reed⁽¹⁹⁾, a 'dual' investigation in both position and momentum space aids discussion towards the total understanding of the effects of electron correlation contained within a particular system. From their subsequent work on HeH^+ , Banyard and Reed^(16,17) showed that these two complementary investigations lead to an increased knowledge of the way in which molecules are formed as the two component subsystems are brought nearer to one another. However, their calculation based on the HeH^+ system was only tractable because of the availability of a single centred wavefunction and, generally, the two-centred nature of any molecular system has meant that very few investigative studies have been performed. Although no comparable position space calculation to that of Banyard and Reed upon HeH^+ has been performed on LiH , the position space investigation of Banyard and Hayns⁽⁵⁶⁾ into the charge distribution in LiH will be of particular interest and their findings will be briefly outlined here.

Banyard and Hayns showed that the contour map for the charge distribution associated with the HF wavefunction reveals the existence of two extensive regions of density of almost spherical symmetry associated with each nucleus. The

spread of the charge cloud around the Li nucleus being reduced in extent, with respect to the charge cloud around the H centre, by the larger nuclear charge. The spherical symmetry suggests an $\text{Li}^+ \text{H}^-$ ionic interpretation of the density. This point is emphasized further by the steep gradient of the charge distribution behind the Li nucleus, a characteristic of an $\text{Li}^+(1s)^2$ core. The influence of electron correlation on the molecular charge distribution reveals several features of interest: in particular, the difference maps produced by Banyard and Hayns indicated a reduction of charge density in the mid-bond region and an increase of charge at, and immediately around each nucleus. Further, an increase in density also occurs in a toroidal outer region around the bond axis at the position of the Li nucleus. The effect of electron correlation also gives rise to a closed negative contour behind the Li nucleus. This implies that, in this region of space, a slight preferential increase of charge has occurred during molecular formation. Such a feature is in general accord with the description by Bader, et al⁽⁵⁷⁾ of the charge movements associated with ionic bonding.

Returning to our investigation on LiH let us now consider the innershell $I_{\text{HF}}(p_1)$ distribution and discuss the effects of correlation by investigating the difference function, $\Delta I(p_1)$, evaluated from $I_{\text{corr}}(p_1) - I_{\text{HF}}(p_1)$. Both of these curves are presented in Figure III.1. The $I_{\text{HF}}(p_1)$ curve for the innershell of LiH are comparable with the results obtained by Youngman⁽⁵⁸⁾ for the $K\alpha K\beta$ shell of Li. Although the function is not a true spin state, ie., cannot

be written as a separable space and spin function, the molecular innershell region shows a similar shape to that obtained for the $d_{\text{HF}}(p_1)$ curve of the atomic system. The $\Delta I(p_1)$ curve for the innershell shows a redistribution of the one-particle probability into two regions. The larger movement, of the distribution, is towards smaller p_1 with a second region showing a very flat but quite extensive redistribution towards larger p_1 ; this implies, of course, that probability is reduced at intermediate values of p_1 . Table III.4 contains one-particle expectation values calculated from the HF one-particle distribution, $I_{\text{HF}}(p_1)$, and from the associated correlated distribution, I_{corr} . Inspection of these results show an increase in $\langle p_1^{-1} \rangle$ and $\langle p_1^{-2} \rangle$ with the largest change for $\langle p_1^2 \rangle$ and only minimal change for $\langle p_1 \rangle$. These results are concomitant with radial correlation where, if we consider the effects of radial correlation on two electrons in position space, one electron moves out away from the nucleus whilst the other move in towards it. The momentum of each of these electrons will, respectively, decrease, for the electron that is further away from the nucleus, and increase, for the nearer electron.

From the innershell radial expectation values given in Table III.6 we notice that the effect of electron correlation is to reduce $\langle p_1^n p_2^n \rangle$ for each n . A similar effect was found for the two-electron systems investigated by Banyard and Reed^(16,17). In particular, their result for $\langle p_1^n p_2^n \rangle$, $n = -1$ and 1 , obtained for Li^+ show comparable magnitudes to those evaluated here for the LiH innershell.

Also, their one-particle expectation values, $\langle p_1^n \rangle$, are quite similar to the values obtained for the molecular innershell. In particular, they obtained a correlated value for $\langle p_1^{-2} \rangle$ and $\langle p_1^2 \rangle$ of 0.756 and 7.279, respectively, which are comparable to the equivalent values shown in Table III.4. Presented in Table III.5 are the one-particle expectation values for the three-electron systems evaluated by Youngman⁽⁵⁸⁾ and Al-Bayati⁽⁵⁹⁾ where comparisons show that the innershell of LiH has similar magnitudes to the intrashell results obtained for Li. It is interesting to note that the results of Banyard and Reed for HeH⁺ showed that the single particle expectation values, evaluated at the equilibrium bond length (R=1.4au), were in closer agreement to their earlier results for He than for an equivalent Z=3 system, i.e., Li. The standard deviation Δp_1 presented in Table III.4 show a slight broadening of the one-particle density as a result of the addition of electron correlation.

The values of $\langle (p_1/p_1^n) \cdot (p_2/p_2^n) \rangle$ given in Table III.10 for $n = 2, 1$ and 0 assess the effects of angular correlation but with emphasis being placed on different regions of the two-particle momentum density. The results for the inner-shell of LiH clearly show small changes in the interparticle angle as a consequence of correlation. The positive sign of all values show that this angle has been reduced from their HF value of 90°. Presented in Table III.11 are the equivalent values obtained for Li and Be⁺, these results taken with the angular values obtained by Banyard and Reed show a similar trend as n decreases from 2 to 0 but the

absolute magnitude of these values are beyond comparison. Once again a possible consequence of the absence of angular terms within the Arrighini wavefunction.

Let us now investigate the effects of correlation on the two-particle properties and consider $\Delta f(p_{12})$ for the inner-shell of LiH. Recalling from Part II of this thesis, analysis of Coloumb shifts in momentum space has revealed that when $\Delta f(p_{12})$ is initially negative this is a feature of radial correlation; whereas, by contrast, a Coulomb shift which is positive at small p_{12} is indicative of angular correlation. From Figure III.4 it is apparent that radial correlation is the dominant effect for this innershell region. This of course is to be expected from the structure of the wavefunction where, as can be seen from Table III.3, the number of σ functions considered is two and half times that of π functions. However, interesting features are to be found when the Coulomb shift for the innershell of LiH is compared with results obtained for other systems. For instance, an obvious comparison must be made between this shift and the comparable K-shell Coulomb shifts evaluated in Part II for atomic Be. In this case the presence of a filled outer 2s shell meant that the atomic K-shell was confined, in terms of any large radial correlation effects, and angular correlation showed as a marginally, dominant effect. In the molecular case the outershell is not as restrictive. Indeed, as discussed above, the work of Banyard and Hayns showed at the HF level of approximation the LiH system behaves like Li^+ and H^- ; even at a correlated level the outershell cannot be considered as having the same

effect as the filled 2s shell of Be. However, similarities do exist between the Be K-shell Coulomb shifts and the results obtained for LiH innershell at larger p_{12} values where, particularly, we once again observe a crossover of the $\Delta f(p_{12})$ curve and the p_{12} axis at a p_{12} value of approximately 6. Although this tail region is not as deep as the result obtained in the Be calculation. Also presented in Figure III.4 is the Coulomb shift evaluated for Be^{2+} by Reed⁽⁵⁴⁾ which offers further similarities with the result for LiH; in particular, the maximum of the Be^{2+} Coulomb shift is comparable to the innershell result and once again the crossover at small p_{12} occur at similar values. Coulomb holes and Coulomb shifts for atomic systems can be brought into reasonable 'coincidence' by scaling the abscissa values to give Zr_{12} in position space and $Z^{-1}p_{12}$ in momentum space, Z being the nuclear charge. Al-Bayati⁽⁵⁹⁾ has presented several such scaled Coulomb shift curves for two electron systems and partitioned subsystems evaluated by himself, Banyard and Reed⁽¹⁹⁾, Youngman⁽⁵⁸⁾ and Mobbs and Banyard⁽⁶⁰⁾. The series includes $\text{Li}^+(1s)$, $\text{Li}(2s)$, $\text{Be}^{2+}(1s)$, $\text{Be}^+(2s)$ and $\text{Be}(1s)$ and all curves show a coincidence at the crossover point at $Z^{-1}p_{12} = 1.5$. If we were to scale in a similar manner the innershell of LiH, by assuming a scaling factor of $Z = 4$, then this curve will also be in agreement with the other two-electron results.

Finally, to conclude the discussion upon the LiH innershell we shall investigate the effect of electron correlation on the expectation value $\langle p_{12}^n \rangle$. From Table III.8 it can be seen that the mean value $\langle p_{12} \rangle$ has been

reduced from its HF value whilst an enhancement is observed for the other two values. Once again comparing these results with the three-electron, Li and Be⁺, values presented in Table III.9 all expectation values have magnitudes comparable to the Li innershell. Further comparisons can be made with the two-electron result, for $\langle p_{12}^n \rangle$, of Banyard and Reed who obtained for Li⁺ HF values, based on the HF wavefunction of Clementi⁽⁶¹⁾, of 0.42501, 3.2961 and 14.473; and correlated values evaluated from the CI description provided by Weiss⁽⁶²⁾ of 0.42592, 3.2540 and 13.979 for $n = -1, 1, 2$

For the outershell of LiH the $\Delta I(p_1)$ curve in Figure III.5 shows similar features observed for the innershell. Electron correlation has redistributed the HF one-particle density towards smaller and larger p_1 values; a consequence, as discussed above, of radial correlation. The range of the outer tail region is not so diffuse as that observed for the innershell. The magnitude of the changes for the outershell region are approximately twenty times those observed for the innershell with a corresponding change in the range of p_1 values of only approximately one third. The one-particle expectation values presented in Table III.4 show an increase in all values over their HF values with the largest increase, as expected from Figure III.2, in $\langle p_1^{-2} \rangle$. An associated change in the two-particle values is observed where both $\langle p_1^{-1} p_2^{-1} \rangle$ and $\langle p_1 p_2 \rangle$ have decreased in magnitude.

At the HF level LiH approximates to a combined system very similar to Li⁺ and H⁻. The results obtained for the

LiH innershell have been shown to exhibit Li^+ characteristics therefore, it is appropriate to assume that the outershell results should be compared to the H^- momentum-space calculation of Banyard and Moore⁽¹⁸⁾ and Banyard and Reed⁽¹⁹⁾. These authors obtained values for $\langle p_1^n \rangle$, with associated n values of -2, -1, 1 and 2, of, respectively, 22.057, 3.248, 0.5566 and 0.5274. These values are consistent with the preface that in the atomic system one electron remains close to the nucleus whilst the second moves out further away from the nucleus. Clearly the smaller $\langle p_1^{-2} \rangle$ result for LiH suggests a movement of both electrons away from the H nucleus, but the confining effect of the Li nucleus prevents the second electron from being as diffuse as in the atomic case.

The Coulomb shift function for the LiH outershell, presented in Figure III.10, reflects the dominance of radial correlation a fact consistent with the behaviour of the radial expectation values discussed above. The magnitude of the $\Delta f(p_{12})$ function is reduced in comparison with the Be result by a factor of approximately 2, but both the atomic and molecular curves have a very similar range, without any scaling of the p_{12} axis, with the atomic system being more diffuse. The γ values given in Table III.10 show the percentage of each $f(p_{12})$ distribution that has been redistributed due to correlation. The result for the outershell is approximately three times that obtained for the innershell, an effect consistent with the results for Be where the L-shell percentages were found to be 5-6 times the K-shell results; remembering, of course, the large Be

results were attributed to the very large angular correlation effect present in the Be L-shell.

Due to the similar nature of the intershell Coulomb shift, presented in Figures III.6 & III.7, both distributions will be discussed simultaneously. Initial observation of these shifts implies that angular correlation is the dominant effect for these regions. However, inspection of Table III.3, and the angular expectation values presented in Table III.10, clearly show that the wavefunction of Arrighini has very few angular configurations that could contribute to such an extent as to outweigh any radial effects which have dominated the intrashells. So, therefore, we must look for some other explanation as to the appearance of the intershell shifts. Recalling the result of Banyard and Hayns who found, as a result of the addition of electron correlation, that the one-particle density was redistributed into a torodial distribution centred around the Li nucleus and at right angles to the bond axis. This increase in the one-particle density arises from a movement of one of the electrons from the H centre towards the Li centre and not just a redistribution of the charge cloud around the Li centre. They also found that for both wavefunction studied in their investigation that the correlated charge cloud was more diffuse throughout space than in the noncorrelated wavefunctions. As a consequence any electron within this distribution will have a smaller momentum than it had when centred on the H nucleus. Returning to the intershell Coulomb shifts we see an enhancement of the $f(p_{12})$

distribution at small p_{12} , this arises from this decrease in the outer electrons momentum. For the intershell $^3\Sigma$ curve the initial values of $\Delta f(p_{12})$ are vanishingly small, and as discussed earlier for atomic Be, this is a direct consequence of Fermi correlation. The extended tail region present on the $^1\Sigma$ Coulomb shift can be attributed to penetration of the outershell electron into the inner regions leading to a high p_{12} tail in the $f(p_{12})$ distribution. No such tail is seen in the triplet case because of the Fermi effect forbidding such a penetration.

The total Coulomb shift for the LiH molecule is presented in Figure III.8 and with a comparison of its individual components in Figure III.9. Once again we see the dominant nature of the intrashell shifts in forming the total shift, in particular the very large contribution from the outershell Coulomb shift, as was found in the atomic four electron study. The intershell shifts marginally reduces the effect of the outershell component whereas the innershell shift contribution leads to a shallow, but extensive, tail region.

Finally we conclude the discussion of electron correlation in LiH by considering the $\Delta g(p_{12}, p_1)$ surfaces presented in Figure III.10. Firstly, a general comment about the overall appearance all of these surfaces. Unlike the results for Be the intrashell Δg surfaces for the molecular system show a diagonal structure not dissimilar to that found in the intershells of the atomic system. Such structure has been associated with 'split-shell' densities

and, clearly, in the molecular system this is attributable to the multicentre nature of the wavefunction as shown by Equation III.1.

Consider the $\Delta g(p_{12}, p_1)$ surface for the innershell of LiH presented in Figure III.10A. The surface has negative values at small p_1 and p_{12} suggesting the dominance of radial correlation in this region. When p_1 is small, approximately 0.9, we see a shift of probability from low p_{12} to higher p_{12} . The minimum of this effect occurs at a p_{12} value of approximately 1.6 with a maximum effect at $p_{12} \approx 3.45$. When p_1 is small, the test electron is in the outer region of the 1σ shell. If the correlation effect is dominantly radial then the other (non-test) 1σ electron will contract towards the nucleus and therefore speed up. Its momentum p_2 will increase and thus a shift in probability towards higher p_{12} will occur since p_1 is at a fixed small value. The second maximum of the surface occurs on the diagonal structure at a p_{12} value approximately equal to the p_1 value of 3.27; this should be compared to the expectation value of $\langle p_{12} \rangle$ which as can be seen from Table III.8 equals 3.28. No other minima are present on this surface, but a zero contour is observed parallel to the p_{12} axis at a p_1 value approximately equal to $\langle p_1 \rangle$.

The outershell surface presented in Figure III.10B shows similar trends to those observe for the innershell Δg surface. Namely, that the surface has a minimum at small p_1 and small p_{12} , showing once again the dominant radial correlation, and two maxima. The magnitudes of these

effects, however, differ vastly from those observed for the innershell surface. The minimum for the outshell has a depth of -0.4 compared with an innershell value of -0.013 ; similarly for the maximum value, the result for the outshell is 0.2 whilst a value of 0.007 is observed for the innershell surface. A corresponding decrease in the range of p_1 and p_{12} values is seen between the two surfaces, the innershell surface ranges from $0-20\text{au}$, the range for the outshell is $0-4\text{au}$. As for the innershell, the general shape of the outshell surface reflects the behaviour of the second electron as the test electron moves through different regions of position space. When the test electron is further away from the nucleus its momentum is small and, since a consequence of radial correlation is that as one electron moves away from the nucleus the other moves towards the nucleus, the momentum of the second electron will be of greater magnitude than its original HF value. For small p_1 the magnitude of p_{12} will be that equivalent to p_2 , the momentum of the second electron, which has enhanced its momentum value, thus an increase in the p_{12} probability would be expected and is indeed observed on the Δg surface. In passing we wish to observe an interesting feature found from the Δg surface. The minimum value of the surface occurs at a p_{12} value of 0.4 , the associated maximum value occurs at a p_{12} value of 1.05 . The mean of these values, which is 0.72 , should be compared to the correlated expectation value $\langle p_1 \rangle$ ($\equiv \langle p_2 \rangle$) for this shell of 0.708 .

As the test electron's momentum p_1 increases its contribution towards p_{12} will also increase. As the test

electron moves closer to the nucleus the second electron moves away with a subsequent reduction in its momentum. A role reversal of what has been discussed above now happens; the second electron's momentum is small so contributions to P_{12} comes solely from the test electron, ie $p_{12} \approx p_1$, leading to the diagonal structure along the $p_1 = p_{12}$ axis. This diagonal structure has no minima just an enhancement of probability centred on $p_1 = 1.05$ and $p_{12} = 1.05$. The two maxima present on the Δg surface share the same p_{12} value of 1.05 which once again has a value comparable to the expectation value $\langle p_{12} \rangle$. Another similar feature shared between the two intrashell surfaces is the zero contour parallel to the p_{12} axis, this occurs, on the outershell Δg surface, at an equivalent distance along the p_1 axis at a value of $\langle p_1 \rangle$.

As can be seen in Figure III.10 the two intrashell surfaces share similar features; likewise the two intershell surfaces have similar features which are, however, unlike those observed for the intrashells. For instance, both intershell surfaces show a positive value for $\Delta g(p_{12}, p_1)$ at small p_1 for all p_{12} values. This initial rise in the surface, which would normally be attributable to angular correlation in an atomic system, has been discussed earlier and has been associated with the movement of an H electron towards the Li nucleus. This redistribution leads to a more diffuse distribution as shown by Banyard and Hayns and hence an increase in probability of small momenta. Also an effect of radial correlation is an increase in momentum of one electron near to the nucleus as the second moves further away. Thus a consequence of these two effects is that for a

small value p_1 of the test electron, the probability distribution for p_{12} will be increased for all values of p_{12} as observed on the intershell Δg surfaces. An exception is observed on the triplet surface at small p_1 and small p_{12} as a consequence of the Fermi effect forbidding two electrons with the same spin sharing the same region of space. No such exclusion is present for the singlet distribution and indeed an enhancement in the p_{12} probability is observed at small p_1 and p_{12} as a result of the second electron being able to penetrate this outer more diffuse region. The maximum feature for the triplet surface occurs at a p_1 and p_{12} value of 0.2 and 1.2, respectively; whilst the two maxima of the singlet surface occurs at the same p_1 value of 0.27, with p_{12} values of 0.5 and 1.7. Both surfaces have a zero contour parallel to the p_{12} axis at a p_1 value of 0.45. After an initial rise at small p_1 the intershell surfaces drop to a minimum with a comparable magnitude for both surfaces of -0.02. As p_1 increases the intershell surfaces have a similar feature to that observed on the intrashell surfaces. Namely an increase in probability centred upon $\langle p_1 \rangle$ and $\langle p_{12} \rangle$ for the two distributions. The diagonal feature is common to all surfaces but for the intershells we observe a more complicated structure. Whereas for the intrashells we observed a rise at small and intermediate p_1 and p_{12} with a tailing off to zero for larger values, the intershell surfaces have no initial rise (indeed we observe a negative trough) and the $p_1 = p_{12}$ axis rises from a value below zero to zero with troughs either side of this structure.

CHAPTER III.5
REFERENCES

- 1 R. McWeeny, The New World of Quantum Chemistry, (Reidel, Dordrecht, Holland, 1976) p.3.
- 2 V.W. Maslen, Proc. Phys. Soc. (London) A69, 734 (1956).
- 3 G. Sperber, Int. J. Quantum Chem. 5, 189 (1971).
- 4 R.J. Boyd and C.A. Coulson, J. Phys. B7, 1805 (1974).
- 5 R. Ahlberg and P. Linder, J. Phys. B9, 2963 (1976).
- 6 C.A. Coulson and A.H. Neilson, Proc. Phys. Soc. (London) 78, 831 (1961).
- 7 R.J. Boyd and C.A. Coulson, J. Phys. B6, 782 (1973).
- 8 R.J. Boyd and J. Katriel, Int. J. Quantum Chem. 8, 255 (1974).
- 9 R.J. Boyd, Can. J. Phys. 53, 592 (1975).
- 10 G. Sperber, Int. J. Quantum Chem. 6, 881 (1972).
- 11 M.A. Besson and M. Suard, Int. J. Quantum Chem. 10, 151 (1976).
- 12 G. Doggett, Molecular Physics 34, 1739 (1977).
- 13 G. Doggett, Molecular Physics 38, 853 (1979).
- 14 R. Benesch and V.H. Smith, Acta Cryst. A26, 579 (1970).
- 15 K.E. Banyard and R.J. Mobbs, J. Chem. Phys. 75, 3433 (1981).
- 16 K.E. Banyard and C.E. Reed, J. Phys. B: Atom. Molec. Phys. 11, 2957 (1978).
- 17 K.E. Banyard and C.E. Reed, J. Phys. B: Atom. Molec. Phys. 14, 411 (1981).
- 18 K.E. Banyard and J.C. Moore, J. Phys. B 10, 2781 (1977).
- 19 K.E. Banyard and C.E. Reed, J. Phys. B 11, 2957 (1978).
- 20 C.A. Coulson, Proc. Camb. Phil. Soc. 37, 55 (1941).
- 21 C.A. Coulson and W.E. Duncanson, Proc. Camb. Phil. Soc. 37, 67 (1941).
- 22 C.A. Coulson, Proc. Camb. Phil. Soc. 37, 74 (1941).
- 23 W.E. Duncanson, Proc. Camb. Phil. Soc. 37, 397 (1941).

- 24 W.E. Duncanson and C.A. Coulson, Proc. Camb. Phil. Soc. 37, 406 (1941).
- 25 C.A. Coulson and W.E. Duncanson, Proc. Camb. Phil. Soc. 38, 100 (1942).
- 26 W.E. Duncanson, Proc. Camb. Phil. Soc. 39, 180 (1943).
- 27 W.E. Duncanson and C.A. Coulson, Proc. Camb. Phil. Soc. 60, 175 (1948).
- 28 W.H. Henneker and P.E. Cade, Chem. Phys. Lett. 2, 575 (1968).
- 29 R.E. Brown and V.H. Smith, Jr., Phys. Rev. 5A, 140 (1972).
- 30 W. Heitler and F. London, Z. Phys. 44, 455 (1927).
- 31 O. Burrau, K. Danske Vidensk. Selsk. Mat. Fys. Meddr. 7, 1805 (1927).
- 32 A. Hibbert, Rep. Prog. Phys. 38, 1217 (1975).
- 33 P.E. Cade and W.M. Huo, J. Chem. Phys. 47, 614 (1967).
- 34 D.D. Ebbing, J. Chem. Phys. 36, 1361 (1962).
- 35 F.E. Harris and H.S. Taylor, Physica 30, 105 (1964).
- 36 J.C. Browne and F.A. Matsen, Phys. Rev. 135, A1227 (1964).
- 37 C.F. Bender and E.R. Davidson, J. Phys. Chem. 70, 2675 (1966).
- 38 R. Ahlrichs and W. Kutzelnigg, J. Chem. Phys. 48, 1819 (1968).
- 39 C.F. Bender and E.R. Davidson, J. Phys. Chem. 49, 4222 (1968).
- 40 W.E. Palke and W.A. Goddard, J. Chem. Phys. 50, 4524 (1969).
- 41 C.C.J. Roothaan, Rev. Mod. Phys. 23, 69 (1951).
- 42 P.O. Löwdin, Phys. Rev. 97, 1474 (1955).
- 43 E.R. Davidson and L.L. Jones, J. Chem. Phys. 37, 2966 (1962).
- 44 E.R. Davidson, J. Chem. Phys. 39, 875 (1963).
- 45 S. Hagstrom and H. Shull, Rev. Mod. Phys. 35, 624 (1963).
- 46 C.F. Bender and E.R. Davidson, J. Phys. Chem. 70, 2675 (1966).

- 47 C.F. Bender and E.R Davidson, Phys. Rev. 183, 23 (1969).
- 48 G.P. Arrighini, J. Tomasi and C. Guidotti, Theoret. Chim. Acta 18, 329 (1970).
- 49 K.E. Banyard and M.M. Mashat, J. Chem. Phys. 67, 1405 (1976)
- 50 O. Sinanoglu and K.A. Brueckner, Three Approaches to Electron Correlation in Atoms, (Yale University Press, 1970).
- 51 P.A.M. Dirac Quantum Mechanics (Oxford University Press, Oxford, 1935), p.103.
- 52 H. Margenau and G.M. Murphy, The Mathematics of Physics and Chemistry (Van Nostrand, Princeton, 1956).
- 53 G.N. Watson, A Treatise on the Theory of Bessel Functions, Cambridge University Press, 2nd edition (1966).
- 54 C.E. Reed, Ph.D. Thesis, Properties of Electron Momentum Distributions: A Study of Correlation Effects in some Two-Electron Systems & An Examination of Directional Compton Profiles for the Lithium Halides, University of Leicester (1980).
- 55 M.E. Rose, Elementary Theory Of Angular Momentum, J. Wiley and Sons, (New York, London).
- 56 K.E. Banyard and M. R. Hayns, J. Phys. Chem. 75, 416 (1971).
- 57 R.F.W. Bader, I. Keaveney and P.E. Cade, J. Chem. Phys. 47, 3381 (1967).
- 58 P.K. Youngman, Private Communication.
- 59 K.H. Al-Bayati, Ph.D. Thesis, Electron Correlation in the $(1s^2 2s)^2 S$ & $(1s^2 2p)^2 P$ states of the Lithium Isoelectronic Sequence in Position & Momentum Space, University of Leicester, (1984).
- 60 R.J. Mobbs and K.E. Banyard, J. Chem. Phys. 78, 6106 (1982).
- 61 E. Clementi, 'Tables of Atomic Functions', a supplement to IBM J. Res. Dev. 9, 2 (1965).
- 62 A.W. Weiss, Phys. Rev. 122, 1826 (1961).
- 63 A.W. Weiss, J. Chem. Phys. 39, 1262 (1963).

Excitation	Coefficient
$(1\sigma)^2(2\sigma)^2$	0.98537
$(1\sigma)^2 - (9\sigma)^2$	-0.02932
$(1\sigma)^2 - (4\pi)^2$	-0.02113
$(1\sigma)^2 - (10\sigma)^2$	-0.02015
$(1\sigma)^2 - 4\sigma 9\sigma$	-0.01461
$(1\sigma)^2 - 9\sigma 11\sigma$	0.00669
$(1\sigma)^2 - 6\sigma 10\sigma$	0.00642
$(1\sigma)^2 - 6\sigma 9\sigma$	-0.00627
$(1\sigma)^2 - 3\sigma 9\sigma$	0.00483
$(2\sigma)^2 - (6\sigma)^2$	-0.06987
$(2\sigma)^2 - 3\sigma 6\sigma$	0.06094
$(2\sigma)^2 - 6\sigma 8\sigma$	0.03998
$(2\sigma)^2 - (1\pi)^2$	-0.03669
$(2\sigma)^2 - 1\pi 3\pi$	-0.03499
$(2\sigma)^2 - (3\pi)^2$	-0.03464
$(2\sigma)^2 - (7\sigma)^2$	-0.03381
$(2\sigma)^2 - 5\sigma 7\sigma$	-0.03205
$(2\sigma)^2 - 1\pi 2\pi$	-0.02115
$(2\sigma)^2 - (8\sigma)^2$	-0.02085
$(2\sigma)^2 - 3\sigma 8\sigma$	-0.02055
$(2\sigma)^2 - 2\pi 3\pi$	-0.01792
$1\sigma 2\sigma - (9\sigma)^2$	-0.00566
$1\sigma 2\sigma - (1\pi)^2$	0.00296
$1\sigma 2\sigma - (4\pi)^2$	-0.00264
$1\sigma 2\sigma - 1\pi 4\pi$	0.00112
	0.00305
$1\sigma 2\sigma - 1\pi 3\pi$	-0.00227
	-0.00229

Table III.1 Important configurations in the 262 configuration wavefunction of Arrighini et al⁽⁴⁸⁾ for the ground state of LiH.

Wavefunction	TOTAL energy E(a.u.)	% Correlation energy	Description of the total wavefunction
Be BUNGE	-14.66419	96.55%	180 configurations 7s, 7p and 4d Orthonormal basis set
HARTREE-FOCK (HF)	-14.57299	0.0%	...
LiH Arrighini et al	-8.05545	82.6%	262 configurations 11 σ and 4 π Orthonormal basis set
HARTREE-FOCK (HF)	-7.98624	0.0%	...

Table III.2 The LiH wavefunction: its total energies E, in atomic units, and composition. The Bunge Be wavefunction included for reference.

Wavefunction	Number of correlation configurations considered			
Be	K(¹ s)	L(¹ s)	KL(¹ s)	KL(³ s)
BUNGE	39	22	46	34
	14[s]	14[s]	15[s]	13[s]
	19[p]	7[p]	22[p]	16[p]
	6[d]	1[d]	9[d]	5[d]
LiH	Inner (¹ Σ)	Outer (¹ Σ)	Inter (¹ Σ)	Inter (³ Σ)
Arrighini	74	74	113	96
	54[σ]	54[σ]	81[σ]	72[σ]
	20[π]	20[π]	32[π]	24[π]

Table III.3 A summary of the correlation configurations considered for each shell. The notation used has been defined earlier, see Table II.4.

Wavefunction	Shell	$\langle p_1^{-2} \rangle$	$\langle p_1^{-1} \rangle$	$\langle p_1 \rangle$	$\langle p_1^2 \rangle$	Δp_1
Be						
BUNGE (B)	K(1S)	0.3930	0.4736	3.0947	13.5927	2.0038
	L(1S)	10.7772	2.4979	0.6712	1.0574	0.7791
	KL(1S)	5.9709	1.5380	1.8692	7.3118	1.9539
	KL(3S)	5.9725	1.5384	1.8696	7.3103	1.9531
	TOTAL	5.8431	1.5208	1.8740	7.3154	1.9502
HARTREE-FOCK (HF)	K(1S)	0.3934	0.4739	3.0919	13.5681	2.0020
	L(1S)	12.2805	2.6874	0.6251	1.0021	0.7819
	KL(1S)	6.3370	1.5806	1.8585	7.2851	1.9573
	KL(3S)	6.3370	1.5806	1.8585	7.2851	1.9573
	TOTAL	6.3370	1.5806	1.8585	7.2851	1.9573
LiH						
Arrighini	Inner($^1\Sigma$)	0.7685	0.6591	2.2433	7.2151	1.4774
	Outer($^1\Sigma$)	8.6964	2.1915	0.7082	0.7882	0.5354
	Inter($^1\Sigma$)	4.7324	1.4253	1.4756	3.9997	1.3499
	Inter($^3\Sigma$)	4.7319	1.4252	1.4758	4.0005	1.3500
	TOTAL	4.7322	1.4253	1.4758	4.0007	1.8227
HARTREE-FOCK (HF) LiH	Inner($^1\Sigma$)	0.7682	0.6588	2.2432	7.2110	1.4762
	Outer($^1\Sigma$)	8.5881	2.1825	0.7071	0.7813	0.5304
	Inter($^1\Sigma$)	4.6781	1.4207	1.4752	3.9962	1.3491
	Inter($^3\Sigma$)	4.6781	1.4207	1.4752	3.9962	1.3491
	TOTAL	4.6781	1.4207	1.4752	3.9962	1.3491

Table III.4 Some one-particle expectation properties for the intra- and intershells of LiH.

Wavefunction	Shell	$\langle p_1^{-2} \rangle$	$\langle p_1^{-1} \rangle$	$\langle p_1 \rangle$	$\langle p_1^2 \rangle$	Δp_1
Li						
	K α K β	0.7634	0.6570	2.2461	7.229	0.576
	K α L α	12.6209	2.2453	1.3332	3.837	2.753
	K β L α	11.6195	2.2455	1.3309	3.822	2.565
	Total	8.3346	1.7159	1.6367	4.962	2.322
	K α K β	0.7644	0.6571	2.2460	7.224	0.577
	K α L α	12.8262	2.2612	1.3298	3.821	2.777
	K β L α	"	"	"	"	"
	Total	8.8056	1.7265	1.6352	4.955	2.413
Be ⁺						
	K α K β	0.3962	0.4744	3.0917	13.576	0.414
	K α L α	4.2931	1.3375	1.9330	7.521	1.582
	K β L α	4.2922	1.3378	1.9284	7.489	1.582
	Total	2.9938	1.0499	2.3177	9.526	1.375
	K α K β	0.3969	0.4744	3.0921	13.575	0.415
	K α L α	4.3251	1.3418	1.9288	7.489	1.589
	K β L α	"	"	"	"	"
	Total	3.0157	1.0527	2.3165	9.518	1.381

Table III.5 Expectation values $\langle p_1^2 \rangle$ and the standard deviations Δp_1 and $\Delta 1/p$ for the $(1s^2 2s)^2 S$ state for the individual shells and the normalized Total values for the Li-like ions. The results are derived by using Weiss⁽⁶²⁾ CI and Weiss⁽⁶³⁾ HF wavefunctions.

WavefunctionShell		$\langle p_1^{-1} p_2^{-1} \rangle$	$\langle p_1 p_2 \rangle$
Be			
BUNGE	K(1S)	0.2233	9.4361
(B)	L(1S)	6.2530	0.4422
	KL(1S)	1.3580	2.3542
	KL(3S)	1.1079	1.6327
	TOTAL	1.8597	2.8551
HARTREE			
-FOCK	K(1S)	0.2246	9.5598
(HF)	L(1S)	7.2219	0.3908
	KL(1S)	1.3994	2.2846
	KL(3S)	1.1480	1.5810
	TOTAL	2.0483	2.8297
LiH			
Arrighini	Inner($^1\Sigma$)	0.4311	4.9681
	Outer($^1\Sigma$)	4.6544	0.4856
et al	Inter($^1\Sigma$)	1.5440	1.6673
	Inter($^3\Sigma$)	1.3460	1.5122
	TOTAL	1.7780	1.9429
HARTREE			
-FOCK	Inner($^1\Sigma$)	0.4340	5.0322
(HF)	Outer($^1\Sigma$)	4.7633	0.4999
	Inter($^1\Sigma$)	1.5352	1.6624
LiH	Inter($^3\Sigma$)	1.3405	1.5099
	TOTAL	1.7923	1.9540

Table III.6 Some two-particle expectation properties for the intra- and intershells of LiH.

Wavefunction	Shell	$\langle p_1^{-1} p_2^{-1} \rangle$	$\langle p_1 p_2 \rangle$
Li			
	K α K β	0.4260	4.9152
	K α L α	2.2827	0.7869
	K β L α	2.5181	0.9334
	Total	1.7423	2.2118
	K α K β	0.4318	5.0446
	K α L α	2.3057	0.7804
	K β L α	2.5400	0.9290
	Total	1.7591	2.2514
Be ⁺			
	K α K β	0.2234	9.3967
	K α L α	0.9156	1.9054
	K β L α	1.0434	2.3630
	Total	0.7275	4.5550
	K α K β	0.2251	9.5668
	K α L α	0.9205	1.8961
	K β L α	1.0481	2.3670
	Total	0.7312	4.6080

Table III.7 Expectation values $\langle p_1^n p_2^n \rangle$ for the $(1s^2 2s)^2 S$ state for the individual shells and the normalized Total values for the Li-like ions. The results are derived by using Weiss⁽⁶²⁾ CI and Weiss⁽⁶³⁾ HF wavefunctions.

Wave-function	Shell	$\langle p_{12}^{-1} \rangle$	$\langle p_{12} \rangle$	$\langle p_{12}^2 \rangle$	Δp_{12}
Be					
BUNGE (B)	K($1s$)	0.3102	4.4735	26.3423	2.5160
	L($1s$)	1.8073	0.9638	2.0525	1.0600
	KL($1s$)	0.5003	3.1678	14.5947	2.1354
	KL($3s$)	0.4070	3.2727	14.4514	1.9341
	TOTAL	0.6398	3.0705	14.3906	2.2276
HARTREE -FOCK (HF)	K($1s$)	0.3082	4.5248	27.0648	2.5673
	L($1s$)	1.7747	0.9591	1.9926	1.0357
	KL($1s$)	0.4999	3.1589	14.5098	2.1286
	KL($3s$)	0.4090	3.2652	14.4112	1.9365
	TOTAL	0.6350	3.0731	14.4668	2.2412
LiH					
Arrigh- ini et al	Inner(1Γ)	0.4263	3.2838	14.2552	1.8633
	Outer(1Γ)	1.3889	1.0468	1.5443	0.6697
	Inter(1Γ)	0.6612	2.2880	7.1423	1.3811
	Inter(3Γ)	0.5535	2.4235	7.9279	1.4334
	TOTAL	0.6895	2.3148	7.7876	1.5585
HARTREE -FOCK (HF)	Inner(1Γ)	0.4234	3.2878	14.2120	1.8445
	Outer(1Γ)	1.3501	1.0624	1.5718	0.6656
	Inter(1Γ)	0.6640	2.2848	7.1352	1.3838
	Inter(3Γ)	0.5553	2.4222	7.9368	1.4387
	TOTAL	0.6839	2.3169	7.7882	1.5556

Table III.8 Some two-particle expectation properties for the intra- and intershells of LiH.

Wave-function	Shell	$\langle p_{12}^{-1} \rangle$	$\langle p_{12} \rangle$	$\langle p_{12}^2 \rangle$	Δp_{12}
Li					
	K α K β	0.4281	3.2384	13.8041	1.8213
	K α L α	0.5749	2.3511	7.5820	1.4332
	K β L α	0.6340	2.3137	7.5387	1.4783
	Total	0.5457	2.6344	9.6416	1.6436
	K α K β	0.4256	3.2923	14.4233	1.8931
	K α L α	0.5753	2.3490	7.5632	1.4301
	K β L α	0.6338	2.3156	7.5553	1.4810
	Total	0.5449	2.6528	9.8473	1.6763
Be ⁺					
	K α K β	0.3103	4.4585	25.8917	2.4523
	K α L α	0.3949	3.3063	14.2575	1.8237
	K β L α	0.4480	3.2478	14.5833	2.0087
	Total	0.3844	3.6709	18.2442	2.1838
	K α K β	0.3083	4.5165	26.7621	2.5226
	K α L α	0.3949	3.3046	14.2341	1.8204
	K β L α	0.4478	3.2521	14.6274	2.0128
	Total	0.3837	3.6910	18.5411	2.2175

Table III.9 Some two-particle expectation properties for the $(1s^2 2s)^2 S$ state for the individual shells and the normalized Total values for the Li-like ions. These results are derived by using Weiss⁽⁶²⁾ CI and Weiss⁽⁶³⁾ HF wavefunctions.

Wavefunction	Shell	$\langle \frac{p_1}{p_1^2} \cdot \frac{p_2}{p_2^2} \rangle$	$\langle \cos \gamma_{12} \rangle$	$\langle p_1 \cdot p_2 \rangle$	Charge Shifted Y%
Be					
BUNGE (B)	K(1S)	0.0033	0.0284	0.4287	0.781
	L(1S)	0.5898	0.1404	0.0298	4.967
	KL(1S)	0.0019		0.0101	0.486
	KL(3S)	0.0025		0.0075	0.286
	TOTAL	0.1004	0.0502	0.0818	0.942
HARTREE-FOCK (HF)	K(1S)	0.0	0.0	0.0	...
	L(1S)	0.0	0.0	0.0	...
	KL(1S)	0.0	0.0	0.0	...
	KL(3S)	0.0	0.0	0.0	...
	TOTAL	0.0	0.0	0.0	...
LiH					
Arrighini et al	Inner($^1\Sigma$)	0.0006	0.0015	0.0123	0.596
	Outer($^1\Sigma$)	0.0021	0.0010	0.0017	1.809
	Inter($^1\Sigma$)	0.0203	0.0150	0.0197	0.185
	Inter($^3\Sigma$)	-0.0244	-0.0211	-0.0370	0.213
	TOTAL	-0.0502	-0.0458	-0.0773	1.533
HARTREE-FOCK (HF)	Inner($^1\Sigma$)	0.0	0.0	0.0	...
	Outer($^1\Sigma$)	0.0	0.0	0.0	...
	Inter($^1\Sigma$)	0.0255	0.0166	0.0218	...
	Inter($^3\Sigma$)	-0.0255	-0.0166	-0.0218	...
	TOTAL	-0.0510	-0.0332	-0.0436	...

Table III.10 Some two-particle expectation properties for the intra- and intershells of LiH. Also included is Y, the percentage of the interparticle distribution function $f_{HF}(p_{12})$ which has been redistributed due to correlation.

Wavefunction	Shell	$\langle \frac{p_1}{p_1^2} \cdot \frac{p_2}{p_2^2} \rangle$	$\langle \cos \gamma_{12} \rangle$	$\langle p_1 \cdot p_2 \rangle$
Li				
	K α K β	0.0083	0.0377	0.3160
	K α L α	0.0075	0.0058	0.0060
	K β L α	0.0083	0.0042	0.0058
	Total	0.0080	0.0159	0.1092
Be⁺				
	K α K β	0.0033	0.0283	0.4472
	K α L α	0.0034	0.0064	0.0167
	K β L α	0.0042	0.0051	0.0162
	Total	0.0036	0.0133	0.1600

Table III.11 Some two-particle expectation properties for the $(1s^2 2s)^2 s$ state for the individual shells and the normalized Total values for the Li-like ions. These results are derived by using Weiss⁽⁶²⁾ CI and Weiss⁽⁶³⁾ HF wavefunctions.

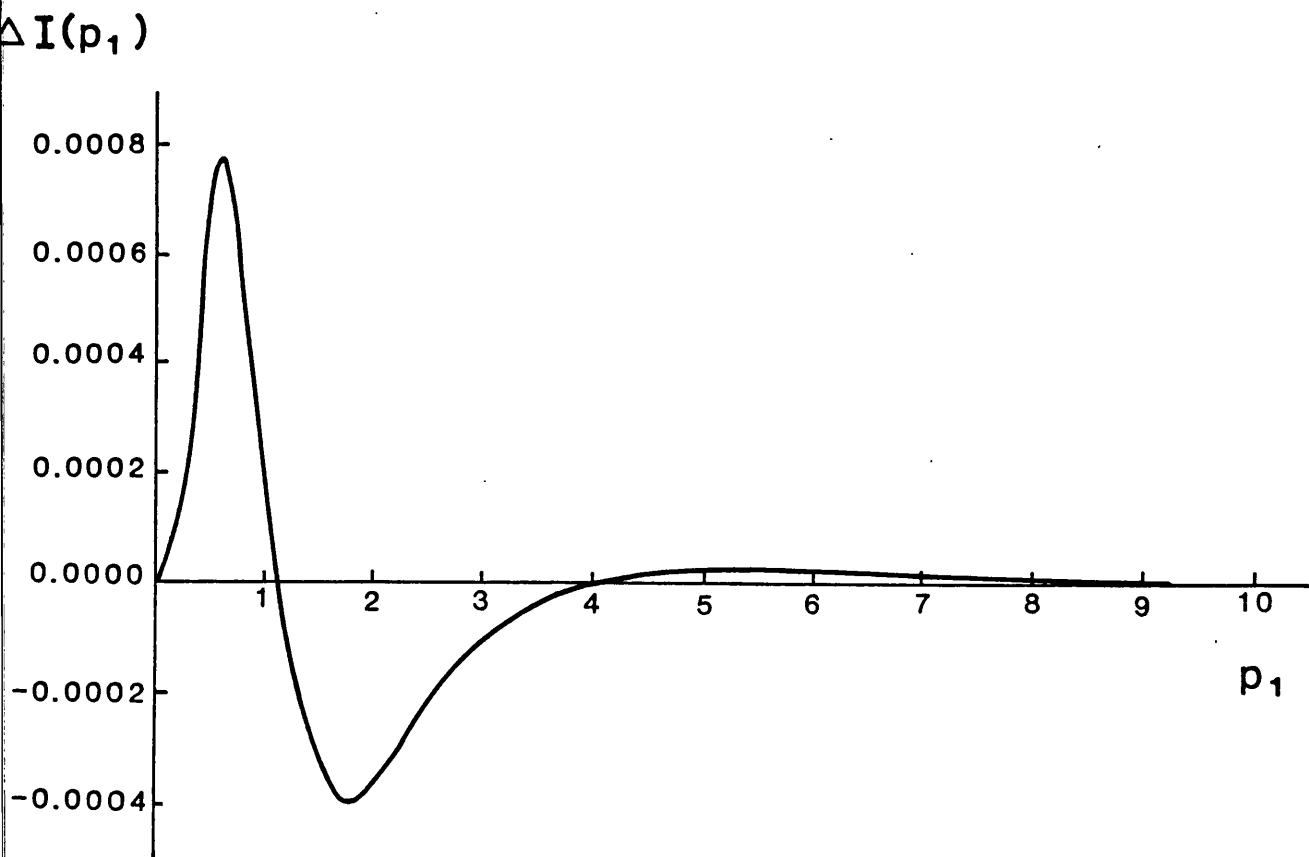
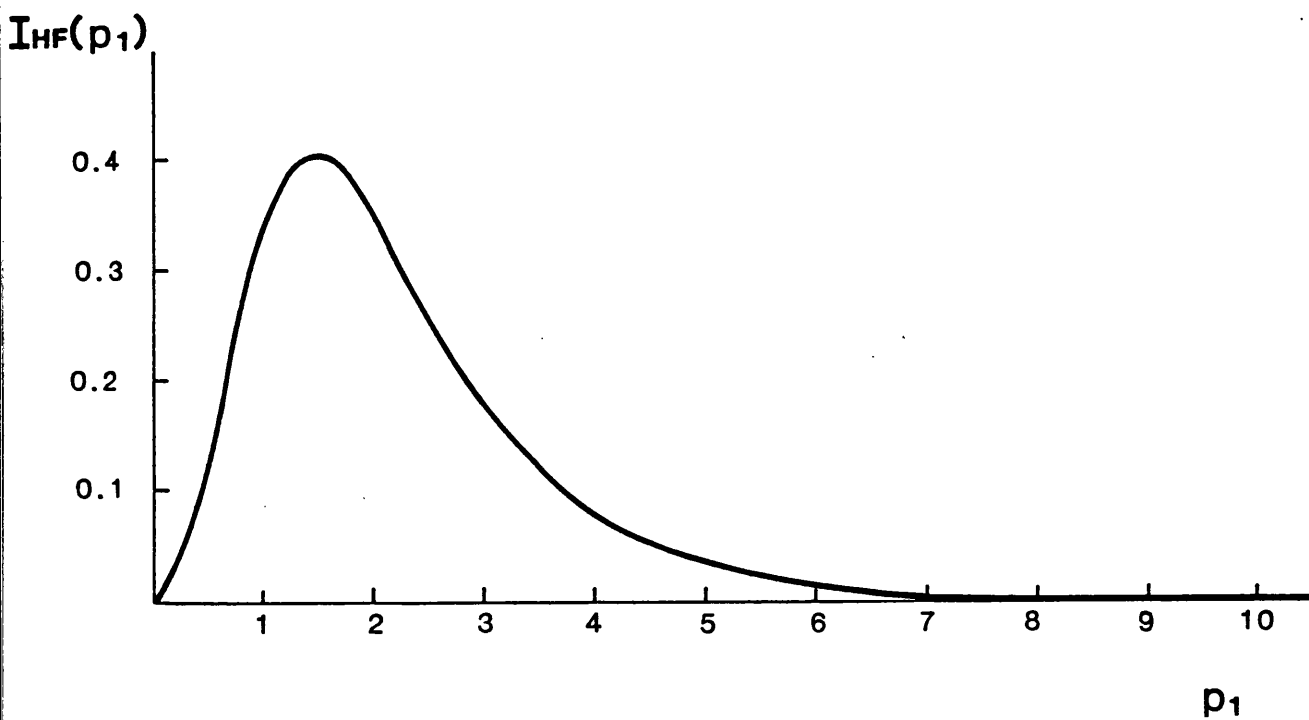


Figure III.1 The LiH innershell radial distribution function $I_{HF}(p_1)$ and the associated difference function given by Equation III.21.

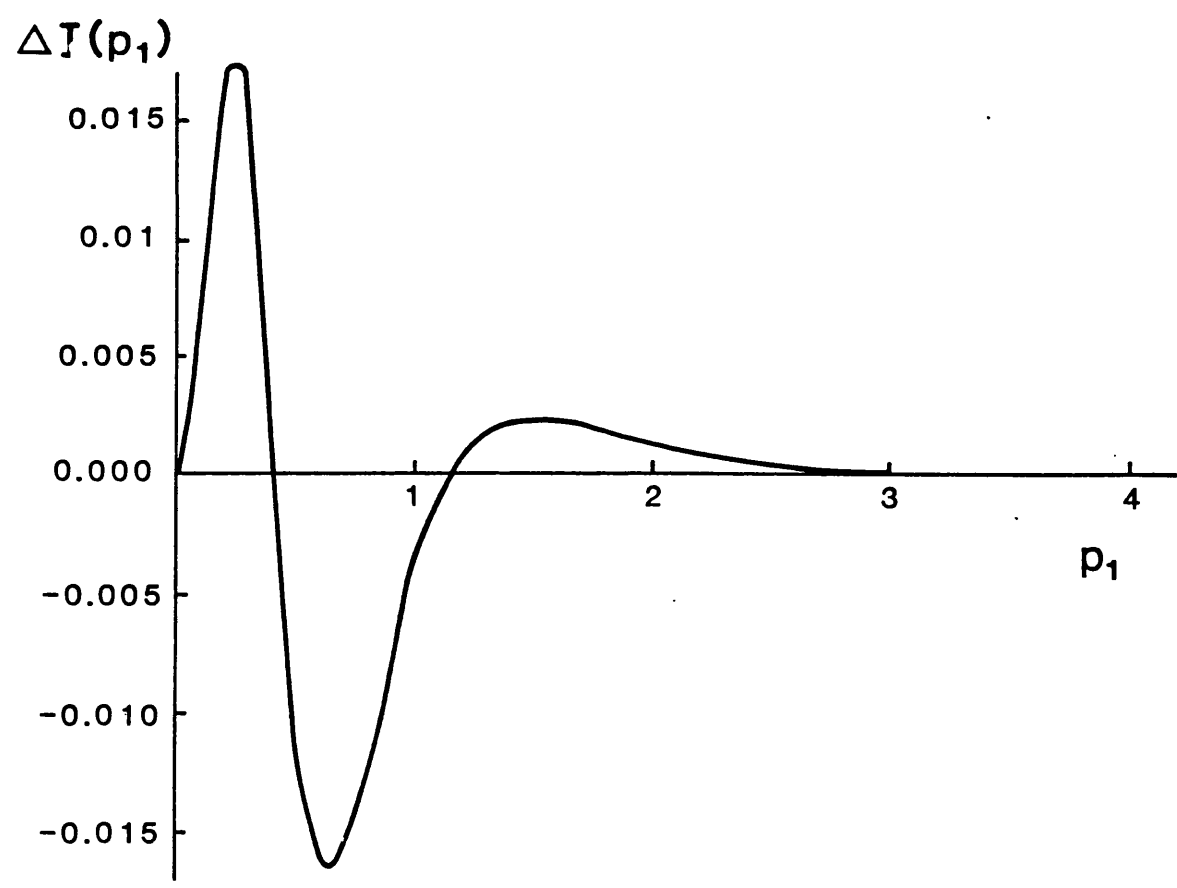
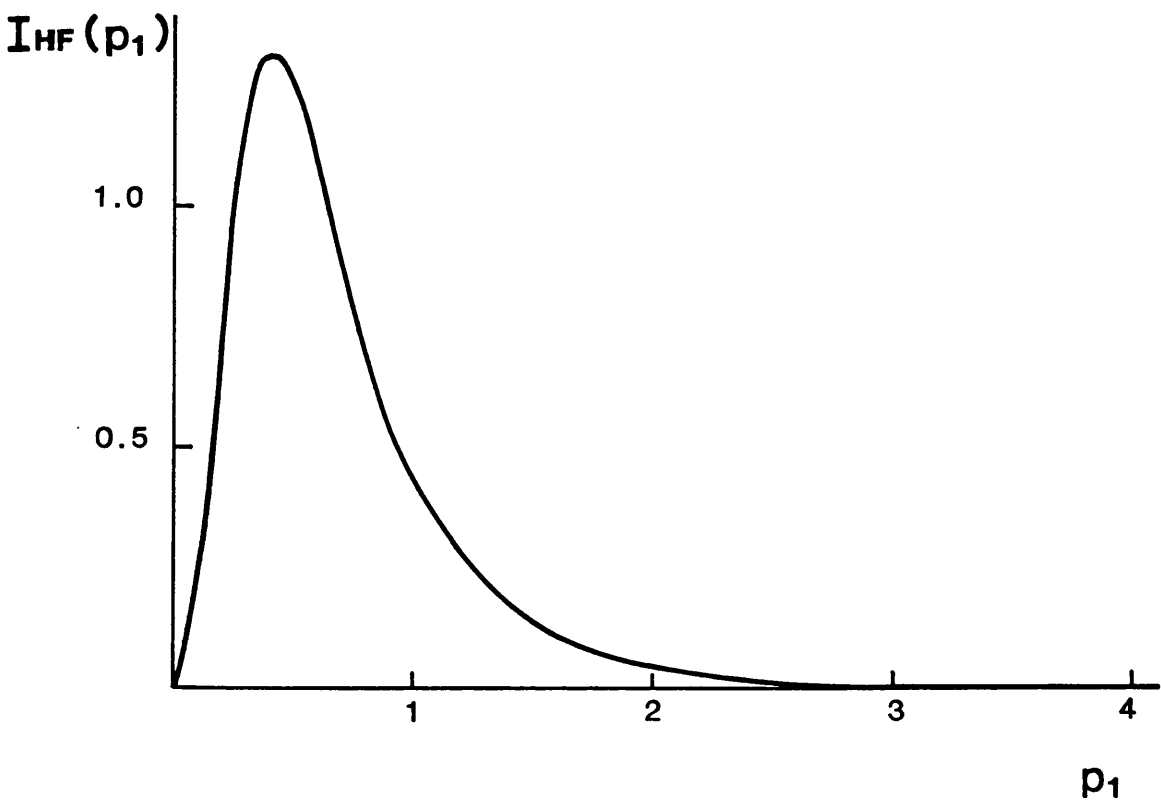


Figure III.2 The LiH outershell radial distribution function $I_{HF}(p_1)$ and the associated difference function given by Equation III.21.

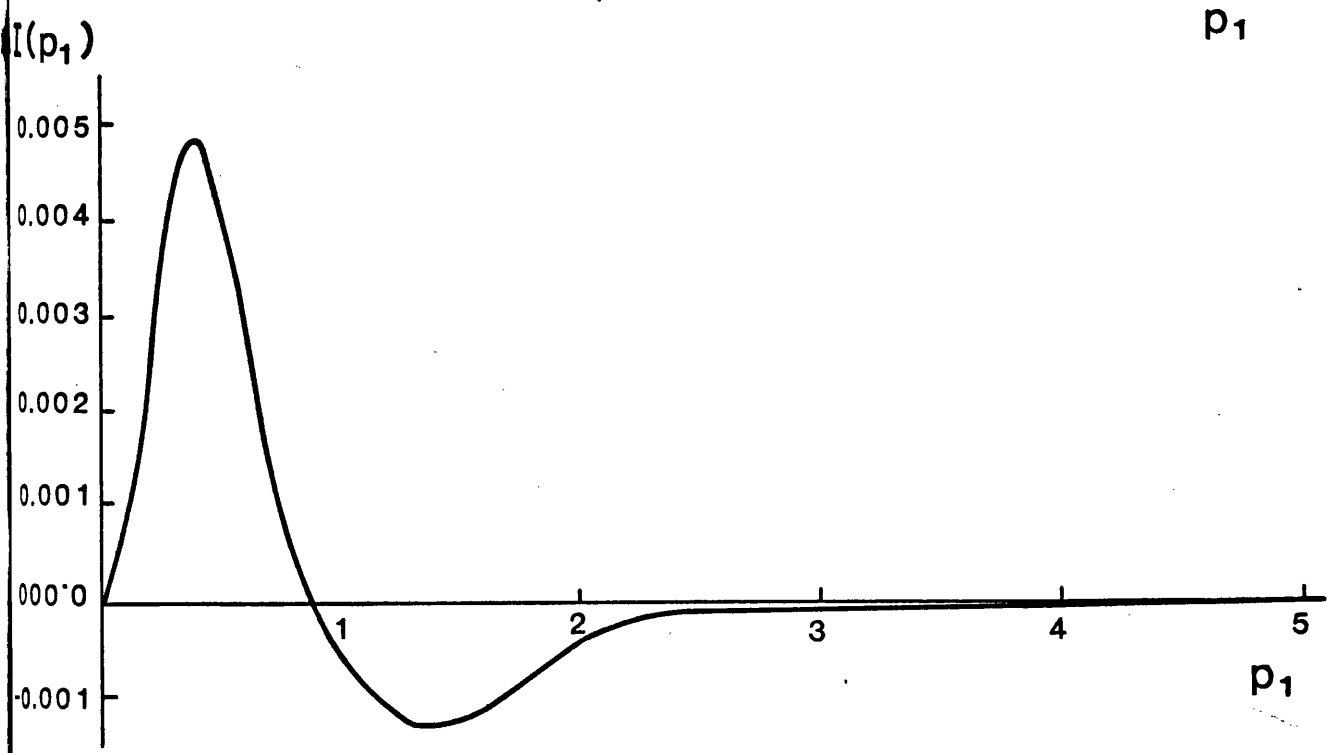
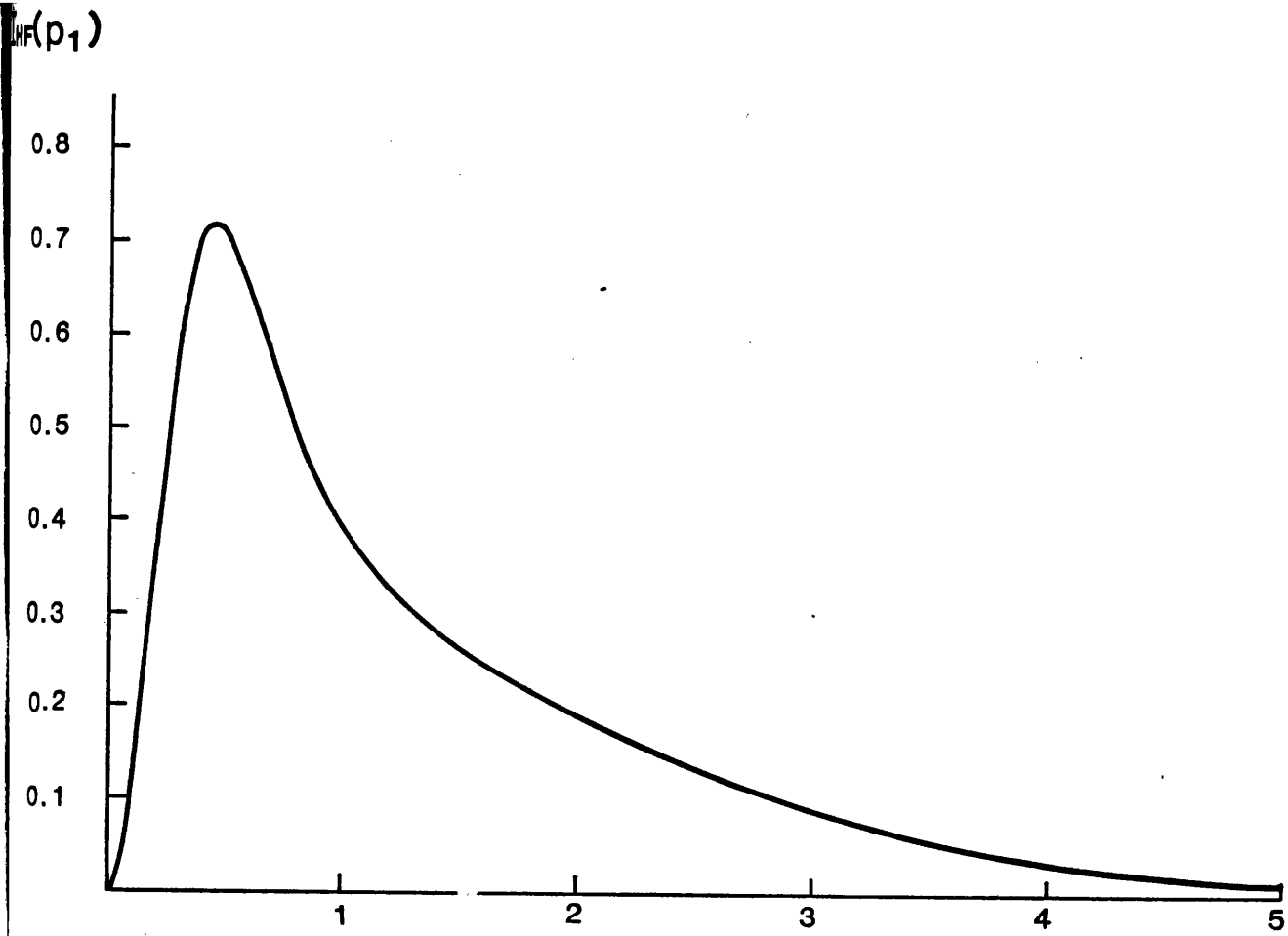


Figure III.3 The total radial distribution function $I_{HF}(p_1)$ and the associated difference function given by Equation III.21 for the LiH molecule.

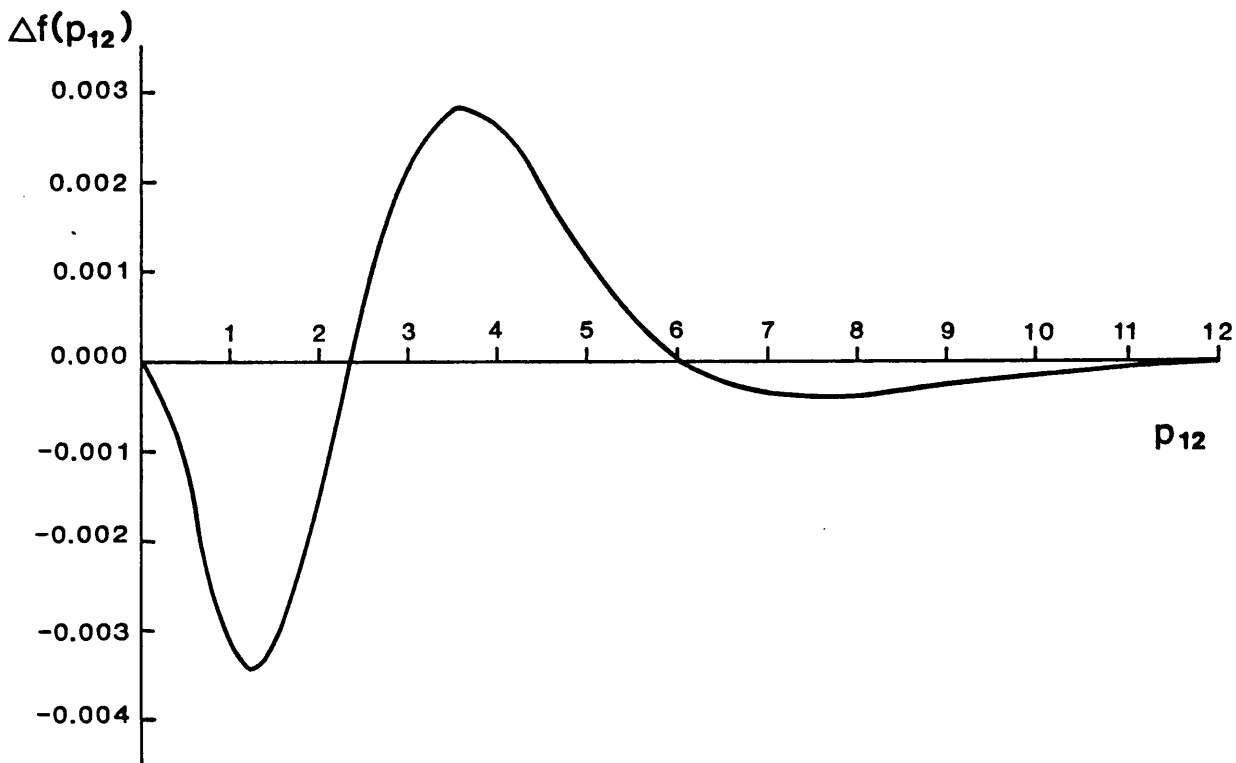


Figure III.4 The LiH innershell Coulomb shift.

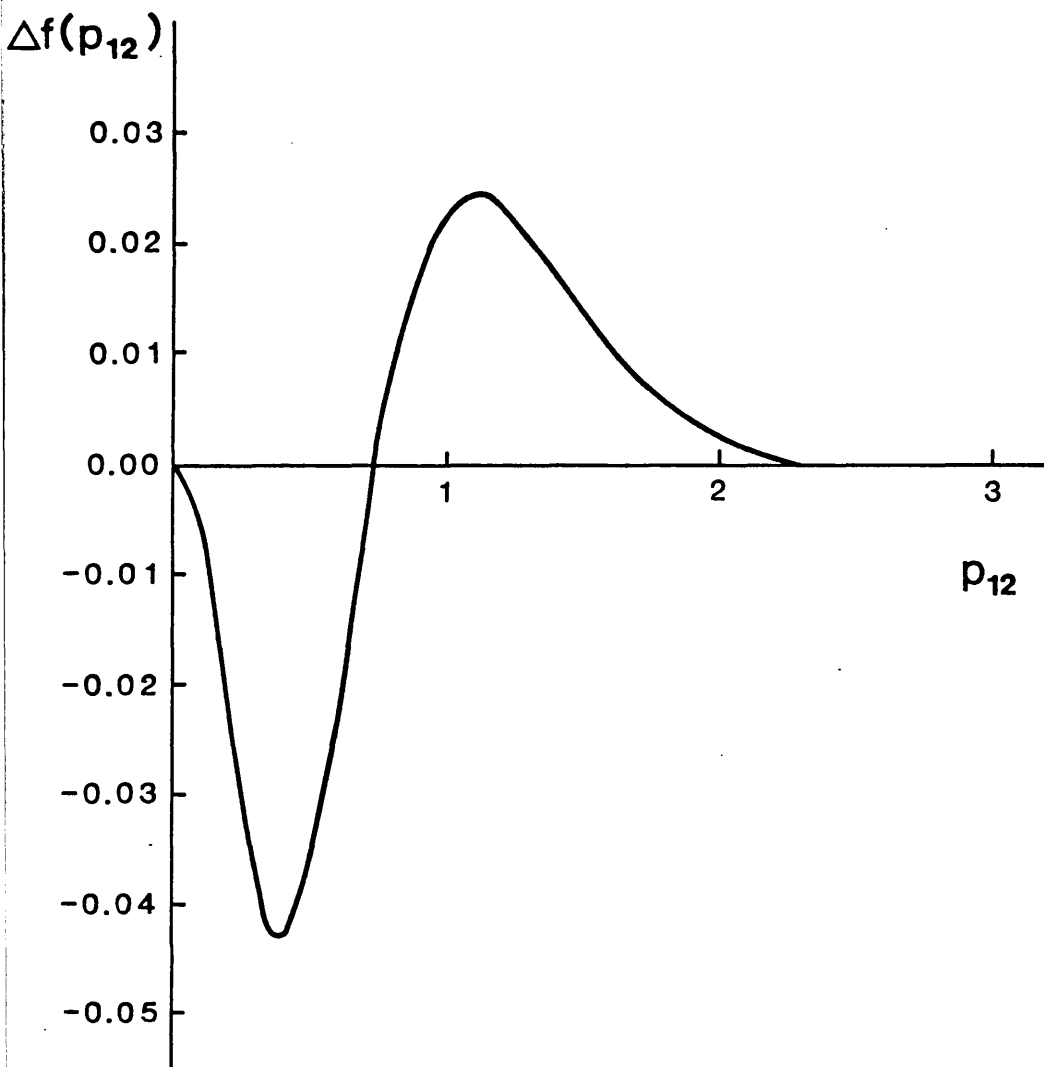


Figure III.5 The LiH outershell Coulomb shift.

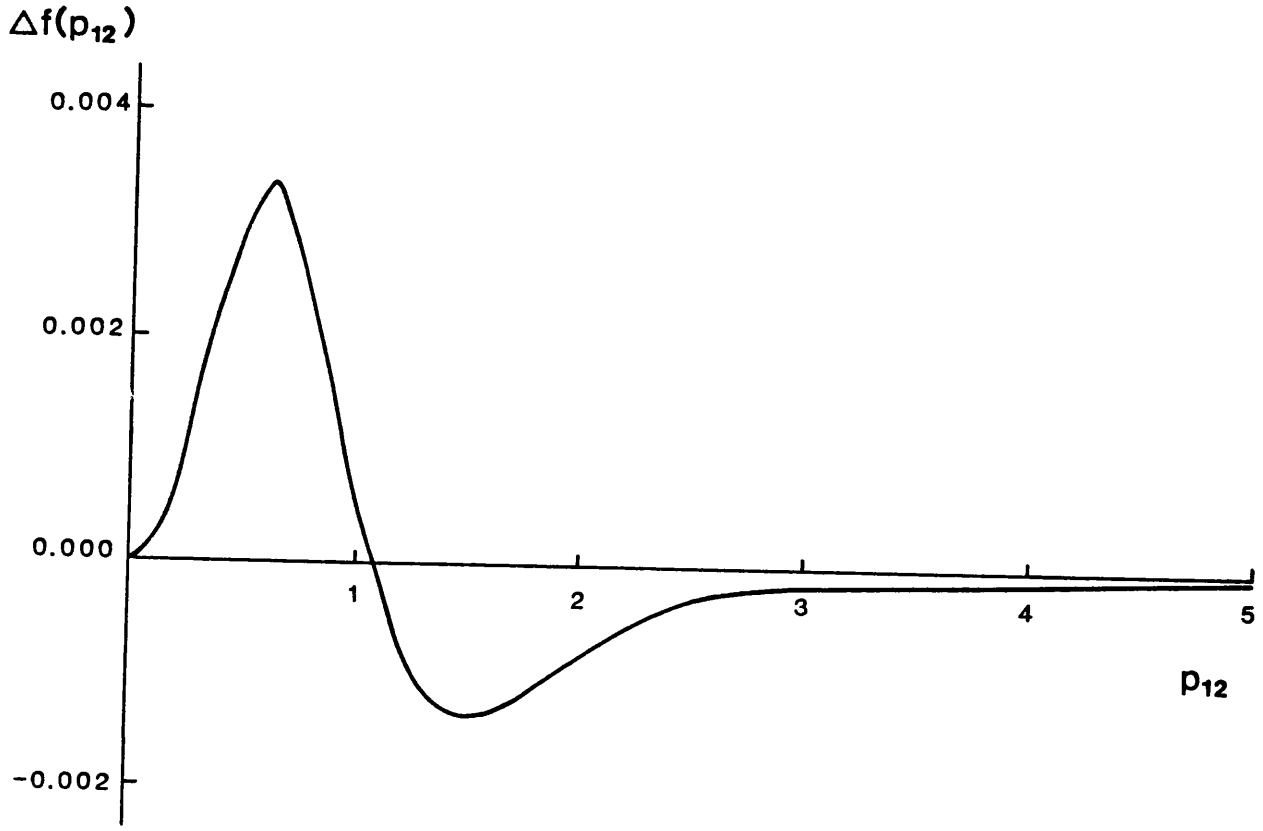


Figure III.6 The LiH intershell (1Σ) Coulomb shift.

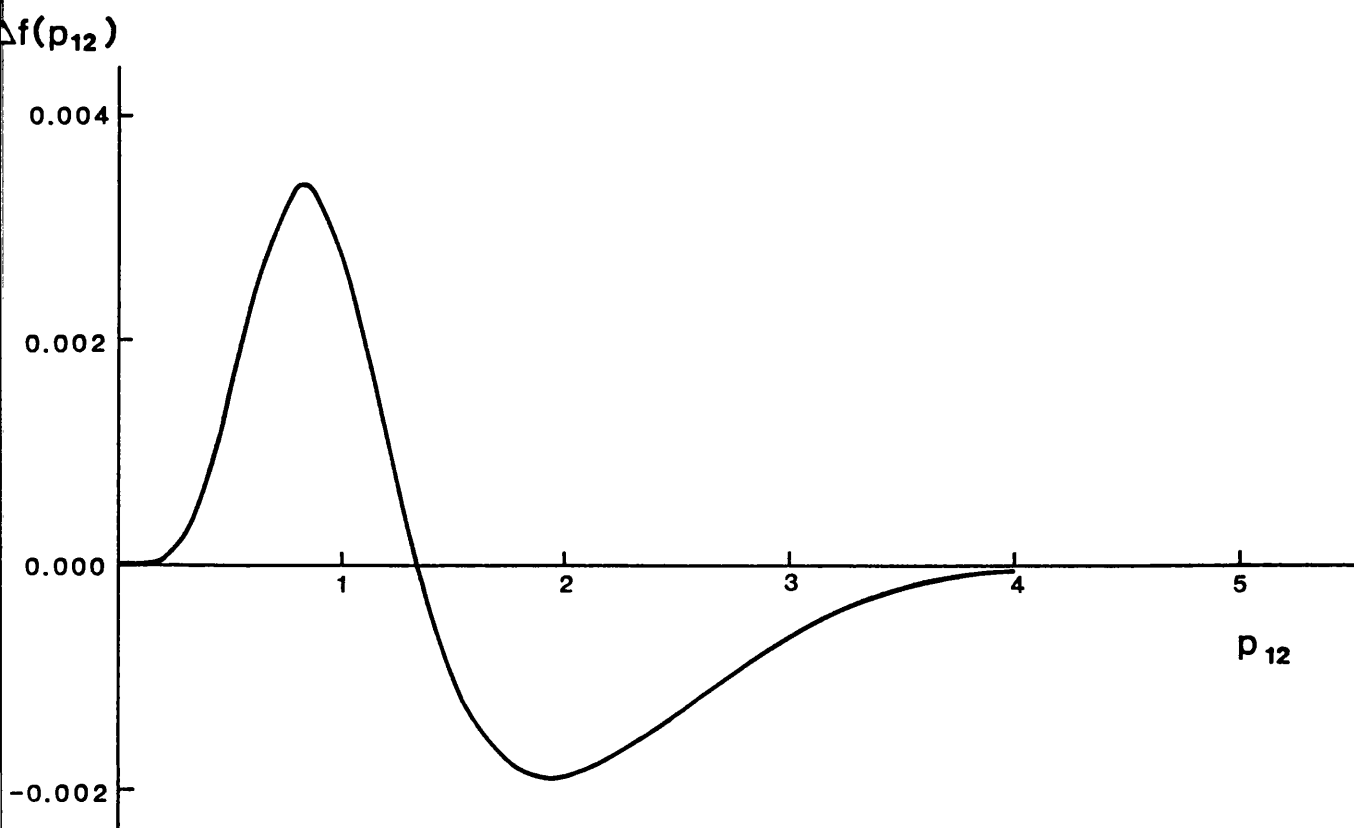


Figure III.7 The LiH intershell ($^3\Sigma$) Coulomb shift.

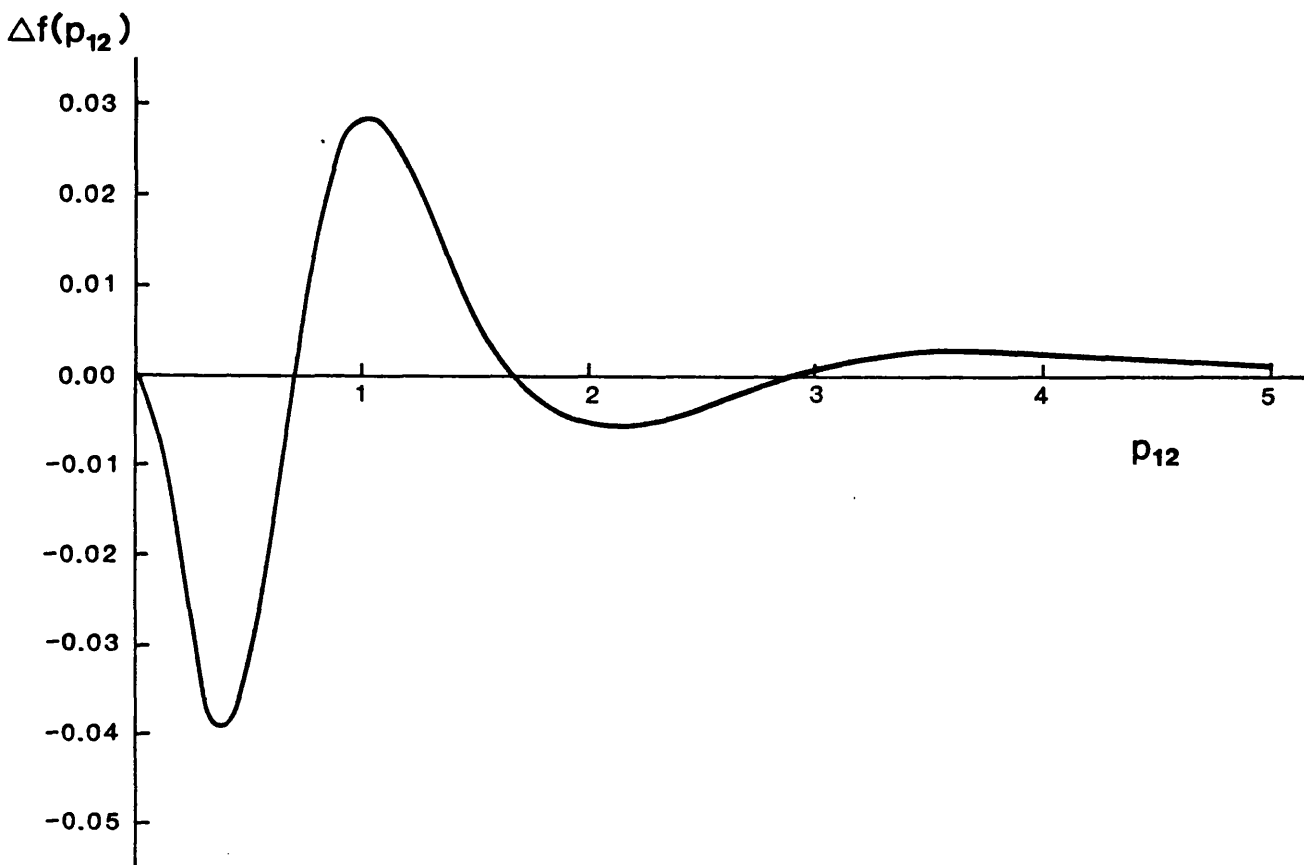


Figure III.8 The LiH total Coulomb shift.

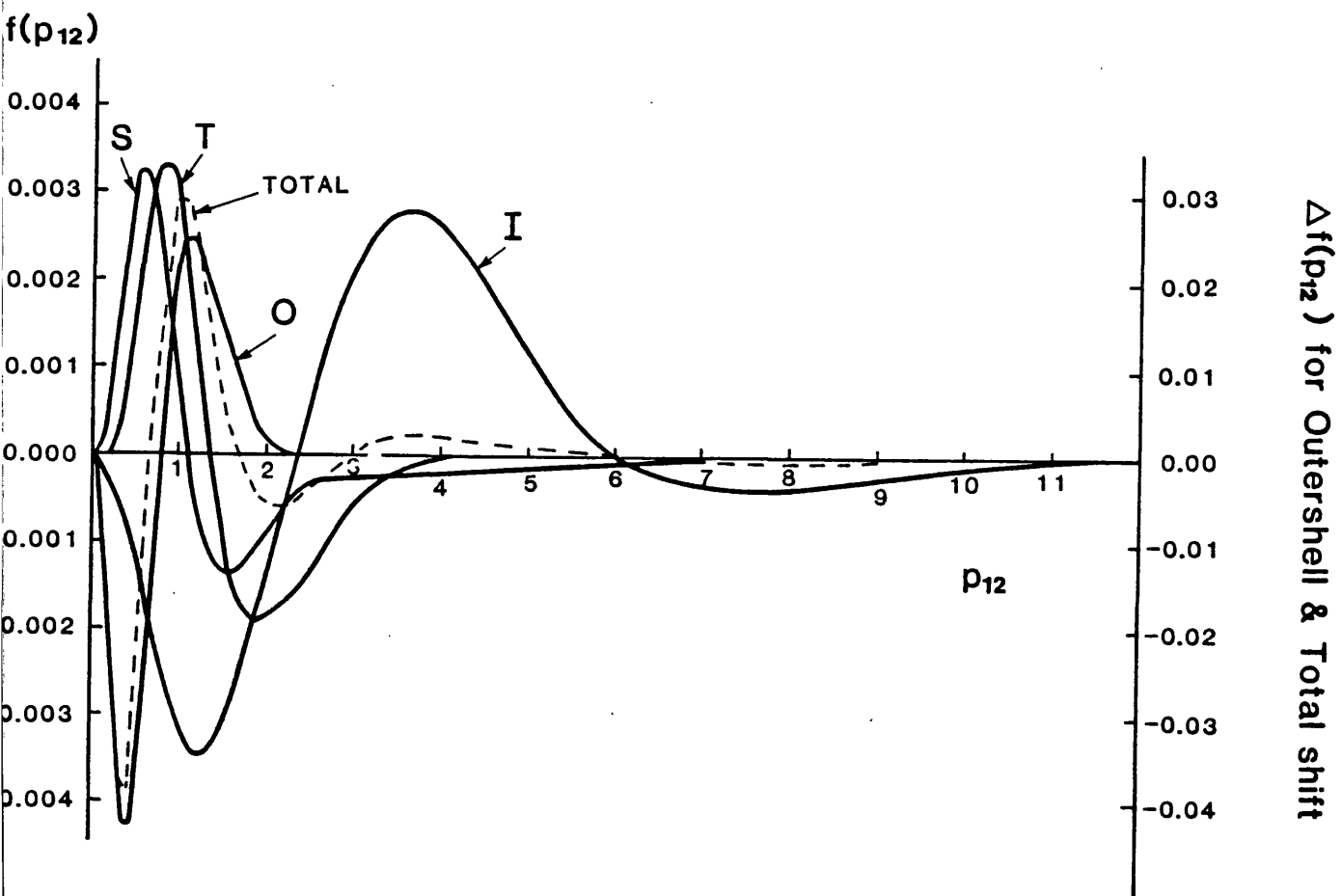
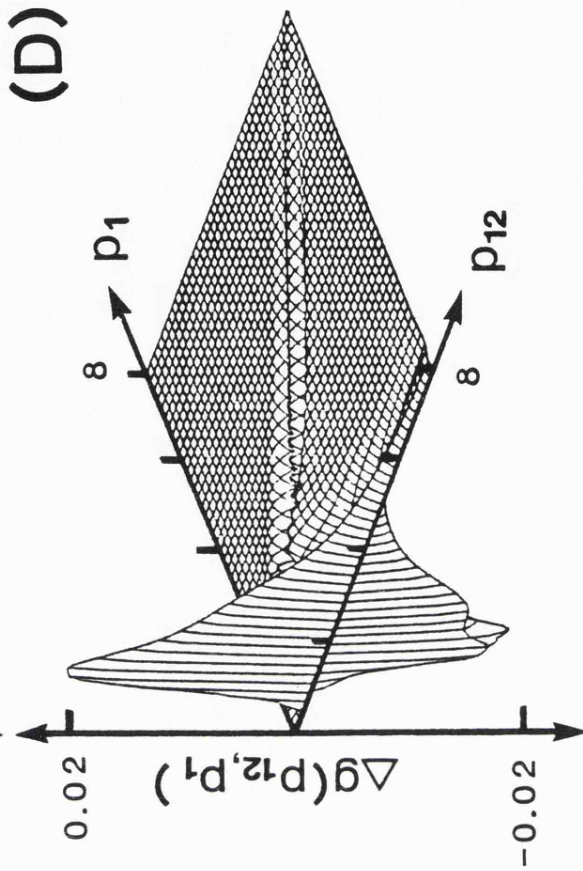
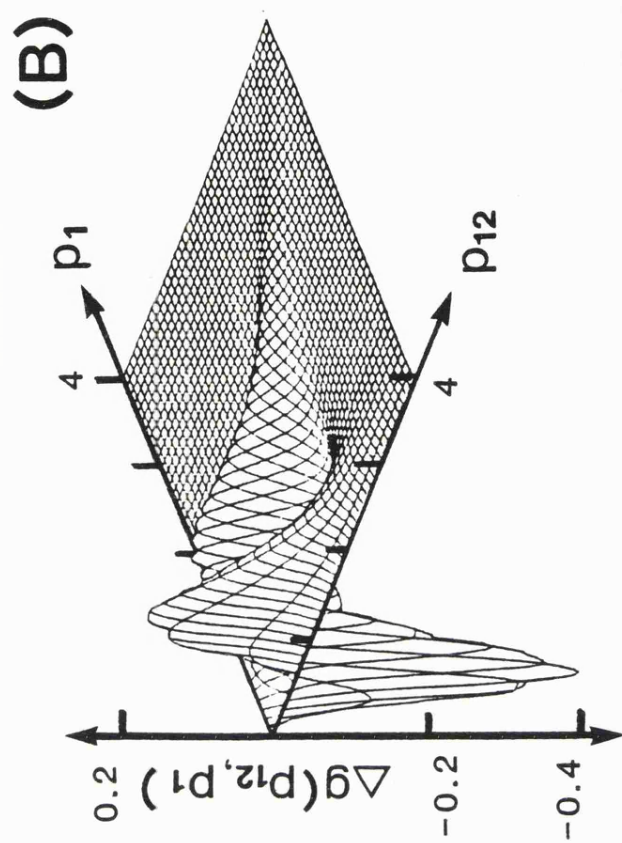
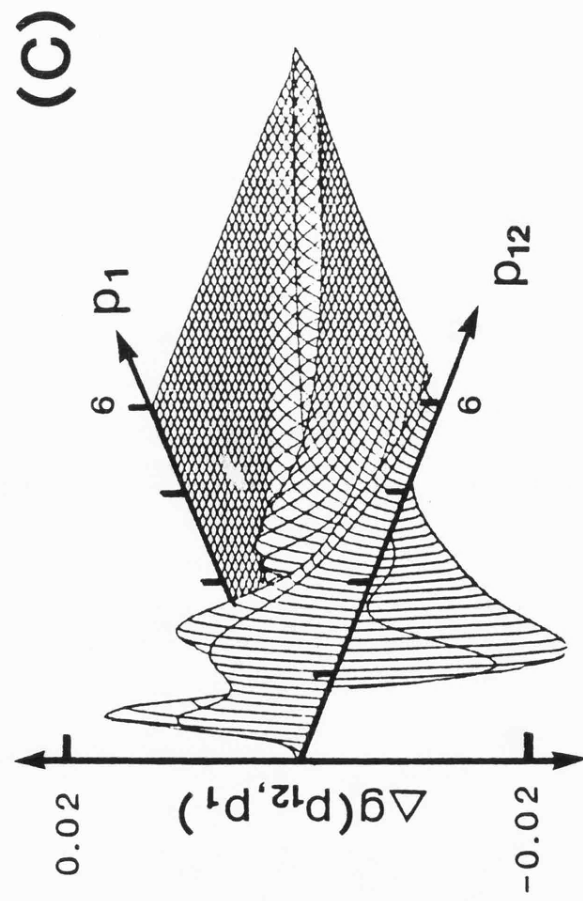
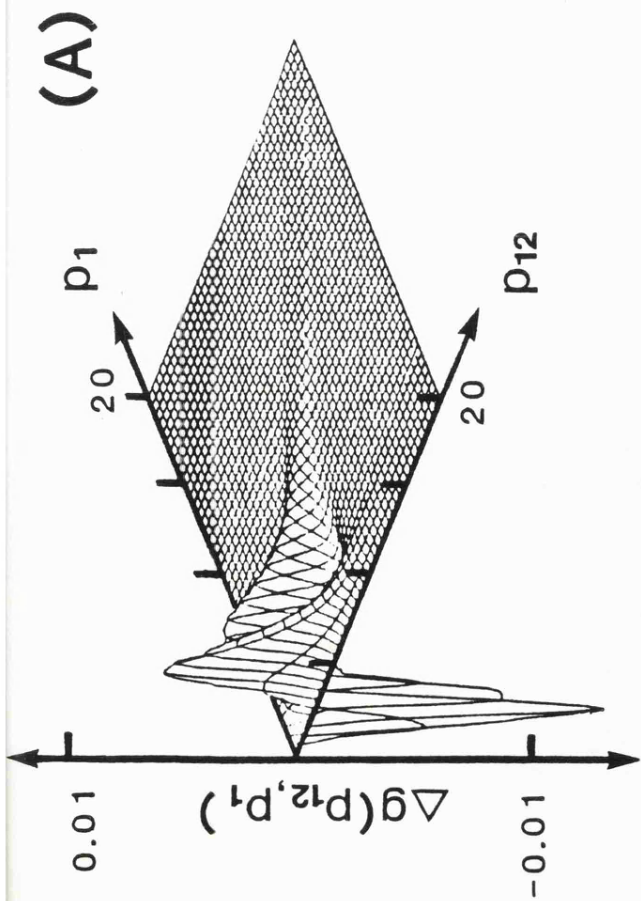


Figure III.9 The LiH total and component Coulomb shifts.

Figure III.10

(see over)

Figure III.10 The partial Coulomb shifts surfaces,
 $\Delta g(p_{12}, p_1)$, for the intra- and intershells of LiH.



PART IV
CORRELATION COEFFICIENTS

CHAPTER IV.1

INTRODUCTION

The term electron correlation, introduced by Wigner and Seitz^(1,2) into the quantum mechanics of electron systems, is apparently borrowed from probability theory and mathematic statistics, where correlation is a well-known concept referring to non-independent variables. Kutzelnigg, Del Re and Berthier⁽³⁾ introduced correlation coefficients to the field of quantum mechanics and discussed their connection with the concept of electron correlation, pointing out that they may be used to analyze both atoms and molecules in ground and excited states. Owing to the difficulty of evaluating the necessary integrals, using reasonably well-correlated wavefunctions, Kutzelnigg et al. restricted their numerical evaluations to two special cases: a radial correlation coefficient and an angular correlation coefficient. Many workers⁽⁴⁻¹²⁾ have subsequently utilised these correlation coefficients in their studies of electron correlation.

During the course of our investigations, King and Rothstein⁽¹³⁾ produced a study of correlation coefficients as applied to an exactly soluble electron correlation problem. They considered the problem of two interacting electrons trapped in an external harmonic oscillator potential and repelling each other via a Hook's law force.

Their conclusion was that although the correlation coefficient provides a measure of electron correlation in the probabilistic sense, it does not necessarily measure electron correlation in the energetic sense of the term. In their view, it appears most sensible to restrict the study of electron correlation, using correlation coefficients, to very accurate wavefunctions.

In this section of this thesis we present a statistical overview outlining the various component terms required in assessing statistical correlation, as applied to the study of electron correlation, and, in particular, we outline the care that must be taken in using correlation coefficients if they are to be employed in calculations involving non-closed shell states.

CHAPTER IV.2

STATISTICAL OVERVIEW

Before we can discuss the application of correlation coefficients to the study of electron correlation in atoms and molecules we must review some of the fundamental concepts behind their construction.

Probability Density and Distribution Functions

A quantity that may assume one of many (or even infinitely many) values within a certain probability range is called a random variable and will be denoted, unless stated otherwise, by the symbol X . A random variable that can assume only discrete values is called a 'discrete random variable'; however within quantum mechanics we concern ourselves with variables that can assume any value from a continuous distribution and such a variable is called a 'continuous random variable'.

The behaviour of a random variable is given by the probability with which the variable will assume certain values. There will in general be a finite probability, P , that the value assumed by the random variable X will lie within an arbitrarily small interval of values dx ; this probability is obviously proportional to the length of that interval:

$$P(x < X < x + dx) \text{ proportional to } dx. \quad \text{IV.1}$$

To convert Equation IV.1 from a statement of proportionality to an equality we must multiply dx by a function $p(x)$ which acts as a kind of weighting function. In general, the probability that a random variable X will assume a value lying between x and $x + dx$ is

$$P(x < X < x + dx) = p(x)dx \quad \text{IV.2}$$

It can be seen from Equation IV.2 that $p(x) = P/dx$ has the dimensions of a probability per unit interval of x ; it is therefore called the probability density (of the random variable X) and completely describes the law governing the behaviour of the random variable X .

Since a probability cannot take a negative value, we have from Equation IV.2 that

$$p(x) \geq 0 \text{ for all } x \quad \text{IV.3}$$

Also, since the assumed value of X will have a value between $-\infty$ and $+\infty$ this is a certain event and so

$$\int p(x) dx = 1 \quad \text{IV.4}$$

All integrations, unless specified otherwise, are assumed to span all the available space. Thus, a probability density must always have the properties of Equations IV.3 and IV.4

and be defined by Equation IV.2, it must of course be a single-valued function of x .

Some common probability densities are: the Normal or Gaussian Probability Density, the Uniform Distribution, the Rayleigh Distribution, the Simpson Distribution and the Lognormal Distribution. Functional forms of these distributions may be found in Ref. 14-16.

Multi-dimensional Distributions

We now consider the extension of the above to two random variables: X assuming values x with probability density $p(x)$, and Y whose probability density is $p(y)$. Let us now, in analogy to the definition of a one-dimensional probability, Equation IV.2, define a two-dimensional probability density $p(x,y)$ by

$$P(x < X < x + dx, y < Y < y + dy) = p(x,y)dxdy \quad . \quad \text{IV.5}$$

Repeating the same considerations as in Equations IV.3 and IV.4 above, we now find for very similar reasons that $p(x,y)$ must be a single-valued function with the properties

$$p(x,y) > 0 \quad \text{IV.6}$$

and

$$\int \int p(x,y)dxdy = 1 \quad . \quad \text{IV.7}$$

By analogy, $p(x,y)$ may now be represented by a surface, see

Figure IV.1, and the probability by the volume $p(x,y)dxdy$. The volume under the surface $p(x,y)$ must by Equation IV.7 be unity. Alternatively, one may represent the surface by plotting 'equiprobability curves' $p(x,y) = \text{const}$. They must obviously be closed curves that do not intersect (contours).

Next, consider the events $x < X < x + dx$, denoted by A, and $y < Y < y + dy$, denoted by B. Let us now consider the conditional probability, $P(A|B)$, which represents the probability of an event A happening having fixed a value (a condition) for event B. As discussed above we can define a density, the conditional probability density, $P_c(x|y)$, by

$$P(x < X < x + dx | y < Y < y + dy) = P_c(x|y)dx \quad \text{IV.8}$$

Note that only X is random, Y is fixed (within the interval $y, y + dy$) and therefore this is a one-dimensional density.

From the theorem of joint probability⁽¹⁴⁻¹⁶⁾

$$P(A,B) = P(A|B)P(B) \quad \text{IV.9}$$

and it follows that

$$p(x,y) = P_c(x|y)p_Y(y) \quad \text{IV.10}$$

The indexes c and Y in Equation IV.10 are needed to indicate that p , P_c and p_Y , though all probability densities, are different functions. We may introduce a simplification to the notation by dropping these indexes and

use the letter p as an operator meaning a probability density of the kind, and of the random variable, evident from the symbol inside the parentheses. Thus Equation IV.10 becomes

$$p(x,y) = p(x|y)p(y) \quad \text{IV.11}$$

which is the theorem of joint probability for continuous random variables. In a similar manner it can be shown that:

$$p(x,y) = p(y|x)p(x) \quad \text{IV.12}$$

Let us now consider the important distinction between independent and dependent continuous random variables. As already indicated by Equation IV.5 it is reasonable to define the (in)dependence of two random variables X and Y as being independent if and only if

$$p(x|y) = p(x) \quad \text{IV.13}$$

that is, if the probability of X assuming a certain value x is unchanged by the value assumed by Y . Substituting Equation IV.13 into IV.12 we find that if X and Y are independent, then

$$p(x,y) = p(x)p(y) \quad \text{IV.14}$$

Thus, Equation IV.14 is a necessary and sufficient condition of independence, and may often lead to the establishment of independence more quickly than Equation IV.5.

Mean Values and Variance

The behavior of a random variable is completely described by its probability distribution, i.e., by its probability density. In many cases we are only interested in certain of its characteristic values, or we are unable to determine the entire distribution and have to restrict ourselves to finding these characteristics.

The most elementary characteristic is the average or the mean value of a random variable. This may be understood to stand for the arithmetic mean of all the values that a random variable may assume. The mean value is thus a rough indication where the variable is to be found, or about which typical value the variable is distributed. It is therefore reasonable to define the mean, or expected, value of a continuous random variable X assuming values x with a probability density $p(x)$ as

$$\langle X \rangle = \int xp(x)dx \quad . \quad \text{IV.15}$$

From the definition given in Equation IV.15 it follows immediately that if C is any constant, then

$$\langle CX \rangle = C \langle X \rangle \quad . \quad \text{IV.16}$$

Now, let $Y = f(x)$ then we also have

$$\langle Y \rangle = \int y p(y) dy = \int f(x) p(x) dx \quad \text{IV.17}$$

and hence an important relationship is

$$\langle f(X) \rangle = \int f(x) p(x) dx \quad \text{IV.18}$$

Equation IV.18 is easily generalised to functions of two (or several) variables. If $Z = f(X, Y)$ then

$$\langle Z \rangle = \int z p(z) dz = \iint p(x, y) f(x, y) dx dy \quad \text{IV.19}$$

In particular, if $f(X, Y) = X + Y$ then from Equation IV.19

$$\begin{aligned} \langle X + Y \rangle &= \iint x p(x, y) dx dy + \iint y p(x, y) dx dy \\ &= \langle X \rangle + \langle Y \rangle \quad \text{IV.20} \end{aligned}$$

Note that we have made no assumptions regarding the possible interdependence of X and Y , and that this result will hold whether X and Y are independent or not.

The mean value is a constant that gives us the crudest information about a random variable, namely, the value around which it is distributed. The next most elementary information concerns the scatter of the individual values, that is, the extent to which the random variable deviates from its mean value. The mean value of the deviations is useless as it is always zero. To characterise the scatter we might use the mean of absolute deviations

$$\langle |X - \langle X \rangle| \rangle \quad \text{IV.21}$$

or its mean square

$$\langle (X - \langle X \rangle)^2 \rangle \quad . \quad \text{IV.22}$$

The second definition proves to be the more useful to statisticians and is called the variance of the random variable X and is denoted by $\text{Var}(X)$ ⁽¹⁴⁻¹⁶⁾. From Equation IV.22 the variance is given by

$$\text{Var}(X) = \langle (X - \langle X \rangle)^2 \rangle = \int (x - \langle X \rangle)^2 p(x) dx \quad . \quad \text{IV.23}$$

Remembering that $\langle X \rangle$ is a constant we may also express the variance using Equation IV.16 as

$$\begin{aligned} \text{Var}(X) &= \langle (X - \langle X \rangle)^2 \rangle = \langle X^2 - 2X\langle X \rangle + \langle X \rangle^2 \rangle \\ &= \langle X^2 \rangle - 2\langle X \rangle^2 + \langle X \rangle^2 \\ &= \langle X^2 \rangle - \langle X \rangle^2 \end{aligned} \quad \text{IV.24}$$

and this formula is usually the most useful for calculating $\text{Var}(X)$. The mean square value $\langle X^2 \rangle$ is found by (see Equation IV.18)

$$\langle X^2 \rangle = \int x^2 p(x) dx \quad . \quad \text{IV.25}$$

The variance of a random variable has the dimension of the square of the random variable, thus to convert to the original dimensions we must take the square root of $\text{Var}(X)$ creating a new quantity called the standard deviation, $\Delta(X)$, given by

$$\Delta(X) = \sqrt{\text{Var}(X)} = \sqrt{(\langle X^2 \rangle - \langle X \rangle^2)}$$

IV.26

which gives a measure to the spread of a distribution.

Covariance

The mean and variance, discussed above, are calculated from the probability density of a single random variable, we now return to the two-dimensional distributions defined by Equations IV.5 - IV.6. Let X and Y be two random variables and consider the mean product of their deviations; namely $\langle (X - \langle X \rangle)(Y - \langle Y \rangle) \rangle$ which, in the light of the above discussion can be expressed as

$$\begin{aligned} \langle (X - \langle X \rangle)(Y - \langle Y \rangle) \rangle &= \langle XY - X\langle Y \rangle - \langle X \rangle Y + \langle X \rangle \langle Y \rangle \rangle \\ &= \langle XY \rangle - \langle X \rangle \langle Y \rangle - \langle X \rangle \langle Y \rangle + \langle X \rangle \langle Y \rangle \\ &= \langle XY \rangle - \langle X \rangle \langle Y \rangle \end{aligned} \quad \text{IV.29}$$

This quantity is called the covariance of X and Y and it may be written as

$$\begin{aligned} \text{Cov}(X, Y) &= \iint (x - \langle X \rangle) (y - \langle Y \rangle) p(x, y) dx dy \\ &= \langle XY \rangle - \langle X \rangle \langle Y \rangle \end{aligned} \quad \text{IV.30}$$

If X and Y are independent, the product of their deviations will be positive as often as negative. Hence, the mean of this product, or the covariance, will be equal to zero. To prove this, we recall that if X and Y are independent, then

$p(x,y) = p(x)p(y)$, and substituting this into Equation IV.30, we have

$$\text{Cov}(X,Y) = \int (x - \langle X \rangle) p(x) dx \int (y - \langle Y \rangle) p(y) dy = 0 \quad \text{IV.31}$$

since both integrals vanish, for example:

$$\int x p(x) dx - \langle X \rangle \int p(x) dx = \langle X \rangle - \langle X \rangle = 0 \quad \text{IV.32}$$

On the other hand, if X and Y are dependent, then Y (if it tends to vary in harmony with X) will tend to be above its mean when X is above its mean, and below its mean when X is below its mean. The product of the deviations will therefore be predominantly positive, and $\text{Cov}(x,y)$, being the mean of this product, will be positive also.

To summarise, $\text{Cov}(x,y)$ is positive when X and Y tend to vary in harmony, negative when X and Y tend to vary in opposition, and zero when X and Y are independent.

The sign of the covariance can often be found simply by inspecting the equiprobability curves $p(x,y) = \text{constant}$. Thus, in Figure IV.2.a it will be seen that increasing X corresponds to increasing Y for the same probability of joint occurrence. Hence X and Y are dependent and tend to vary in harmony; similarly, in the case of Figure IV.2.b, X and Y tend to vary in opposition.

If the equiprobability curves have an axis of symmetry parallel to one of the coordinate axes (the x axis in Figure

IV.2.c) then the covariance vanishes, as may be seen from Equation IV.30, since every element in the integrand will be cancelled by an equal element of opposite sign.

Let us next investigate the maximum value of $\text{Cov}(X, Y)$. Let $U = X - \langle X \rangle$ and $V = Y - \langle Y \rangle$ be the deviations of X and Y , respectively, and consider Schwarz's inequality⁽¹⁷⁾

$$\begin{aligned} \left(\iint uv p(u, v) du dv \right)^2 &\leq \iint u^2 p(u, v) du dv \iint v^2 p(u, v) du dv \\ &\leq \iint u^2 p(u) du \iint v^2 p(v) dv \\ &\leq \langle U^2 \rangle \langle V^2 \rangle \end{aligned} \quad \text{IV.33}$$

Since the expression on the left hand side is the square of the $\text{Cov}(X, Y)$, see Equation IV.30, and $\langle U^2 \rangle$, $\langle V^2 \rangle$ are, by definition, the variances of X and Y , respectively, therefore Equation IV.33 may be written as

$$[\text{Cov}(X, Y)]^2 \leq \text{Var}(X) \text{Var}(Y) \quad ,$$

from which we may derive the following expression

$$- \sqrt{[\text{Var}(X) \text{Var}(Y)]} \leq \text{Cov}(X, Y) \leq + \sqrt{[\text{Var}(X) \text{Var}(Y)]} \quad ,$$

that is,

$$-1 \leq \text{Cov}(X, Y) / \sqrt{[\text{Var}(X) \text{Var}(Y)]} \leq +1 \quad \text{IV.34}$$

This enables us to introduce the dimensionless quantity, τ , defined by

$$\tau = \text{Cov}(X,Y) / \sqrt{[\text{Var}(X)\text{Var}(Y)]}$$

IV.35

and is called a correlation coefficient of X and Y, which, by Equation IV.34, must lie within the range

$$-1 \leq \tau \leq +1$$

IV.36

If X and Y are independent, then, by Equation IV.31, $\tau=0$; if τ is positive, X and Y vary in harmony, if it is negative, they vary in opposition. In both cases the absolute magnitude of τ is an indication of how strongly X and Y are dependent. The value $\tau=1$ (full correlation) corresponds to linear dependence of X and Y; the value $\tau=0$ corresponds to 'non-correlation', and $\tau=-1$ represents complete anti-correlation.

Thus, correlation and non-correlation are something similar to dependence and independence. However, the two are not identical. Independence is a stronger concept than non-correlation. If X and Y are independent, they are automatically uncorrelated, as we have seen in Equation IV.31. However, the converse is not always true; that is, it may happen that even though $\tau=0$, X and Y are not independent as is illustrated in the following example:

Let $X = \cos\theta$, $Y = \sin\theta$, where θ is a random variable. Then X and Y are certainly not independent, since they are related to each other by the functional relationship

$$Y = \sqrt{1 - X^2}$$

IV.37

Now let θ be distributed uniformly from zero to 2π .
Then, from Equation IV.30,

$$\begin{aligned}\text{Cov}(X,Y) &= \langle \cos\theta \sin\theta \rangle - \langle \cos\theta \rangle \langle \sin\theta \rangle \\ &= (1/2) \langle \sin 2\theta \rangle \\ &= 0\end{aligned}\tag{IV.38}$$

and, hence, $\tau = 0$ in spite of IV.37.

Thus, independence implies non-correlation and correlation implies dependence; but the converse is not necessarily true, ie., independence does not follow from $\tau=0$, and $\tau \neq 0$ does not follow from inter-dependence.

CHAPTER IV.3

AN APPRAISAL OF CORRELATION COEFFICIENTS

The term electron correlation is commonly used in two different senses. In the conventional quantum mechanical sense electron correlation effects are those that are not taken into account by the Hartree-Fock approximation^(21,22). In the statistical sense electron correlation is the manner in which the electron pair density differs from the product of the one-electron densities⁽²³⁾. It is difficult to visualise the correlation density because it is a rather complex function of six variables, hence, it is useful to have numerical indices which provide overall measures of correlation. (Some idea of the complexity of the pair correlation density can be obtained by examining detailed cross-sectional diagrams such as those given by Maslen⁽²⁴⁾, Sperber⁽²⁵⁾ and Besson & Suard⁽²⁶⁾) Such indices were introduced by Kutzelnigg, Del Re and Berthier⁽³⁾ who used concepts from probability theory and mathematical statistics to define generalised correlation coefficients, τ , involving functions of the position vectors, \underline{r}_1 and \underline{r}_2 . They considered the use of two such functions, a radial correlation coefficient and an angular coefficient.

Radial correlation coefficients depend only on the radial part of the two-electron density and are defined by

$$\tau_{\text{radial}} = (\langle r_1^n r_2^n \rangle - \langle r_1^n \rangle^2) / (\langle r_1^{2n} \rangle - \langle r_1^n \rangle^2) . \quad \text{IV.39}$$

The coefficients corresponding to specific choices $n=1$ and $n=-1$ were introduced by Kutzelnigg and coworkers⁽³⁾. This coefficient clearly depends on the choice of origin, the nucleus is a natural origin for atoms whereas molecules generally do not have a natural origin.

Kutzelnigg and his colleagues defined an angular correlation coefficient for atoms, choosing the nucleus as the origin, and, interpreting the product vectors as a scalar product, we can obtain a generalized expression for this correlation coefficient as

$$\begin{aligned} \tau_{\text{angular}} &= \langle \underline{r}_1 / r_1^n \cdot \underline{r}_2 / r_2^n \rangle / \langle r_1^{2(1-n)} \rangle \\ &= \langle r_1^{1-n} r_2^{1-n} \cos \gamma_{12} \rangle / \langle r_1^{2(1-n)} \rangle \end{aligned} \quad \text{IV.40}$$

where, $n = 0, 1$ and 2 and γ_{12} is the angle subtended at the nucleus by the position vectors \underline{r}_1 and \underline{r}_2 . The particular case $n=0$ was introduced by Kutzelnigg et al. and the specific case $n=1$ leads to the particularly simple angular correlation coefficient $\langle \cos \gamma_{12} \rangle$. These angular correlation coefficients, as indeed for any correlation coefficient, are bounded in absolute value by unity. Perfect positive correlation ($\tau = 1$) means that the position vectors of a pair of electrons are expected to coincide whereas perfect negative correlation ($\tau = -1$) implies that electron pairs are expected to be at diametrical positions with respect to the nucleus. If the angular correlation coefficient is zero

then the electrons are either independent or merely uncorrelated by virtue of the orthogonality of their position vectors.

King and Rothstein⁽¹³⁾ have pointed out that care must be taken when using correlation coefficients in the investigation of electron correlation. A discussion of their work will be left to the following section. Let us now outline further considerations that have to be undertaken if correlation coefficients are to be used, sensibly, in the analysis of electron correlation. To aid the discussion, in Figures IV.4 and IV.5 we present diagrammatic representations of the two-particle radial density distribution $D_{\text{HF}}(r_1, r_2)$ and the function $g_{\text{HF}}(r_{12}, r_1)$ for the intra- and intershells of beryllium, evaluated using the Hartree-Fock wavefunction of Watson⁽²⁰⁾. The $D_{\text{HF}}(r_1, r_2)$ function is defined by:

$$D_{\text{HF}}(r_1, r_2) = \int \Gamma_{\text{HF}}(\underline{r}_1, \underline{r}_2) r_1^2 r_2^2 \sin\theta_1 \sin\theta_2 d\theta_1 d\theta_2 d\phi_1 d\phi_2 \quad \text{IV.41}$$

and $g_{\text{HF}}(r_{12}, r_1)$, used previously in the construction of partial Coulomb holes, is defined such that

$$\int g_{\text{HF}}(r_{12}, r_1) dr_1 = f_{\text{HF}}(r_{12}) \quad \text{IV.42}$$

where, $\Gamma_{\text{HF}}(\underline{r}_1, \underline{r}_2)$ is the partitioned Hartree-Fock two-particle density as given in Equation II.22 and $f_{\text{HF}}(r_{12})$ is the interparticle separation distribution function⁽²⁷⁾. The $D_{\text{HF}}(r_1, r_2)$ and $g_{\text{HF}}(r_{12}, r_1)$ functions have the following normalisation conditions

$$\int D(r_1, r_2) dr_1 dr_2 = 1$$

and

$$\iint g_{HF}(r_{12}, r_1) dr_{12} dr_1 = \int f_{HF}(r_{12}) dr_{12} = 1 .$$

A more detailed discussion of the derivation of $g_{HF}(r_{12}, r_1)$ may be found in Ref 28 Appendix A.2.

Figure IV.4 show the $D_{HF}(r_1, r_2)$ surfaces for atomic Be as studied in Part II of this thesis, evaluated from the Hartree-Fock wavefunction⁽²⁰⁾. Figures IV.4(A) and IV.4(B) show very similar details both for the K- and L-shells; each distribution being homogeneous. Figures IV.4(C) and IV.4(D), for the intershells of $1s$ and $3s$ symmetry, clearly show two distinct features, the third structure found on the $1s$ surface, in Figure IV.4(C), is associated with the penetration of the outer L-shell electron into the inner K-shell region, no such feature is found on the $3s$ surface because of the Fermi effect forbidding any such penetration. The main features found on these surfaces are attributable to 'non-correlation' or independence, each electron is effectively localised in its own region of space and appears unaffected by the presence of the other. Non-correlation is associated with structures parallel to the variable axis.

A dangerous assumption is the ability to combine data from two or more separate groups as though they were a single homogeneous population. A scatter diagram such as Figure IV.3 helps to show what will occur if we do this.

The data in Group I show a good positive correlation, measured about the mean (X_1, Y_1) , whereas the data in Group II show hardly any relationship, measured about their mean (X_2, Y_2) . If we try to compute a single correlation coefficient for the whole of the data, we are of course making the calculation relative to the overall mean (X, Y) , which in Figure IV.3 happens to fall between the two groups of observations; this in itself should be warning enough. The r value will be very large because all the observations fall in the first and third quadrants relative to (X, Y) . Returning to Figures IV.4(C) and IV.4(D), we can see that each surface possess structural forms which constitute separate population distributions. Although not completely analogous with the scatter diagram, Figure IV.3, discussed above, where the probability is zero between the two groups of information, the probability is sufficiently small to consider these surfaces as being constructed of quasi-homogenous distributions. Thus, as pointed out above, any discussion about the composite implies discussing changes about a mean value that will not lie within either, or any, of these distributions. This type of structure will always manifest itself in any split shell state or system. So the original results of Kutzelnigg, Del Re and Berthier⁽³⁾, who applied correlation coefficients to the 3S , 1P and 3P states of helium, must be treated with some caution. This, of course, implies that the correlation coefficients present in Tables II.10, II.11, II.17 and II.18 for the intershells of Be, which were only presented for comparison and completeness, should be treated with the same caution, and used only as a relative guideline.

The question, of course, then arises as to how we can study electron correlation effects within split shell states, such as the $\text{He}(1s2s)^1S$ state, or the intershell distributions of an atom such as Be. Investigating another probability distribution function, such as $g_{\text{HF}}(r_{12}, r_1)$, might be a solution to the problem. As can be seen in Figure IV.5, this transformation of the problem does not produce the required single homogenous structure. Indeed each structure in the $g_{\text{HF}}(r_{12}, r_1)$ surfaces for the intershells KL^1S and KL^3S of Be, Figures IV.5(C) and IV.5(D), can be associated with the various structures found in the $D_{\text{HF}}(r_1, r_2)$ surfaces, each is attributable to different types of statistical correlation. The parallel structure can be assigned to 'noncorrelation' or independence and the diagonal structure to 'harmonic' correlation as discussed earlier. Even tranposing to another coordinate system, such as momentum space coordinates p_1 and p_2 or p_1 and p_{12} , does not destroy these structures. Although not presented in any detail the momentum distribution $g(p_{12}, p_1)$ and the $\Delta g(p_{12}, p_1)$ surfaces, defined by Equation II.57 and presented in Figure II.13, for the intra- and intershells of Be show similar features found in their position space counterparts: that is, the intershells, once again, do not form homogeneous distributions.

Thus, in conclusion, the use of correlation coefficients must be reserved for systems that include only intrashells giving homogeneous bivariant distributions and the investigation of electron correlation for any other effect

must be limited to discussion of overall changes of these distributions by forming, for example, difference-surfaces, such as the Δg -type surfaces discussed above.

CHAPTER IV.4

AN ASSESSMENT OF THE WORK OF KING AND ROTHSTEIN

Introduction

The system considered by King and Rothstein⁽¹³⁾ was one of two interacting electrons trapped in an external harmonic oscillator potential. The Hamiltonian for the problem is given by

$$H = -1/2 (\nabla_1^2 + \nabla_2^2 - k(r_1^2 + r_2^2) + \alpha r_{12}^2) \quad \text{IV.43}$$

where k and α are spring constants, obeying a Hook's Law of interaction, and represents the electron-nucleus and a form of electron-electron interaction, respectively. Davidson⁽¹⁹⁾ reported an exact solution for this type of Hamiltonian by introducing the variables $\underline{R} = \sqrt{2}(\underline{r}_1 + \underline{r}_2)$ and $\underline{r} = \sqrt{2}(\underline{r}_1 - \underline{r}_2)$. The solution for the Schrödinger equation is of the following form

$$\Psi = \psi(\underline{R})\phi(\underline{r})[\sigma] \quad \text{IV.44}$$

where $[\sigma]$ is the usual antisymmetric normalized two-particle spin function and the spatial functions ψ and ϕ are given by

$$\psi(\underline{R}) = (\sqrt{k/\pi})^{3/4} \exp(-\sqrt{k}R^2/2) \quad \text{IV.45}$$

and

$$\varphi(\underline{r}) = (\sqrt{k_\alpha}/\pi)^{3/4} \exp(-\sqrt{k_\alpha} r^2/2) \quad \text{IV.46}$$

where $k_\alpha = (k - 2\alpha)$. The exact ground-state energy for such a system is given by $E(k, \alpha) = 3/2(\sqrt{k} + \sqrt{k-2\alpha}) \equiv 3/2(\sqrt{k} + \sqrt{k_\alpha})$. We note that since the energy involves $\sqrt{k_\alpha}$, in order to obtain a non-imaginary value α must be bounded by the range $0 \leq \alpha \leq k/2$. At $\alpha > k/2$, the repulsive spring constant α is sufficiently strong that the two electrons repel each other to the extent that the external harmonic oscillator potential cannot bind both electrons.

King and Rothstein examined an angular correlation coefficient for the system which, being dependent on the angle between the electronic position vectors, follows the definition given by Equation IV.40 when $n = 0$. Using the exact solution as set out in Equations IV.44 - 46, the corresponding expression for τ is

$$\tau(k, \alpha) = (\sqrt{k_\alpha} - \sqrt{k}) / (\sqrt{k_\alpha} + \sqrt{k}) \quad \text{IV.47}$$

Figure IV.6 shows the variation of $E(k, \alpha)$, the true ground state energy, and $\tau(k, \alpha)$ with α . For simplicity, a value for k , the electron-nuclear spring constant, has been taken to be equal to unity. Note that if $k_\alpha = k$ (ie., $\alpha = 0$) $\tau(k, \alpha)$ is zero corresponding to two independent electrons. They are indeed truly independent because the probability density can be written in the form specified by Equation IV.14. As k_α tends to 0 (ie., $2\alpha \rightarrow k$) we find that $\tau(k, \alpha)$

tends to -1. This corresponds to two perfectly negatively correlated electrons; that is, the electrons are on opposite sides of the nucleus.

King and Rothstein then considered the problem variationally by considering the approximate wavefunction $\bar{\Psi}$ given by

$$\bar{\Psi} = \psi(\underline{R})\varphi^\beta(\underline{r})[\sigma] \quad \text{IV.48}$$

where $\psi(\underline{R})$ is given by Equation IV.45 and

$$\varphi^\beta(\underline{r}) = (\sqrt{\beta/\pi})^{3/4} \exp(-\sqrt{\beta}r^2/2) \quad \text{IV.49}$$

with β being regarded as a variational parameter and $[\sigma]$ is the spin function as discussed earlier.

The angular correlation coefficient for the system, given by Equation IV.40, may be evaluated in terms of this variational parameter β giving

$$\tau(k, \beta) = (\sqrt{\beta} - \sqrt{k})/(\sqrt{\beta} + \sqrt{k}) \quad \text{IV.50}$$

and Figure IV.7 shows the variation of this function, $\tau(k, \beta)$, with β . To assist the discussion we present in Figure IV.8 the variation of $E(k, \beta)$, the variational energy of the system, with β , which is given by $E(k, \beta) = 3/2[\sqrt{k} + 1/2\sqrt{\beta}(k/\beta + 1)]$. Note that this expression for $E(k, \beta)$ is also a function of α .

Discussion

Figure IV.6 shows the variation of the correlation coefficient, $\tau(k,\alpha)$, and energy, $E(k,\alpha)$, with changing α , the interparticle spring constant, evaluated for the system investigated by King and Rothstein⁽¹³⁾. Following King and Rothstein, "if the parameter α in the Hamiltonian H ", see Equation IV.43, "is small, the exact correlation coefficient, $\tau(k,\alpha)$, is a small negative number", and as can be seen in Figure IV.6 when $\alpha \rightarrow 0$ the energy has a value of $\sqrt{3k}$ corresponding to the system possessing two independently charged particles. The associated correlation coefficient, $\tau(k,\alpha)$, is seen to be of zero value. As α varies from 0 to an upper limit of $k/2$, the correlation coefficient can be considered to reflect the energy of the system; varying from 0 to -1 corresponding to an energy variation of $3\sqrt{k}$ to $3\sqrt{k}/2$ over the same range of α .

King and Rothstein then compared this solution, for the exact wavefunction, to one obtained using Equation IV.49 with the parameter β chosen, not via the energy criteria, but to give a correlation coefficient close to -1. As can be seen from Figure IV.7 this corresponds to a value for β of near zero value. This, says King and Rothstein, "is a poor approximation to the true ground state energy of $3\sqrt{k}$ despite the nearly perfect, negative correlation coefficient". The energy, $E(k,\beta)$, corresponding to such a value of β is in the region of $3\sqrt{k}/2$ having selected an appropriate choice for α of $k/2$. Any other choice for α would lead to an infinite value for the energy having fixed

the value for β as described above, see Figure IV.8. From Figure IV.6 an energy value corresponding to $3\sqrt{k}$ is not the lowest energy state of the system but is equivalent to the independent particle energy, which has an associated correlation coefficient of zero value. However, the energy $3\sqrt{k}/2$ does correspond to the lowest correlated energy, and is evaluated from $\alpha = k/2$ (ie., $k_\alpha = 0$) which has an associated value for the correlation coefficient equal to -1. It appears that King and Rothstein are comparing two physically different systems. In the first instance, to quote King and Rothstein, α has a small value, giving the system the appearance of two independent particles and in the second case, in order to obtain a physically meaningful energy for an associated non-optimized variation parameter β of small magnitude, α must have a value of $k/2$, thus producing a system on the limit of stability.

However, if we decide to operate outside of the variation method and not energy-minimize with respect to β we believe the following argument might lead to the same conclusions as that of King and Rothstein: namely, that an energetically poor wavefunction (but not variationally optimized) could have a more negative τ value than the exact solution. Following King and Rothstein we will take α to be a small non-zero value. The behaviour of the variational energy for the system as a function of β , and α , is presented in Figure IV.8 where it is seen that for a fixed choice for α , other than $k/2$, $E(k,\beta)$ vs. β has a variational minimum with the optimum β being of non-zero value. As β gets smaller the energy for the system rises away from its

(variational) minimum. Again, if we decide to follow King and Rothstein by insisting on a large negative correlation coefficient then this will, as before, preselect a value for β of near zero value. Selecting the energy appropriate to this choice of small β , and small α , we would indeed conclude that the energy of the system was a poor approximation to the ground state energy despite the correlation coefficient for the system having a value of -1. But, of course, we are indeed operating outside of the variational theorem and the value obtained for the energy of the system has no useful meaning.

Thus, in conclusion, the results of King and Rothstein can only be proven satisfactorily by ignoring one of the most fundamental concepts of quantum mechanics, that of the energy variation method. Contrary to their findings, Figure IV.6 illustrates that correlation coefficients do appear to give a global measure of electron correlation in the energetic sense and their conclusion that the usefulness of correlation coefficients should be limited only to a discussion of exact, or very accurate, wavefunctions has not been substantiated.

CHAPTER IV.5

SUMMARY

The investigative elements of electron correlation have been examined in terms of their fundamental concepts from the field of statistical mathematics. The distribution function $g_{\text{HF}}(r_{12}, r_1)$ is a joint probability function comprising of individual conditional probability functions $g_{\text{HF}}(r_{12}|r_1)$. Integrating the joint probability function with respect to r_1 leads to the probability density $f_{\text{HF}}(r_{12})$, the inter-particle separation distribution function, which has been used extensively in the study of electron correlation. Additional indexes help us to describe the shape of the various distribution functions: the covariance describes the variation of two random variables with respect to each other, that is, whether they vary in harmony or are independent, and the standard deviation which measures the spread of a distribution. These two indexes are themselves functions of more fundamental components called expectation values. A quotient function, involving the covariance and standard deviation, allows us to define a quantity, for a homogenous bivariant distribution, called a correlation coefficient which is a dimensionless quantity that gives a single value which is a global measure of correlation.

These quantities have been used to analyse the effects of electron correlation in atoms and molecules; initially

just using the fundamental expectation values. However, in more recent years, the conditional and joint probability functions $g_{HF}(r_{12}|r_1)$ and $g_{HF}(r_{12},r_1)$, along with their electron-correlated counterparts $g_{corr}(r_{12}|r_1)$ and $g_{corr}(r_{12},r_1)$, have played a more leading role; culminating in the use of correlation coefficients. In this section of the thesis we have warned against the "blind" use of correlation coefficients. In particular, we have emphasized that their usefulness is only applicable to homogenous bivariant distributions.

Finally, the recent work of King and Rothstein, has been studied in order to examine their claim that correlation coefficients should only be applied to highly correlated or exact wavefunctions. Their work was found to be inconclusive within the normal bounds of the energy variation method and to accomplish their results we had to ignore this underlying concept of modern physics.

CHAPTER IV.6

REFERENCES

1. E.P. Wigner and F. Seitz, Phys. Rev. 43, 804 (1933).
2. E.P. Wigner and F. Seitz, Phys. Rev. 46, 509 (1934).
3. W. Kutzelnigg, G. Del Re and G. Berthier, Phys. Rev. 172, 49 (1968).
4. W.A. Bingel and W. Kutzelnigg, Adv. Quantum Chem. 5, 201 (1970).
5. W.A. Bingel, Chem. Phys. Lett. 5, 367 (1970).
6. K.E. Banyard and D.J. Ellis J. Phys. B 8, 2311 (1975).
7. K.E. Banyard and M.M. Mashat J. Chem. Phys. 67, 1405 (1977).
8. K.E. Banyard and J.C. Moore, J. Phys. B 10, 2781 (1977).
9. Ajit J. Thakkar and V.H. Smith, Jr., Phys. Rev. A 18, 841 (1978).
10. Ajit J. Thakkar and V.H. Smith, Jr., Phys. Rev. A 23(2), 473 (1981).
11. K.E. Banyard and R.J. Mobbs, J Chem. Phys. 75, 3433 (1981).
12. R.J. Mobbs and K.E. Banyard, J Chem. Phys. 78, 6106 (1983).
13. F.W. King and S.M. Rothstein, Phys. Rev. A 21(5), 1376 (1980).
14. C.E. Weatherburn, A First Course in Mathematical Statistics (Cambridge U.P., 1968).
15. R.Z. Yeh, Modern Probability Theory (Harper and Row, London, 1973).
16. Y. Chou, Statistical Analysis (Holt, Rinehart and Winston, London, 1975).
17. Derived, for example, in Margenau and G.M. Murphy, Theoretical Mathematics of Physics and Chemistry (Princeton, N.J.: Van Nostrand, 1943), pp. 134-135.

18. W.Feller, An Introduction to Probability Theory and its Applications, 3rd. Ed. (Wiley, New York, 1968).
19. E.R. Davidson, Reduced Density Matrices and Quantum Chemistry, (Academic, New York, 1976).
20. R.E. Watson, Phys. Rev. 119, 170 (1960).
21. O. Sinanoglu and K.A. Brueckner, Three Approaches to Electron Correlation in Atoms (Yale U.P., New Haven, 1970).
22. A.C. Hurley, Electron Correlation in Small Molecules (Academic Press, London, 1976).
23. R. McWeeny, Rev. Mod. Phys. 32, 335 (1960). For a review see R. McWeeny, Int. J. Quantum Chem. Symp. 1, 351 (1967).
24. V. Maslen, Proc, Phys. Soc. London A69, 734 (1956).
25. G. Sperber, Int. J. Quantum Chem. 5, 188 (1971).
26. M.A. Besson and M. Suard, Int. J. Quantum Chem. 10, 151 (1976).
27. C.A. Coulson and A.H. Neilson, Proc. Phys. Soc. London 78, 831 (1961).
28. K.H. Al-Bayati, Ph.D. Thesis, Electron Correlation in the $(1s^2 2s)^2 S$ & $(1s^2 2p)^2 P$ States of the Lithium Isoelectronic Sequence in Position and Momentum Space, University of Leicester (1984).

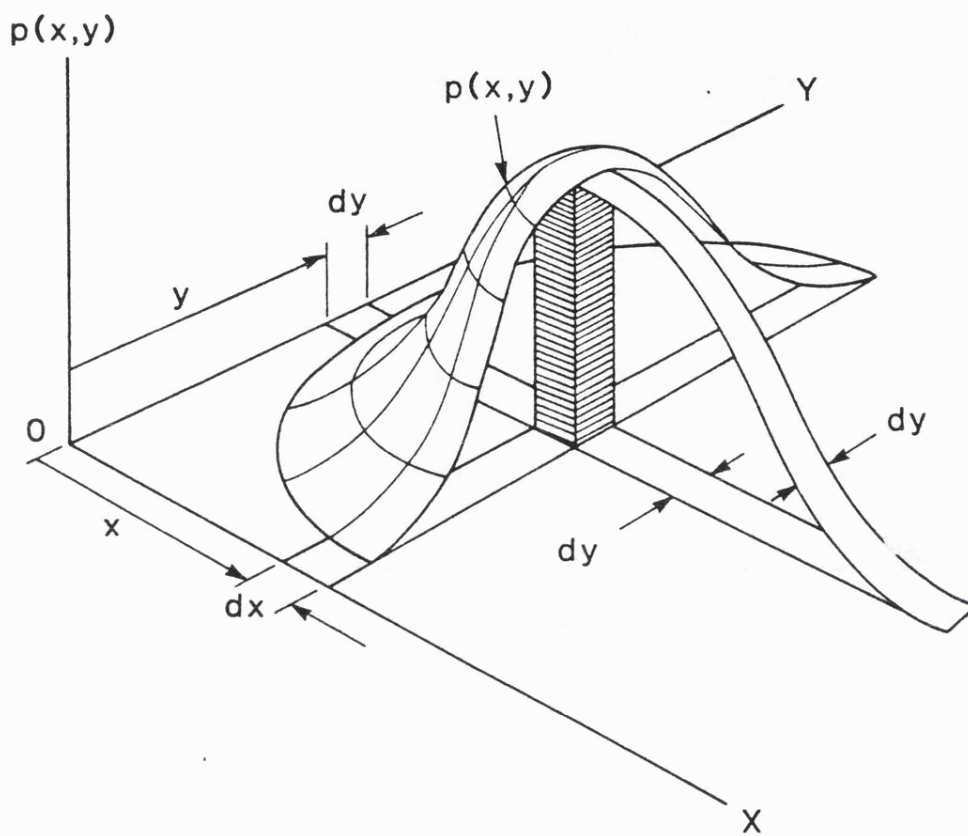


Figure IV.1 A two-dimensional probability density.

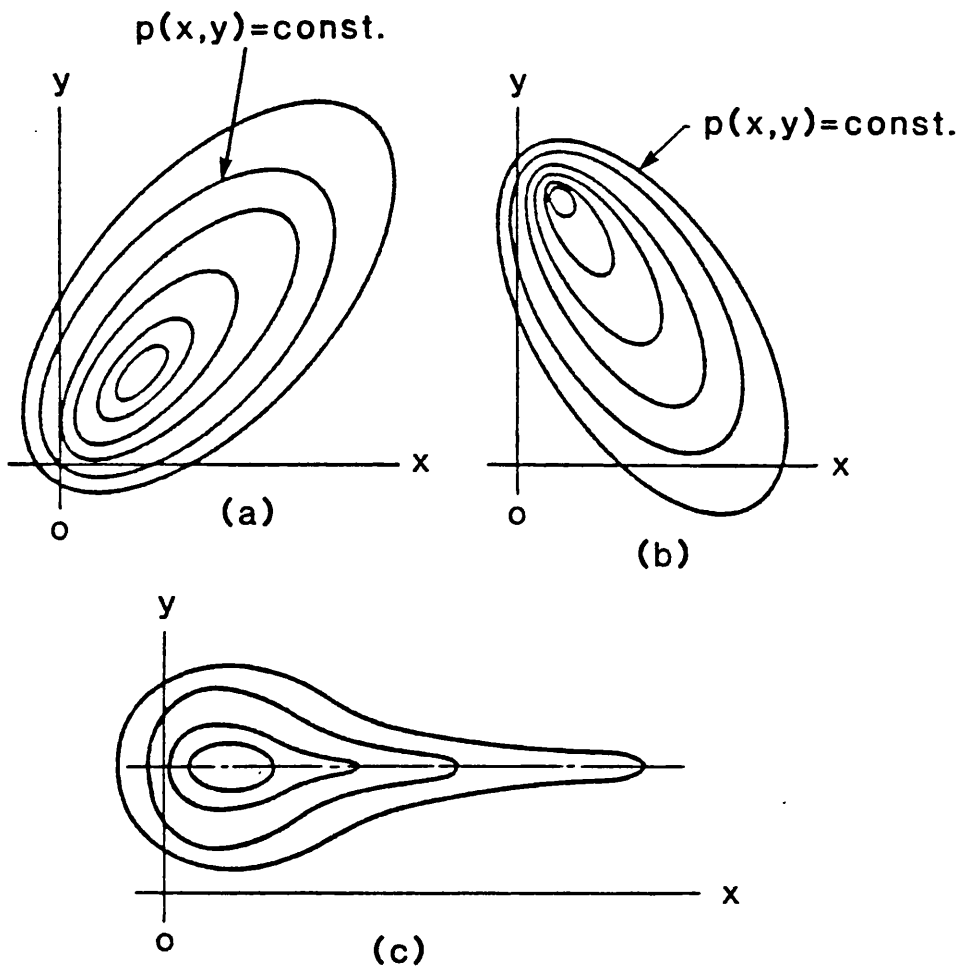


Figure IV.2 Equiprobability curves of two correlated or uncorrelated variables. (a) X and Y dependent (in harmony), (b) X and Y dependent (in opposition), (c) X and Y uncorrelated.

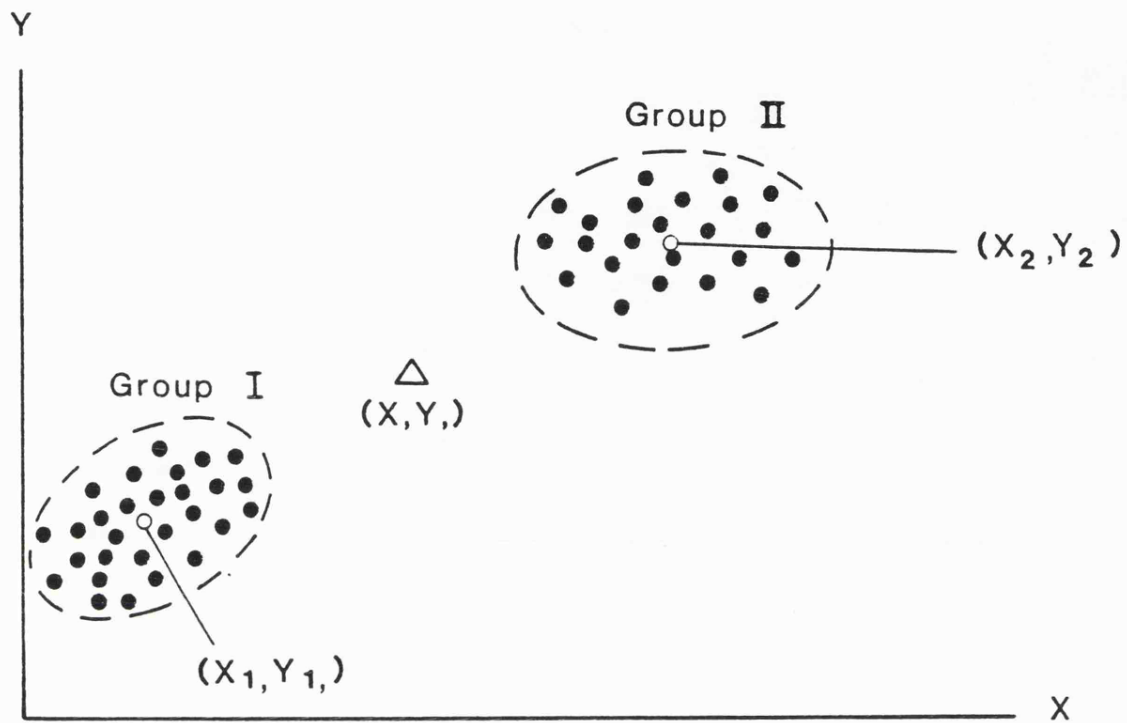
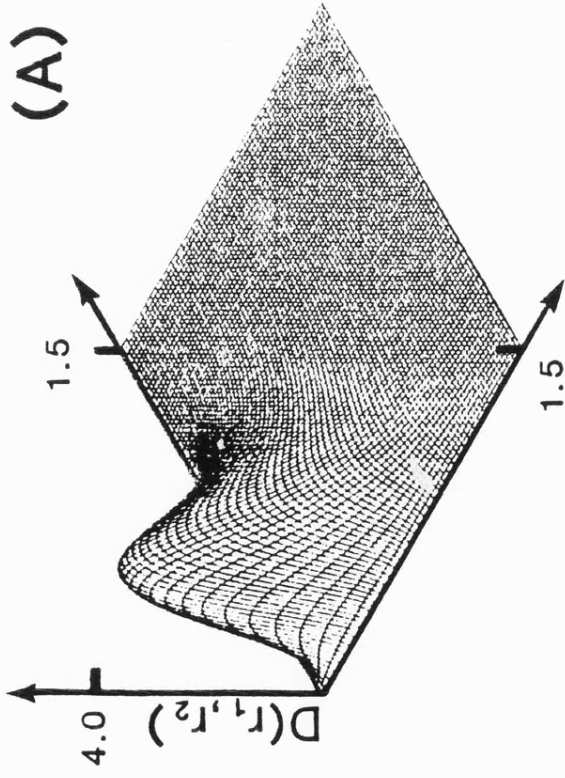


Figure IV.3 A scatter diagram including two distinct populations in which the correlations are different.

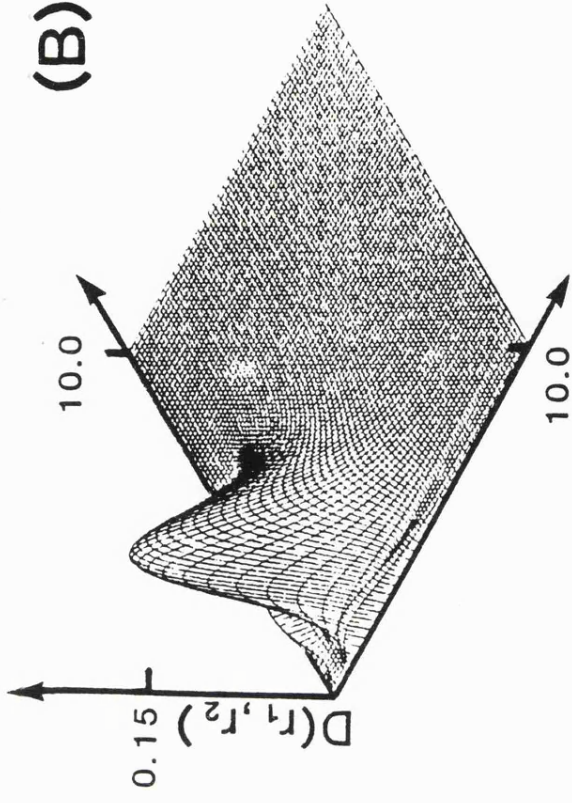
Figure IV.4
(see over)

Figure IV.4 The HF two-particle radial densities,
 $D_{\text{HF}}(r_1, r_2)$, for the intra- and intershells of atomic Be
evaluated from the HF function of Watson⁽²⁰⁾.

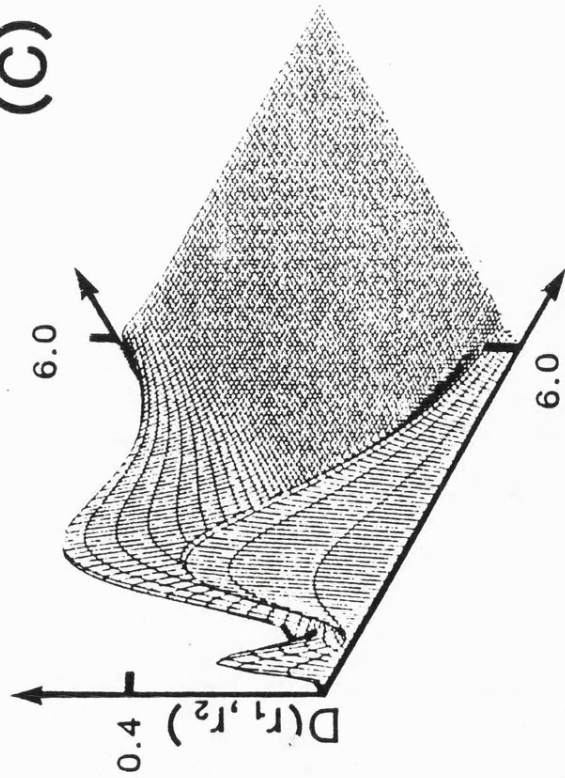
(A)



(B)



(C)



(D)

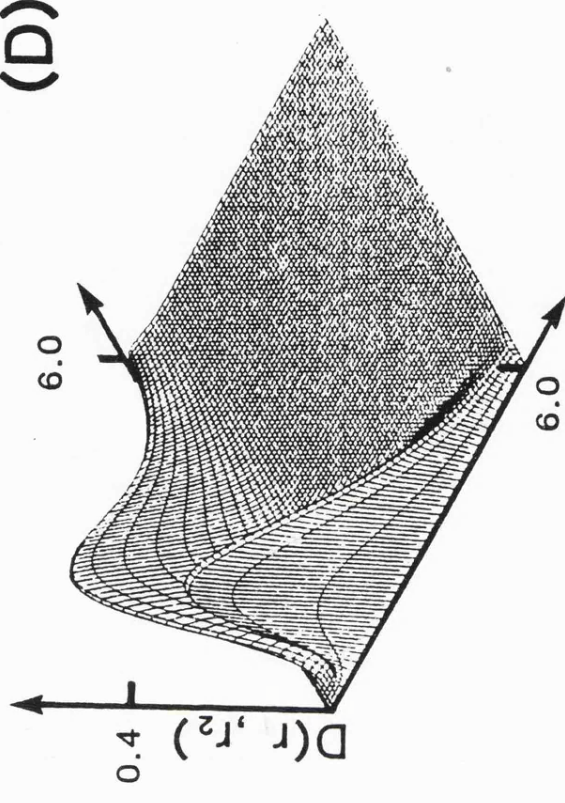
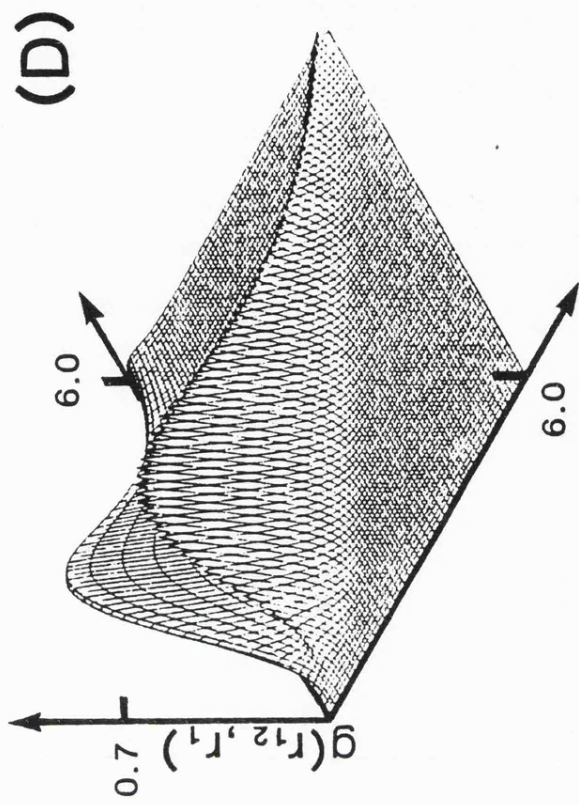
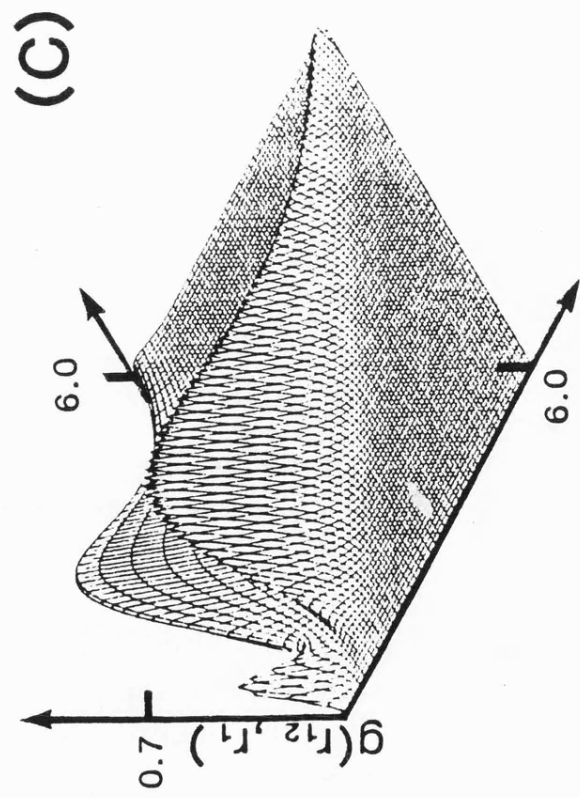
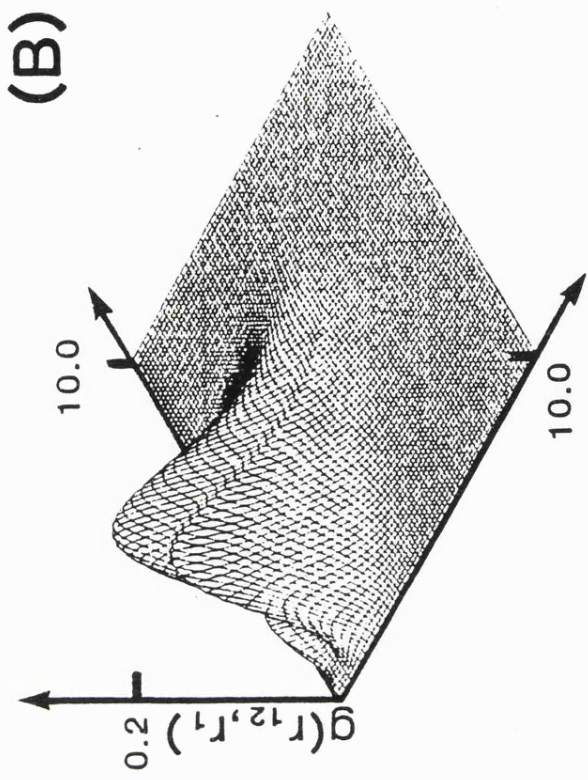
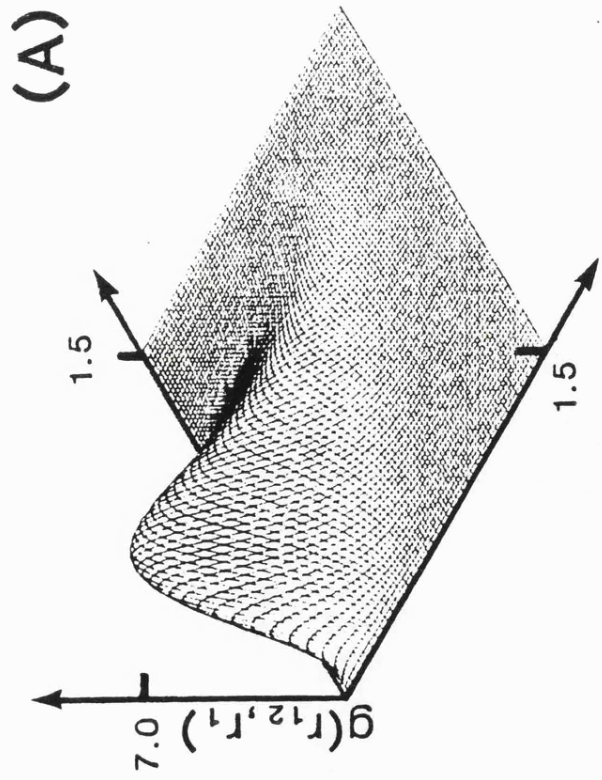


Figure IV.5
(see over)

Figure IV.5 The HF $g_{\text{HF}}(r_{12}, r_1)$ vs. (r_{12}, r_1) surface for the intra- and intershells of atomic Be evaluated from the HF function of Watson⁽²⁰⁾.



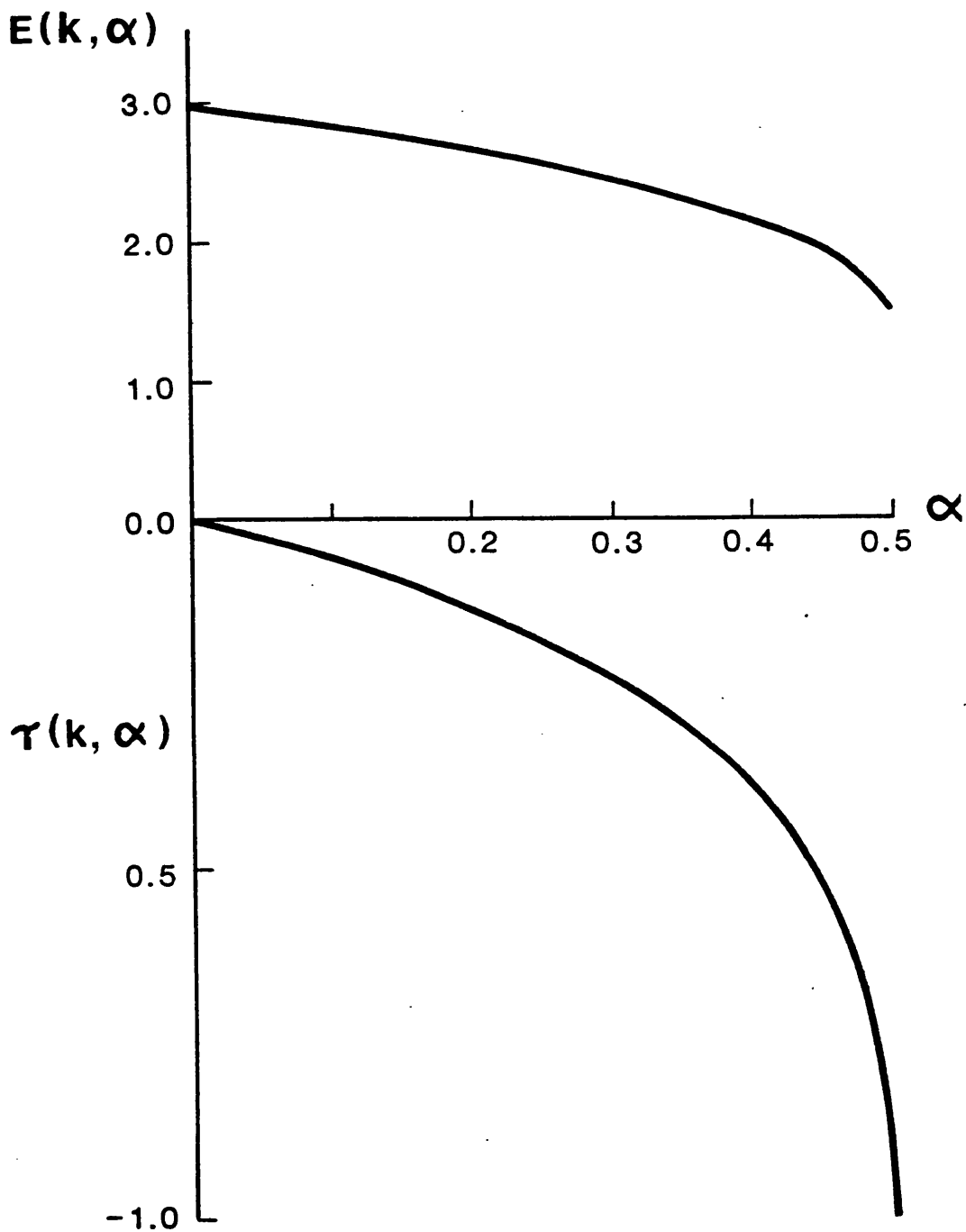


Figure IV.6 The variation of the ground-state energy, $E(k, \alpha)$, and correlation coefficient, $\tau(k, \alpha)$ for the two-electron system considered by King and Rothstein⁽¹³⁾ ($k=1$).

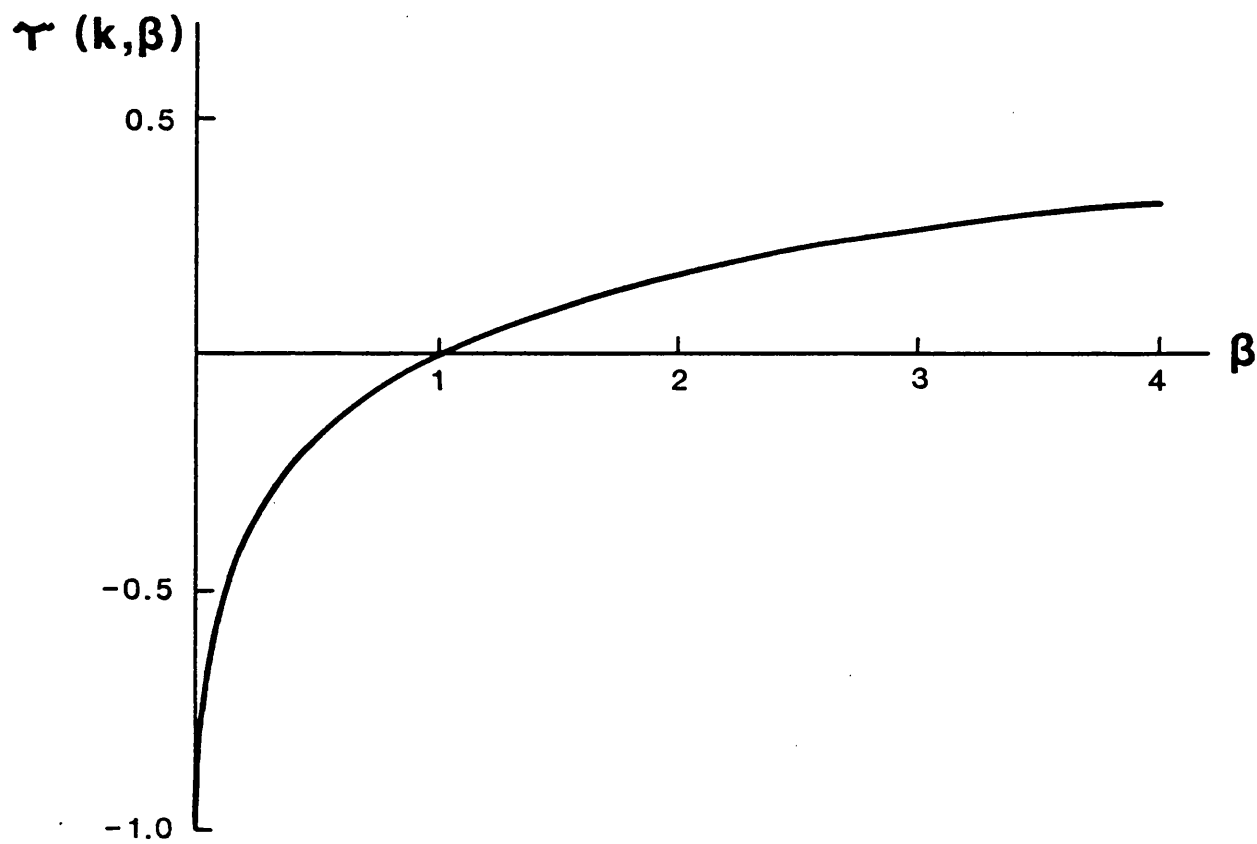


Figure IV.7 The dependence of the correlation coefficient $\tau(k, \beta)$ with the variational parameter β for the two-electron system considered by King and Rothstein⁽¹³⁾ ($k=1$).

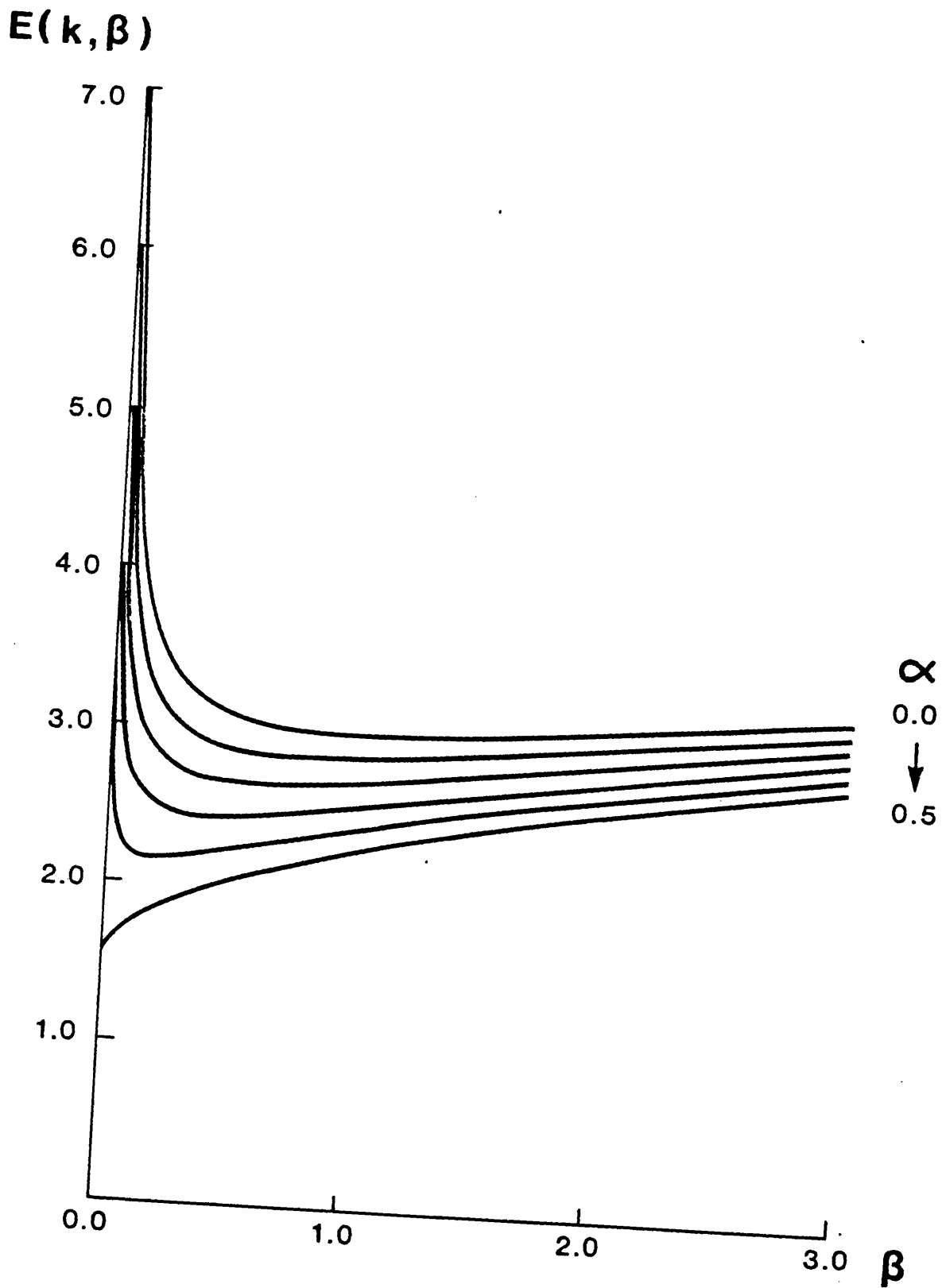


Figure IV.8 The variational energy $E(k, \beta)$ for the two-electron system considered by King and Rothstein⁽¹³⁾ ($k=1$).

Coulomb holes and correlation coefficients for electronic shells: A comparative analysis of several wave functions for Be

K. E. Banyard and R. J. Mobbs

Department of Physics, University of Leicester, Leicester, England
(Received 10 April 1980; accepted 16 September 1980)

A partitioning technique used previously to examine correlation trends in individual electronic shells for a series of ions has been extended and applied to a detailed comparison of four well-correlated wave functions for the Be atom. The present analysis of a correlated two-particle density, generalized for any N -electron system, retained all contributions from products of *all* terms in the wave function up to and including the pair-correlation effects. For each correlated description of Be, Coulomb holes have been evaluated and compared for the $K(^1S)$, $L(^1S)$, $KL(^1S)$, and $KL(^3S)$ shells. The inverted nature of the inter-shell holes, relative to the intra-shell effect, has been examined and rationalized in terms of the $2s-2p$ near-degeneracy which exists in Be. The total Coulomb holes for the two energetically best wave functions showed a previously unseen structure which was directly attributable to the inter-shells. Several one- and two-particle expectation values are reported and these were used to determine various angular and radial correlation coefficients τ . Thus, for each wave function, a global assessment could be obtained of the correlation effects within different regions of the intra- and inter-electronic shells.

I. INTRODUCTION

Electron correlation can be examined in terms of the Coulomb hole $\Delta f(r_{mn})$, this being the difference between the correlated and the Hartree-Fock (HF) distribution functions for the interparticle separation r_{mn} for an electron pair (m, n) .¹ However, such an analysis has generally been confined to two-electron systems.²⁻⁷ In an endeavor to gain insight into correlation effects for specific electronic shells within an N -electron system, Banyard and Mashat⁸ used the many-electron theory (MET) proposed by Sinanoğlu^{9,10} to partition the two-particle difference density required for the evaluation of $\Delta f(r_{mn})$. Coulomb holes were then determined for the individual shells in a Be-like series of ions using the correlated wavefunctions of Weiss¹¹ and the HF functions of Clementi.¹² The partitioning technique was carried out to within first order up to and including the pair-correlation functions U_{ij} .

The K -shell "holes" for the Be-like ions were found to be very similar to those obtained for the two-electron series whereas, by comparison, the influence of correlation on the L -shells was quite striking. Of especial interest were the characteristics of the Coulomb holes for the $K\alpha L\beta$ - and $K\alpha L\alpha$ -shells. In particular, it was observed that the $K\alpha L\alpha$ curves were *inverted* by comparison with the "holes" obtained by Boyd and Katriel⁶ for the 2^3S state of the He-like ions. Clearly, such findings could be dependent on the restrictions imposed by Weiss¹¹ when constructing his wave functions. Consequently, it was suggested that it would be of considerable interest to compare the observations for Be with the results of a corresponding analysis of other highly correlated wave functions and, in the process, one could then establish whether the intershell behavior was acceptable or not.

Thus, for the ground state of Be, we examine the inter- and intrashell correlation effects embodied in four configuration-interaction (CI) wave functions reported by Watson,¹³ Bunge,¹⁴ and Olympia and Smith¹⁵; two

functions were taken from the latter work. In addition to calculating the Coulomb holes $\Delta f(r_{m,n})$, we also determine the *partial* "holes" $\Delta g(r_{m,n}, r_m)$ defined by Boyd and Coulson.⁵ A brief summary of some one- and two-particle expectation values is reported and, following the earlier analysis,⁸ these are used to derive various radial and angular correlation coefficients τ .

Since we are comparing relatively sophisticated wave functions for a given system, it was thought advisable to extend the partitioning technique for the two-particle correlated density to a higher level of approximation. Finally, a limited comparison is made between these results and those obtained for the Bunge¹⁴ wave function when partitioned according to the original first-order approach.⁸

II. THEORY AND WAVE FUNCTIONS

Following Banyard and Mashat,⁸ if the change in the two-particle density due to electron correlation can be written as

$$\Delta \Gamma(\mathbf{x}_m, \mathbf{x}_n) \approx \sum_{i < j}^N \Delta \Gamma_{ij}(\mathbf{x}_m, \mathbf{x}_n), \quad (1)$$

where i and j label occupied spin-orbitals in the restricted HF description of an N electron system, then the Coulomb hole associated with the spin-orbital pair (i, j) is given by

$$\Delta f_{ij}(r_{mn}) = \int \frac{\Delta \Gamma_{ij}(\mathbf{x}_m, \mathbf{x}_n) d\mathbf{x}_m d\mathbf{x}_n}{dr_{mn}}. \quad (2)$$

The integrations for electrons m and n are performed over spin and all space coordinates except r_{mn} , as described by Coulson and Neilson.¹ The definition of $\Delta \Gamma(\mathbf{x}_m, \mathbf{x}_n)$ in terms of $\Psi_{\text{corr}}(1, 2, \dots, N)$ and $\Psi_{\text{HF}}(1, 2, \dots, N)$ follows as before⁸; see also McWeeny and Sutcliffe.¹⁶ For the HF two-particle density, the partitioning into pair-wise components (i, j) is both exact and straightforward, yielding

$$\Gamma_{\text{HF}}(\mathbf{x}_m, \mathbf{x}_n) = \binom{N}{2} \sum_{i < j}^N [\phi_i(\mathbf{x}_m) \phi_j(\mathbf{x}_n) - \phi_j(\mathbf{x}_m) \phi_i(\mathbf{x}_n)]^2, \quad (3)$$

here, for example, ϕ_i is the i th occupied normalized HF spin-orbital. The partitioning of $\Gamma_{\text{corr}}(\mathbf{x}_m, \mathbf{x}_n)$ is, however, approximate.

For a closed-shell system, we may write^{9,10} the correlated wave function as

$$\Psi_{\text{corr}}(1, 2, \dots, N) = C \left\{ \alpha \left[\pi(1, 2, \dots, N) \times \left(1 + \sum_{i=1}^N \frac{f_i}{\phi_i} + \frac{1}{\sqrt{2!}} \sum_{i < j}^N \frac{U_{ij}}{\phi_i \phi_j} + \frac{1}{\sqrt{3!}} \sum_{i < j < k}^N \frac{U_{ijk}}{\phi_i \phi_j \phi_k} + \dots \right) \right] \right\} \quad (4)$$

where $\pi(1, 2, \dots, N)$ is the product of all occupied HF spin-orbitals, such that $\alpha \pi(1, 2, \dots, N)$ represents the

normalized N -particle HF wave function, f_i is an orbital correction function, and U_{ij} is the pair-correlation function associated with ϕ_i and ϕ_j . The remaining notation and the orthogonality conditions imposed on f_i , U_{ij} , etc., have been defined elsewhere.^{10,17,18} Equation (4) is now truncated to exclude U_{ijk} and the higher correlation functions and, in the present work, $\Gamma_{\text{corr}}(\mathbf{x}_m, \mathbf{x}_n)$ is then formulated without further approximation by retaining products of all terms and integrating over all electron coordinates except those associated with electrons m and n . After some considerable manipulation, the resulting two-particle density can be expressed in partitionable form as

$$\begin{aligned} \Gamma_{\text{corr}}(\mathbf{x}_m, \mathbf{x}_n) = & \sum_{i < j}^N \sum_{h \neq i, j}^N C'_{ij} \left[\frac{\langle \Psi_{\text{corr}} | \pi_{ij} \rangle^* \langle \Psi_{\text{corr}} | \pi_{ij} \rangle}{\langle \Psi_{\text{corr}} | \pi \rangle^2} \right. \\ & + \frac{8}{\sqrt{2}} (\phi_i \phi_j - \phi_j \phi_i) \alpha_{mn} (-f_h^{ij} \phi_h + f_h^{ih} \phi_j + f_h^{hj} \phi_i) + 2\alpha' (\langle U_{ij} | U_{ij} \rangle \phi_h \phi_h + 4 \langle U_{ik} | U_{kj} \rangle \phi_i \phi_j) \\ & + 2(\phi_i \phi_j - \phi_j \phi_i) \left(\sum_{s < t}^N (\phi_s \phi_t - \phi_t \phi_s) \sum_{\langle g < h \rangle \neq i, j}^N \sum_{\langle p < q \rangle \neq s, t}^N \langle U_{gh} | U_{pq} \rangle \right) \\ & \left. + 2(\phi_i \phi_j - \phi_j \phi_i)^2 \langle f_h | f_h \rangle - 4(\phi_i \phi_h - \phi_h \phi_i) (\phi_j \phi_h - \phi_h \phi_j) \langle f_i | f_j \rangle \right] \quad (5) \end{aligned}$$

The constants C'_{ij} ensure that, as in Eq. (3), the density for each pair (i, j) is normalized to unity. In this analysis, π_{ij} represents the product of all occupied HF spin orbitals except $\phi_i(m)$ and $\phi_j(n)$ and, owing to the antisymmetrizer α in Eq. (4), the remaining $(N-2)$ electron coordinates can be arranged arbitrarily among the available $(N-2)$ spin orbitals. The integrations in $\langle \Psi_{\text{corr}} | \pi_{ij} \rangle$ are over all the coordinates occurring in π_{ij} and thus we obtain a function of \mathbf{x}_m and \mathbf{x}_n only. With the restriction that $g < h$, the summations over g and h each span all the spin-orbital labels except i and j ; corresponding restrictions hold for the ranges of p and q . For compactness, we have also introduced the following antisymmetrizers for the electronic coordinates

$$\alpha_{mn} \equiv \mathbf{x}_m \mathbf{x}_n - \mathbf{x}_n \mathbf{x}_m,$$

and

$$\alpha' \equiv \mathbf{x}_m \mathbf{x}_n \mathbf{x}_m \mathbf{x}_n - \mathbf{x}_m \mathbf{x}_n \mathbf{x}_n \mathbf{x}_m - \mathbf{x}_n \mathbf{x}_m \mathbf{x}_m \mathbf{x}_n + \mathbf{x}_n \mathbf{x}_m \mathbf{x}_n \mathbf{x}_m.$$

In addition, the abbreviated notation for terms like $f_h^{ij} \phi_h$ and the single integration $\langle U_{ij} | U_{ij} \rangle_a$, for example, are to be interpreted as

$$f_h^{ij} \phi_h \equiv \left(\int U_{ij}(\mathbf{x}_a, \mathbf{x}_r) f_h(\mathbf{x}_r) d\mathbf{x}_r \right) \phi_h(\mathbf{x}_a),$$

and

$$\langle U_{ij} | U_{ij} \rangle_a \equiv \int U_{ij}^*(\mathbf{x}_a, \mathbf{x}_r) U_{ij}(\mathbf{x}_b, \mathbf{x}_r) d\mathbf{x}_r,$$

where a and b are chosen according to the prescription given by α_{mn} and α' , respectively. Finally, the dependence on electron coordinates for the remaining terms in Eq. (5) is to be taken as

$$U_{ij} \equiv U_{ij}(\mathbf{x}_m, \mathbf{x}_n),$$

and

$$\phi_i \phi_j - \phi_j \phi_i \equiv \phi_i(\mathbf{x}_m) \phi_j(\mathbf{x}_n) - \phi_j(\mathbf{x}_m) \phi_i(\mathbf{x}_n).$$

For a given HF description of the system and a chosen CI representation of Ψ_{corr} , the functions f_i and U_{ij} can be determined by the method of successive partial orthogonalizations.⁹

Thus, using Eqs. (5) and (3) in conjunction with Eq. (2), approximate Coulomb holes for Be could be obtained for the $K(^1S)$, $L(^1S)$, $KL(^1S)$, and $KL(^3S)$ shells. It is to be noted that in the present work the (i, j) pairs (1, 4) and (2, 3) have been combined and rewritten to produce pure spin states for the intershells. As before, it is convenient, henceforth, to set $m = 1$ and $n = 2$.

The four CI wave functions analyzed here each possess the restricted HF wave function of Watson¹³ as the leading configuration. The correlation effect is achieved by using an orthonormal basis set to form additional configurations involving various excitations from this HF reference state. Thus, to assist the discussion, Table I not only includes the total energies E but we also quote, for each shell, the number of single- and double-excitation terms and, in addition, we summarize their composition. Atomic units are used throughout this work.

The complexity represented by the use of Eq. (5) to partition $\Gamma_{\text{corr}}(\mathbf{x}_1, \mathbf{x}_2)$ was eased by defining the present "holes" for Be with respect to the HF wave function of Watson.¹³ Pilot calculations indicate that differences due to changing from the Clementi¹² to the Watson¹³ HF function will be negligible. Ideally, it would have been desirable to include in our analysis the 650-term CI wave function of Bunge¹⁹ but the added labor and the required computer time proved to be prohibitive.

TABLE I. The Be ground-state correlated wave functions, their total energies E , in atomic units, and a summary of the correlation configurations considered here for each shell. For a given shell, $N[l]$ indicates that N correlation configurations were formed by either a single- or double-excitation from that shell into a basis orbital of l -type symmetry, the remaining electrons retaining their Hartree-Fock descriptions. Also listed is the total number of such configurations for a given shell within each Ψ . The reference Hartree-Fock (HF) wave function is that determined by Watson.

Wave function Ψ^a	Total energy E (a. u.)	% correlation energy ^b	Description of the total Ψ^c	Number of correlation configurations considered			
				K (¹ S)	L (¹ S)	KL (¹ S)	KL (³ S)
Bunge (B) ^d	-14.664 19	96.55%	180 configurations; 7s, 7p, and 4d orthonormal basis set	39 14[s], 19[p], 6[d]	22 14[s], 7[p], 1[d]	46 15[s], 22[p], 9[d]	34 13[s], 16[p], 5[d]
Olympia and Smith (OS95) ^e	-14.663 55	95.87%	95 configurations; 7s, 7p, and 4d orthonormal basis set	26 11[s], 12[p], 3[d]	15 10[s], 4[p], 1[d]	28 8[s], 16[p], 4[d]	21 6[s], 13[p], 2[d]
Watson (W) ^f	-14.657 40	89.36%	37 configurations; 6s, 5p, 4d, 2d, and 2g orthonormal basis set	22 6[s], 8[p], 4[d], 2[f], 2[g]	6 5[p], 1[d]	4 1[s], 3[p]	1 1[p]
Olympia and Smith (OS85) ^e	-14.655 34	87.18%	85 configurations; 4s, 2p, and 1d orthonormal basis set	9 5[s], 3[p], 1[d]	9 5[s], 3[p], 1[d]	11 7[s], 3[p], 1[d]	6 5[s], 1[p]
Hartree-Fock ^g (HF)	-14.572 99	0.0% ^g

^aFor comparison, the 55-term CI wave function of Weiss (Ref. 11) for Be used a nonorthogonal basis set and yielded $E = -14.660 90$ a. u., giving 93.06% of the correlation energy.

^bThe exact nonrelativistic energy for Be is $-14.667 45$ (quoted from Ref. 15).

^cThe leading configuration in each correlated Ψ is the restricted Hartree-Fock wave function of Watson (Ref. 13).

^dReference 14.

^eReference 15.

^fReference 13.

^gBy definition.

The intra- and intershell Coulomb holes are shown in Figs. 1 and 2, respectively. The sum total of the "holes" for each correlated description is given in Fig. 3(a) and, for the energetically best wave function,¹⁴ the total Coulomb hole is compared with its components in Fig. 3(b). For the Bunge wave function, we evaluated the partial Coulomb holes $\Delta g(r_{12}, r_1)$ for each shell and the results are displayed in Fig. 4. These "holes" are defined⁵ such that

$$\int_0^\infty \Delta g_{ij}(r_{12}, r_1) dr_1 = \Delta f_{ij}(r_{12}), \quad (6)$$

and, therefore, they enable us to examine the effect of electron correlation when a test electron, say electron 1, is located at a specific distance from the nucleus.

Selected one- and two-particle expectation values are given in Tables II and III, respectively. As before, Δx is the standard deviation of x . Because of space, results are quoted only for the Bunge¹⁴ and 95-term Olympia and Smith¹⁵ wave functions. For reference, both tables include the expectation values derived from the Watson HF function.

Statistical correlation coefficients were first applied to the analysis of electron correlation by Kutzelnigg, Del Re and Berthier.²⁰ For our two-electron shells we evaluated the radial coefficients

$$\tau_r = \frac{\langle r_1 r_2 \rangle - \langle r_1 \rangle^2}{\langle r_1^2 \rangle - \langle r_1 \rangle^2}, \quad (7)$$

$$\tau_{1/r} = \frac{\langle r_1^{-1} r_2^{-1} \rangle - \langle r_1^{-1} \rangle^2}{\langle r_1^{-2} \rangle - \langle r_1^{-1} \rangle^2}, \quad (8)$$

and the angular coefficients

$$\tau_\gamma = \frac{\langle \mathbf{r}_1 \cdot \mathbf{r}_2 \rangle}{\langle r_1^2 \rangle}, \quad (9)$$

$$\tau_{\gamma'} = \frac{\langle (\mathbf{r}_1/r_1^2) \cdot (\mathbf{r}_2/r_2^2) \rangle}{\langle r_1^{-2} \rangle}, \quad (10)$$

and

$$\tau_{\gamma''} = \langle \cos \gamma \rangle, \quad (11)$$

where γ is the angle between the electronic position vectors \mathbf{r}_1 and \mathbf{r}_2 . This selection of τ enables us to emphasize different regions of the two-particle density when assessing either radial or angular effects. We also note that each τ is bounded between -1 and $+1$. For consistency, we followed the definition of the Coulomb hole and formed $\Delta\tau = \tau(\text{corr}) - \tau(\text{HF})$. The results are presented in Table IV for all four CI wave functions.

III. DISCUSSION

From Table I it is seen that the wave function due to Bunge is not only the best energetically but, not surprisingly, it is also the most complex in its description of each shell. The E values in Table I also indicate that the correlated wave functions fall into two groups: the Bunge¹⁴ (B) and 95-term Olympia and Smith¹⁵ (OS95) functions followed by the Watson¹³ (W) and 85-term

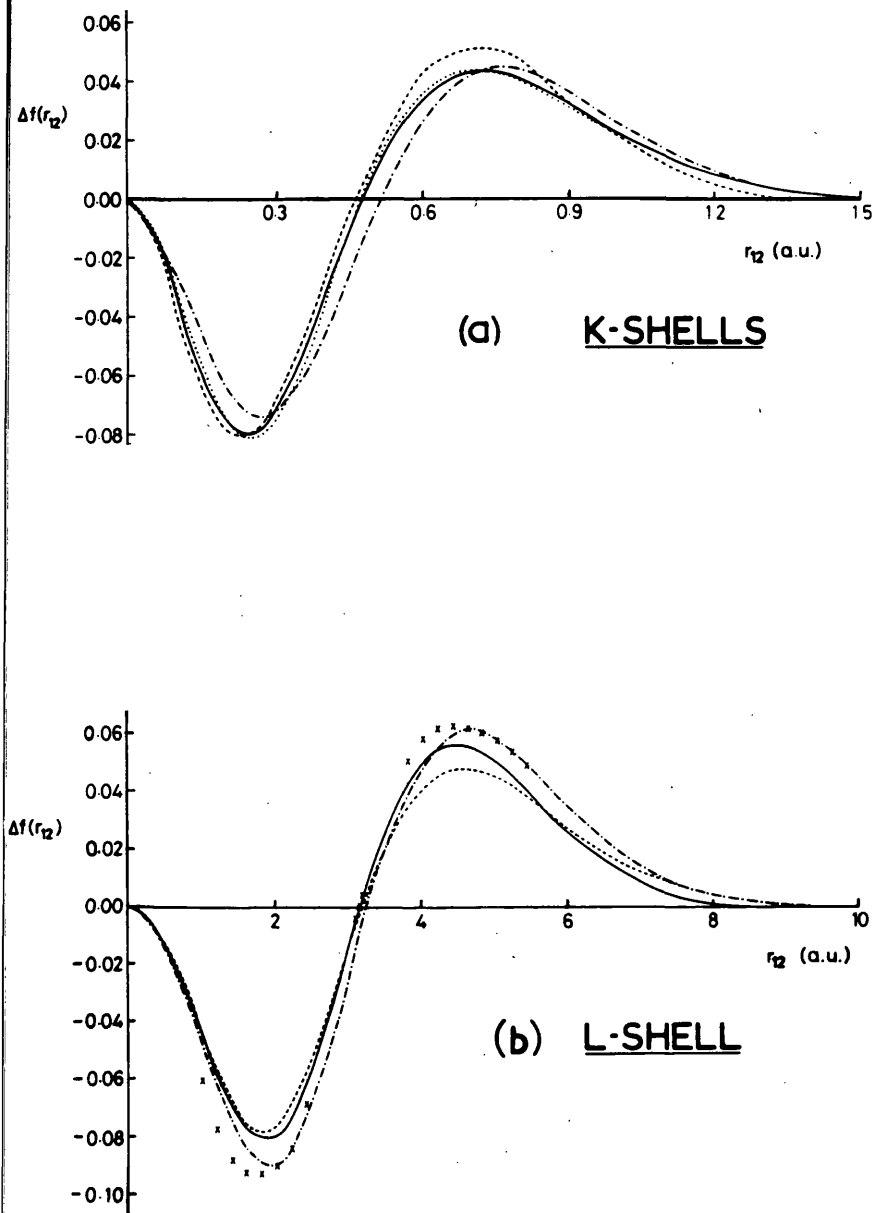


FIG. 1. The Coulomb holes $\Delta f(r_{12})$ for the (a) K and (b) L shell in Be. $\Delta f(r_{12})$ is the difference between a correlated and an HF description of the interparticle distribution function. Each $f_{ij}(r_{12})$ is normalized to unity and r_{12} is measured in atomic units (a. u.). The correlated descriptions are given by the Bunge¹⁴ (B) wave function (solid curve), the Olympia and Smith¹⁵ 95-term (OS95) function (dotted curve), the Watson¹³ (W) function (dashed curve), and the Olympia and Smith¹⁵ 85-term (OS85) function (dot-dashed curve). The HF wave function is taken from Watson.¹³ The crosses for the L shell indicate the $\Delta f(r_{12})$ values derived from the B function using the first-order partitioning technique of Banyard and Mashat³; the corresponding K -shell results are coincident with the solid curve for the B function.

Olympia and Smith¹⁵ (OS85) descriptions. The Weiss¹¹ wave function for Be, analyzed by Banyard and Mashat, has an energy of -14.66090 a.u. and therefore lies between these two groups. However, since the Weiss configurations were constructed from a nonorthogonal basis set, his 55-term wave function does not lend itself to a summary in the form of Table I. Nevertheless, the truncated natural expansion of the Weiss wave function presented by Barnett, Linderberg, and Shull²¹ should provide a useful comparison in this context. As a preliminary to our main discussion, we note that the HF expectation values in Tables II and III are in excellent accord with those derived previously from the HF wave function of Clementi.¹²

Figure 1(a) reveals a high degree of correspondence between the K -shell Coulomb holes derived from the B and OS95 functions. By comparison, the Watson curve is seen to be slightly too compact and the OS85 function

yields a K -shell hole which is too diffuse. The crossover points for the B and OS95 functions are almost coincident with the value obtained from the earlier analysis and, like the Weiss result, both curves show a strong similarity with the Coulomb hole for Be^{2+} . In Fig. 1(b) the L -shell holes for the B and OS95 wave functions are coincident and, along with the Watson curve, their crossover points are comparable with that of the Weiss curve. Relative to the Bunge curve, the Watson L -shell hole is somewhat too shallow whereas the OS85 function produces a hole which is not only too deep but is, once again, too diffuse. A comparison between the L -shell effect and that for the K shell can be obtained in terms of the percentage of each $f_{\text{HF}}(r_{12})$ density which has been redistributed due to correlation: these results, labeled Υ , are given in Table IV. For the four wave functions analyzed here, the L -shell percentages are about 6.5 times those for the K shell; an exception is the L shell for the OS85 function. Note also the com-

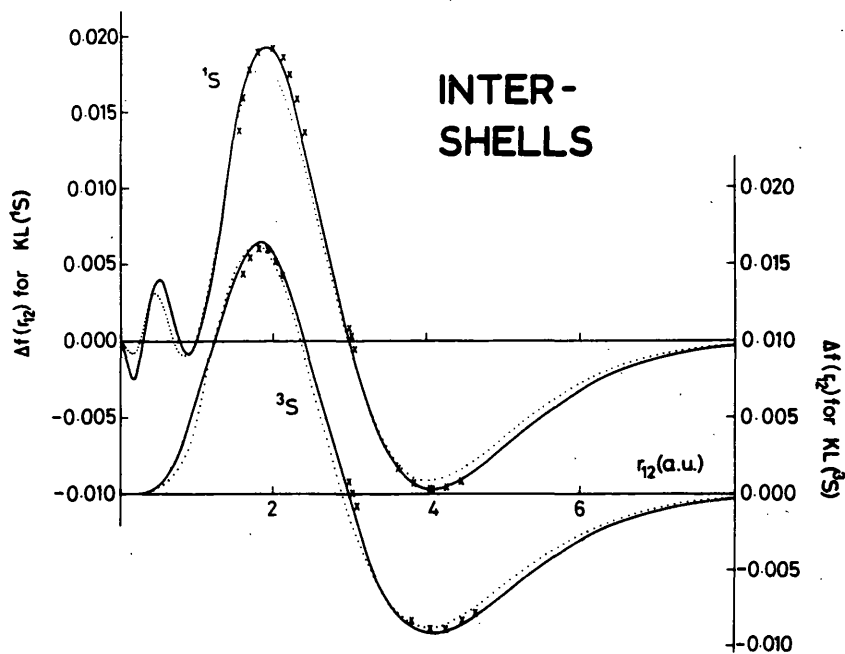


FIG. 2. $\Delta f(r_{12})$ vs r_{12} for the $1S$ and $3S$ intershells for the B (solid curve) and OS95 (dotted curve) correlated wave functions. The crosses are for the B function using the first-order partitioning technique.

parison of these T values with those derived from the previous $\Delta f(r_{12})$ curve⁸ obtained from the first-order partitioning of the Weiss wave function.

For the W wave function, Barnett, Linderberg, and Shull²¹ suggested that a deficiency appears to exist in the description of the outer-shell p -character, thus influencing angular correlation. However, inspection of Table I indicates that, for the L shell of Watson, a greater inadequacy may exist when describing radial correlation; this is confirmed by the correlation coefficients in Table IV, where the consequences are seen to be quite marked for $\Delta\tau_r$ and $\Delta\tau_{1/r}$. The OS85 wave function is, with the exclusion of the configuration d^4 , a complete CI expansion over a small basis set. Therefore, the overdiffuseness in both shells must be associated with an imbalance between the radial and angular components of correlation due to the restricted number of basis orbitals.

For the L shell, correlation caused a significant contraction in the one- and two-particle radial density distributions. This is illustrated in Tables II and III for the B and OS95 wave functions by the changes in $\langle r^n \rangle$, $\langle r_1^{-1} r_2^{-1} \rangle$, and $\langle r_1 r_2 \rangle$. Such radial contractions are only compatible with the sizeable increase in the interparticle separation (see Table III) because of the $2s-2p$ near-degeneracy in Be which produces a large angular correlation effect. The magnitude of the angular separation for each shell can be judged by inspection of $\Delta\tau_r$, $\Delta\tau_{1/r}$, and $\Delta\tau_{r^2}$ in Table IV and, as seen, the L -shell coefficients are by far the largest.

The intershell Coulomb holes shown in Fig. 2 are for the B and OS95 wave functions and, for each shell, the similarity between the curves is quite impressive. The intershell curves for the two remaining CI wave functions were, by comparison, small (less than 8% of the Bunge values) and contracted towards the origin; thus, for clarity, they are not presented. However, a mea-

sure of each $\Delta f(r_{12})$ is provided by the values of T in Table IV. In passing we note that, for the B and OS95 wave functions, the T values for the intershells are comparable with those for the K shell. Figure 2 reveals that the $3S$ curves are of the same shape as the $K\alpha L\alpha$ hole derived previously from the Weiss function. Although the maxima and minima of the $3S$ curves are about 14% larger than those of the Weiss curve, the crossover values of $r_{12} = 2.91$ and 2.95 are only slightly smaller than the $K\alpha L\alpha$ result of 3.08 . Like the Weiss result, these $3S$ intershell curves are inverted by comparison with the 2^3S holes obtained by Boyd and Katriel⁶ for the He-like ions. Nevertheless, at small r_{12} , each Be curve follows the He-like trend by being vanishingly small, a feature which arises from the influence of Fermi correlation on $f_{\text{corr}}(r_{12})$ and $f_{\text{HF}}(r_{12})$. By contrast, we note that the $1S$ curves in Fig. 2 possess a structure very similar to that reported by Boyd and Coulson⁵ for the 2^1S hole in He. Although not strictly comparable, the $1S$ curves are also seen to be of the same shape as the $K\alpha L\beta$ Weiss curve and their final crossover point at $r_{12} = 3.00$ is remarkably close to the Weiss result of 3.13 . Therefore, it would appear that the intershell characteristics contained in the Weiss Be-like wave functions are, indeed, quite reliable.

To rationalize the shape of the intershell curves we recall that, for Be, the pair-correlation energies for the K and L shells are about seven times larger than those for the intershells,^{22,18} thus illustrating the dominance of intrashell correlation. In addition, it is noted from Table II that, for the K shell, correlation produces only a marginal expansion of the radial density whereas, for the L shell, a significant contraction occurs as discussed above. That correlation has brought the K and L shells closer together implies that, at large r_{12} , the interparticle distribution function $f(r_{12})$ for each intershell should decrease relative to the HF values. At small r_{12} , the interpenetration of the L shell into the K -

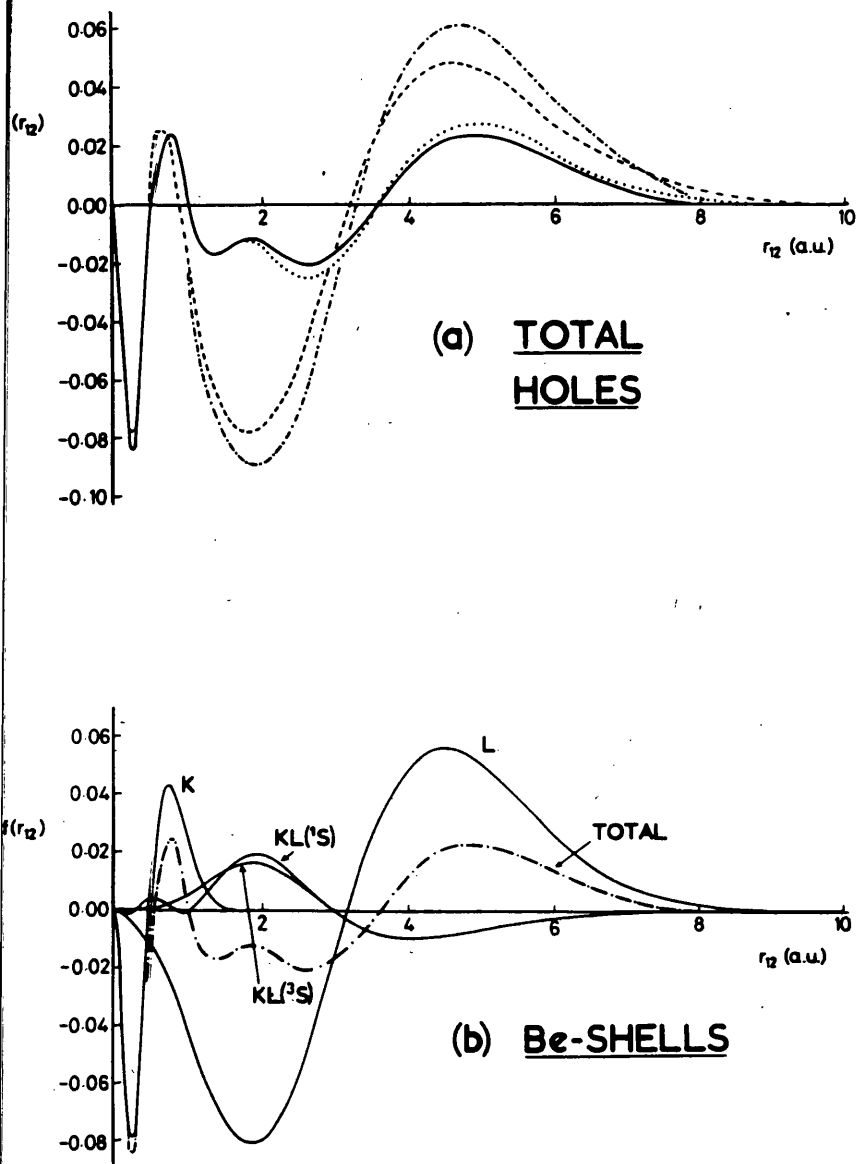


FIG. 3. (a) The sum total of the intra- and intershell Coulomb holes given by $\Delta f(r_{12}) = K(^1S) + L(^1S) + KL(^1S) + 3KL(^3S)$ for the B (solid curve), OS95 (dotted curve), W (dashed curve), and OS85 (dot-dashed curve) correlated wave functions. (b) A comparison of intra- and intershell Coulomb holes for the B wave function. The sum total of these holes for the B wave function, given by $K(^1S) + L(^1S) + KL(^1S) + 3KL(^3S)$, is shown here by the dot-dashed curve.

shell region will provide the major contribution to the evaluation of $f(r_{12})$. Thus, for the 1S intershell, we would expect that $\Delta f(r_{12})$ may be of conventional Coulomb hole shape when $r_{12} \gtrsim 1$ say, this r_{12} value being comparable with the extent of $\Delta f(r_{12})$ for the K shell. By contrast, as already mentioned, the Fermi effect is operative at small r_{12} for the 3S case and, consequently, this will obviate the need for Coulomb correlation. For both intershells, the effect at large r_{12} should be greater than that at small r_{12} because a large interparticle separation can, of course, span the distance between the K- and L-shell regions of maximum density. Finally, the requirement that each $\Delta f(r_{12})$ curve should integrate to zero implies the existence of a maximum at intermediate r_{12} for both 1S and 3S . The magnitude and extent of the characteristics outlined above are clearly dependent on the quality of the intershell pair descriptions contained in the correlated wave function. Consequently, only the B and OS95 wave functions produce $f(r_{12})$ curves with such features. That the 3S intershell curves for the Be-like ions should be different

from the 2^3S Coulomb holes for the two-electron systems is now clear since the correlation effect within the excited state of a He-like ion is not constrained by the presence of any intrashell effects.

The total holes in Fig. 3(a) fall into two quite distinct pairs with the similarity between the B and OS95 wave functions being very good. In marked contrast with the previous Coulomb holes for Be,^{23,8} these two functions produce some well-defined structure which is directly attributable to the improved description of the two intershells. This is substantiated by a comparison with the component curves in Fig. 3(b) for the example of the B wave function. The 1S and 3S contributions also cause a significant reduction in the size of the L-shell maximum. The W and OS85 functions yield total holes which appear reasonable within the K-shell region but, elsewhere, Fig. 3(a) shows that these curves are too exaggerated and, as expected, they possess no intershell features. A relative measure of the four total holes is provided by the corresponding T values in Table IV. That the

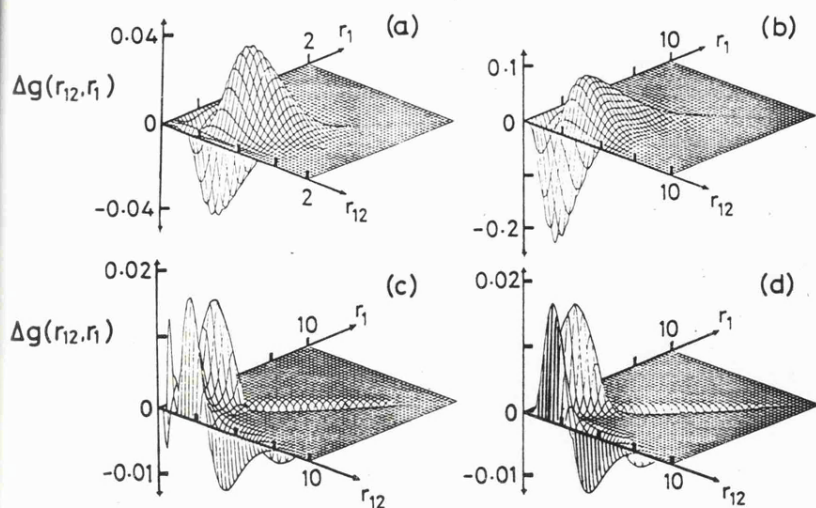


FIG. 4. The partial Coulomb holes $\Delta g(r_{12}, r_1)$ vs r_{12} and r_1 for the (a) $K(1S)$, (b) $L(1S)$, (c) $KL(1S)$, and (d) $KL(3S)$ shells derived from the B correlated wave function.

major differences between the two sets of Coulomb holes in Fig. 3(a) are due to the inadequate descriptions of the intershell correlation effects in the W and OS85 functions can be illustrated as follows. If, when forming total holes for the W and OS85 functions, one replaced their $1S$ and $3S$ contributions by those derived from either the B or OS95 functions (see Fig. 2), then the resulting curves would be found to be comparable in shape and magnitude with the total holes shown in Fig. 3(a) for the B and OS95 functions. We note that the $KL(3S)$ contribution has to be multiplied by 3 when evaluating the total Coulomb hole.

Having discussed the changes in the distribution functions for the interparticle separation, let us now make a brief comment about the individual $f(r_{12})$ distributions. The spread or diffuseness of $f(r_{12})$ about the mean value $\langle r_{12} \rangle$ is measured by the magnitude of Δr_{12} . Table III shows that, for each shell, the correlated value of Δr_{12} derived from either the B or OS95 wave function is less than the corresponding HF result. This indicates that

the introduction of electron correlation has caused each $f(r_{12})$ distribution to sharpen up around its $\langle r_{12} \rangle$ value. However, when comparing the Δr_{12} values for the whole atom (determined from the total $f(r_{12})$ distributions), we observe that the correlated results are now larger than the HF value. This contrast between the behavior of the total distributions and that for their component parts arises from the varying effect of correlation on $\langle r_{12} \rangle$ for the individual electronic shells. Because correlation produces a large increase in $\langle r_{12} \rangle$ for the L shell but causes a small decrease in $\langle r_{12} \rangle$ for both intershells, for example, it immediately suggests that the correlated description of the total $f(r_{12})$ distribution will be more diffuse about the mean than its HF counterpart. This behavior of the $f(r_{12})$ distributions, illustrated by the results in Table III, also occurs for the Be-like ions⁸ when described by the correlated wave functions of Weiss.¹¹

The partial Coulomb holes $\Delta g(r_{12}, r_1)$ shown in Fig. 4 for the K and L shells are of conventional shape for all

TABLE II. Some one-particle expectation properties for the intra- and intershells of Be derived from the partitioned form of the second-order density $\Gamma(\mathbf{x}_1, \mathbf{x}_2)$; see Eqs. (3) and (5). Results are quoted for the Bunge and Olympia and Smith 95-term CI wave functions and, for reference, the corresponding HF values are given. Atomic units are used.

Wave function	Shell	$\langle r_1^{-2} \rangle$	$\langle r_1^{-1} \rangle$	$\langle r_1 \rangle$	$\langle r_1^2 \rangle$	Δr_1
Bunge (B)	$K(1S)$	27.737	3.6803	0.4152	0.2334	0.2470
	$L(1S)$	1.1048	0.5331	2.5794	7.9423	1.1357
	$KL(1S)$	14.425	2.1084	1.4969	4.0954	1.3618
	$KL(3S)$	14.431	2.1088	1.4970	4.0959	1.3619
	Total ^a	14.426	2.1080	1.4971	4.0931	1.3608
Olympia and Smith (OS95)	$K(1S)$	27.741	3.6799	0.4149	0.2328	0.2464
	$L(1S)$	1.0709	0.5325	2.5798	7.9632	1.1435
	$KL(1S)$	14.455	2.1092	1.4992	4.1151	1.3666
	$KL(3S)$	14.458	2.1094	1.4995	4.1154	1.3663
	Total ^a	14.440	2.1083	1.4987	4.1095	1.3651
Hartree-Fock (HF)	$K(1S)$	27.759	3.6819	0.4149	0.2330	0.2465
	$L(1S)$	1.0560	0.5225	2.6498	8.4318	1.1875
	$KL(1S) = 3KL(3S)$	14.408	2.1022	1.5324	4.3324	1.4086

^aThe sum total listed here for each expectation value $\langle r_1^n \rangle$ is given by $\frac{1}{6}[K(1S) + L(1S) + KL(1S) + 3KL(3S)]$. For the HF wave function the total is numerically equal to the intershell value.

TABLE III. Some two-particle expectation properties for the intra- and intershells of Be derived from the partitioned form of the second-order density $\Gamma(\mathbf{x}_1, \mathbf{x}_2)$. Results are quoted for the Bunge and Olympia and Smith 95-term CI wave functions and, for reference, the corresponding HF values are given. Atomic units are used.

Wave function	Shell	$\langle r_1^{-1} r_2^{-1} \rangle$	$\langle r_1 r_2 \rangle$	$\left\langle \left(\frac{r_1}{r_1^2} \right) \cdot \left(\frac{r_2}{r_2^2} \right) \right\rangle$	$\langle r_1 \cdot r_2 \rangle$	$\langle r_{12}^{-1} \rangle$	$\langle r_{12} \rangle$	Δr_{12}
Bunge (B)	K (1S)	13.289	0.1702	-0.3132	-0.0070	2.1925	0.6194	0.3100
	L (1S)	0.2788	6.5462	-0.0608	-2.0008	0.2789	4.1966	1.5111
	KL (1S)	2.1425	1.0781	-0.0071	-0.0044	0.5119	2.6490	1.1866
	KL (3S)	1.7801	1.0602	-0.0247	-0.0064	0.4599	2.6585	1.1675
	Total ^a	3.5084	1.8291	-0.0759	-0.3386	0.7272	2.5734	1.5469
Olympia and Smith (OS95)	K (1S)	13.186	0.1702	-0.3076	-0.0071	2.1946	0.6194	0.3102
	L (1S)	0.2791	6.5547	-0.0599	-1.9956	0.2789	4.2028	1.5137
	KL (1S)	2.1665	1.0824	-0.0059	-0.0042	0.5125	2.6519	1.1877
	KL (3S)	1.7803	1.0623	-0.0194	-0.0059	0.4594	2.6601	1.1711
	Total ^a	3.4954	1.8324	-0.0719	-0.3355	0.7274	2.5757	1.5500
Hartree-Fock (HF)	K (1S)	13.556	0.1722	0	0	2.2732	0.6071	0.3119
	L (1S)	0.2730	7.0215	0	0	0.3432	3.7559	1.6602
	KL (1S)	2.1077	1.1095	0	0	0.5063	2.6819	1.2099
	KL (3S)	1.7399	1.0897	0	0	0.4555	2.6921	1.1902
	Total ^a	3.5261	1.9287	0	0	0.7482	2.5202	1.5204

^aThe sum total listed here for each expectation value is given by $\frac{1}{6}[K(^1S)+L(^1S)+KL(^1S)+3KL(^3S)]$.

TABLE IV. The changes $\Delta\tau$ in the radial and angular correlation coefficients τ . The various τ are defined in Eqs. (7)-(11) and $\Delta\tau = \tau(\text{corr}) - \tau(\text{HF})$. Also included is Υ , the percentage of the interparticle distribution function $f_{\text{HF}}(r_{12})$ which has been redistributed due to electron correlation. For comparison, the results obtained for the Weiss wave function by Banyard and Mashat are quoted where possible.

Wave function ^a	Shell	$\Delta\tau_r$	$\Delta\tau_{1/r}$	$\Delta\tau_\gamma$	$\Delta\tau'_\gamma$	$\Delta\tau''_\gamma$	Charge Shifted $\Upsilon\%$
Bunge (B)	K (1S)	-0.0358	-0.0180	-0.0301	-0.0113	-0.0331	2.130
	L (1S)	-0.0832	-0.0066	-0.2519	-0.0550	-0.3035	13.919
	KL (1S)	-0.0026	+0.0007	-0.0010	-0.0017	-0.0060	2.350
	KL (3S)	-0.0024	+0.0011	-0.0015	-0.0005	-0.0048	2.266
	Total ^b	-0.0111	-0.0043	-0.0827	-0.0053	-0.0595	0.999
Olympia and Smith (OS95)	K (1S)	-0.0316	-0.0250	-0.0306	-0.0111	-0.0333	2.181
	L (1S)	-0.0773	-0.0056	-0.2506	-0.0559	-0.3021	13.975
	KL (1S)	-0.0004	+0.0034	-0.0010	-0.0013	-0.0053	2.158
	KL (3S)	-0.0013	+0.0015	-0.0014	-0.0004	-0.0048	2.122
	Total ^b	-0.0106	-0.0056	-0.0816	-0.0053	-0.0592	1.323
Watson (W)	K (1S)	-0.0367	-0.0259	-0.0239	-0.0110	-0.0306	2.141
	L (1S)	+0.0053	-0.0001	-0.2208	-0.0575	-0.2819	13.437
	KL (1S)	-0.0005	-0.0021	+0.0046	+0.0006	+0.0059	0.124
	KL (3S)	+0.0005	+0.0000	+0.0046	+0.0004	+0.0040	0.036
	Total ^b	-0.0057	-0.0066	-0.0707	-0.0039	-0.0491	2.252
Olympia and Smith (OS85)	K (1S)	-0.0389	-0.0169	-0.0299	-0.0100	-0.0337	2.157
	L (1S)	-0.0804	-0.0102	-0.2511	-0.0634	-0.3064	15.889
	KL (1S)	-0.0022	-0.0046	-0.0010	-0.0003	-0.0017	0.085
	KL (3S)	+0.0027	+0.0010	+0.0049	-0.0003	-0.0036	0.063
	Total ^b	-0.0114	-0.0042	-0.0818	-0.0042	-0.0588	2.728
Weiss	K (1S)	-0.0399	-0.0185	-0.0296	2.064
	L (1S)	-0.0866	-0.0095	-0.2809	16.341
	K α L β	1.990
	K α L β	2.040
	Total ^b	1.702

^aAll τ for the HF wave function are zero except for the radial coefficients for the intershells. For KL (1S), τ_r and $\tau_{1/r}$ are -0.6243 and -0.2314 and, for KL (3S), the values are -0.6343 and -0.2682, respectively.

^bThe totals for $\Delta\tau$ were evaluated from Eqs. (7)-(11) by using the sum totals for the appropriate expectation values. The total for Υ was determined from the sum total Coulomb hole for the corresponding correlated wave function and, in this instance, is equal to $1/6$ (the area of the curve below the r_{12} axis) $\times 100\%$.

locations r_1 of the test electron. The K -shell diagram shows that the largest hole occurs when $r_1 \approx \langle r_1 \rangle_K$ whereas, for the L shell, the surface is not only more extensive but the greatest effect, which is considerably larger than that for the K shell, occurs at $r_1 \approx 0.5 \langle r_1 \rangle_L$. The structure of each intershell surface is comparatively complicated, although the inverted nature of the "holes" is immediately apparent in both cases.

To examine the sensitivity of our $\Delta f(r_{12})$ curves with respect to the partitioning technique, we calculated the Coulomb holes for the Bunge wave function using the first-order analysis of Banyard and Mashat.⁸ The K -shell curve was essentially unchanged to within graphical accuracy and, as indicated by the crosses in Fig. 2, the changes for the intershells are not large. The greatest effect occurred for the L shell. The crosses in Fig. 1(b) show that retaining only first-order terms in the correlated density gives rise to $\Delta f(r_{12})$ values which are too large when compared with the previous Bunge curve. Extending the partitioning of $\Gamma_{\text{corr}}(\mathbf{x}_1, \mathbf{x}_2)$ to the present level of analysis but adding only those contributions involving the $(s_1^2 p_1^2)$ -configuration reduced the magnitude of the L -shell hole and made it virtually coincident with the solid curve. Graphical coincidence was also achieved for the intershell curves. This not only re-emphasizes the importance of the $2s-2p$ near-degeneracy effect but also suggests that part of the difference between the Bunge and Weiss L -shell curves will be due to the level of partitioning for $\Gamma_{\text{corr}}(\mathbf{x}_1, \mathbf{x}_2)$.

The changes in τ provide global measures of electron correlation because each coefficient involves expectation values based on both the one- and two-particle densities. A common scale for each τ allows intercomparisons to be made. Table IV shows that an overall similarity exists between the $\Delta\tau$ for the B and OS95 wave functions. For the K shells, we observe that $\Delta\tau_r$ and $\Delta\tau_{r'}$ are of roughly comparable magnitude but, for the L shells, the angular effect is seen to be at least three times larger than $\Delta\tau_r$. We note that the Watson L -shell values for $\Delta\tau_{1/r}$ and $\Delta\tau_r$ are exceedingly small, thus indicating a lack of radial correlation; by contrast, the angular coefficients are of a more reasonable magnitude. This is understandable by inspection of Table I where it is seen that the correlation configurations listed for the L shell of Watson are all of angular form. For the intershells, the $\Delta\tau$ values are found to be more varied; in particular, we observe that for the B and OS95 functions $\Delta\tau_{1/r}$ and $\Delta\tau_r$ are now of opposite sign. The positive values of $\Delta\tau_{1/r}$ arise from an increase in $\langle r_1^{-1} r_2^{-1} \rangle$, thus indicating that correlation causes a contraction in the inner regions of the intershell two-particle radial density. However, from an angular viewpoint, the signs of $\Delta\tau_r$, $\Delta\tau_{r'}$, and $\Delta\tau_{r''}$ imply an increase in interparticle separation; an exception is the W function, due to an inadequacy in the number of correlation configurations. The net effect of correlation on $\langle r_{12} \rangle$ for the intershells in the B and OS95 wave functions can be seen from Table III.

IV. SUMMARY

The first-order partitioning technique used by Banyard and Mashat for studying Coulomb holes for electronic

shells in Be-like ions has been extended and applied to a comparison of different wave functions for Be. An overall assessment of the radial and angular correlation within each shell is provided by the change in various correlation coefficients. When partitioning the second-order correlated density, the present inclusion of all products of terms up to and including the pair-correlation functions U_{ij} produced greatest change, relative to the earlier work, in the Coulomb hole for the L shell. This was related to the $2s-2p$ near-degeneracy effect which exists in Be. For systems in which such effects do not occur it is felt that first-order partitioning may prove adequate.

The total energies E of the four CI wave functions examined here group into two pairs and this was clearly reflected in the behavior of the Coulomb holes for each shell. The effect was particularly noticeable for the intershells.

The $\Delta f(r_{12})$ curves for the 1S and 3S intershell states were inverted by comparison with the intrashell holes, thus substantiating the characteristics observed earlier when analyzing the Weiss wave functions for the Be-like ions. The shape of such curves was rationalized in terms of the significant contraction of the L shell towards the nucleus which, in turn, arises primarily from a large nondynamical angular correlation effect. As a consequence, a study of the intershells in a system like Ne, with its completed K and L shells, would be quite informative.

The total Coulomb holes for the two energetically best descriptions of Be revealed that, even when combined with the K - and L -shell holes, the intershell effects were of sufficient magnitude to produce clearly identifiable characteristics not seen in earlier work.

The examination of Coulomb holes and correlation coefficients for individual electronic shells, via a partitioning technique, can be applied to more complex atoms and molecules in both position and momentum space. Work along these lines is now in progress.

ACKNOWLEDGMENT

One of us (R.J.M.) wishes to thank the Science Research Council for the award of a Maintenance Grant.

¹C. A. Coulson and A. H. Neilson, Proc. Phys. Soc. London **78**, 831 (1961).

²R. F. Curl and C. A. Coulson, Proc. Phys. Soc. London **85**, 647 (1965).

³W. A. Lester, Jr. and M. Krauss, J. Chem. Phys. **44**, 207 (1966).

⁴K. E. Banyard and G. J. Seddon, J. Chem. Phys. **58**, 1132 (1973).

⁵R. J. Boyd and C. A. Coulson, J. Phys. B **6**, 782 (1973).

⁶R. J. Boyd and J. Katriel, Int. J. Quantum Chem. **8**, 255 (1974).

⁷N. Moiseyev, J. Katriel, and R. J. Boyd, Theor. Chim. Acta **45**, 61 (1977).

⁸K. E. Banyard and M. M. Mashat, J. Chem. Phys. **67**, 1405 (1976).

⁹O. Sinanoğlu, Rev. Mod. Phys. **35**, 517 (1963).

¹⁰For a general review of Sinanoğlu's many-electron theory

- see O. Sinanoğlu and K. A. Brueckner, *Three Approaches to Electron Correlation in Atoms* (Yale University, New Haven, 1970).
- ¹¹A. W. Weiss, *Phys. Rev.* **122**, 1826 (1961).
- ¹²E. Clementi, "Tables of Atomic Functions," a supplement to *IBM J. Res. Dev.* **9**, 2 (1965).
- ¹³R. E. Watson, *Phys. Rev.* **119**, 170 (1960).
- ¹⁴C. F. Bunge, *Phys. Rev.* **168**, 92 (1968).
- ¹⁵P. L. Olympia, Jr. and D. W. Smith, *J. Chem. Phys.* **52**, 67 (1970).
- ¹⁶R. McWeeny and B. T. Sutcliffe, *Methods of Molecular Quantum Mechanics* (Academic, New York, 1969).
- ¹⁷G. K. Taylor and K. E. Banyard, *Phys. Rev. A* **8**, 1157 (1973).
- ¹⁸K. E. Banyard and G. K. Taylor, *Phys. Rev. A* **10**, 1972 (1974).
- ¹⁹C. F. Bunge, *Phys. Rev. A* **14**, 1965 (1976).
- ²⁰W. Kutzelnigg, G. Del Re, and G. Berthier, *Phys. Rev.* **172**, 49 (1968).
- ²¹G. P. Barnett, J. Linderberg, and H. Shull, *J. Chem. Phys.* **43**, S80 (1965).
- ²²F. W. Byron and C. J. Joachain, *Phys. Rev.* **157**, 7 (1967).
- ²³R. Benesch and V.H. Smith, Jr., *J. Chem. Phys.* **55**, 482 (1971).

Correlation effects in momentum space for the electronic shells in Be

R. J. Mobbs and K. E. Banyard

Department of Physics, University of Leicester, Leicester, England
(Received 27 January 1982; accepted 9 August 1982)

Our previous partitioning technique for analyzing correlation effects within the individual electronic shells of Be in position space has been applied here to a corresponding examination in momentum space. Comparability with the results in position space was ensured by considering the same configuration-interaction (CI) wave functions and Hartree-Fock (HF) description as before; the functions were transformed into momentum space by applying the standard Dirac procedure. By analogy with position space, Coulomb shifts $\Delta f(p_{12})$ vs p_{12} were derived for the $K(^1S)$, $L(^1S)$, $KL(^1S)$, and $KL(^3S)$ shells in Be. Selected one- and two-particle momentum expectation values are also reported along with various radial and angular correlation coefficients. The opposing effects of radial and angular correlation in momentum space for Be gave a K -shell Coulomb shift which, being small, suggested a rough balance between these correlation components. For the L shell, however, the large excess of angular correlation produced a "shift" which, relative to the K shell, was of considerable magnitude. Thus, when forming the sum total Coulomb shift for the whole atom, the L -shell component virtually masked all contributions arising from the other shells. This is in direct contrast with position space where the intershell effects in Be produced some detailed structure in the total Coulomb hole $\Delta f(r_{12})$ vs r_{12} . The characteristics of the momentum curves for the various shells are rationalized and their relationship with the corresponding results in position space is discussed.

I. INTRODUCTION

Recently,¹ we examined and compared the intra- and intershell correlation effects in position space for the ground state of Be when described by several configuration-interaction (CI) wave functions.²⁻⁴ The analysis was performed by determining Coulomb holes^{5,6} and various expectation values for each electronic shell. The expectation values were used to calculate several statistical correlation coefficients τ : these were of particular interest when assessing the angular and radial components of electron correlation in the intrashells. The description of an individual shell, at both a correlated and Hartree-Fock (HF) level, was obtained by partitioning the second-order density for the total system into its pair-wise components. To achieve such partitioning we neglected the three- and four-particle correlation terms in the many-body representation⁷ of the correlated wave function. In the present work, a parallel investigation of Be is carried out in momentum space.

When forming the Coulomb hole in position space, the effects of radial and angular correlation are known to work in unison whereas, by contrast, in momentum space, these components yield characteristics which are in opposition.⁸ Consequently, momentum space is a particularly useful and sensitive medium for highlighting the differences between the radial and angular components of correlation for both atoms and molecules. In a study of some two-electron systems,^{9,10} it has been found that, by comparison with position space, such differences give rise to a relatively complicated structure for the Coulomb hole; thus, for momentum space, it is preferable to use the term "shift" rather than "hole."⁹

For Be(¹S), the Coulomb shifts and the changes in τ in momentum space reported here are derived from the CI wave functions of Bunge³ and Olympia and Smith.⁴

In each instance, the HF reference state for Be is taken, as before,¹ from the work of Watson.² Since position and momentum coordinates are conjugate quantities, the present results, taken together with our earlier findings, will provide an overall view of correlation within the individual intra- and interelectronic shells for this example of a many-electron atom.

II. CALCULATIONS AND RESULTS

The correlated descriptions of Be provided by the 180-term CI wave function of Bunge (B) and the 95-term function of Olympia and Smith (OS95) account for 96.55% and 95.87% of the correlation energy,¹ respectively. The analysis of these ground-state wave functions is eased because not only are they constructed from a common orthonormal basis set but, in addition, they each contain the restricted HF wave function of Watson² as the *leading* configuration.

Electron correlation may be investigated by examining the differences between the correlated two-particle density $\Gamma_{\text{corr}}(\mathbf{x}_m, \mathbf{x}_n)$ and the corresponding HF density $\Gamma_{\text{HF}}(\mathbf{x}_m, \mathbf{x}_n)$. The definition of $\Gamma(\mathbf{x}_m, \mathbf{x}_n)$ in terms of an N -particle wave function follows McWeeny and Sutcliffe¹¹ and is normalized to equal the number of independent electron pairs within the system; as usual \mathbf{x}_m , e.g., represents the combined position space and spin coordinates of electron m . The density for the individual electronic shells is obtained by partitioning Γ into its pair-wise components (i, j) , where (i, j) labels the occupied normalized spin-orbitals ϕ in the restricted HF description of our closed-shell system. For $\Gamma_{\text{HF}}(\mathbf{x}_m, \mathbf{x}_n)$, the partitioning is both straightforward and exact. The resolution of $\Gamma_{\text{corr}}(\mathbf{x}_m, \mathbf{x}_n)$ into its intra- and intershell components alone may be achieved only approximately and, in our analysis, requires the use of the many-body expansion of Ψ_{corr} proposed by Sinanoğlu.⁷ This expan-

sion for Ψ_{corr} is truncated after the pair-correlation functions U_{ij} and $\Gamma_{\text{corr}}(\mathbf{x}_m, \mathbf{x}_n)$ is then constructed without further approximation by retaining products of all terms and integrating over all electron coordinates except those associated with electrons m and n . Thus, the resulting expression for $\Gamma_{\text{corr}}(\mathbf{x}_m, \mathbf{x}_n)$ can be written as

$$\Gamma_{\text{corr}}(\mathbf{x}_m, \mathbf{x}_n) = \sum_{i,j}^N \Gamma_{ij}(\mathbf{x}_m, \mathbf{x}_n) \quad (1)$$

The correlated form of $\Gamma_{ij}(\mathbf{x}_m, \mathbf{x}_n)$ is lengthy and complicated and, since it was presented previously,¹ it will not be repeated. The energies and structure of the Ψ_{corr} examined here were reported in Table I of Ref. 1. It is to be noted that, when presenting our results, the (i, j) pair (1, 4) and (2, 3) have been combined and rewritten to yield pure spin states 1S and 3S for the intershells. In addition, the m and n labels in each two-particle density have, henceforth, been set to be 1 and 2, respectively. The partitioned two-particle densities in momentum space for the $K(^1S)$, $L(^1S)$, $KL(^1S)$, and $KL(^3S)$ shells were obtained by applying the Dirac transformation procedure¹² to the primitive spin-orbitals in position space used to represent each Be wave function. Atomic

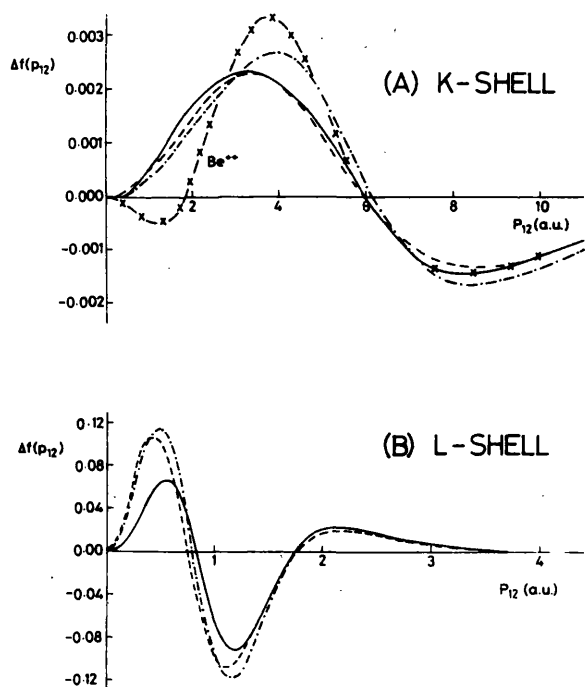


FIG. 1. The Coulomb shifts $\Delta f(p_{12})$ for the (A) K and (B) L shell in Be. $\Delta f(p_{12})$ is the difference between a correlated and an HF description of the interparticle momentum distribution function. Each $f_{ij}(p_{12})$ is normalized to unity and p_{12} is measured in atomic units (a. u.). The correlated descriptions are given by the Bunge (Ref. 3) (B) wave function (—) and the Olympia and Smith (Ref. 4) 95-term (OS95) function (the resulting K- and L-shell curves are coincident with those obtained from the Bunge wave function). Results are also shown for the Watson (Ref. 2) (W) function (---) and the Olympia and Smith (Ref. 4) 85-term (OS85) function (-·-·-·-). The HF wave function for Be is taken from Watson (Ref. 2). For comparison with the Be K shell, diagram (A) includes the Coulomb shift for the Be^{2+} ion (-x-x-x-x) derived from the correlated wave function of Weiss (Ref. 14) and the HF function of Clementi (Ref. 15).

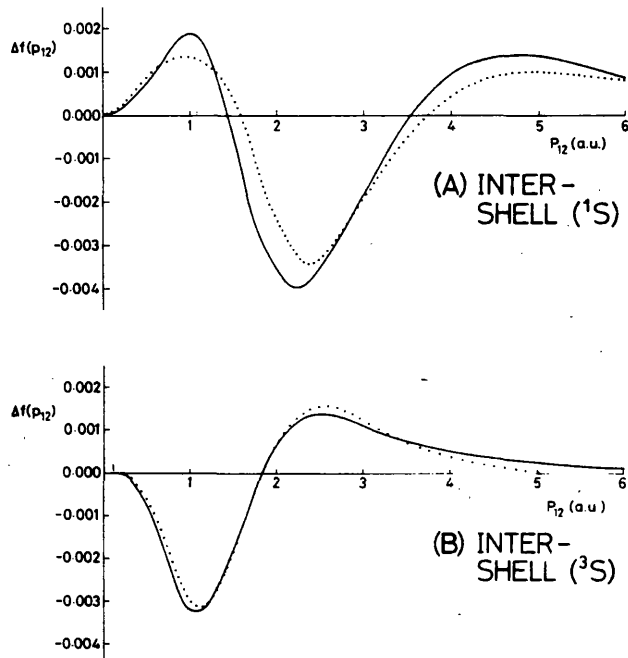


FIG. 2. $\Delta f(p_{12})$ vs p_{12} for the 1S and 3S intershells in Be as described by the B (—) and OS95 (····) correlated wave functions. The HF wave function for Be is taken from Watson (Ref. 2).

units are used throughout this work.

The Coulomb shift associated with the HF spin-orbital pair (i, j) is given by

$$\Delta f_{ij}(p_{12}) = \int \Delta \Gamma_{ij}(p_1, p_2) dp_1 dp_2 / dp_{12} \quad (2)$$

where the limits of integration are analogous to those discussed by Coulson and Neilson⁵ in position space; spin has been integrated out of Eq. (2). $\Delta f_{ij}(p_{12})$ is the change, due to correlation, in the distribution function $f_{ij}(p_{12})$ for a given magnitude of the momentum difference $p_{12} = |\mathbf{p}_1 - \mathbf{p}_2|$ between electrons 1 and 2 and $\Delta \Gamma_{ij}(p_1, p_2)$ is the change in the partitioned two-particle density after transformation into momentum space. Each $f_{ij}(p_{12})$ is normalized to unity. The Coulomb shifts $\Delta f(p_{12})$ vs p_{12} for the intra- and intershells of Be are shown in Figs. 1 and 2, respectively. To provide some correspondence with our Coulomb hole analysis,¹ Fig. 1 also includes results derived from the correlated wave function of Watson² and the 85-term CI function of Olympia and Smith.⁴ These functions (W and OS85) account for 89.36% and 87.18% of the correlation energy; however, their intershell effects are too small to justify inclusion in Fig. 2. For the B wave function,³ the curves for the individual shells are compared with their sum total effect in Fig. 3(A). The sum total shifts for the various correlated wave functions are presented in Fig. 3(B).

Reported in Table I are some one- and two-particle expectation values for the B and OS95 wave functions and, for reference, we also include the HF results. Table I also contains Υ —the percentage of each $f_{\text{HF}}(p_{12})$ probability density which has been redistributed due to

TABLE I. Some one- and two-particle momentum expectation values for the intra- and intershells of Be derived from the partitioned form of the second-order density $\Gamma(p_1, p_2)$ for the Bunge (Ref. 3) and Olympia and Smith 95-term (Ref. 4) CI wave functions. For reference, we quote the corresponding HF values. Also included is T —the percentage of the interparticle momentum distribution function $f_{HF}(p_{12})$ which has been redistributed due to electron correlation. Atomic units are used throughout.

Wave function	Shell	$\langle p_1^{-1} \rangle$	$\langle p_1 \rangle$	$\langle p_1^2 \rangle$	$\langle p_1^{-1} p_2^{-1} \rangle$	$\langle p_1 p_2 \rangle$	$\langle p_1 \cdot p_2 \rangle$	$\langle p_{12} \rangle$	Density shifted $T\%$
Bunge (B)	$K(1S)$	0.4736	3.0947	13.593	0.2233	9.4361	0.4287	4.4735	0.781
	$L(1S)$	2.4979	0.6712	1.0574	6.2530	0.4422	0.0298	0.9638	4.967
	$KL(1S)$	1.5380	1.8692	7.3118	1.3580	2.3542	0.0102	3.1678	0.486
	$KL(2S)$	1.5384	1.8696	7.3103	1.1079	1.6327	0.0075	3.2727	0.286
	Total ^a	1.5208	1.8740	7.3154	1.8597	2.8551	0.0818	3.0705	0.942 ^b
Olympia and Smith (OS95)	$K(1S)$	0.4737	3.0950	13.597	0.2234	9.4369	0.4282	4.4718	0.786
	$L(1S)$	2.4963	0.6690	1.0559	6.2454	0.4394	0.0302	0.9621	4.959
	$KL(1S)$	1.5424	1.8695	7.3197	1.3641	2.3670	0.0134	3.1672	0.405
	$KL(2S)$	1.5426	1.8692	7.3189	1.1116	1.6294	0.0079	3.2720	0.265
	Total ^a	1.5233	1.8735	7.3216	1.8613	2.8552	0.0826	3.0695	0.935 ^b
Hartree-Fock (HF)	$K(1S)$	0.4739	3.0919	13.5681	0.2246	9.5598	0.0	4.5248	...
	$L(1S)$	2.6874	0.6251	1.0021	7.2219	0.3908	0.0	0.9591	...
	$KL(1S)$	1.5806	1.8585	7.2851	1.3994	2.2846	0.0	3.1589	...
	$KL(2S)$	1.5806	1.8585	7.2851	1.1480	1.5810	0.0	3.2652	...
	Total ^a	1.5806	1.8585	7.2851	2.0483	2.8297	0.0	3.0731	...

^aThe sum total listed here for each expectation quantity is given by $\frac{1}{6}[K(1S) + L(1S) + KL(1S) + 3KL(2S)]$.

^bThe total for T was determined from the sum total Coulomb shifts for the corresponding correlated wave function and, in this instance, is equal to $\frac{1}{6} \times (\text{the area of the curve below the } p_{12} \text{ axis}) \times 100\%$.

correlation. By analogy with position space,¹ the radial and angular components of correlation were assessed by evaluating the statistical correlation coefficients $\tau_{1/p}$, τ_p , τ_γ , $\tau_{\gamma'}$, and $\tau_{\gamma''} = \langle \cos \gamma \rangle$, where $p = |p|$ and γ is the angle between the electronic momentum vectors p_1 and p_2 . The results for $\Delta\tau = \tau(\text{corr}) - \tau(\text{HF})$ for the K and L shells and the total atom are given in Table II; for brevity we omit the less interesting $KL(1S)$ and $KL(2S)$ values.

III. DISCUSSION

In Fig. 1(A) we note that the K shell curves derived from the B and OS95 wave functions are graphically indistinguishable. By comparison, it is seen that the OS85 function gives a Coulomb shift which is not only of

greater magnitude at its peak but is also somewhat more diffuse. The W wave function produces a curve which crosses the axis at a point coincident with the B and OS95 curves but differs from them slightly in magnitude. Included in Fig. 1(A) is the Coulomb shift for Be^{2+} since a comparison between it and the K shell of Be is of obvious interest; the ionic curve was obtained by Reed¹³ using the CI wave function of Weiss¹⁴ and the HF function of Clementi.¹⁵ We observe that although the B and OS95 functions give results which are very similar to the Be^{2+} curve when $p_{12} > 6$, significant differences exist for $0 < p_{12} < 6$. For two-electron systems it has been established⁹ that, at small p_{12} , the radial component of electron correlation gives rise to negative values for $\Delta f(p_{12})$ whereas, by contrast, angular correlation produces a curve which is initially positive. Thus, when

TABLE II. The changes $\Delta\tau$ in the radial and angular statistical correlation coefficients τ for the Be K and L shells and the total atom, where $\Delta\tau = \tau(\text{corr}) - \tau(\text{HF})$. The various τ in momentum space are defined by analogy with Eqs. (7)–(11) of Ref. 1.^a

Wave function	Shell	$\Delta\tau_{1/p}$	$\Delta\tau_p$	$\Delta\tau_\gamma$	$\Delta\tau_{\gamma'}$	$\Delta\tau_{\gamma''}$
Bunge (B)	$K(1S)$	-0.0058	-0.0352	+0.0315	+0.0083	+0.0284
	$L(1S)$	+0.0029	-0.0136	+0.0282	+0.0547	+0.1404
	Total ^b	-0.0111	-0.0097	+0.0112	+0.0172	+0.0302
Olympia and Smith (OS95)	$K(1S)$	-0.0058	-0.0354	+0.0315	+0.0082	+0.0283
	$L(1S)$	+0.0031	-0.0134	+0.0300	+0.0549	+0.1397
Total ^b	-0.0115	-0.0088	+0.0113	+0.0170	+0.0299	

^aThe radial coefficients $\tau_{1/p}$ and τ_p emphasize the inner and outer regions of the radial two-particle momentum density, respectively. The angular coefficients τ_γ , $\tau_{\gamma'}$, and $\tau_{\gamma''}$ are related, in turn, to $\langle p_1 \cdot p_2 \rangle$, $\langle (p_1/p_1^2) \cdot (p_2/p_2^2) \rangle$ and $\langle \cos \gamma \rangle$, where γ is the angle between the momentum vectors p_1 and p_2 for electrons 1 and 2.

^bThe total for $\Delta\tau$ is obtained by using the sum totals for the appropriate expectation values to determine each total τ .

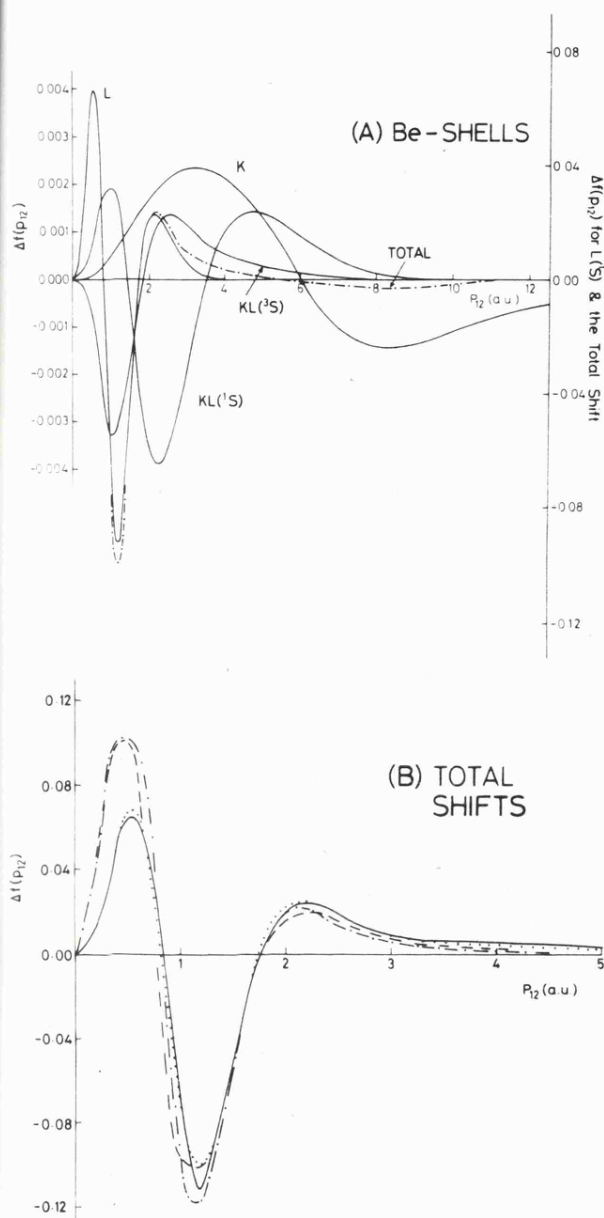


FIG. 3. (A) A comparison of intra- and intershell Coulomb shifts for the B wave function. The sum total of these shifts for the B wavefunction, given by $K(^1S) + L(^1S) + KL(^1S) + 3KL(^3S)$, is shown here by the chain-dot curve. The $\Delta f(p_{12})$ scale for the sum total Coulomb shift is the same as that for the $L(^1S)$ shell; see the right of the diagram. (B) The sum total of the intra- and intershell Coulomb shifts given by $\Delta f(p_{12}) = K(^1S) + L(^1S) + KL(^1S) + 3KL(^3S)$ for the B (—), OS95 (····), W (---), and OS85 (- · - · -) correlated wave functions.

p_{12} is small, Fig. 1(A) shows that, like the other two-electron ions, the overall effect in Be^{2+} is one of radial correlation. However, for the K shell in Be, it appears that the occupation of the L shell causes an *initial* cancellation between the angular and radial components. These differences between Be^{2+} and Be at small p_{12} are in general accord with a comparison between the corresponding $\Delta\tau$ values. Although the K -shell angular correlation coefficients for Be were found to be only

marginally larger than those for Be^{2+} , it was noted that the $\Delta\tau_{1/p}$ value of -0.0058 for the K shell was *considerably* smaller than the ionic result of -0.0197 . Thus, by comparison with Be^{2+} , radial correlation at small momenta in the Be K shell is inhibited by the presence of the L shell electrons. In the light of the momentum analysis by Banyard and Reed,⁹ the *overall* behavior of the curves in Fig. 1(A) suggests that angular correlation has, on balance, the major influence in the K shell of Be.

The L -shell Coulomb shifts in Fig. 1(B) show that the B and OS95 wave functions yield results which are graphically coincident, as was found in position space. However, unlike position space, these $\Delta f(p_{12})$ values are noticeably different from the results derived from *both* the W and OS85 functions. Figure 1(B) highlights the dominance of angular correlation at small p_{12} , the effect being greatest for the energetically poorer W and OS85 functions. The magnitude of the L -shell Coulomb shift is considerably greater than that for the K shell although, as would be expected, it is much less extensive in its p_{12} range. Like position space, the Υ values in Table I indicate that the L -shell effect is about 6.5 times larger than that for the K shell.

In position space, correlation caused a significant contraction of the L -shell distribution in Be. This is reflected here as an *expansion* in the one- and two-particle radial densities, as revealed by the changes in $\langle p_1^2 \rangle$ and $\langle p_1^2 p_2^2 \rangle$ in Table I. For the angular-related properties in Tables I and II, we see that each intrashell value possesses a positive sign. Thus, correlation has enhanced the alignment of the two momentum vectors, a result which is in keeping with the ground-state studies of the He-like ions.^{8,9} The large amount of angular correlation in the L shell in both momentum and position space is due, of course, to the high degree of near $2s-2p$ degeneracy in Be and, as such, is a nondynamical effect.¹⁶

In position space,¹ the $KL(^1S)$ and $KL(^3S)$ Coulomb holes for Be were found to be of similar shape and magnitude except in the region of small r_{12} . However, in momentum space, Fig. 2 shows that the opposing effects of angular and radial correlation produce intershell shifts which are quite distinct in character *and* range. The Coulomb shifts for 1S suggest that angular correlation is dominant for $p_{12} < 1.5$, whereas, for the 3S curves, it appears that radial correlation is paramount. When $p_{12} = |p_1 - p_2|$ is close to zero, Fermi correlation causes $f_{\text{corr}}(p_{12})$ and $f_{\text{HF}}(p_{12})$ to be vanishingly small, thus accounting for the graphically negligible values of $\Delta f(p_{12})$ in Fig. 2(B) when $p_{12} < 0.25$. Inspection of Table I shows that, for the intershells, electron correlation has produced an expansion in the one- and two-particle radial momentum densities.

The rationalization of the shape of these Coulomb shifts requires, of necessity, some general comments about the HF model. Since each shell within the HF reference state for Be uses basis orbitals with zero angular momentum, the momentum vector p for an electron will be parallel to its position vector r . Moreover, the HF description indicates that, in each space,

the average angle between two electronic vectors is 90° . If, for a given shell in position space for Be, the two electrons can be thought of as oscillating about the nucleus along mutually perpendicular axes then, to minimize the electron-electron repulsion energy, it is reasonable to assume a phase difference between their motions of $\pi/2$. As the initial example, let us now comment on the expected behavior of $\Delta f(p_{12})$ for the L shell. The introduction of correlation was found^{17,18} to cause a relatively large increase in the average angle between the position vectors r_1 and r_2 . In the context of the HF model discussed above, this implies that correlation produces a corresponding decrease in the average angle between p_1 and p_2 , as observed. Such a change in angle predicts an increase in $f(p_{12})$ for small p_{12} . Correlation also produced a contraction of the L shell in position space which, as seen from Table I, means a move towards higher momentum values. Consequently, the Coulomb shifts should also be positive at large p_{12} . Because each $f(p_{12})$ distribution is normalized, a compensating decrease in probability is to be expected at intermediate p_{12} . These correlation characteristics are indeed seen in Fig. 1(B).

For the K shell of Be in position space, we found¹ that the radial and angular correlation coefficients were not only of the same sign but, in contrast with the L shell, they were also of roughly similar magnitude when applied to a common region of space. This similarity of magnitude also occurs in momentum space but, as Table II shows, the K shell radial and angular coefficients are now of opposite sign. Thus, as seen in Fig. 1, the almost equal and opposing effects of radial and angular correlation in the K shell produces maximum and minimum values for $\Delta f(p_{12})$ which are very small by comparison with the L shell. In passing, we recall that, in position space, the extremum values of $\Delta f(r_{12})$ for the K shell were comparable with those for the L shell. The approximate balance between the correlation components in momentum space for the K shell makes it difficult to predict a shape for the corresponding Coulomb shift. Figure 1(A) indicates that the K -shell curves are, in fact, characterized by an angular correlation effect.

The pair correlation energies for Be^{19,20} suggest that the behavior of the 1S and 3S intershell Coulomb shifts may be largely dictated by the intrashell correlation effects. For the 1S intershell, the interpenetration of the K - and L -shell orbitals will give rise to overlap regions where the occupying electron pair will experience $K(^1S)$ or $L(^1S)$ type correlation. At small p_{12} it is reasonable to suggest that the main contribution to $f(p_{12})$ should arise from this double-occupancy effect within the individual intrashell regions. Therefore, one expects that $\Delta f(p_{12})$ for $KL(^1S)$ will follow the common feature of the $K(^1S)$ and $L(^1S)$ curves by being positive at small p_{12} . A large p_{12} value implies that the intershell electrons will be physically separated by being located essentially in their respective shells. The correlation effect ought now to be dominated by the significant shift of an L -shell electron towards a region of higher momentum; the change in the K -shell momentum due to correlation is comparatively small.

Since the average angle between p_1 and p_2 for the $KL(^1S)$ is barely decreased by correlation from its HF value of 90° (viz. $\langle \cos \gamma \rangle_{\text{corr}} = +0.0007$ for $KL(^1S)$ and $+0.0038$ for $KL(^3S)$ using the B function), the increase in L -shell momentum will produce a transfer in p_{12} probability towards larger p_{12} values. Thus, $\Delta f(p_{12})$ should be positive at large p_{12} and negative at intermediate p_{12} , as seen in Fig. 2(A). The behavior of the 3S Coulomb shift at large p_{12} may be rationalized in the same way. However, because of the Fermi effect, it is not too surprising that the 3S curve has the smaller p_{12} range. When p_{12} is small, the 3S and 1S curves in Fig. 2 are seen to be quite different in shape. The presence of the Fermi effect in the 3S intershell stops the Coulomb shift from possessing any $K(^1S)$ or $L(^1S)$ characteristics at small p_{12} . Consequently, the structure of the $KL(^3S)$ curve will be governed mainly by the increase in the L -shell momentum vector which, as seen above, retains an average orientation of almost 90° with respect to the marginally increased K -shell vector. Thus, after the initial flat part of the curve, due to the near-zero values of $f_{\text{corr}}(p_{12})$ and $f_{\text{HF}}(p_{12})$, correlation will reduce $f(p_{12})$ and increase it at the larger p_{12} values, as mentioned before.

The most noticeable feature in Fig. 3(A) is the massive influence of the $L(^1S)$ curve which, in Be, almost completely masks any variation in the other curves when forming the sum total Coulomb shift. This is in marked contrast with position space where intershell effects were quite discernible in the total $\Delta f(r_{12})$ curve. The change in behavior on transforming to momentum space arises because, as noted earlier, angular and radial correlation effects are now in opposition. A comparison of Fig. 3(B) with Fig. 1(B) shows that, for $p_{12} < 2$, the main differences between the various total Coulomb shifts arise from variations in the correlated description of the L -shell electrons. At large p_{12} , the total shifts essentially reflect K -shell characteristics. Figure 3(B) also shows that the B and OS95 wave functions produce results which are in good agreement over the whole p_{12} range. The similarity between these functions is also demonstrated by the T values in Table I.

An overall assessment of angular and radial correlation components in different regions of momentum space is provided by the change in the correlation coefficients listed in Table II. As seen, these results support our findings not only for the K and L shells but also for the total atom. The correspondence between the two sets of $\Delta \tau$ values is quite striking. In passing, we note that when the average $\gamma = \arccos \{ \Delta \tau_{\gamma} \} \equiv \langle \cos \gamma \rangle_{\text{corr}}$ in momentum space was added to the corresponding interparticle angle in position space, the total was $180^\circ (\pm 0.3^\circ)$ for each shell, except L , within each correlated wave function. That the L -shell values are always somewhat in excess of 180° may be a consequence of the large nondynamical angular correlation effect. Generally, however, the sum of the two angles was in keeping with our HF and correlated models discussed above.

IV. SUMMARY

Because angular and radial correlation produce opposing effects in momentum space, the structure of the

Coulomb shift reflects the nature of the dominant correlation component for a given electronic shell. The Coulomb shift for the Be K shell indicates that, overall, the angular component is slightly in excess of the radial effect. Compared with the K shell, the correlation effects in momentum space for the L shell are massive. The disparity between the K - and L -shell Coulomb shifts in Be is so great that, irrespective of the contributions from the two intershells, the $\Delta f(p_{12})$ curve for the atom as a whole is almost completely dominated by the L -shell component. This is in contrast with position space where not only did the K and L shells possess comparable extremum values for $\Delta f(r_{12})$ but, more interestingly, the total Coulomb hole for Be exhibited distinct intershell features. With these points in mind, it would be intriguing to examine a system like Ne, with a completed L shell, in both position and momentum space.

The Coulomb shifts for the intershells in Be showed marked differences in behavior at small p_{12} : the $KL(^1S)$ curve for $p_{12} < 1$ was influenced primarily by angular correlation while $KL(^3S)$ was dominated by radial correlation. Finally, when rationalizing the shapes of the $\Delta f(p_{12})$ curves for the individual electronic shells, Fermi correlation proved to be the important factor in differentiating between the two intershells.

ACKNOWLEDGMENT

One of us (RJM) wishes to thank the Science Research Council for the award of a Maintenance Grant.

- ¹K. E. Banyard and R. J. Mobbs, *J. Chem. Phys.* **75**, 3433 (1981). A misprint exists in Eq. (3) of this work, the constant ($\frac{1}{2}$) should be ($\frac{1}{3}$).
- ²R. E. Watson, *Phys. Rev.* **119**, 170 (1960).
- ³C. F. Bunge, *Phys. Rev.* **168**, 92 (1968).
- ⁴P. L. Olympia, Jr. and D. W. Smith, *J. Chem. Phys.* **52**, 67 (1970).
- ⁵C. A. Coulson and A. H. Neilson, *Proc. Phys. Soc. London* **78**, 831 (1961).
- ⁶R. E. Curl and C. A. Coulson, *Proc. Phys. Soc. London* **85**, 647 (1965).
- ⁷O. Sinanoğlu, *Rev. Mod. Phys.* **35**, 517 (1963). For a general review of many-body theory applied to electron correlation see O. Sinanoğlu and K. A. Brueckner, *Three Approaches to Electron Correlation in Atoms* (Yale University, New Haven, 1970).
- ⁸K. E. Banyard and J. C. Moore, *J. Phys. B* **10**, 2781 (1977).
- ⁹K. E. Banyard and C. E. Reed, *J. Phys. B* **11**, 2957 (1978).
- ¹⁰C. E. Reed and K. E. Banyard, *J. Phys. B* **13**, 1519 (1980).
- ¹¹R. McWeeny and B. T. Sutcliffe, *Methods of Molecular Quantum Mechanics* (Academic, New York, 1969).
- ¹²P. A. M. Dirac, *Quantum Mechanics* (Oxford University, Oxford, 1935), p. 103.
- ¹³C. E. Reed, Ph.D. thesis, Leicester University, 1980.
- ¹⁴A. W. Weiss, *Phys. Rev.* **122**, 1826 (1961).
- ¹⁵E. Clementi, *Tables of Atomic Functions*, a supplement to *IBM J. Res. Devel.* **9**, 2 (1965).
- ¹⁶V. McKoy and O. Sinanoğlu, *J. Chem. Phys.* **41**, 2689 (1964).
- ¹⁷K. E. Banyard and D. J. Ellis, *Mol. Phys.* **24**, 1291 (1972).
- ¹⁸K. E. Banyard and M. M. Mashat, *J. Chem. Phys.* **67**, 1405 (1976), see also Ref. 1.
- ¹⁹F. W. Byron and C. J. Joachain, *Phys. Rev.* **157**, 7 (1967).
- ²⁰K. E. Banyard and G. K. Taylor, *Phys. Rev. A* **10**, 1972 (1974).